frontiers | Research Topics

Maize stress ecophysiology and regulation

Edited by
Jiwang Zhang, Baizhao Ren and Xuecai Zhang

Published in
Frontiers in Plant Science

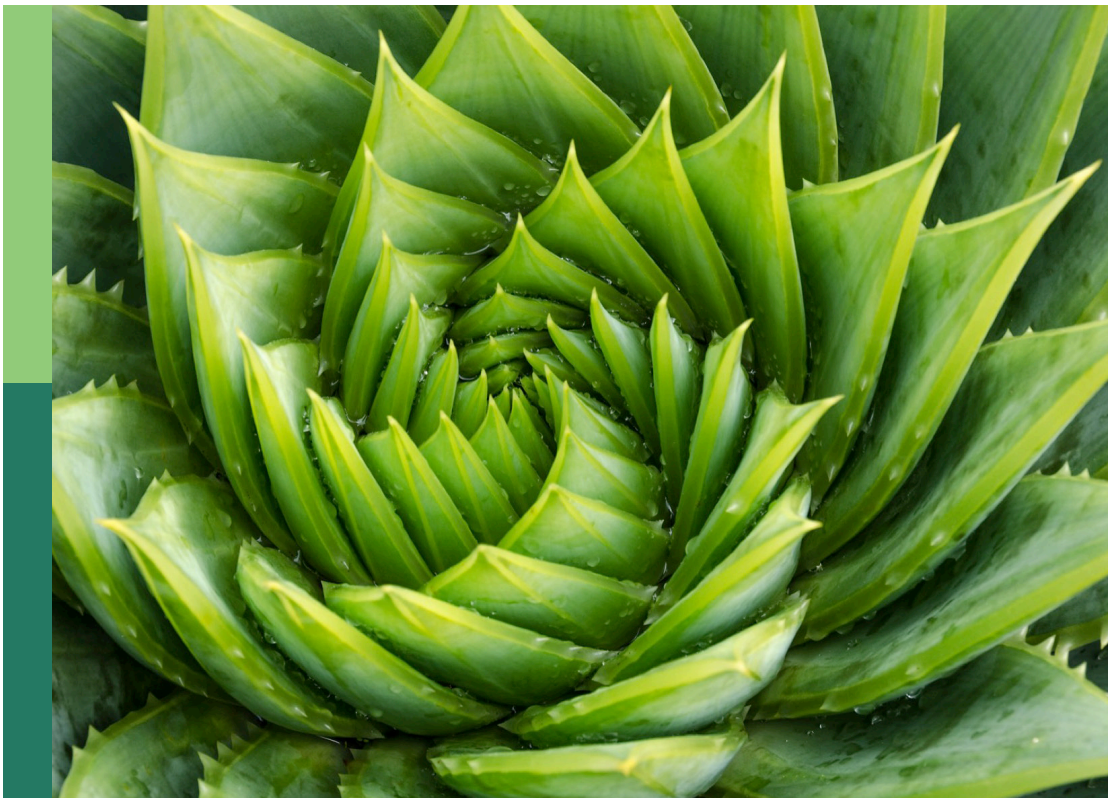

ISSN 1664-8714
ISBN 978-2-8325-3968-2
DOI 10.3389/978-2-8325-3968-2

About Frontiers

Frontiers is more than just an open access publisher of scholarly articles: it is a pioneering approach to the world of academia, radically improving the way scholarly research is managed. The grand vision of Frontiers is a world where all people have an equal opportunity to seek, share and generate knowledge. Frontiers provides immediate and permanent online open access to all its publications, but this alone is not enough to realize our grand goals.

Frontiers journal series

The Frontiers journal series is a multi-tier and interdisciplinary set of open-access, online journals, promising a paradigm shift from the current review, selection and dissemination processes in academic publishing. All Frontiers journals are driven by researchers for researchers; therefore, they constitute a service to the scholarly community. At the same time, the *Frontiers journal series* operates on a revolutionary invention, the tiered publishing system, initially addressing specific communities of scholars, and gradually climbing up to broader public understanding, thus serving the interests of the lay society, too.

Dedication to quality

Each Frontiers article is a landmark of the highest quality, thanks to genuinely collaborative interactions between authors and review editors, who include some of the world's best academicians. Research must be certified by peers before entering a stream of knowledge that may eventually reach the public - and shape society; therefore, Frontiers only applies the most rigorous and unbiased reviews. Frontiers revolutionizes research publishing by freely delivering the most outstanding research, evaluated with no bias from both the academic and social point of view. By applying the most advanced information technologies, Frontiers is catapulting scholarly publishing into a new generation.

What are Frontiers Research Topics?

Frontiers Research Topics are very popular trademarks of the *Frontiers journals series*: they are collections of at least ten articles, all centered on a particular subject. With their unique mix of varied contributions from Original Research to Review Articles, Frontiers Research Topics unify the most influential researchers, the latest key findings and historical advances in a hot research area.

Find out more on how to host your own Frontiers Research Topic or contribute to one as an author by contacting the Frontiers editorial office: frontiersin.org/about/contact

Maize stress ecophysiology and regulation

Topic editors

Jiwang Zhang — Shandong Agricultural University, China

Baizhao Ren — Shandong Agricultural University, China

Xuecai Zhang — International Maize and Wheat Improvement Center, Mexico

Citation

Zhang, J., Ren, B., Zhang, X., eds. (2023). *Maize stress ecophysiology and regulation*. Lausanne: Frontiers Media SA. doi: 10.3389/978-2-8325-3968-2

Table of contents

frontiers | Frontiers in Plant Science

TYPE Original Research
PUBLISHED 04 January 2023
DOI 10.3389/fpls.2022.1087652

OPEN ACCESS

EDITED BY
Baizhao Ren,
Shandong Agricultural University, China

REVIEWED BY
Bo Ming,
Institute of Crop Sciences (CAAS), China
Dongqing Yang,
Shandong Agricultural University, China

*CORRESPONDENCE
Yongjun Wang
yjwang2004@126.com
Lichun Wang
wlc1960@163.com

SPECIALTY SECTION
This article was submitted to Plant Abiotic Stress, a section of the journal Frontiers in Plant Science

RECEIVED 02 November 2022
ACCEPTED 05 December 2022
PUBLISHED 04 January 2023

CITATION
Yang J, Meng X, Yang S, Yang J, Li Z, Yang Q, Zheng P, Shao X, Wang Y and Wang L (2023) A simple method for lodging resistance evaluation of maize in the field.
Front. Plant Sci. 13:1087652.
doi: 10.3389/fpls.2022.1087652

A simple method for lodging resistance evaluation of maize in the field

Jinsheng Yang[1,2], Xiangzeng Meng[1], Shuangyuan Yang[3], Jinzhong Yang[4], Zhaoxia Li[4], Qinglong Yang[1], Peifeng Zheng[1], Xiwen Shao[1], Yongjun Wang[1,2]* and Lichun Wang[1,2]*

[1]Agronomy College, Jilin Agricultural University, Changchun, Jilin, China, [2]Jilin Academy of Agriculture Sciences/Key Laboratory of Crop Eco-Physiology and Farming System in the Northeastern, Institute of Agricultural Resources and Environment, Ministry of Agriculture and Rural Affairs, Changchun, Jilin, China, [3]Senior Department, No.1 Middle School Laizhou City Shandong Province, Yantai, Shandong, China, [4]Agronomy College, Qingdao Agricultural University, Qingdao, Shandong, China

The increase of planting density is a dominant approach for the higher yield of maize. However, the stalks of some varieties are prone to lodging under high density conditions. Much research has been done on the evaluation of maize lodging resistance. But there are few comprehensive reports on the determination of maize lodging resistance *in situ* without injury under field conditions. This study introduces a non-destructive *in situ* tester to determine the lodging resistance of the different maize varieties in the field. The force value can be obtained by pulling the stalk to different angles with this instrument, which is used to evaluate the lodging resistance of maize varieties. From 2018 to 2020, a total of 1,172 sample plants from 113 maize varieties were tested for the lodging resistance of plants. The statistical results show that the values of force on maize plants at 45° inclination angles (F_{45}) are appropriate to characterize maize lodging resistance *in situ* by nondestructive testing in the field. According to the F_{45} value, the maximum lodging resistance F_{max} can be inferred. The formula is: F_{max} =1.1354 F_{45} – 0.3358. The evaluation results of lodging resistance of different varieties of this study are basically consistent with the test results of three-point bending method, moving wind tunnel and other methods. Therefore, the F_{45} value is the optimal index for nondestructive evaluation of maize stalk-lodging resistance under the field-planting conditions.

KEYWORDS

maize, lodging resistance, tester, nondestructive evaluation, *in situ*, actual measured value, presumptive value

1 Introduction

Maize is the most widespread global food and feed crop. Reasonable densing planting can make full use of natural resources and is the most effective way to achieve high-yield and high-efficiency maize cultivation (Li et al., 2017). Increased maize planting density increases harvest ears and grain yield. However, when the planting density increases beyond a certain extent, lodging is prone to occur (Sun et al., 2021). Maize lodging is extremely harmful to production, not only affecting the stalk character of maize and greatly reducing yield and quality, but also bringing difficulties to field management and harvesting (Deng et al., 2017; Zhang et al., 2018; Sun and Wang, 2020). Therefore, the accurate evaluation of maize stalk lodging resistance has important practical significance for realizing high-yield and high-efficiency cultivation of maize.

Maize lodging generally occurs after the jointing stage, and can be caused by storms, cultivation measures, diseases, insect pests, etc., and especially by strong wind, which causes the maize plants to tilt or fall to the ground after rain (Kamara et al., 2003; Sun and Wang, 2020). The lodging of maize plants can occur in three ways: (1) the bending strength of the stalk is not sufficient to resist the external wind pressure and the stalk is broken (the phenomenon of "stem breaking"); (2) the rigidity of the stalk may be sufficient to resist the external wind force, but the root system has insufficient grip to resist the external wind pressure (the phenomenon of "root collapse"); or (3) the root system has a strong grip and can resist the external wind pressure, and the stalk has poor rigidity and is sufficiently tough that it does not break under the external wind pressure (Robertson et al., 2017), but the inclination exceeds 45° (the phenomenon of "stem lodging"). The lodging degree of maize plants can be divided into mild (tilting 0°–30°), moderate (tilting 30°–60°), and severe (above 85°). Different degrees of lodging have different effects on maize yield. Generally, light lodging reduces yield by 10%–20%, moderate lodging reduces yield by 30%–45%, heavy lodging reduces yield by more than 50%, and even more severe lodging can result in a 100% reduction in yield (Huang and Zhang., 2007; Cheng et al., 2011; Li, 2012). Much research has been done on the evaluation of maize lodging resistance. Laboratory methods of testing stem lodging resistance mainly include the crush test (Zuber and Grogan, 1961; Thompson, 1963), the peel penetration test (Peiffer et al., 2013; Li et al., 2014), and the bending test (Kokubo et al., 1989; Ennos et al., 1993; Li et al., 2003; Gou et al., 2008; Hu et al., 2013; Robertson et al., 2014). In addition, if a correlation between various chemical or morphological factors of plants (e.g., stem diameter, stem lignin content, and stem bark thickness) and the lodging resistance of stems is established, it could be used to predict the lodging resistance of plants. However, these methods usually require a great deal of labor and time, and cannot directly determine the lodging resistance *in situ* of plants in the field. Sibale et al. (1992) measured the puncture resistance of the rind using a modified electronic penetrometer to aid in the selection of plants with higher maize stalk strength. Zhang et al. (2018) evaluated the crushing strength of stems by measuring the force required to break the stems using a hydraulic press. Wen et al. (2019) used a mobile wind turbine to conduct an *in situ* assessment of the stalk lodging resistance of different maize varieties; this research has shown that a new cumulative lodging index (CLI) is more reliable than mechanical properties, failure wind speed (FWS), and wind speed reduction index (RI) when evaluating lodging resistance in terms of reliability and resolution. Cook et al. (2019) invented a maize lodging resistance tester called Darling that breaks the maize stalk by giving it a thrust at a fixed height to obtain the maximum lodging resistance and bending moment, which can evaluate the lodging resistance of maize stalks in the field. Darling is a device capable of inducing a natural destruction and, as such, the device was destructive in assessing maize lodging resistance. Although methods of measuring maize stem strength are becoming convenient and efficient, they are all performed under controlled conditions and can cause some damage to the plant. There are few comprehensive reports on the determination of maize lodging resistance *in situ* without damage under field conditions. When testing the lodging resistance of maize plants from jointing stage to mature stages, it is best to use a non-destructive method and the same population (sample); this can not only objectively evaluate the differences of lodging resistance among different genotypes, but effectively reduce the workload and error caused by different populations (samples). Maize researchers urgently need a technology for the evaluation of maize lodging resistance that can achieve non-destructive *in situ* determination in the field.

Therefore, a simple lodging resistance evaluation method was developed *in situ* for maize plants in the field, which showed simple, fast, efficient and accurate determination of maize lodging resistance. The instrument used the lever principle to pull the maize plants to different angles and measure the real-time pulling force at different angles, which performed the synchronous acquisition of the three parameters of angle, force and displacement (i.e., distance between the main machine and the rotating shaft of the tester). The testing instrument is used to determine the maize lodging resistance using non-destructive measurement *in situ*. The goals of the current study were (1) to establish a simple method for evaluating lodging resistance in the field and (2) to quantify the plant lodging resistance of different maize varieties.

2 Lodging resistance tester and testing method

2.1 Field experiment design

2.1.1 Experimental design

Field experiments were conducted at the location in Test Site 16, Shandong Denghai Seed Industry Co., Ltd. (E: 119°56.6′, N:

37°20.7′), and Hanting District, Weifang City (E: 119°4.8′, N: 36° 53.3′), in Shandong Province, and arranged in 3 years with 113 varieties. The lodging resistance of plants at different planting densities was determined during the flowering period, at the milk ripening stage, and at maturity. The design was shown in Table 1. Three replicates were designed for each variety in a location.

2.1.2 Meteorological factors

The meteorological factors for 2018–2020 were given in Figure 1.

2.1.3 Agronomy strategy managements

In this study, fertilization was applied according to the yield standard of 11.25 mg ha^{-1}, the total fertilization ratio of N:P:K was 3:1:2, and top dressing was applied four times: at the bottom fertilizer stage, at the jointing stage, at the large trumpet stage, and at the male pumping stage. The bottom fertilizer had a N:P:K ratio of 6:6:6, and the remaining phosphate fertilizer and potassium fertilizer were applied once at the jointing stage. Nitrogen fertilizer was applied such that 40% of the total N required was provided at the jointing stage and 50% of the total N required was provided at the large trumpet stage; the remaining nitrogen fertilizer was applied once at the male pumping stage.

2.2 Test method

2.2.1 Placement of lodging resistance tester

A sample of maize plants in the field were selected for testing. Plants with similar plant height, ear height and stalk thickness were selected within the population to eliminate the marginal effect on the experiment. The lodging resistance tester was placed in parallel wit the target maize plant and at a fixed distance away from the tester. The pedal was pressed to insert the fork head into the soil for fixation and the fixing nut of the main machine loosened to slide it along the vertical rod to the ear height. The fixing nut again was then tightened again and the stalk of the maize clamped to test (Figures 2A, B).

2.2.2 Determination of lodging resistance

2.2.2.1 Maximum lodging resistance determination

The test key was pressed to start the test procedure, the upper part of the tester was manually pulled evenly, and the vertical rod slowly turned, until the plant snapped or pulled to 90°. During the test, the main machine automatically recorded the angle, tension, and displacement. The maximum tension reflected the maximum lodging resistance of the plant.

2.2.2.2 Measurement of lodging resistance non-destructive

The test button was pressed to start the test, the upper part of the tester was pulled by hand, trn the vertical rod was turned at a constant speed to pull the plant until it was tilted at a 45° angle, then the main machine was loosened, and the plant returned to its normal growth state. During the test, the main machine automatically recorded the angle, tension, and displacement (Figure 2C) for the determination of lodging resistance.

2.2.2.3 Calculation of expected values

F_{max} and F_{45} were fitted, $y = ax + b$ (a and b are constants, x was the bending force of the stalk when the stalk was bent 45° (F_{45}), and the expected value (y) is calculated by the fitted equation.

2.3 Field non-destructive *in situ* maize lodging resistance tester

2.3.1 Design principle

In the absence of external wind, the maize plant was supported only by gravity mg and ground support T, and the two forces reach balance (Figure 3A).

Assuming that the wind was horizontal, the wind pressure was P, and the windward area of the maize was S. If point A was the concentrated stress point on the windward side of the maize, the wind force received by the maize plants at point A was PS. When subjected to wind, the plant's swaying motion can be resolved as a series of motions on the vertical plane with the root system as the origin. Under the combined action of wind PS and gravity, mg, the plant would be inclined and bent, and the resistance moment Mo was produced by the anchoring of the root system. If maize plants are divided into two independent parts, stalk and ear, the mass of the stalk was m_1 and the mass of ear was m_2. Maize plants reached a force equilibrium state under the action of wind, gravity, and self-resistance (Figure 3B). At this time, the torque produced by wind and gravity was equal to the bending torque produced by maize plants. The equilibrium equation of its force (Liu, 2017) was as follows:

$$\begin{cases} PS - F_{ox} = 0 & (1) \\ m_1 g + m_2 g - F_{oy} = 0 & (2) \\ M_O = PS \cdot L_1 + m_1 g \cdot L_2 + m_2 g \cdot L_3 & (3) \end{cases}$$

In the absence of wind, we use the instrument to pull the maize plant to tilt and bent it (Figure 3C). The balance equation of its force (Liu, 2017) is as follows:

TABLE 1 Test varieties in three years.

Years	Locations	Varieties	Test periods	Planting density (plants ha^{-1})	Notes
2018	Test Site 16, Shandong Denghai Seed Industry Co., Ltd., Laizhou, Shandong Province	Denghai661 (DH661)a, Denghai 605(DH605)b, Denghai618(DH618)a, Denghai3622(DH3622)c, Xianyu335 (XY335)b, Zhengdan958(ZD958)c	Tasseling stage, milk stage and physiological maturity stage.	4.5, 6.0, 7.5, 9.0, 10.5	The comparisons of lodging resistance at different developmental stages (a: low-ear varieties; b: mid-ear varieties; c: high-ear varieties)
2020	Test Site 16, Shandong Denghai Seed Industry Co., Ltd., Laizhou City, Shandong Province	Denghai605(DH605)b, Denghai618(DH618)a, Xianyu335(XY335)b, Zhengdan958 (ZD958)c, Xundan18(XD18)c, Xundan20(XD20)c	Tasseling stage, milk stage and physiological maturity stage.	4.5, 6.0, 7.5, 9.0	The comparisons of lodging resistance at different developmental stages test
2019	Test Site 16, Shandong Denghai Seed Industry Co., Ltd., Laizhou City, Shandong Province	45S01, 45S02, 45S03, 45S04, 45S05, 45S06, 45S07, 45S08, 45S09, 45S10, 45S11, 45S12, 45S13, 45S14, 45S15, 45S16, 45S17, 45S18, 45SCK1, 45SCK2, 45SCK3, Zhengdan958, IY3541, MC588, MC876, NK809, WH1288, ZY303, Chengyu826, Chuangyu188, Dahua1870, Deke501, Denghai125, Guanyu162, Heyu337, Hongsuo899, Huayu688, Jiyu338, Jiyu39, Jidan958, Jinlai318, Jingke9297, Jinnongke445, Jinnongke738, Jiuheyu1, Liyuan296, Luxing617, Mingyu815, Qinliang505, Ruiyou288, Shandan650, Shandan660, Shiyu1502, Tianci1898, Weiyu191, Wugu654, Xianyu1867, Xianyu1871, Xiandai567, Xiandai978, Xundan528, Xianyunuo046, Xianyunuo335, Xiangnong16, Yefeng168, Yongyou988, Yudan188, Yuhong987, Zhaoyu610, Kongfeng191, Zhongbo919, Zhongdan182, Zhongjinyu303.	Physiological maturity stage.	6.75	Regional experimental varieties of maize in Shandong Province
2019	Test Site 16, Shandong Denghai Seed Industry Co., Ltd., Laizhou City, Shandong Province	50S01, 50S02, 50S03, 50S04, 50S05, 50S06, 50S07, 50S08, 50S09, 50S10, 50S12, 50S13, 50S14, 50S15, 50S16, 50S17, 50SCK, 50SCK2, 50CK3, Z50S01, Z50S02, Z50S03, Z50S04, Z50S05, Z50SCK1.	Physiological maturity stage.	7.5	Regional experimental varieties of maize in Shandong Province
2020	Hanting District, Weifang City, Shandong Province	JNK728, DK517, SD650, FK159, FK139, XY047, LP638.	Physiological maturity stage.	7.5	Variety screening test

$$\begin{cases} F_\theta \cdot cos\theta - F_{ox} = 0 & (4) \\ F_\theta \cdot sin\theta + m_1 g + m_2 g - F_{oy} = 0 & (5) \\ M_O{}' = F_\theta \cdot L + m_1 g \cdot L_2 + m_2 g \cdot L_3 & (6) \end{cases}$$

The moment *Mo* of the maize plant resisting the resultant force of wind and gravity was equal to the moment *Mo′* of the maize plant resisting the pulling force, when we used the instrument to pull the maize plant to tilt to the same degree as when exposed to the wind. Therefore, in the horizontal direction, the moment $PS{\cdot}L_1$ of wind was equal to the moment $F_\theta{\cdot}L$ of instrument tension in the horizontal direction of the stem and, in the vertical direction, the moment of gravity "$m_1g{\cdot}L_2 + m_2g{\cdot}L_3$" was constant.

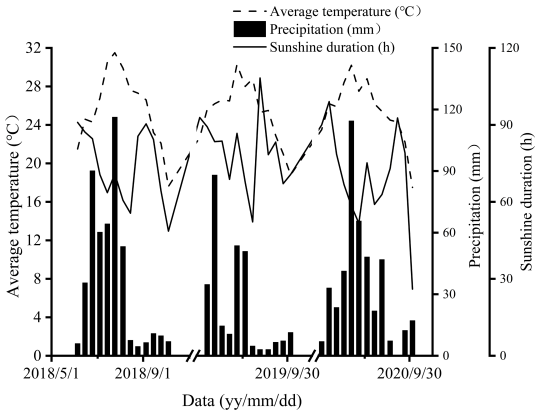

FIGURE 1
The meteorological factors for 2018–2020.

For the same variety, the center of gravity of the stalk part was the same, and the weight moment $m_1g{\cdot}L_2$ of the stem was constant. However, the difference in L_3 was caused by the difference in the height of the ear position. The higher the ear position, the greater the moment $m_2g{\cdot}L_3$ of the ear weight. Because $F_\theta{\cdot}L$ was equivalent to $PS{\cdot}L_1$, the windward area S is roughly the same, and L_3 was positively correlated with L, so P was positively correlated with F_θ.

The maximum bending moment was fixed as the same variety. When the critical bending moment M_{max} was reached, according to formula (3), the height of ear leads to an increase in $m_2g{\cdot}L_3$, the corresponding wind power PS decreases, and the wind resistance of the maize decreases.

Different varieties had different ear height and their tensile force varies. This change was reflected in the fact that when Mo' was the same, the larger L_3 was, the smaller F_θ was at the same angle. Because the height of the maize ear was the main influencing factor, the F_θ produced by the instrument pulling at the ear position could be used to evaluate the wind resistance of maize.

When the wind was low, the maize plants swing back and forth with the root system as the origin. With the increase in wind force, the resultant moment of wind force PS and gravity will also increase. At this time, if the anchoring force of root system was weak, root fall would occur. If the anchoring force of the root system was strong but the quality of the stem was poor, plastic deformation would occur, which will cause the stem to break. Mo' at the inclination angle of the plant was the maximum lodging resistance moment of the plant when the root falls or the stem breaks, and F_θ was the critical lodging resistance force.

The stalk material of the same maize plant was the same, the center of gravity and ear position are the same in the same

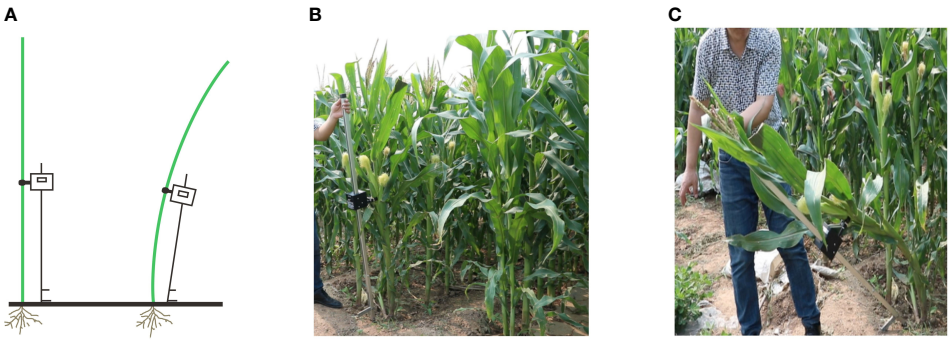

FIGURE 2
Test process of lodging resistance tester. **(A)** Schematic diagram of instrument placement during a test process. **(B)** Place the instrument parallel to the plant at the beginning of the test. **(C)** Pull the instrument vertical rod by hand for testing.

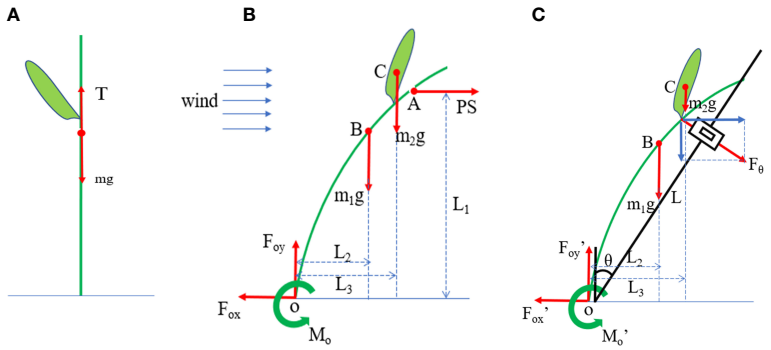

FIGURE 3
Analysis of maize plant force. **(A)** Stress analysis of maize plants under windless conditions. *T*, ground support force; *mg*, gravity of maize plant. **(B)** Stress analysis of maize plants under the influence of external wind. **(A)**, the concentrated stress point on the windward side of a maize plant; B, the center of gravity of stalk part of maize plant; **(C)**, the center of gravity of ear part of maize plant. *PS*, wind force exerted on maize plant; m_1g, gravity of stalk part of maize plant; m_2g, gravity of ear part of maize plant; F_{ox}, horizontal force on maize root; F_{oy}, vertical force on maize root; L_1, arm of force of *PS*; L_2, arm of force of m_1g; *L*, arm of force of m_2g; *O*, stem base; M_o, resistance moment of maize plant. **(C)** Pulling force given to the maize plant by the apparatus during the resistance to overturning test. θ, inclination angle of vertical shaft of instrument, F_θ, tension at inclination angle θ; L, the arm of F_θ, $F_{ox'}$, horizontal force on maize root, $F_{oy'}$, vertical force on maize root; $M_{o'}$, resistance moment of maize plant.

growth period, and the arm of force *L* is the same. As long as F_θ was measured, the lodging resistance of the maize stalk can be evaluated. If F_θ was measured before lodging or folding, the evaluation can be realized without damaging maize plants (Figure 3C).

2.3.2 Non-destructive maize lodging resistance tester

Based on the above idea, Shuangyuan Yang invented the field non-destructive *in situ* lodging resistance tester (NDT) for maize plants, which was commercially produced by Laizhou Kaitian Instrument Co., Ltd. The instrument model was KTDF-1 (Figure 4). At present, three patents had been granted, namely, a Chinese invention patent (patent no. ZL201510176119.9), a Chinese utility model patent (patent no. ZL201720355104.3), and a German utility model patent (patent no. 202017106298).

The field non-destructive *in situ* lodging resistance tester for maize (Figure 4A) could be used to determine the force and dynamic displacement at different angles, until the maximum bending force that leads to the breaking of maize stalk is found. The tester could be automatically adjusted for displacement measurement. The displacement is produced by the force vector of the plant at different angles. By using the tester, the dynamic determination of pull forces and the changes of angles could be achieved. The main engine of the instrument is controlled by a microcontroller (Figure 4B) and operated through the user interface (Figure 4C). The force and stalk position obtained at different angles during the test could replace F_θ (the wind force *PS*). According to Equations (4) and (5), the lodging resistance of maize plants under the force of wind could be evaluated. Data from the test can be imported into a computer for analysis (Figure 4D).

2.4 Statistical analysis and processing

IBM SPSS Statistics 26 (IBM Corporation, Armonk, NY, USA) was used for data statistics and analysis. Maize varieties were clustered according to the squared Euclidean distance method. Origin 2021 (Origin Lab, Northampton, MA, USA) was used for data processing and plotting. Comparisons among groups were tested by one-way analysis of variance and the least significant difference test, and differences between the means were considered significant at $p<0.05$.

3 Results

3.1 Evaluation for the criteria of maize lodging resistance by F_{max} values

From 2018 to 2020, 1,172 maize plants were tested in Laizhou and Weifang Region, Shandong Province, at the flowering, milk ripening, and maturity period. As the plant tilted angle increases, the pull trajectory of the plant determined by a tester complies with the equation $y = -0.0028x^2 + 0.3989x + 2.4187$ ($R^2 = 0.9991$, $n = 1172$), where x represents the tilted angle, and y represents the pull value at the angle (Figure 5A).

The F_{max} values of the above maize plants were clustered by Euclidean distance and divided into four categories (Figure 5B)

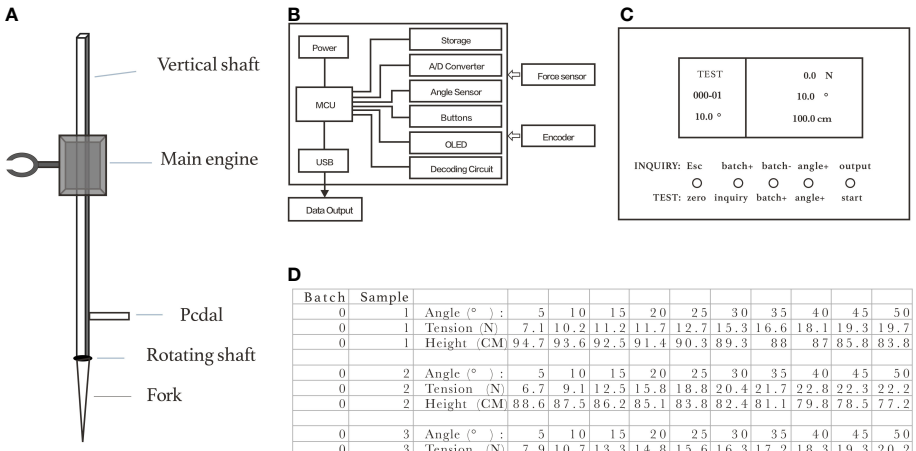

D

Batch	Sample											
0	1	Angle (°) :	5	10	15	20	25	30	35	40	45	50
0	1	Tension (N)	7.1	10.2	11.2	11.7	12.7	15.3	16.6	18.1	19.3	19.7
0	1	Height (CM)	94.7	93.6	92.5	91.4	90.3	89.3	88	87	85.8	83.8
0	2	Angle (°) :	5	10	15	20	25	30	35	40	45	50
0	2	Tension (N)	6.7	9.1	12.5	15.8	18.8	20.4	21.7	22.8	22.3	22.2
0	2	Height (CM)	88.6	87.5	86.2	85.1	83.8	82.4	81.1	79.8	78.5	77.2
0	3	Angle (°) :	5	10	15	20	25	30	35	40	45	50
0	3	Tension (N)	7.9	10.7	13.3	14.8	15.6	16.3	17.2	18.3	19.3	20.2
0	3	Height (CN)	91.3	90.3	89	87.8	86.5	85.2	83.9	82.5	81.1	79.7

FIGURE 4
The physical appearance, major components and export data format of lodging resistance tester *in situ* for maize. **(A)** Tester structure: it consists of the main engine, vertical shaft, rotating shaft, pedal and fork head. The vertical shaft is connected to the fork head through the rotating shaft, and the pedal is located at the lower part of the vertical shaft. The test host can slide up and down along the vertical bar. **(B)** Electronic system: the main engine integrates the angle, tension, and height sensors, which is controlled by microcontroller. The angle sensor uses a single-axial gyroscope, output to MCU through I2C port, with accuracy of 0.1°; the tensile sensor adopts an S-type tension integrated weighing sensor, output voltage signal into digital signal to MCU through AD conversion, with accuracy of 0.1 N; the height sensor adopts a displacement encoder, transmitted to MCU, measuring reference to the bottom end of vertical rod rotating shaft, with accuracy of 0.1 cm. Other types of sensors can also be connected to this device. The power supply device comes from the charging lithium battery, which can power the device for more than six hours. **(C)** User interface: consists of a 3.5-inch LCD screen and five selection buttons at the bottom of the device. These five buttons integrate the two functions of preparation mode and query mode. The user interface is written in the C programming language. **(D)** Export data format: each set of data has three group values: angle, force, and displacement (distance between vertical line and the rod of the tester). After the test ends, import the data into the U disk in a XLS file format.

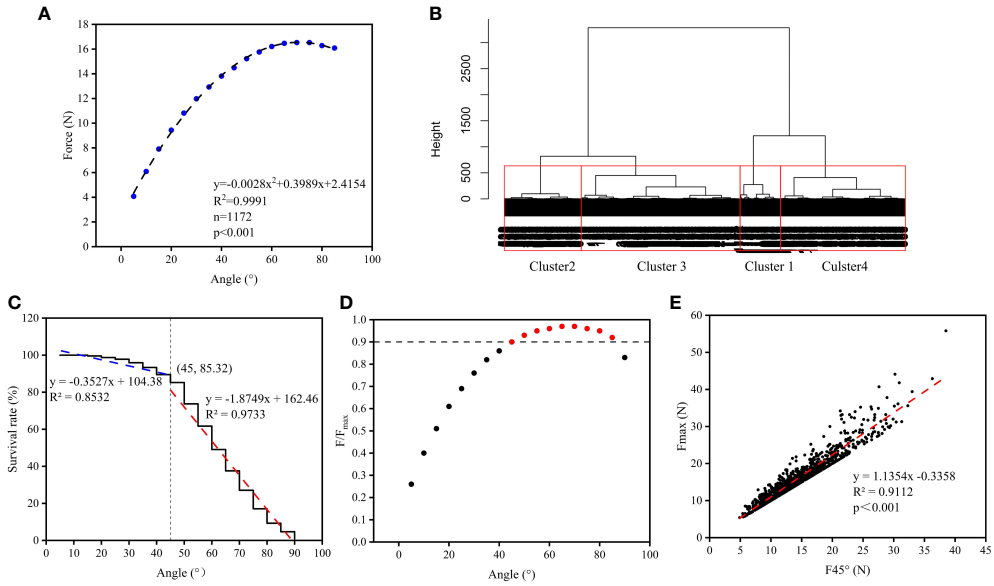

FIGURE 5
The data analysis of lodging resistance from maize plants at different locations in three years. **(A)** Stress values of maize plants at different angles. **(B)** Clustered lodging level of maize plants according to the tested F_{max}. **(C)** The survival rate of maize plants under different tilted angles. **(D)** The ratio of F to F_{max} under different tilted angles. **(E)** Correlation between F_{45} and F_{max}.

with a mean of 9.25 N, 14.53 N, 20.61 N, and 31.33 N, which consisted of 32.25%, 37.88%, 22.70%, and 7.17% in the total number of varieties. Accordingly, the lodging resistance levels of maize was divided into four levels: poor lodging resistance (cluster 3, F_{max} ≤11.8 N), low lodging resistance (cluster 2, F_{max} > 11.8 N but ≤17.5 N), medium lodging resistance (cluster 1, F_{max} >17.5 N but ≤25.8 N), and high lodging resistance (cluster 4, F_{max} >25.8 N) (Table 2).

3.2 A correlation between F_{45} and F_{max}

As shown in Figure 5E, F_{45} and F_{max} are strongly correlated, and F_{max} predicted by F_{45} can be used to assess the lodging resistance of maize plants according to the correlation. Simulation results agree well with measurements.

As the tilt angle of the maize plant increased, the breaking ratio of the plants gradually increased. When the tilt angle was below 45°, the breaking ratio was relatively low. When tilt angle was between 5° and 40° the cumulative proportion of breaking plants was 10.41%; at 45° the proportion was 4.27%, and at 50° the proportion was 11.60%, indicating that a plant tilt angle of 45° was the critical point for a significant decrease in the survival rate of plants. The proportion of plants breaking increases slowly as tilt angle increases up to<45°, and the survival rate of plants has a curve slope of –0.3527; when the tilt angle goes beyond 45°, the survival rate of plants decreases quickly, accompanied by a curve slope of –1.8749 (Figure 5C).

In the process of the test, as the tilted angle θ of the plant increases, the pull force of the F value (expressed as F_θ) increases until the plant breaks or does not break at a 90° angle. Subsequently,the maximum F value (expressed as F_{max}) can be determined. As the results, the larger the tilt angle, the closer to F_{max} is F_θ. A map was made by using F_θ/F_{max} values and tilted angles (Figure 5D). It wis interesting that, at tilt angles in the 15–55° range, th F_θ/F_{max} increases proportionally, and F_θ/F_{max} is about 0.9 at a 45° tilt angle (Figure 5D), which could characterize the lodge resistance of maize plants.

Out of 1,172 tested maize plants, 1,000 tilted by 45° without the stalk breaking and were selected to determine F_{45} values and F_{max}, and comparing F_{45} with its corresponding F_{max} developed the equation $y = 1.1354x - 0.3358$ ($R^2 = 0.9112$), indicating that a strong correlation exists between F_{45} and F_{max} (Figure 5E). By measuring F_{45} and applying the formula, expected values for maximum stalk resistance can be obtained. The maize plants under a 45° tilt angle maintained a 85.32% survival rate in a large complex population; therefore, F_{45} can be used to evaluate the lodging resistance of maize plants with a simple method.

3.3 Evaluation of lodging resistance for the different varieties of maize

The F_{max} was predicted by F_{45} and the lodging resistance of plants were evaluated under non-damaged conditions. Comparing the measured and expected values in pairs, the results are shown in Table 3. In the low-resistance group the accuracy reached 97.28%; in the high-resistance group the accuracy was 88.57%, which was the lowest accuracy (Table 3). It was concluded that the two tests produced similar results for the lodging resistance of plants.

The traits of plants from different varieties, planting density, and development period were principal factors for the lodging resistance of maize plants. The planting density usually is negatively associated with F_{max}, that is, higher planting density usually led to a lower F_{max}. Under low-density conditions, the differences of varieties are significant, that is, the data of lodging resistance from a population consisting of different varieties show great heterogeneity, while at high density, the differences

TABLE 2 The F_{max} clustering by the Euclidean distance method.

	F_{mean}	F_{min}	F_{max}	Samples in each cluster
cluster 1	31.33	26	55.8	84
cluster 2	20.61	17.6	25.8	266
cluster 3	14.53	11.9	17.5	444
cluster 4	9.25	3.4	11.8	378

TABLE 3 Comparing of the lodging resistance levels of plants by measured and inferred values.

Levels of lodging resistance	Lodge-prone	Low resistance	Moderate resistance	High resistance	Total
Individual distribution from expected values	258	415	249	78	1000
Individual distribution from measured values	248	404	278	70	1000
Accuracy (%)	96.0	97.28	89.57	88.57	

FIGURE 6
Measurement of lodging resistance of six varieties in different densities of maize plants. I: inferior lodging resistance, II: medium lodging resistance, III: high lodging resistance range, IV: strong lodging resistance. VT, flowering period; R3, grain filling period; R6, maturation period; AV, actual measured value F_{max} value; PV, presumptive value. The missing value of the force indicates that the angle at which the plant breaks is less than 45°.

between varieties become smaller. Maize plants at different developmental stages or in different reproductive periods show obvious differences in lodging resistance. From Figure 6, it is obvious that the F_{max} estimation and F_{max} measurement produced consistent results.

The eight varieties of maize were rated according to their lodging resistance in different planting densities in 2018 and 2020. Based on F_{max}, DH661, DH618, and DH605 were high lodging-resistant varieties, with inferior lodging resistance detected in only 2.6%, 10.7% and 11.5% of total plants in two years. DH3622, ZD958, XY335, XD20, and XD18 had poor lodging resistance, with 22.7%, 37.1%, 36.1%, 40.0%, and 63.0% of plants having inferior lodging resistance (Figures 7A, C). The same conclusion was obtained by using the F45 measurement method (Figures 7B, D).

4 Discussion

4.1 Advantages of non-destructive testing in the field

In 2019, Cook published a paper in which a lodging resistance tester, Darling, was developed. Darling was the first instrument for the lodging resistance measurement of crops in the field. The Darling tester produces a thrust at a fixed height to assess the lodging resistance of maize and sorghum, but actually evaluates the strength and toughness of the plant stalk. The Darling uses a destructive test for maximum lodging resistance.

The purpose of our test is to assess the lodging resistance of plants in a non-destructive way, which is important for the selection of commercial cultivars and cultivation of crops. For the lack of appropriate tools and test methods, the maximum lodging resistance of plants was determined and used to evaluate the maize lodging resistance, which is based on the stalk-breaking of plants and tensile strength from different angles, and inevitably causes the breaking of plants, resulting in maize plants that could not grow normally after the test. In order to evaluate maize lodging resistance in maize without injuring the plant, the maize stalk breaking rate and tensile value at different angles were determined. F_{45} gave an index of maize lodging resistance with a very low breaking rate, and from the correspondence between F_{max} and F_{45} (Figure 5E), the lodging resistance of plant was determined with F_{45}. It is concluded that F_{45} can represent maize lodging resistance, which can be obtained by an NDT method in the fields. In this study, the F_{45} values were determined by a lodging

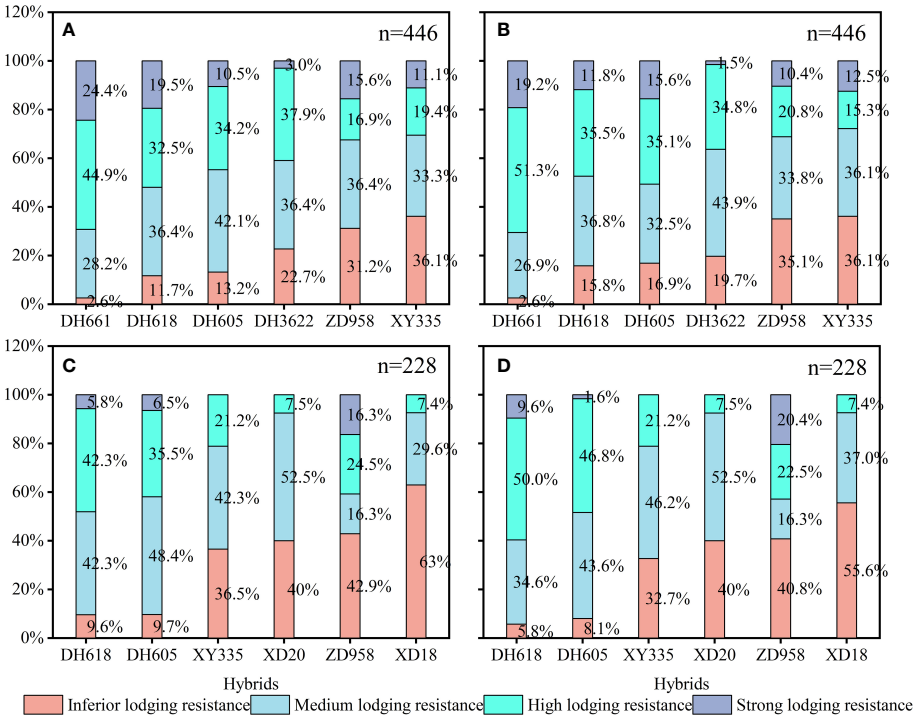

FIGURE 7
(A) In 2018, the actual measured value (AV) of all plants was rated for lodging resistance and the proportion of different grades of plants was determined. **(B)** In 2018, all plants were rated for lodging resistance based on presumptive value (PV) and the proportion of different grades of plants was determined. **(C)** In 2020, the AV of all plants was rated for lodging resistance and the proportion of different grades of plants was determined. **(D)** In 2018, all plants were rated for lodging resistance based on EV and the proportion of different grades of plants was determined.

resistance tester in the field and the lodging resistance of plants was calculated to predict the maximum lodging resistance, which achieved the *in situ* non-destructive testing of lodging resistance in maize.

4.2 Accuracy of non-destructive evaluation of maize lodging resistance in the field

This field non-destructive testing method can evaluate lodging resistance under different conditions. In 2018 and 2020, six varieties were selected to experiment on different densities, and the results show (1) among the varieties there existed significant differences in lodging resistance (DH661 > DH618 > DH605 > DH3622 > ZD958 > XY 335 > XD 20 > XD18); (2) the lodging resistances of plants from one variety were determined by differences in planting density, and higher planting density led to lower lodging resistance in all varieties; and (3) when the plants of one variety were tested for lodging resistance in different developmental periods, conclusions were usually consistent.

4.3 Reliability of the non-destructive *in situ* lodging resistance tester method in the field

At present the determination of maize lodging resistance usually uses the three-point bending method or the moving wind tunnel method. There are multiple instruments for the three-point bending method evaluation; the most popular tester is the YYD-1 lodging resistance tester produced by Zhejiang Topu Yunnong Technology Co., Ltd. With this instrument, DH661 (Ren et al., 2016) and DH618 showed strong lodging resistance (Ren et al., 2016; Gu et al., 2017; Yang et al., 2022), and XY335, ZD958, and XD20 showed weaker lodging resistance (Gu et al., 2017; Xue et al., 2020; Yang et al., 2022). By using digital detector FGJ-5, the stem breaking resistance of different varieties of maize was rated as XY335 > ZD958 > XD20, and the bending resistance of plant was ZD958 > XD20 (Cheng, 2010). By using a mobile wind tunnel to detect lodging resistance, Wen rated the wind resistance performance of different varieties as XY335 > ZD958 > XD20 (Wen et al., 2019). The results from non-destructive testing used in this study were nearly identical.

5 Conclusion

This non-destructive *in situ* method can test the lodging resistance of a maize stem by determining the angle values of bending plant in constant pull force, or reading the values of pull force on a plant that is inclined 45°°, based on the force strength on the plants in the field, composed of gravity and wind force. Non-destructive determination for maize lodging resistance in the field by using the lodging resistance tester can be successfully performed. The accuracy of the method was examined with different plants of 113 varieties for 3 years under different planting densities and developmental periods. F_{45} on maize plants at a 45° inclination was suitable to characterize maize lodging resistance in the field, and was the best index for the evaluation of maize lodging resistance in this study. According to the F_{45} value, the maximum lodging resistance F_{max} can be inferred, and the formula is $F_{max} = 1.1354F_{45} - 0.3358$.

Data availability statement

The original contributions presented in the study are included in the article/supplementary material. Further inquiries can be directed to the corresponding authors.

Author contributions

All authors have contributed significantly to the research. JSY: investigation, writing – original; XM, ZL, QY, and PZ: data curation, data analysis, visualization; SY: the inventor of the maize inversion resistance tester; JZY: the experimentalist in Weifang, sampling; XS: supervision; YW and LW: conceptualization, funding acquisition. All authors contributed to the article and approved the submitted version.

Conflict of interest

The authors declare that the research was conducted in the absence of any commercial or financial relationships that could be construed as a potential conflict of interest.

Publisher's note

All claims expressed in this article are solely those of the authors and do not necessarily represent those of their affiliated organizations, or those of the publisher, the editors and the reviewers. Any product that may be evaluated in this article, or claim that may be made by its manufacturer, is not guaranteed or endorsed by the publisher.

Supplementary material

The Supplementary Material for this article can be found online at: https://www.frontiersin.org/articles/10.3389/fpls.2022.1087652/full#supplementary-material

References

Cheng, F. L. (2010). *Effect of plant density, potash fertilizer on lodging resistance ability of summer maize* (Baoding, Hebei: Hebei Agriculture University).

Cheng, F. L., Du, X., Liu, M. X., Ji, X. L., and Cui, Y. H. (2011). Maize lodging and its influence on yield. *Maize Sci.* 19, 105–108.

Cook, D. D., Chapelle, W. D. L., and Lin, T. C. (2019). Darling: a device for assessing resistance to lodging in grain crops. *Plant Methods* 15, 102–110.

Deng, Y., Wang, C. Y., Guo, H. X., Zhang, L. G., Zhao, Li., Wang, L. J., et al. (2017). Effects of population density on agronomic characters, mechanical properties and yield of maize stem. *Crop Magazine* 4, 89–95.

Ennos, A. R., Crook, M. J., and Grimshaw, C. (1993). The anchorage mechanics of maize (*Zea mays* l). *J. Exp. Bot.* 44, 47–153. doi: 10.1093/jxb/44.1.147

Gou, L., Zhao, M., Huang, J. J., Zhang, B., Li, T., and Sun, R. (2008). Bending mechanical properties of stalk and lodging resistance of maize. *Acta Agronomica Sinica* 34, 653–661.

Guo, Q. Q., Chen, R. P., Sun, X. Q., Jiang, M., Sun, H. F., Wang, S., et al. (2018). A non-destructive and direction-insensitive method using a strain sensor and two single axis angle sensors for evaluating corn stalk lodging resistance. *Sensors* 18, 1852–1863. doi: 10.3390/s18061852

Gu, L. M., Qiao, J. F., Zhang, M. W., Zhu, W. H., Huang, L., Dai, S. T., et al. (2017). Effect of planting density on stalk characteristics and lodging-resistant capacity of different density-resistant summer maize varieties. *J. Maize Sci.* 25, 91–97.

Huang, J. P., and Zhang, J. F. (2007). Influence of summer maize lodging on yield and control measures. *Henan Agric.* 13, 21.

Hu, H. X., Liu, W. X., Fu, Z. Y., Homann, L., Technow, F., Wang, H. W., et al. (2013). QTL mapping of stalk bending strength in a recombinant inbred line maize population. *Theor. Appl. Genet.* 126, 2257–2266. doi: 10.1007/s00122-013-2132-7

Kamara, A. Y., Kling, J. G., Menkir, A., and Ibikunle, O. (2003). Association of vertical root-pulling resistance with root lodging and grain yield in selected S1 maize lines derived from a tropical low-nitrogen population. *J. Agron. Crop Sci.* 189, 129–135. doi: 10.1046/j.1439-037X.2003.00023.x

Kokubo, A., Kuraishi, S., and Sakurai, N. (1989). Culm strength of barley: correlation among maximum bending stress, cell wall dimensions, and cellulose content. *Plant Physiol.* 91, 876–882. doi: 10.1104/pp.91.3.876

Li, J. P. (2012). Influence of corn lodging on yield and preventive measures. *Modern Rural Sci. Technol.* 15, 14–15.

Li, Y., Qian, Q., Zhou, Y., Yan, M., Sun, L., Zhang, M., et al. (2003). BRITTLE CULM1, which encodes a COBRA-like protein, affects the mechanical properties of rice plants. *Plant Cell* 15, 2020–2031. doi: 10.1105/tpc.011775

Liu, H. W. (2017). *Mechanics of materials I. 3th Edition* (Beijing: Higher Education Press), 353–355.

Li, K., Yan, J., Li, J., and Yang, X. (2014). Genetic architecture of rind penetrometer resistance in two maize recombinant inbred line populations. *BMC Plant Biol* 14, 152-162. doi: 10.1186/1471-2229-14-152

Li, S. K., Zhao, J. R., Dong, S. T., and Zhao, M. (2017). Research progress and prospect of maize cultivation in China. *Chin. Agric. Sci.* 50, 1941–1959.

Peiffer, J. A., Flint-Garcia, S. A., DeLeon, N., McMullen, M. D., Kaeppler, S. M., and Buckler, E. S. (2013). The genetic architecture of maize stalk strength. *PloS One* 8, e67066.

Ren, B. Z., Li, L. L., Dong, S. T., and Liu, P. (2016). Effects of plant density on stem traits and lodging resistance of summer maize hybrids with different plant heights. *Acta Agronomica Sin.* 42, 1864–1872.

Robertson, D. J., Julias, M., Lee, S. Y., and Cook, D. D. (2017). Maize stalk lodging: morphological determinants of stalk strength. *Crop Sci.* 57, 926–934. doi: 10.2135/cropsci2016.07.0569

Robertson, D. J., Smith, S., Gardunia, B., and Cook, D. (2014). An improved method for accurate phenotyping of corn stalk strength. *Crop Sci.* 54, 2038–2044.

Sibale, E. M., Darrah, L. L., and Zuber, M. S. (1992). Comparison of two rind penetrometers for measurement of stalk strength in maize. *Maydica* 37, 111–114.

Sun, N., Bian, S. F., Meng, X. M., Zhao, H. X., Zhang, L. H., Tan, G. B., et al. (2021). Effects of chemical regulation on maize lodging resistance under high density conditions. *Mol. Plant Breed.* 19, 1–7.

Sun, W. C., and Wang, Y. Q. (2020). Causes and countermeasures of maize lodging. *Modern Agric.* 12, 26–27.

Thompson, D. L. (1963). Stalk strength of corn as measured by crushing strength and rind thickness. *Crop Sci* 3, 323–329. doi: 10.2135/cropsci1963.0011183X000300040013x

Wen, W. L., Gu, S. H., Xiao, B. X., Wang, C. Y., Wang, J. L., Ma, L. M., et al. (2019). *In situ* evaluation of stalk lodging resistance for different maize (*Zea mays* l) cultivars using a mobile wind machine. *Plant Methods* 15, 96–112. doi: 10.1186/s13007-019-0481-1

Xue, J., Gao, S., Fan, Y. H., Li, L. L., Ming, B., Wang, K. R., et al. (2020). Traits of plant morphology, stalk mechanical strength, and biomass accumulation in the selection of lodging-resistant maize cultivars. *Eur. J. Agron.* 117, 126073. doi: 10.1016/j.eja.2020.126073

Yang, J. S., Geng, W. J., Zhang, J. W., Ren, B. Z., and Wang, L. C. (2022). Responses of the lodging resistance of summer maize with different gene types to plant density. *Agronomy* 12, 10–25. doi: 10.3390/agronomy12010010

Zhang, L. L., Sun, S. J., Chen, Z. J., Jiang, H., Zhang, X. D., and Chi, D. C. (2018). Effects of different color plastic film and planting density on dry matter accumulation and yield of spring maize. *J. Appl. Ecol.* 29, 113–124. doi: 10.13287/j.1001-9332.201801.019

Zuber, M. S., and Grogan, C. O. (1961). A new technique for measuring stalk strength in corn. *Crop Sci.* 1, 378–380. doi: 10.2135/cropsci1961.0011183X000100050028x

frontiers | Frontiers in Plant Science

TYPE Original Research
PUBLISHED 27 January 2023
DOI 10.3389/fpls.2023.1069551

OPEN ACCESS

EDITED BY
Jiwang Zhang,
Shandong Agricultural University, China

REVIEWED BY
Muhammad Ishaq Asif Rehmani,
Ghazi University, Pakistan
Wangfeng Zhang,
Shihezi University, China

*CORRESPONDENCE
Kai Zhang
zhangkai@henau.edu.cn
Zhandong Liu
liuzhandong@caas.cn

†These authors have contributed equally to this work

SPECIALTY SECTION
This article was submitted to Crop and Product Physiology, a section of the journal Frontiers in Plant Science

RECEIVED 14 October 2022
ACCEPTED 09 January 2023
PUBLISHED 27 January 2023

CITATION
Huang C, Qin A, Gao Y, Ma S, Liu Z, Zhao B, Ning D, Zhang K, Gong W, Sun M and Liu Z (2023) Effects of water deficit at different stages on growth and ear quality of waxy maize.
Front. Plant Sci. 14:1069551.
doi: 10.3389/fpls.2023.1069551

Effects of water deficit at different stages on growth and ear quality of waxy maize

Chao Huang[1†], Anzhen Qin[1†], Yang Gao[1], Shoutian Ma[1], Zugui Liu[1], Ben Zhao[1], Dongfeng Ning[1], Kai Zhang[2*], Wenjun Gong[3], Mengqiang Sun[3] and Zhandong Liu[1*]

[1]Institute of Farmland Irrigation, Chinese Academy of Agriculture Sciences, Key Laboratory of Crop Water Use and Regulation, Ministry of Agriculture and Rural Affairs, Xinxiang, China, [2]College of Tobacco Science, Henan Agricultural University, Zhengzhou, China, [3]Guangli Irrigation Authority, Jiaozuo, China

Introduction: Extreme weather has occurred more frequently in recent decades, which results in more frequent drought disasters in the maize growing season. Severe drought often decreases remarkably plant growth and yield of maize, and even reduces significantly the quality of maize production, especially for waxy maize.

Results: To study the changes in plant growth, fresh ear yield, and fresh grain quality of waxy maize under water deficits occurring at different growth stages, and further strengthen the field water management of waxy maize, water deficit experiments were carried out under a rain shelter in 2019 and 2020. Water deficit treatments were imposed respectively at the V6–VT (D_{V6-VT}), VT–R2 (D_{VT-R2}), and R2–R3 (D_{R2-R3}) stages of waxy maize, and treatment with non-water deficit in the whole growing season was taken as the control (CK). The lower limit of soil water content was 50% of field capacity for a water deficit period and 65% of field capacity for a non-water deficit period.

Results: In this study, water deficits imposed at V6–VT and VT–R2 stages decreased plant growth rate and leaf gas exchange parameters, accelerated leaf senescence, and limited ear growth of waxy maize, which resulted in 11.6% and 23.1% decreases in grains per ear, 19.4% and 7.3% declines in 100-grain weight, 20.3% and 14.2% losses in fresh ear yield in 2019 and 2020 growing seasons, respectively, while water deficit at R2–R3 stage had no significant effect on ear traits and fresh ear yield, but the fresh ear yield with husk of DR2–R3 decreased by 9.1% ($P<0.05$). The obvious water deficit imposed at the V6–VT and VT–R2 stages also lowered grain quality. Water deficits at the V6–VT and VT–R2 stages led to accelerated maturity, resulting in increased total protein, starch, and lysine content in grains at the R3 stage and decreased soluble sugar content. Principal component analysis revealed that when water deficits occurred in the waxy maize growing season, they firstly altered maize physiological processes, then affected ear characteristics and yield, and finally resulted in significant grain quality changes. In conclusion, a water deficit during V6–VT and VT–R2 not only reduced fresh ear yield but also adversely affected grain quality. However, water deficit during R2–R3 had little effect on total protein, starch, and soluble sugar content, but increased obviously lysine content.

Discussion: The above results suggested that avoiding serious water deficits at the V6–VT and VT–R2 stages of waxy maize while imposing a slight water deficit at the R2–R3 stage has not only little effects on fresh ear yield but also a remarkable improvement in grain quality.

KEYWORDS

waxy maize, water deficit, leaf physiological characteristic, fresh ear yields, grain quality

Introduction

Drought is one of the main disasters affecting agricultural production around the world. Climate change has led to the aggravation of drought in many regions and significantly increased the frequency of extreme drought (IPCC, 2014). Since 1950, the land area affected by drought in China's agricultural production has shown a gradual upward trend, and the loss of food due to drought is about 25–30 × 10^6 t, accounting for 60% of the total loss from natural disasters (Hao and Singh, 2015; Song et al., 2018).

Water deficit can lead to a large number of physiological stress reactions in plants, thus changing the physiological characteristics of plants, thereby affecting the growth of plants, and the yield and quality of final products (Wang and Frei, 2011). Under conditions of water deficit, plant cells will produce reactive oxygen species (ROS) due to oxidative damage and synthesize a large amount of malondialdehyde (MDA). Meanwhile, the enhanced activities of catalase (CAT), superoxide dismutase (SOD), and peroxidase (POD) prevent severe damage (Ye et al., 2020a). At the same time, soluble sugar, soluble protein, and proline content in plant cells will gradually increase to maintain normal cell osmotic pressure (Liu et al., 2015). Drought stress also significantly reduced the photosynthetic rate of maize leaves. On the one hand, stomatal opening would decrease under drought stress, leading to a decrease in CO_2 supply and a decrease in the photosynthetic rate of maize leaves (Yao et al., 2012). On the other hand, peroxidation can reduce the activity of leaf photosynthetic enzymes (ribulose-1, 5-diphosphate carboxylase, and phosphoenolpyruvate carboxylase), resulting in a lower photosynthetic rate and final yield reduction of maize (Markelz et al., 2011; Ye et al., 2020a).

Water deficits can also affect the quality of crop products. Studies have shown that drought can reduce grain starch content and increase protein content in many crops (Wang and Frei, 2011; Thitisaksakul et al., 2012). Drought was shown to lower starch concentration in cassava tubers (Santisopasri et al., 2001), and water deficit during the flowering stage caused the process of starch accumulation in advance, and reduced the total starch accumulation (Yi et al., 2014). Some studies also showed that water deficit during the whole growth stage increased starch accumulation, starch accumulation rate, and the activities of key enzymes for starch synthesis (AGPase (glucose-1-ATP transferase), SS (starch synthase), and SBE (1,4-glucan branching enzyme)) at early filling stage in wheat, but decreased starch accumulation and amylose content at late filling stage (Dai et al., 2008; Singh et al., 2008). Studies also showed that drought stress increased total protein concentrations but decreased the contents of alcohol-soluble protein, glutenin, and oat protein contents in wheat grains (Begcy and Walia, 2015; Flagella et al., 2010; Ozturk and Aydin, 2004).

It was also reported that a water deficit reduced lysine content and increased protein content in maize grains and changed maize grain quality by increasing nitrogen, magnesium, zinc, and alcohol-soluble protein concentrations and reducing potassium and glutenin concentrations (Erbs et al., 2015). However, some studies suggested that drought at different growing stages had different effects on the grain quality of maize. Compared with normal irrigation, a drought at the whole growth stage was shown to decrease starch content by 3% and increase protein content in normal maize (Liu et al., 2013a). Sandhya et al. (2010) reported that drought stress at the seedling stage reduced the content of protein and starch in grains, while Ma et al. (2006) found that the content of protein and lysine in grains would be increased under moderate drought but decreased under excessive drought at the maize seedling stage. Drought imposed at the silking stage decreased starch content and increased protein content in maize grains (Wang and Frei, 2011; Thitisaksakul et al., 2012; Beckles and Thitisaksakul, 2014; Wang et al., 2021a). Drought stress at the flowering and post-anthesis stages both decreased grain protein content and fresh ear yield (decreased by 16.2%), but increased grain starch content in waxy maize (Zhao, 2017; Shi et al., 2018; Wang et al., 2021a). However, drought stress at the filling stage had no significant effects on the starch content but increased the protein content in the grains of fresh waxy maize. (Lu et al., 2015). In the process of grain formation, drought stress reduced the final starch content but increased the protein content (Wang et al., 2021b).

As a fresh-eating food, waxy maize places a high value on grain quality. Higher quality can bring better edible value and economic value (Wang et al., 2020). With the rapid improvement of citizen living standards, the planting area of fresh waxy maize increased significantly in the last decade in China. It can be expected that waxy maize will have a better market prospect and that the plantation area will continue to develop in the future. Although about 70% of the average annual rainfall of 582 mm occurred in the period of June to October in the Huang-Huai-Hai Plain (Si et al., 2020), most of the rainfall was given in several heavy rainstorms (Ma et al., 2016), which usually results in long periods without any effective rainfall and severe droughts during the maize growing season. The use of appropriate measurements and techniques is vital for high-yield, good-quality, and sustainable waxy maize production in the region. For the effects of water deficits on grain quality of waxy maize, most of the previous

studies-imposed water deficits after flowering. They mainly explored the changes in grain quality of waxy maize at complete maturity under different water-deficit treatments. However, few studies have focused on the effects of water deficits occurring in the vegetative growth stage, especially on grain quality in the fresh stage. Therefore, the main objectives of this experiment were focused on: (1) clarifying the changes in plant growth, physiological characteristics, fresh ear yield, and fresh grain quality of waxy maize under water deficit at the jointing stage, flowering stage, and filling stage; and (2) revealing in detail the tolerance of waxy maize to water deficit at different growing stages for determining suitable water management during the waxy maize growing period. This research contributes to the rapid development of waxy maize production in the Huang-Huai-Hai Plain.

Materials and methods

Site description

The experiment was carried out in lysimeters under a large-scale rain shelter at the Xinxiang Comprehensive Experimental Station of the Chinese Academy of Agricultural Sciences located in Qiliying Town, Xinxiang, Henan, China (35°18′N, 113°54′E, 75 m a.s.l.) with temperate monsoon weather in the 2019 and 2020 maize growing seasons. All lysimeters are non-weighing with well-equipped irrigation and drainage systems. The dimensions of each lysimeter were 2.0 m wide × 3.33 m length × 2.0 m in depth. The top side of the steel outer frame of the lysimeter is 10 cm higher than the soil surface in the lysimeter to prevent runoff during rain or irrigation events. A total of 24 lysimeters were arranged in two rows under a rain shelter. There was a 2 m space between the rows and 20 cm between lysimeters in the same row. The physical and chemical properties of the top 40 cm of the soil layer are shown in Table 1. A mobile rain shelter was installed above the two rows of lysimeters and closed before a rainfall and opened after the rainfall. This was done to avoid the severe effects of natural rainfall on the experiment of signed water deficit at different stages in maize growing seasons. An automatic weather station (YM-HJ03, Handan Chuangmeng Electronic Technology Co., Ltd., Hebei, China) was set on the edge of the lysimeter area. The average daily temperature and accumulated precipitation during the whole growing season of waxy maize in the two experiment seasons are shown in Figure 1.

Experimental design

The experimental waxy maize variety was "Shenkenuo 1," bred by the Shanghai Academy of Agricultural Sciences. The variety is a multi-resistant waxy maize variety with high taste quality and great planting promotion value (Wang et al., 2014). A total of 40 plants of waxy maize were maintained in each lysimeter, with row spacing of 60 cm and plant spacing of 30 cm. The experiment arranged only one factor (water deficit stage) with four treatment levels, i.e., water deficit occurred at V6–VT, VT–R2, and R2–R3 stages, and no water deficit in the whole waxy maize growing season (as CK), respectively. Following the soil water content arrangement shown in Xiao et al. (2011), no irrigation was carried out when the soil water contents were higher than 50% of field capacity during the process of water deficit treatment at the V6–VT, VT–R2, and R2–R3 stages of waxy maize, and irrigation was performed when the soil water content was reduced to or less than 50% of field capacity, or at the end of a growing stage with water deficit treatment. During the periods without arranging water deficit treatment, the soil water contents were maintained at more than 65% of field capacity, so the soil water contents in CK treatment were maintained at higher than 65% of field capacity in whole growing seasons. All four treatments were replicated three times. The planned soil water lower limits for all four treatments are shown in Table 2. The beginning date of each growth stage is shown in Table 3.

Measurement set-up

Measurements of soil water content

Soil water content (SWS, cm^{-3} cm^{-3}) in the 0–100 cm soil layer was measured in real time with Insentek sensors (Oriental Zhigan Technology Ltd., Zhejiang, China) with a 10 cm increment. The sensor parameters were shown in Qin et al. (2019).

Measurements of plant height and leaf area index

At the six-leaf stage of waxy maize, three representative waxy maize plants with similar growth status were selected and marked in each lysimeter. The plant height and the leaf length and largest leaf width of all leaves on the three marked plants were measured at the end of each water deficit period of V6–VT, VT–R2, and R2–R3 in 2019 and 2020, and the leaf area index of each lysimeter was calculated by using Eq. (1) (Huang et al., 2022).

TABLE 1 Basic parameters of topsoil of 0–40 cm in lysimeters.

Location	Soil texture	pH	Soil bulk density (g cm^{-3})	Soil field capacity (cm^3 cm^{-3})	Organic matter (g kg^{-1})	Total nitrogen (g kg^{-1})	Available potassium (mg kg^{-1})	Total phosphorus (g kg^{-1})	Available phosphorus (g kg^{-1})	NO_3^--N (mg kg^{-1})	NH_4^+-N (mg kg^{-1})
Xinxiang	Silt loam soil	8.8	1.51	0.31	10.72	0.73	138.96	0.94	72.00	18.34	2.54

Soil pH was determined in 1:5, soil to CO_2-free water suspension by pH meter (120P-02A, Thermo Fisher Scientific); soil bulk density was measured by ring knife method; soil field capacity was measured by infiltration method; organic carbon was determined by potassium dichromate volumetric method; total nitrogen was determined by microcalorimetric method; exchangeable potassium was determined by flame photometric method; total phosphorus was determined by perchloric acid–sulfuric acid method; available phosphorus was determined by sodium hydrogen carbonate solution-Mo-Sb anti spectrophotometric method; NO_3^--N was determined by immerse-UV spectrophotometry method; NH_4^+-N was determined by indophenol blue colorimetry.

10.3389/fpls.2023.1069551

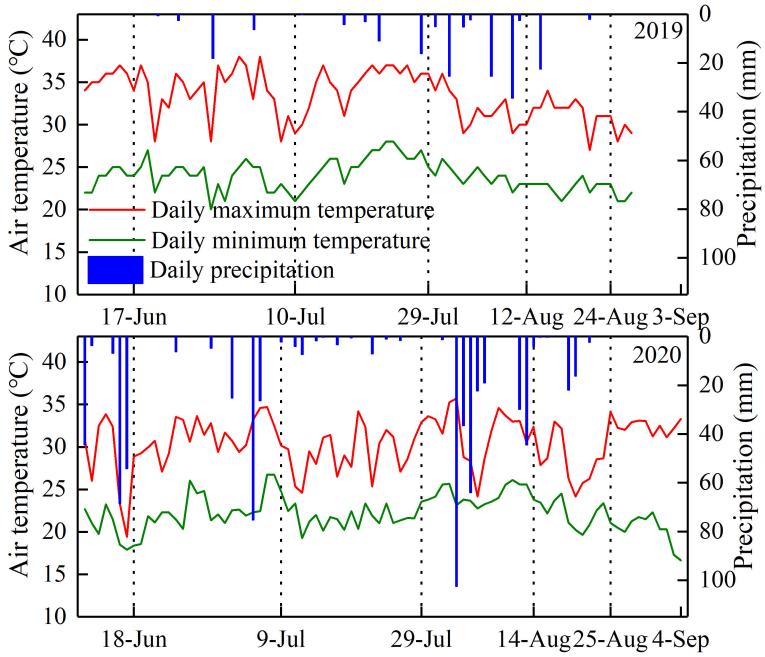

FIGURE 1
Daily air temperature and precipitation during the 2019 and 2020 growing seasons.

$$LAI = 0.75 \times \frac{\sum_{i=1}^{m}\sum_{j=1}^{n}(L_{ij} \times W_{ij})}{m} \times \frac{N}{S} \quad (1)$$

where LAI is the leaf area index (dimensionless), L_{ij} is the leaf length (cm) of the jth leaf on ith plant, W_{ij} is the largest width (cm) of the jth leaf on ith plant, m is the measured number of plants, n is the number of leaves per plant, N is the plant number on a lysimeter, and S is the soil surface area of a lysimeter (cm^2).

Measurements of gas exchange

A Li-6400 portable photosynthesis analyzer (LI-COR, USA) was used to measure the gas exchange parameters (including net photosynthetic rate (P_n), stomatal conductance (G_s), transpiration rate (T_r), and intercellular CO_2 concentration (C_i)) of the ear leaves on the marked plants at the end of each water deficit period of V6–VT, VT–R2, and R2–R3 in 2019 and 2020. Measurements were carried out between 9:00 and 11:00 a.m. on a sunny day. A SPAD-502 portable chlorophyll meter (Konica Minolta Holdings, Inc., Japan) was used to measure the *SPAD* value of the ear leaves on the marked plants at the end of the three water deficit periods (Huang et al., 2022). The leaf water use efficiency ($LWUE$) was calculated with Eq. (2) (Huang et al., 2022).

$$LWUE(\mu mol \quad mmol^{-1}) = \frac{P_n(\mu mol \quad m^{-2} \quad s^{-1})}{T_n(\mu mol \quad m^{-2} \quad s^{-1})} \quad (2)$$

Determination of enzyme activities and osmotic adjustment substances in waxy maize leaves

Five ear leaves of waxy maize in each lysimeter were sampled at the R3 stage in 2019 for determining the soluble protein content (determined with the BCA protein method), soluble sugar content (with the anthrone colorimetry method), proline content (with the ninhydrin method), and malondialdehyde (MDA, determined with the thiobarbituric acid method) contents of ear leaves of waxy maize. The methods of determining the activities of antioxidant enzymes such as superoxide dismutase (SOD, NBT method), peroxidase (POD, guaiacol method), and catalase (CAT, ammonium molybdate method) also were consistent with those described by Huang et al. (2022).

TABLE 2 Designed low limit of soil water content for different treatments at different waxy maize growing stages.

Water deficit treatment	Lower limit of soil moisture content			
	V1–V6 stage	V6–VT stage	VT–R2 stage	R2–R3 stage
CK	65	65	65	65
D_{V6-VT}	65	50	65	65
D_{VT-R1}	65	65	50	65
D_{R1-R3}	65	65	65	50

The values in the table are the lower limit controlled of soil water content, and presented as percentage of field capacity. V1, first leaf; V6, sixth leaf; VT, tasseling; R2, blister stage; R3, milk stage.

TABLE 3 Beginning date of each growth stage of waxy maize in two growing seasons.

Year	Sowing	Second leaf	Sixth leaf	Tasseling	Blister stage	Milk stage	Harvest
2019	10.6.2019	17.6.2019	10.7.2019	29.7.2019	12.8.2019	24.8.2019	27.8.2019
2020	11.6.2020	18.6.2020	9.7.2020	29.7.2020	14.8.2020	25.8.2020	4.9.2020

Fresh ear grain yield and ear characters

Fresh ears with husks were taken on all lysimeters (the harvest date is shown in Table 2) at the end of the R3 stage in the 2019 and 2020 seasons. A total of 20 representative ears were sampled on each lysimeter to measure the yield of fresh ears with husks and the yield of fresh ears without husks. Ear characters such as ear length, ear diameter, bald tip length, grain rows per ear, grains per row, and grains per ear were also determined simultaneously by averaging the relevant values of the 20 sample ears. After threshing, three groups of 100 grains were randomly sampled to determine the 100-grain weight for each experimental lysimeter.

Grain quality

The waxy maize grains were collected at late R3 stages for determining fresh grain quality using the method described by Huang et al. (2022) in the 2019 and 2020 seasons. The soluble sugar content (determined with the anthrone colorimetric method), starch content (with the anthrone-sulfuric acid method), total protein content (with the total nitrogen content method, total protein content = total nitrogen content × 6.25), and lysine content (with the ninhydrin chromogenic method) of waxy maize grains were measured for each sample. The contents of amylopectin, amylose, gliadin, gluten, albumin, and globulin were measured by the Sanshu Bio-Tech company in China. The amylose content of starch was determined using a colorimetric amylose content assay (Knutson and Grove, 1994). The amylose content was analyzed using the GPC-RI-MALLs system developed by Park et al. (2007). Glutenins and gliadins were extracted and quantitated subsequently from two biological replicates by reverse-phase ultra-performance liquid chromatography (RP-UPLC) according to a method described by Han et al. (2015), and the sample size was modified in minor ways according to the protein concentration of waxy maize grain. The albumin and globulin content was analyzed using an automatic microplate reader (Multiskan GO, Thermo, USA).

Statistical analysis

The effects of water deficits imposed at different stages on the waxy maize growth index, grain yield, yield components, and grain quality were analyzed by analysis of variance using the General Linear Model procedure (GLM) in SPSS 19.0 (IBM Inc., Chicago, IL, USA). Duncan's new multiple range difference method was used to test the significance of the difference at the $P<0.05$ level. Figures were drawn with Origin 2017 (OriginLab, USA). Principal component analysis was used to determine the comprehensive impact of the water deficit.

Results

Effects of water deficits on plant height and leaf area index

Plant height and leaf area index (*LAI*) of waxy maize varied significantly with growing stages and growing seasons ($P<0.01$; Table 4). The results of the two growing seasons showed that plant height and *LAI* decreased most significantly under the water deficit imposed at the V6–VT and VT–R2 stages (Table 4), and the change trends in the two growing seasons were basically the same (Figure 2). At the end of the water deficit period of V6–VT and VT–R2, all plant heights and *LAI* values of D_{V6-VT} and D_{VT-R2} were significantly lower than those of the CK treatment. Compared with CK, the plant height under D_{V6-VT} and D_{VT-R2} treatments at the R3 stage decreased by 10.7% and 9.0% ($P<0.05$), and the *LAI* decreased by 22.4% and 19.5% ($P<0.05$), respectively. The D_{R2-R3} treatment did not exhibit significant effects on plant height and *LAI*, but because of temperature, light, and other reasons factors, the plant height of waxy maize in 2019 was higher than in 2020. It was clearly indicated that a water deficit imposed at the V6–VT and VT–R2 stages may severely limit the plant growth and leaf development of waxy maize.

Effects of water deficits on MDA, antioxidant enzymes, and osmotic adjustment substances in maize leaves

MDA content and antioxidant enzyme activities in waxy maize leaves under different water-deficit treatments are shown in Figure 3. Compared with CK, the MDA content in D_{V6-VT} and D_{VT-R2} increased by 40.8% and 46.0%, respectively ($P<0.05$, Figure 3A), while the MDA content in D_{R2-R3} was significantly decreased by 30.1% ($P<0.05$). These results indicated that the recovery of plants in the D_{V6-VT} and D_{VT-R2} treatments was weak after re-watering. It may be the main reason that changes in CAT were insignificant under D_{V6-VT} treatment, and the activities of SOD and POD were significantly decreased by 26.8% and 25.8%, respectively, compared with CK ($P<0.05$). The oxidative damage to waxy maize plants still appeared obviously at the milk stage, even after a long-term release of the water deficit imposed at the jointing stage. D_{VT-R2} significantly increased CAT by 33.6% ($P<0.05$) but decreased significantly SOD and POD by 19.1% and 18.4% ($P<0.05$), which indicated that the oxidative damage caused by the water deficit at the VT–R2 stage can only be alleviated to a certain extent. D_{R2-R3} exhibited less oxidative damage and obvious increases in SOD, CAT, and POD by 24.5%, 83.8%, and 24.5%, respectively ($P<0.05$), which indicated that the damage caused by water deficit at the R2–R3 stage may have been almost completely alleviated at the milk stage.

10.3389/fpls.2023.1069551

TABLE 4 ANOVA results of relevant waxy maize indices in the 2019 and 2020 growing seasons.

Effect		Plant height (cm)	Leaf area index	Ear length (cm)	Ear diameter (mm)	Bald tip length (cm)	Rows per ear	Grains per row	Grains per ear	100-grain weight (g)	Fresh ear yield with husk (t hm^{-2})	Fresh ear yield (t hm^{-2})	Total protein (mg g^{-1})	Grain soluble sugar (mg g^{-1})	Starch (mg g^{-1})	Lysine (mg g^{-1})
Stage	CK	213a	2.05a	17.35a	46.01a	1.16a	14.6ab	32.8a	505a	36.56a	15.24a	10.77a	80.52b	80.80a	77.55d	7.93b
	V6–VT	189c	1.60b	15.47c	46.33a	0.98a	14.0b	33.3a	453b	29.50c	12.51c	8.13d	87.37a	55.53c	161.66a	9.26a
	VT–R2	193c	1.65b	16.21b	44.25b	1.23a	12.7c	28.0b	402c	33.88b	13.75b	8.74c	86.26a	69.14b	145.32b	9.81a
	R2–R3	201b	1.95a	17.20a	45.38ab	1.02a	15.0a	32.2a	459b	35.93a	13.84b	10.11b	82.08b	77.41a	97.08c	9.26a
Year	2019	206a	1.93a	14.60a	47.04a	0.35a	15.0a	38.4a	590a	35.67a	15.54a	10.11a	88.53a	73.83a	107.32b	8.98b
	2020	184b	1.69b	13.64b	43.94b	1.85a	13.1b	24.8b	319b	32.27b	12.12b	8.76b	79.58b	67.62b	133.48a	9.14a
Stage		**	**	**	**	**	**	**	**	**	**	**	**	**	**	ns
Year		**	**	**	*	ns	**	**	**	**	**	**	**	**	**	*
Stage × Year		ns	ns	**	*	ns	ns	**	*	ns	Ns	ns	ns	**	**	ns

Same lowercase letters indicated no significance between different stages and years at a = 0.05. The mean is reported. *P<0.05, **P<0.01, ns P ≥0.05.

The soluble protein, soluble sugar, and free proline in waxy maize leaves at the R3 stage are shown in Figure 4. Results showed that the recovery of waxy maize plants after re-watering was poor under $D_{V6–VT}$ and $D_{VT–R2}$ treatments. Compared with CK, the soluble sugars and soluble proteins in the $D_{V6–VT}$ treatment increased by 95.4% and 38.1% (P<0.05) and by 42.0% and 26.4% (P<0.05) in the $D_{VT–R2}$ treatment, respectively. These increases were beneficial to maintaining cell water potential under water deficits, reducing leaf water loss, and improving leaf water use efficiency. The $D_{V6–VT}$ treatment had the highest levels of soluble sugar, soluble protein, and proline. Meanwhile, the soluble sugar content in the $D_{R2–R3}$ treatment increased by 30.9% (P<0.05), but the soluble protein decreased by 19.1% compared with the CK treatment. It was further indicated that a water deficit in the V6–VT stage had the greatest impact on the relevant index in waxy maize leaves and the smallest effects from a water deficit in the R2–R3 stage.

Effects of water deficits on photosynthetic characteristics

Under water deficit, plants usually reduced water loss by closing partially stomates, while the photosynthetic recovery of waxy maize was different after release from the water deficit imposed at different growing stages (Figure 5). The changes in *SPAD* and photosynthetic characteristics in the two growing seasons were basically the same (Figure 5). After water deficit at the V6–VT stage, *SPAD* and gas exchange parameters of leaves decreased, but leaf water use efficiency (*LWUE*) increased. After a water deficit at the VT–R2 stage, P_n, G_s, C_i, and T_r of leaves decreased significantly. Compared with CK, the $D_{V6–VT}$ treatment reduced the *SPAD* of waxy maize leaves (Figure 5A), and the $D_{V6–VT}$ and $D_{VT–R2}$ treatments significantly decreased P_n, G_s, and T_r (Figures 5B, C, E) and C_i of waxy maize leaves at the R3 stage. Both $D_{V6–VT}$ and $D_{VT–R2}$ treatments increased *LWUE* significantly (Figure 5F). But no significant differences in P_n, C_i, G_s, T_r, and *LWUE* between $D_{R2–R3}$ and CK were investigated. With the postponement of the water deficit stage, P_n, G_s, and T_r showed an increasing trend, while C_i showed a trend of decreasing at the beginning and then increasing later (Figure 5D), while *LWUE* showed a firmly decreasing trend (Figure 5F).

Effects of water deficits on ear traits

The results of the ANOVA in two growing seasons showed that there were significant differences in grains per ear and 100-grain weight under different water deficits imposed at different growth stages of waxy maize (P<0.01; Table 4). The 100-grain weight of $D_{V6–VT}$ was significantly lower than those of other treatments, decreasing by 19.4% compared with CK (P<0.05; Figure 6A). Meanwhile, the grain yield per ear of the $D_{VT–R2}$ treatment was the lowest and was 23.1% lower than that of CK (P<0.05; Figure 6B).

Ear length, ear diameter, bald tip length, grain rows per ear, and grains per row significantly varied with water deficit treatments (P<0.01; Table 4; Figures 7A–E). The results of multiple comparisons in two growing seasons showed that the ear length of $D_{V6–VT}$, compared with CK, decreased the most obviously, followed

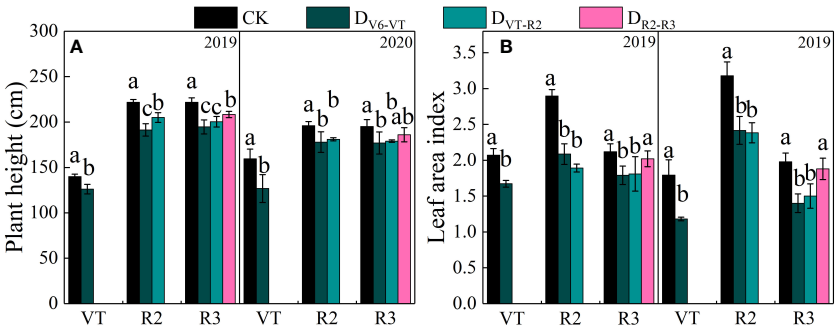

FIGURE 2
Plant heights and *LAI* of waxy maize under water deficits at different growing stages in the 2019 and 2020 seasons. Different lowercase letters during the same year indicated significant at 0.05 level. The X axes are years. CK, control; D_{V6-VT}, water deficit from six leaf stage (V6) to tasseling stage (VT); D_{VT-R2}, water deficit from tasseling stage to blister stage (R2); D_{R2-R3}, water deficit from blister stage to milk stage (R3); VT, tasseling stage; R2, blister stage; R3, milk stage. **(A)** plant height of waxy maize; **(B)** leaf area index of waxy maize.

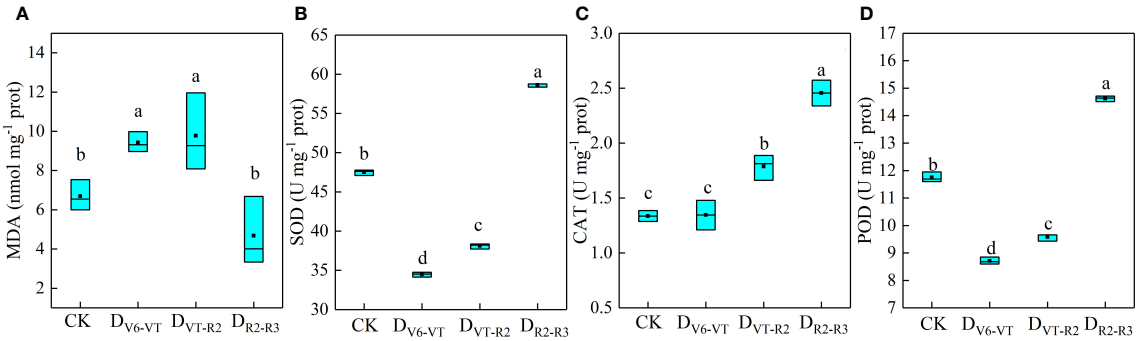

FIGURE 3
MDA contents and antioxidant enzyme activities of waxy maize leaves under water deficits at different growing stages in the 2019 season. Lowercase letters indicate the difference of different treatments at 0.05 level; MDA, malonaldehyde; SOD, superoxide dismutase; CAT, catalase; POD, peroxidase. the box from bottom to top indicated the lower quartile, median and upper quartile respectively, and the middle black box indicated the mean value. CK, control; D_{V6-VT}, water deficit from six leaf stage (V6) to tasseling stage (VT); D_{VT-R2}, water deficit from tasseling stage to blister stage (R2); D_{R2-R3}, water deficit from blister stage to milk stage (R3). **(A)** MDA content of leaves; **(B)** SOD activities of leaves; **(C)** CAT activities of leaves; **(D)** POD activities of leaves.

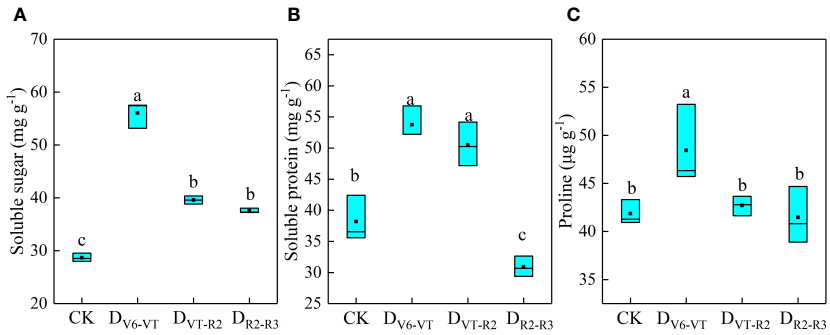

FIGURE 4
Contents of osmotic adjustment substances of waxy maize leaves under water deficits imposed at different growing stages in the 2019 season. Lowercase letters indicate the difference of different treatments at 0.05 level; the box from bottom to top indicated the lower quartile, median and upper quartile respectively, and the middle black box indicated the mean value. CK, control; D_{V6-VT}, water deficit from six leaf stage (V6) to tasseling stage (VT); D_{VT-R2}, water deficit from tasseling stage to blister stage (R2); D_{R2-R3}, water deficit from blister stage to milk stage (R3). **(A)** soluble sugar contents of leaves; **(B)** soluble protein contents of leaves; **(C)** proline contents of leaves.

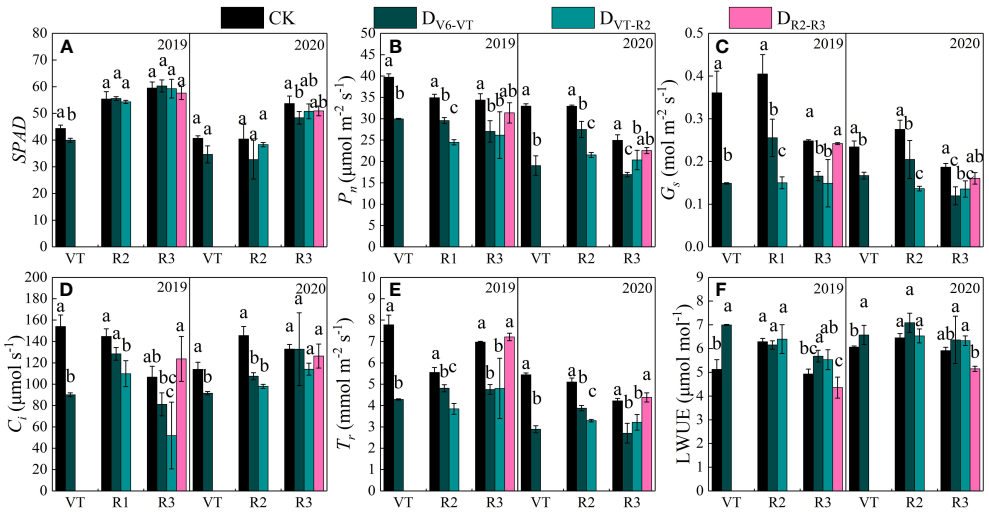

FIGURE 5
Photosynthetic characteristics of waxy maize leaves under water deficits at different growing stages in the 2019 and 2020 seasons. Different lowercase letters during the same stage indicated significant at 0.05 level. *SPAD*, leaf chlorophyll content index; P_n, net photosynthetic rate; G_s, stomatal conductance; C_i, intercellular CO_2 concentration; T_r, transpiration rate; LWUE, leaf water use efficiency. The X axes are years. CK, control; D_{V6-VT}, water deficit from six leaf stage (V6) to tasseling stage (VT); D_{VT-R2}, water deficit from tasseling stage to blister stage (R2); D_{R2-R3}, water deficit from blister stage to milk stage (R3). **(A)** SAPD value of leaves; **(B)** net photosynthetic rate of leaves, P_n; **(C)** stomatal conductivity of leaves, G_s; **(D)** intercellular CO_2 concentration of leaves, C_i; **(E)** transpiration rate of leaves, T_r; **(F)** leaf water use efficiency of leaves, LWUE.

by D_{VT-R2}. Meanwhile, the ear diameter under the D_{VT-R2} treatment decreased the most significantly, and grain rows per ear and grains per row of D_{VT-R2} decreased significantly due to the decrease in ear length and ear diameter (Table 4). Compared with CK, the ear length of D_{V6-VT} and D_{VT-R2} decreased by 12.7% and 8.5%, respectively (P<0.05; Figure 7A), while the ear diameter, grain rows per ear, and grains per row of D_{VT-R2} decreased by 3.2%, 12.6%, and 16.8%, respectively (P<0.05; Figures 7B, D, E). It was the decrease in grain rows per ear and grains per row that resulted in the decrease in grains per ear. Due to the stage differences in imposed water deficit stages, the maturity dates of ears were obviously different, which resulted in different grain moisture contents at harvest. The grain moisture content of D_{V6-VT} treatment was significantly lower than that of CK, while no remarkable differences were investigated between the grain moisture contents of D_{VT-R2} or D_{R2-R3} treatments and that of CK at the end of R3 stage (Figure 7F).

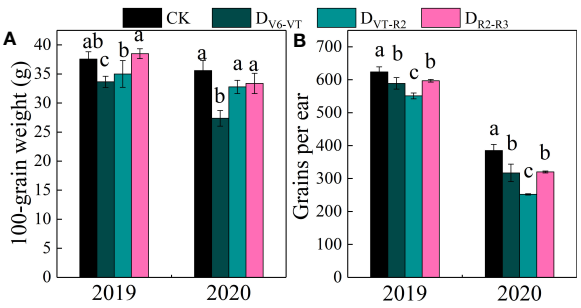

FIGURE 6
100-grain weight and grains per ear of waxy maize under water deficits at different growing stages in the 2019 and 2020 seasons. Different lowercase letters during the same stage indicated significant at 0.05 level. The X axes are years. CK, control; D_{V6-VT}, water deficit from six leaf stage (V6) to tasseling stage (VT); D_{VT-R2}, water deficit from tasseling stage to blister stage (R2); D_{R2-R3}, water deficit from blister stage to milk stage (R3). **(A)** 100-grain weight of fresh grains; **(B)** grains per ear of fresh ear.

Effects of water deficits on fresh ear yield

Fresh ear yield with husks (HFY) and fresh ear yield (FY) were affected very significantly by the water deficit stage and growing seasons (P<0.01; Table 4). The ear yield of waxy maize varied under different water deficit treatments. Water deficit at the V6–VT stage showed the greatest effect on the ear yield, followed by those at the VT–R2 stage, and the least effect under water deficit at the R2–R3 stage (Figure 8). Compared with those under CK, mainly due to the varying grain number per ear and 100-grain weight under water deficit at different stages, the HFY and FY decreased by 22.0% and 20.3% under D_{V6-VT} (P<0.05), by 14.3% and 14.2% under D_{VT-R2} (P<0.05), and both less than 10.0% under D_{R2-R3}, respectively.

Effects of water deficits on grain quality

Total protein, grain soluble sugar, and starch contents in waxy maize grains varied significantly with the different water deficit stage treatments and growing seasons (P<0.01; Table 4). Water deficit increased the contents of total protein, starch, and lysine in fresh waxy maize grains, but reduced the content of soluble sugar in fresh waxy maize grains. However, the effects of water deficits at different growing stages on grain quality were obviously different, and the changing trends in the two growing seasons were consistent (Figure 9). The soluble sugar content of the D_{V6-VT} treatment was the lowest due to a 31.6% decrease over that of CK (Figure 9B; P<0.05), followed by the D_{VT-R2} treatment with a decrease of 14.1% (P<0.05), while the decrease was 4.0% under the D_{R2-R3} treatment.

10.3389/fpls.2023.1069551

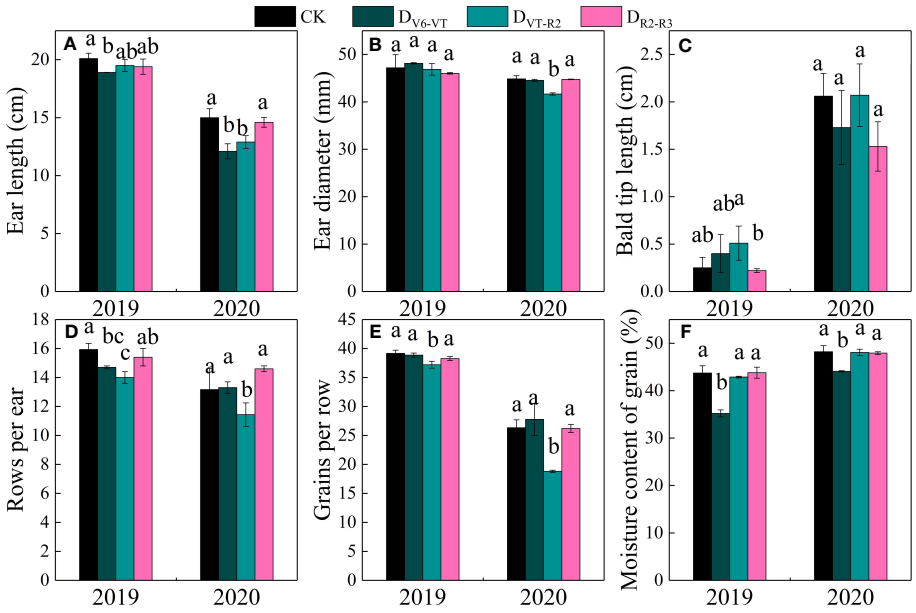

FIGURE 7
Ear traits of waxy maize under water deficits at different growing stages in the 2019 and 2020 seasons. Different lowercase letters during the same stage indicated significant at 0.05 level. The X axes are years. CK, control; D_{V6-VT}, water deficit from six leaf stage (V6) to tasseling stage (VT); D_{VT-R2}, water deficit from tasseling stage to blister stage (R2); D_{R2-R3}, water deficit from blister stage to milk stage (R3). **(A)** ear length; **(B)** ear diameter; **(C)** bald tip length; **(D)** rows per ear; **(E)** grains per row; **(F)** moisture content of grains.

The total protein content and starch content were the greatest under the D_{V6-VT} treatment (Figures 9A, C) with an increase of 8.5% and 66.5%, respectively (P<0.05) than those under CK, respectively (P<0.05). The following were those under the D_{VT-R2} treatment with an increase of 7.1% and 20.1% (P<0.05), and under the D_{R2-R3} treatment with an increase of 2.0% and 1.5% under the D_{R2-R3} treatment. Compared with the CK treatment, the D_{V6-VT}, D_{VT-R2}, and D_{R2-R3} treatments increased the lysine content in grains by 16.7%, 23.8%, and 16.7%, respectively.

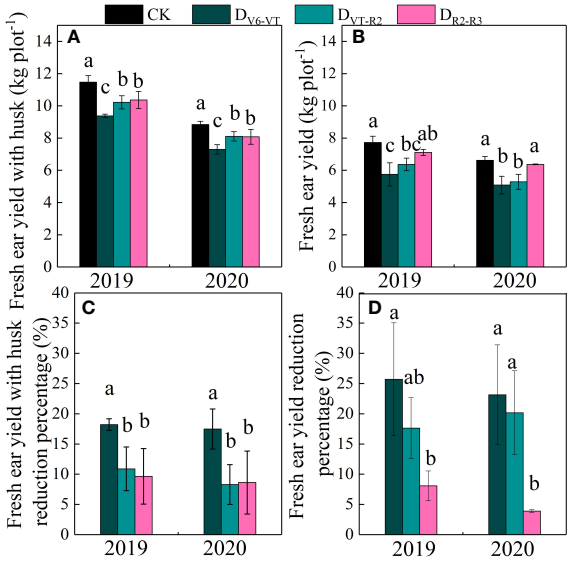

FIGURE 8
Ear yields of waxy maize under water deficits at different growing stages in the 2019 and 2020 seasons. Different lowercase letters during the same stage indicated significant at 0.05 level. The X axes are years. CK, control; D_{V6-VT}, water deficit from six leaf stage (V6) to tasseling stage (VT); D_{VT-R2}, water deficit from tasseling stage to blister stage (R2); D_{R2-R3}, water deficit from blister stage to milk stage (R3). **(A)** fresh ear yield with husk; **(B)** fresh ear yield; **(C)** fresh ear yield with husk reduction percentage; **(D)** fresh ear yield reduction percentage.

Figure 9 indicated that the water deficit at the V6–VT stage had the most significant effects on the total protein and starch content of waxy maize grains, so the changes in amylose, amylopectin, and component protein content of waxy maize grains under the D_{V6-VT} treatment were selected as representative to show the effects of water deficit on grain quality index (Table 5). Compared with CK, the amylose and amylopectin content under the D_{V6-VT} treatment increased by 15.9% and 92.5% (P<0.05), the contents of glutelin and globulin decreased by 9.1% and 56.9%, respectively (P<0.05), while the contents of alcohol-soluble protein and albumin increased by 24.0% and 59.9%, respectively (P<0.05).

Principal component analysis

Principal component analysis (PCA) was performed on all measured indexes of waxy maize in the two growing seasons. Three principal components (PC1, PC2, and PC3) were extracted in 2019 and 2020 (λ >1), and the eigenvalues (λ) of principal component 1 (PC1) in 2019 and 2020 were 18.88 and 13.37, and explained 69.9% and 66.9% of the total variation, respectively. λ of PC2 in 2019 and 2020 were 5.19 and 4.22, which contributed 19.2% and 21.1% of the total variation, respectively. λ of PC3 in 2019 and 2020 were 2.93 and 2.41, which explained 10.9% and 12.0% of the total variation, respectively (Table 6). The largest loading variable in 2019 was CAT, followed by bald tip length, SPAD, lysine, and ear diameter. The largest loading variable in 2020 was C_i, followed by ear length, ear diameter, grain number per ear, and fresh ear yield with husks. These

10.3389/fpls.2023.1069551

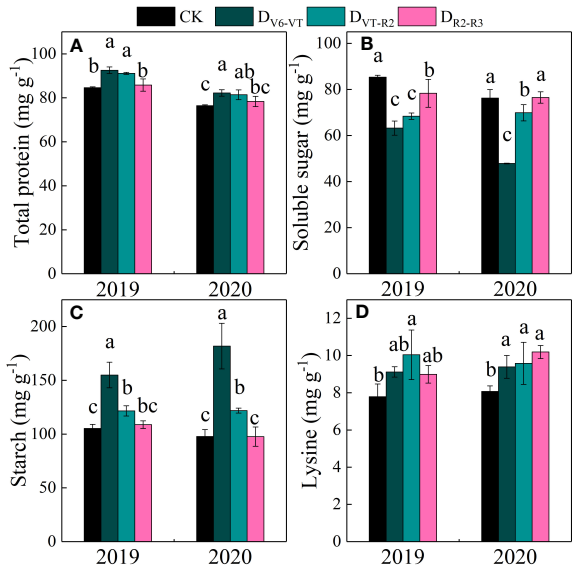

FIGURE 9
Grain quality traits of waxy maize under water deficits at different growing stages in the 2019 and 2020 seasons. Different lowercase letters during the same stage indicated significant at 0.05 level. The X axes are years. CK, control; D_{V6-VT}, water deficit from six leaf stage (V6) to tasseling stage (VT); D_{VT-R2}, water deficit from tasseling stage to blister stage (R2); D_{R2-R3}, water deficit from blister stage to milk stage (R3). **(A)** total protein of fresh grains; **(B)** soluble sugar of fresh grains; **(C)** starch of fresh grains; **(D)** Lysine of fresh grains.

results indicated that leaf physiology traits were most sensitive to water deficit, followed by ear traits and fresh ear yield in waxy maize (Figure 10).

Discussion

Effects of water deficits at different growing stages on leaf physiological characteristics of waxy maize

When plants are subjected to water stress, a large amount of reactive oxygen species will accumulate in the tissues, which will break the mechanism of reactive oxygen species production and scavenging, triggering the production of MDA by cell membrane peroxidation (Liu et al., 2015). Meanwhile, plant cells produce many kinds of antioxidant enzymes such as SOD, CAT, and POD to scavenge reactive radicals (Simova et al., 2008). Studies have shown that the accumulation of MDA varies with growing stages and that the longer a water deficit lasted, the more MDA was accumulated (Liu, 2013b). In our study, the MDA content in waxy maize leaves under the D_{V6-VT} and D_{VT-R2} treatments was significantly higher than that under the CK treatment at the R3 stage, and the MDA value under D_{V6-VT} was greater than that under D_{VT-R2}. Our results are similar to the results of Li et al. (2017), which indicated that the magnitude of MDA accumulation at the jointing stage was greater than that at the filling stage. On the one hand, SOD, CAT, and POD activities in the cells increased to scavenge excessive reactive oxygen species (Liu et al., 2015). In this study, both SOD and POD activities were significantly lower in the D_{V6-VT} treatment compared with those in CK, mainly due to the inhibition of SOD and POD activities by excessive MDA (Liu, 2013b). But SOD, CAT, and POD activities in the D_{R2-R3} treatment increased significantly, which indicated that the plant functions recovered better after re-watering from the R2 to the R3 water deficit. Bu et al. (2009) also demonstrated an increase in protective enzyme activity after re-watering. Meanwhile, the increases in proline and total carbohydrate contents under water deficit are beneficial to protect maize plant tissues from oxidative damage (Bu et al., 2009; Anjum et al., 2016). Previous studies have shown that proline and MDA are in a reciprocal relationship, with proline accumulation helpful for reducing MDA damage to the plant, while soluble sugars and soluble proteins increase beneficial for maintaining cellular osmotic pressure (Liu et al., 2015; Li et al., 2017). In our study, the soluble sugar, soluble protein, and proline contents of waxy maize leaves under D_{V6-VT} were significantly higher than those under CK at the R3 stage, while these contents under both D_{VT-R2} and D_{R2-R3} were similar to those under the CK treatment. Even though the soluble sugar content increased after re-watering (Bu et al., 2009), the damage caused by the water deficit imposed at the V6–VT stage remained unrecovered. After re-watering, the recovery of antioxidant enzyme activity was very poor, photosynthesis was adversely affected, and an irreversible effect resulted in waxy maize plants grown under the D_{V6-VT} treatment in our study, mainly due to the long water deficit period (approximately 20 d, see Table 3) in the V6–VT stage.

Photosynthesis is the main physiological process driving plant growth and is highly sensitive to water deficits (Chaves et al., 2009). Water deficits reduce P_n, T_r, and G_s, which in turn reduce maize plant biomass and grain yield (Ali and Ashraf, 2011; De Carvalho et al., 2011; Li et al., 2018). In our study, P_n and G_s decreased significantly under both the D_{V6-VT} and D_{VT-R2} treatments with nearly the same variation pattern, which was very similar to those results from Cai et al. (2017). C_i was also significantly reduced in the D_{VT-R2}

TABLE 5 Effects of water deficit imposed at jointing stage on starch and protein contents of waxy maize grains in the 2019 and 2020 growing seasons.

Year	Treatment	Amylose (mg g^{-1})	Amylopectin (mg g^{-1})	Alcohol soluble protein (mg g^{-1})	Glutenin (mg g^{-1})	Albumin (mg g^{-1})	Globulin (mg g^{-1})
2019	CK	33.69 ± 0.47b	71.61 ± 3.85b	24.00 ± 0.17b	37.86 ± 0.65a	2.97 ± 0.11b	1.55 ± 0.05a
	D_{V6-VT}	36.44 ± 0.39a	118.55 ± 11.87a	31.54 ± 0.57a	35.19 ± 0.87b	4.59 ± 0.12a	0.67 ± 0.06b
2020	CK	34.28 ± 0.40b	63.55 ± 6.34b	26.76 ± 1.34b	32.58 ± 0.71a	3.33 ± 0.26b	1.50 ± 0.03a
	D_{V6-VT}	42.39 ± 3.83a	139.46 ± 21.23a	31.23 ± 0.81a	28.95 ± 1.68b	5.50 ± 0.56a	0.65 ± 0.01b

The lowercase letters in the same column are the differences at the 0.05 level in the same year; the same uppercase letters are different between the two regions at 0.05 level. CK, control; D_{V6-VT}, water deficit from six leaf stage (V6) to tasseling stage (VT).

TABLE 6 Eigenvalues and variances of principal component analysis in the 2019 and 2020 growing seasons.

Year	Principal Component Number	Eigenvalue (λ)	Total variation (%)	Cumulative (%)
2019	PC1	18.88	69.93	69.93
	PC2	5.19	19.20	89.14
	PC3	2.93	10.86	100.00
2020	PC1	13.37	66.86	66.86
	PC2	4.22	21.10	87.96
	PC3	2.41	12.04	100.00

treatment, mainly due to stomatal limitation, but was not significantly affected in the D_{V6-VT} treatment. SPAD value decreased obviously under the D_{V6-VT} treatment, because reactive oxygen species generated by water deficit severely degraded severely chlorophyll pigments (Anjum et al., 2016) and significantly decreased chlorophyll content (Ye et al., 2020b). Water deficit also may reduce photosynthetic enzyme (PEPCase, RuBPase) activity (Ye et al., 2020a), and it caused a remarkable reduction in photosynthetic rate under the D_{V6-VT} treatment in this study. Reduced G_s also limited transpiration and resulted in a significant decrease in T_r under the D_{V6-VT} and D_{VT-R2} treatments. But *LWUE* increased when plants were exposed to a water deficit, due mainly to the obvious reduction in transpiration and water consumption (Yao et al., 2012).

Effects of water deficits at different growing stages on yield and yield traits of waxy maize

The reduction of photosynthetic rate under water deficit may lead to a reduction of plant photoassimilate deposition and ultimately the loss of grain yield (Kimaro et al., 2015; Ye et al., 2020a; Ulfat et al., 2021). Previous studies have shown that a water deficit during grain filling reduced the grain fresh weight, water content, and grains per ear of waxy maize (Guo et al., 2022). In this study, fresh ear yield with husk and fresh ear yield were significantly reduced, and the grain number per ear and 100-grain weight also showed some reducing trends under the D_{V6-VT} and D_{VT-R2} treatments. The most obvious decrease in grain number per ear was investigated in the D_{VT-R2} treatment, while the most remarkable decrease in 100-grain weight occurred in the D_{V6-VT} treatment. Previous results already indicated that a water deficit imposed at the tasseling, flowering, and filling stages could reduce the grain number per ear and grain weight of waxy maize, resulting in yield loss (Sun, 2014). Similar to the results of Xiao et al. (2011), the yield loss under treatment with a water deficit that occurred at the jointing stage was less than that under a water deficit imposed at the filling stage. The yield loss trend under water deficit may be described as that the yield loss reduces gradually as the period of water shortage becomes later and later. The yield reduction was mainly caused by the decrease in grain number per ear and 100-grain weight (Wen, 2020). Yang et al. (2019) also showed that a water deficit imposed at the tasseling stage significantly reduced the grain number per ear and 100-grain weight of fresh waxy maize, mainly due

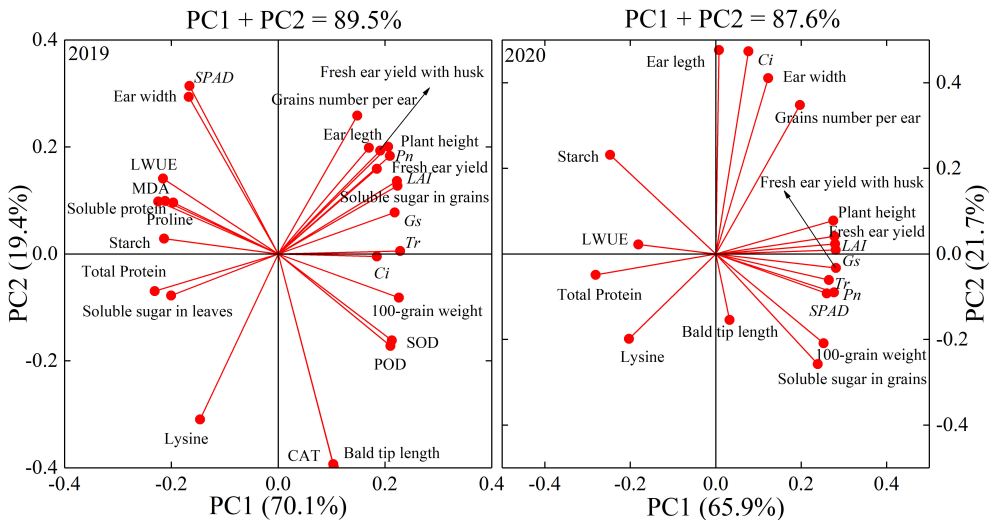

FIGURE 10
Loading diagram of principal component analysis in the 2019 and 2020 seasons. *LAI*, leaf area index; MDA, malonaldehyde; SOD, superoxide dismutase; CAT, catalase; POD, peroxidase; *SPAD*, leaf chlorophyll content index; P_n, net photosynthetic rate; G_s, stomatal conductance; C_i, intercellular CO_2 concentration; T_r, transpiration rate; *LWUE*, leaf water use efficiency. PCn indicates the extracted principal component.

to the decreases in pollen dispersal and grain filling rates. Water deficit not only affects the formation and vitality of pollen but also affects the differentiation of maize spikelets (Li et al., 2022), resulting in a decrease in the number of rows per ear, grain number per ear, and final yield reduction. This study showed that high accumulation of MDA in leaves resulted in quicker leaf senescence, and then decreases in *LAI*, photosynthesis rate, and dry matter accumulation under the D_{V6-VT} treatment. The greatest reductions in 100-grain weight and grain moisture content were investigated under D_{V6-VT} in this study, indicating that the D_{V6-VT} treatment caused the process of starch accumulation in advance and led to poor filling quality. The P_n values in 2020 were generally lower than those in 2019, mainly due to less radiation and a lower temperature in 2020 (Figure 5B), which resulted in a lower 100-grain weight and less dry matter accumulation in 2020 (Gao et al., 2017). The worse radiation environment in the 2020 growing season also led to a decrease in pollen viability and a subsequent decline in grains per ear, which may be the main reason for the remarkable differences in fresh ear yields between the two growing seasons (Zhou et al., 2013).

Effects of water deficits at different growing stages on grain quality of waxy maize

Grain quality was closely related to leaf physiology and yield. Studies have shown that an increase in wheat grain protein content is closely associated with a decrease in yield under water deficit (Ozturk and Aydin, 2004; Flagella et al., 2010). It is also indicated that the starch content of grain was also closely related to yield in barley (Worch et al., 2011). In this experiment with waxy maize, the D_{V6-VT} and D_{VT-R2} treatments increased the total protein contents while decreasing the soluble sugar contents. In addition, the starch and lysine contents were increased by the water deficit imposed at all growing stages. Several studies have shown that water deficit at the grain formation stage may reduce the starch content and increase the total protein content of waxy maize grain (Sun, 2014; Wang et al., 2021b). The increase in protein content was mainly due to the concentration effect of reduced biomass under water deficits (Rotundo and Westgate, 2009). Ma et al. (2006) also showed that the protein and lysine contents of maize grains increased under moderate water deficit conditions. The changes in protein and lysine contents in this study showed very similar trends to those in Ma et al. (2006). D_{V6-VT} resulted in increases in glutenin and albumin contents, but decreases in alcoholic-soluble protein and globulin contents in grains. For the grain quality of waxy maize, the effects of water deficit on grain starch content in this study were opposite to those shown in some previous studies (Sun, 2014; Wang et al., 2021b), maybe mainly because the previous results were investigated from matured grains, whereas fresh grains were used in this study. Debon et al. (1998) and Silva et al. (2001) found that the increase in the starch concentration of fresh fruit of potato was mainly due to the concentration effect caused by the decrease in water content in fresh fruit. Guo et al. (2022) and Shi et al. (2018) also showed an increase in starch content in fresh waxy maize grains under drought stress and indicated that acceleration of grain filling and decreases in grain water content under drought (Figure 7F) might be the main reasons for the starch content increase. Meanwhile, water deficit caused a significantly increase in abscisic acid (ABA) content in maize plant tissues, and then led to the activity increases of four key enzymes related closely to converting soluble sugar into starch (Zhang et al., 2012). Yi et al. (2014) indicated that a water deficit imposed at V6–VT advanced the starch accumulation process in sorghum, and Dai et al. (2008) also indicated that a water deficit increased starch accumulation in wheat at the early filling stage. In our study, both amylose and amylopectin increased under water deficit at the V6–VT period, and the percentage of amylopectin increase was much greater than that of amylose. Water deficit reduced the expression of starch branching enzymes SEBI and SBEIIb genes, which resulted in decreases in amylose and amylopectin content, and then the final total starch content (Wu et al., 2022). The results of PCA (Figure 10) showed that the antioxidant enzymes and gas exchange parameters in leaves were items affected early by water deficit, and ear growth, grain number per ear, 100-grain weight, the water content of fresh grains were affected lately, and fresh ear yield and grain quality as the finally affected items.

Conclusion

The water deficit imposed at the V6–VT stage limits severely the growth of waxy maize plants in the vegetative stage, reduces the 100-grain weight of waxy maize, and results in a significant reduction in fresh ear yield and grain starch accumulation, mainly due to accelerated grain ripening. A water deficit imposed at the VT–R2 stage affects the flowering and pollination of waxy maize plants and results in a significant reduction in grain number per ear and the final ear yield. However, a moderate water deficit imposed at the R2–R3 stage had little effect on growth and development, fresh ear yield, total protein, soluble sugar, and starch content in fresh grains of waxy maize but had significant effects on increasing the lysine content in fresh grains. The results in this study also suggested that more in-depth and comprehensive studies on the effects of water deficit duration imposed at different growing stages should be performed, and suitable techniques for reducing loss of yield and quality caused by water deficit should be developed.

Data availability statement

The raw data supporting the conclusions of this article will be made available by the authors, without undue reservation.

Author contributions

CH: investigation, data curation, formal analysis, visualization, and writing—original draft preparation. AQ: conceptualization, methodology, data curation, formal analysis, writing, and manuscript reviews. YG and SM: methodology, writing—editing and funding acquisition. ZuL, BZ, and DN: provided guidance and manuscript reviews. WG and MS: investigation. KZ and ZiL: conceptualization, writing—editing, supervision, project

administration, and funding acquisition. All authors contributed to the article and approved the submitted version.

Funding

This research was jointly supported by the China Agriculture Research System (CARS-02-18), the Key R&D and promotion projects in Henan Province (212102110291 and 222102110163), the Henan Provincial Natural Science Foundation (202300410553), the Agricultural Science and Technology Innovation Program (ASTIP), the National Natural Science Foundation of China (32101856), and the Key Project of Water Conservancy Science and Technology in Henan Province (Key Technology Innovation and Application of Agricultural Intensive and Efficient Water Use in Irrigation Areas).

Conflict of interest

The authors declare that the research was conducted in the absence of any commercial or financial relationships that could be construed as a potential conflict of interest.

Publisher's note

References

Ali, Q., and Ashraf, M. (2011). Induction of drought tolerance in maize (Zea mays l.) due to exogenous application of trehalose: Growth, photosynthesis, water relations and oxidative defence mechanism. *J. Agron. Crop Sci.* 197, 258–271. doi: 10.1111/j.1439-037X.2010.00463.x

Anjum, S. A., Tanveer, M., Ashraf, U., Hussain, S., Shahzad, B., Khan, I., et al. (2016). Effect of progressive drought stress on growth, leaf gas exchange, and antioxidant production in two maize cultivars. *Environ. Sci. pollut. R.* 23 (17), 17132–17141. doi: 10.1007/s11356-016-6894-8

Beckles, D. M., and Thitisaksakul, M. (2014). How environmental stress affects starch composition and functionality in cereal endosperm. *Die Stärke* 66 (1-2), 58–71. doi: 10.1002/star.201300212

Begcy, K., and Walia, H. (2015). Drought stress delays endosperm development and misregulates genes associated with cytoskeleton organization and grain quality proteins in developing wheat seeds. *Plant Sci.* 240, 109–119. doi: 10.1016/j.plantsci.2015.08.024

Bu, L. D., Zhang, R. H., Han, M. M., Xu, J. Q., and Chang, Y. (2009). The physiological mechanism of compensation effect in maize leaf by re-watering after drought stress. *Acta Agr. Bor-Occid. Sin.* 8 (2), 88–92.

Cai, F., Mi, N., Ji, R. P., Zhao, X. L., Shi, K. Q., Yang, Y., et al. (2017). Effects of drought stress and subsequent rewatering on major physiological parameters of spring maize during the key growth periods. *Chin. J. Appl. Ecol.* 28 (11), 3643–3652. doi: 10.13287/j.1001-9332.201711.015

Chaves, M. M., Flexas, J., and Pinheiro, C. (2009). Photosynthesis under drought and salt stress: Regulation mechanisms from whole plant to cell. *Ann. Bot.* 103 (4), 551–560. doi: 10.1093/aob/mcn125

Dai, Z. M., Wang, Z. L., Zhang, M., Li, W. Y., Yan, S. H., Cai, R. G., et al. (2008). Starch accumulation and activities of enzymes involved in starch synthesis in grains of wheat grown under irrigation and rain-fed conditions. *Sci. Agr. Sinica.* 46 (5), 34–37. doi: 10.1016/0921-8696(86)90292-6

Debon, S. J., Tester, R. F., Millam, S., and Davies, H. V. (1998). Effect of temperature on the synthesis, composition and physical properties of potato microtuber starch. *J. Sci. Food Agr.* 76 (4), 599–607. doi: 10.1002/(SICI)1097-0010(199804)76:43.0.CO;2-F

De Carvalho, R. C., Cunha, A., and Da Silva, J. M. (2011). Photosynthesis by six Portuguese maize cultivars during drought stress and recovery. *Acta Physiol. Plant* 33, 359–374. doi: 10.1007/s11738-010-0555-1

Erbs, M., Manderscheid, R., Hüther, L., Schenderlein, A., Wieser, H., Dänicke, S., et al. (2015). Free-air CO2 enrichment modifies maize quality only under drought stress. *Agron. Sustain. Dev.* 35 (1), 203–212. doi: 10.1007/s13593-014-0226-5

Flagella, Z., Giuliani, M. M., Giuzio, L., Volpi, C., and Masci, S. (2010). Influence of water deficit on durum wheat storage protein composition and technological quality. *Eur. J. Agron.* 33 (3), 197–207. doi: 10.1016/j.eja.2010.05.006

Gao, J., Shi, J. G., Dong, S. T., Liu, P., Zhao, B., and Zhang, J. W. (2017). Effect of different light intensities on root characteristics and grain yield of summer maize (Zea mays l.). *Sci. Agr. Sin.* 50 (11), 2104–2113. doi: 10.3864/j.issn.0578-1752.2017.11.016

Guo, J., Qu, L. L., Wang, L. F., Lu, W. P., and Lu, D. L. (2022) Effects of post-silking drought stress degree on grain yield and quality of waxy maize. *J. Sci. Food Agr.* 1–11. doi: 10.1002/jsfa.12250

Han, C., Lu, X., Yu, Z., Li, X., Ma, W., and Yan, Y. (2015). Rapid separation of seed gliadins by reversed-phase ultraperformance liquid chromatography (RP-UPLC) and its application in wheat variety and germplasm identification. *Biosci. Biotech. Bioch.* 79 (5), 808–815. doi: 10.1080/09168451.2014.998618

Hao, Z. C., and Singh, V. P. (2015). Drought characterization from a multivariate perspective: A review. *J. Hydrol.* 527, 668–678. doi: 10.1016/j.jhydrol.2015.05.031

Huang, C., Zhang, W. Q., Wang, H., Gao, Y., Ma, S. T., Qin, A. Z., et al. (2022). Effects of waterlogging at different stages on growth and ear quality of waxy maize. *Agr. Water Manage.* 266, 207603. doi: 10.1016/j.agwat.2022.107603

IPCC (2014). "Contribution of working group II to the fifth assessment report of the intergovernmental panel on climate change," in *Climate change 2014: Impacts, adaptation, and vulnerability. part a: Global and sectoral aspects.* Eds. C. B. Field, V. R. Barros, D. J. Dokken, K. J. Mach and M. D. Mastrandrea (Cambridge, United Kingdom and New York, NY, USA: Cambridge University Press).

Kimaro, A. A., Mpanda, M., Rioux, J., Aynekulu, E., Shaba, S., Thiong'o, M., et al. (2015). Is conservation agriculture 'climate-smart' for maize farmers in the highlands of Tanzania. *Nutr. Cycl. agroecosys.* 105 (3), 217–228. doi: 10.1007/s10705-015-9711-8

Knutson, C., and Grove, M. (1994). Rapid method for estimation of amylose in maize starches. *Cereal. Chem.* 71 (5), 469–471.

Li, T. L., Hu, X. T., Wang, W. E., Du, B., and Ma, W. G. (2017). Effects of water stress on proline and malondialdehyde content in leaves of spring maize. *Water Saving Irrig.* 6), 34–37.

Li, X. J., Kang, S. Z., Zhang, X. T., Li, F. S., and Lu, H. N. (2018). Deficit irrigation provokes more pronounced responses of maize photosynthesis and water productivity to elevated CO2. *Agr. Water Manage.* 195, 71–83. doi: 10.1016/j.agwat.2017.09.017

Li, H. W., Tiwari, M., Tang, Y. L., Wang, L. J., Yang, S., Long, H. C., et al. (2022). Metabolomic and transcriptomic analyses reveal that sucrose synthase regulates maize pollen viability under heat and drought stress. *Ecotox. Environ. Safe* 246, 114191. doi: 10.1016/j.ecoenv.2022.114191

Liu, Y. H. (2013b). Physiological responses and adaptation of summer maize (Zea mays l) to water stress during different growth periods. *J. Arid Land Resour. Environ.* 27 (2), 171–175. doi: 10.13448/j.cnki.jalre.2013.02.009

Liu, L. M., Klocke, N., Yan, S. P., Rogers, D., Schlegel, A., Lamm, F., et al. (2013a). Impact of deficit irrigation on maize physical and chemical properties and ethanol yield. *Cereal. Chem.* 90, 453–462. doi: 10.1094/CCHEM-07-12-0079-R

Liu, C., Li, Z. T., Yang, K. J., Xu, J. Y., Wang, Y. F., Zhao, C. J., et al. (2015). Effects of water stress and subsequent rehydration on physiological characteristics of maize (Lea mays) with different drought tolerance. *J. Plant Physiol.* 51 (5), 702–708. doi: 10.13592/j.cnki.ppj.2015.0038

Lu, D., Cai, X., Zhao, J., Shen, X., and Lu, W. (2015). Effects of drought after pollination on grain yield and quality of fresh waxy maize. *J. Sci. Food Agr.* 95 (1), 210–215. doi: 10.1002/jsfa.6709

Ma, X. L., Cui, Z. H., Chen, J., Xiao, C. L., Zhang, L. J., and Wang, Q. X. (2006). Effect of drought stress during seedling stage on the content of grain crude protein, and lysine of maize. *J. Maize Sci.* 14 (2), 71–74. doi: 10.13597/j.cnki.maize.science.2006.02.026

Markelz, R. J. C., Strellner, R. S., and Leakey, A. D. B. (2011). Impairment of C4 photosynthesis by drought is exacerbated by limiting nitrogen and ameliorated by elevated [CO2] in maize. *J. Exp. Bot.* 62, 3235–3246. doi: 10.1093/jxb/err056

Ma, Y. P., Sun, L. L., and Ma, X. Q. (2016). Ecophysiological responses of summer maize to drought and waterlogging in Huang-Huai-Hai plain. *Agr. Res. Arid Area* 34 (4), 85–93. doi: 10.7606/j.issn.1000-7601.2016.04.13

Ozturk, A., and Aydin, F. (2004). Effect of water stress at various growth stages on some quality characteristics of winter wheat. *J. Agron. Crop Sci.* 190 (2), 93–99. doi: 10.1046/j.1439-037X.2003.00080.x

Park, I. M., Ibanez, A. M., and Shoemaker, C. F. (2007). Rice starch molecular size and its relationship with amylose content. *Starch-Stärke* 59 (2), 69–77. doi: 10.1002/star.200600568

Qin, A., Ning, D., Liu, Z., Sun, B., Zhao, B., Xiao, J., et al. (2019). Insentek sensor: An alternative to estimate daily crop evapotranspiration for maize plants. *Water* 11 (1), 25. doi: 10.3390/w11010025

Rotundo, J. L., and Westgate, M. E. (2009). Meta-analysis of environmental effects on soybean seed composition. *Field Crop Res.* 110 (2), 147–156. doi: 10.1016/j.fcr.2008.07.012

Sandhya, V. S. K. Z., Ali, S. Z., Grover, M., Reddy, G., and Venkateswarlu, B. (2010). Effect of plant growth promoting pseudomonas spp. on compatible solutes, antioxidant status and plant growth of maize under drought stress. *Plant Growth Regul.* 62 (1), 21–30. doi: 10.1007/s10725-010-9479-4

Santisopasri, V., Kurotjanawong, K., Chotineeranat, S., Piyachomkwan, K., Sriroth, K., and Oates, C. G. (2001). Impact of water stress on yield and quality of cassava starch. *Ind. Crop Prod.* 13, 115–129. doi: 10.1016/S0926-6690(00)00058-3

Shi, L. J., Wen, Z. R., Zhang, S. B., Wang, J., Lu, W. P., and Lu, D. L. (2018). Effects of water deficit at flowering stage on yield and quality of fresh waxy maize. *Acta Agron. Sin.* 44 (8), 1205–1211. doi: 10.3724/SP.J.1006.2018.01205

Silva, J. A. B., Otoni, W. C., Martinez, C. A., Dias, L. M., and Silva, M. (2001). Microtuberization of andean potato species (solanum spp.) as affected by salinity. *Sci. Hortic-Amsterdam* 89 (2), 91–101. doi: 10.1016/S0304-4238(00)00226-0

Simova, S. L., Demirevska, K., Petrova, T., Tsenov, N., and Feller, U. (2008). Antioxidative protection in wheat varieties under severe recoverable drought at seedling stage. *Plant Soil Environ.* 54, 529–536. doi: 10.17221/427-PSE

Si, Z., Muhammad, Z., Mehmood, F., Wang, G., Gao, Y., and Duan, A. (2020). Effects of nitrogen application rate and irrigation regime on growth, yield, and water-nitrogen use efficiency of drip-irrigated winter wheat in the north China plain. *Agr. Water Manage.* 231, 106002. doi: 10.1016/j.agwat.2020.106002

Singh, S., Singh, G., Singh, P., and Singh, N. (2008). Effect of water stress at different stages of grain development on the characteristics of starch and protein of different wheat varieties. *Food Chem.* 108, 130–139. doi: 10.1016/j.foodchem.2007.10.054

Song, H., Li, Y., Zhou, L., Xu, Z., and Zhou, G. (2018). Maize leaf functional responses to drought episode and rewatering. *Agr. For. Meteorol.* 249, 57–70. doi: 10.1016/j.agrformet.2017.11.023

Sun, X. L. (2014). *Effects of soil moisture stress during grain filling on grain yield and starch quality of waxy maize* (Yangzhou, China: Yangzhou Univ).

Thitisaksakul, M., Jiménez, R. C., Arias, M. C., and Beckles, D. M. (2012). Effects of environmental factors on cereal starch biosynthesis and composition. *J. Cereal. Sci.* 56 (1), 67–80. doi: 10.1016/j.jcs.2012.04.002

Ulfat, A., Shokat, S., Li, X., Fang, L., Großkinsky, D. K., Majid, S. A., et al. (2021). Elevated carbon dioxide alleviates the negative impact of drought on wheat by modulating plant metabolism and physiology. *Agr. Water Manage.* 250, 106804. doi: 10.1016/j.agwat.2021.106804

Wang, Y., and Frei, M. (2011). Stressed food-the impact of abiotic environmental stresses on crop quality. *Agr. Ecosyst. Environ.* 141 (3-4), 271–286. doi: 10.1016/j.agee.2011.03.017

Wang, J., Fu, P. X., Lu, W. P., and Lu, D. L. (2020). Application of moderate nitrogen levels alleviates yield loss and grain quality deterioration caused by post-silking heat stress in fresh waxy maize. *Crop J.* 8 (6), 1081–1092. doi: 10.1016/j.cj.2019.11.007

Wang, H., Lu, Y. L., Sun, D. P., Yu, D. S., Shi, B., Lin, J. Y., et al. (2014). Breeding of a new waxy maize cultivar 'Shenkenuo 1'. *Acta Agr. Shanghai* 30 (6), 50–53.

Wang, J., Mao, Y., Huang, T., Lu, W., and Lu, D. (2021b). Water and heat stresses during grain formation affect the physicochemical properties of waxy maize starch. *J. Sci. Food Agr.* 101 (4), 1331–1339. doi: 10.1002/jsfa.10743

Wang, L., Yan, Y., Lu, W., and Lu, D. (2021a). Application of exogenous phytohormones at silking stage improve grain quality under post-silking drought stress in waxy maize. *Plants* 10 (1), 48. doi: 10.3390/plants10010048

Worch, S., Rajesh, K., Harshavardhan, V. T., Pietsch, C., and Sreenivasulu, N. (2011). Haplotyping, linkage mapping and expression analysis of barley genes regulated by terminal drought stress influencing seed quality. *BMC Plant Biol.* 11 (1), 1–14. doi: 10.1186/1471-2229-11-10

Wu, W. H., Qu, J. Z., Blennow, A., Herburger, K., Hebelstrup, K. H., Guo, K., et al. (2022). The effects of drought treatments on biosynthesis and structure of maize starches with different amylose content. *Carbohyd. Polym.* 297, 120045. doi: 10.1016/j.carbpol.2022.120045

Xiao, J. F., Liu, Z. D., Liu, Z. G., and Nan, J. Q. (2011). Effects of drought at different growth stages and different water availabilities on growth and water consumption characteristics of summer maize. *J. Maize Sci.* 19 (4), 54–58, 64. doi: 10.13597/j.cnki.maize.science.2011.04.025

Yang, H., Gu, X. T., Ding, M. Q., Lu, W. P., and Lu, D. L. (2019). Activities of starch synthetic enzymes and contents of endogenous hormones in waxy maize grains subjected to post-silking water deficit. *Sci. Rep-Uk* 9 (1), 1–8. doi: 10.1038/s41598-019-43484-0

Yao, C. X., Zhang, S. Q., and Yan, X. J. (2012). Effects of drought and re-watering on photosynthetic characteristics of maize leaf. *Res. Soil Water Conserv.* 19 (3), 278–283.

Ye, Y. X., Lu, D. L., Wang, F. B., Chen, X. H., Qi, M. Y., He, R., et al. (2020b). Effects of exogenous trehalose on physiological characteristics in waxy maize seedlings under drought stress. *J. Maize Sci.* 28 (3), 80–86. doi: 10.13597/j.cnki.maize.science.20200310

Ye, Y. X., Wen, Z. R., Yang, H., Lu, W. P., and Lu, D. L. (2020a). Effects of post-silking water deficit on the leaf photosynthesis and senescence of waxy maize. *J. Integr. Agr.* 19 (9), 2216–2228. doi: 10.1016/S2095-3119(20)63158-6

Yi, B., Zhou, Y. F., Gao, M. Y., Zhang, Z., and Han, Y. (2014). Effect of drought stress during flowering stage on starch accumulation and starch synthesis enzymes in sorghum grains. *J. Integr. Agr.* 13 (11), 2399–2406. doi: 10.1016/S2095-3119(13)60694-2

Zhang, H., Li, H., Yuan, L., Wang, Z., Yang, J., and Zhang, J. (2012). Post-anthesis alternate wetting and moderate soil drying enhances activities of key enzymes in sucrose-to-starch conversion in inferior spikelets of rice. *J. Exp. Bot.* 63 (1), 215–227. doi: 10.1093/jxb/err263

Zhao, Q. (2017). *Selection of waxy maize materials and comprehensive evaluation* (Changchun, China: Jilin Agr. Univ).

Zhou, W. X., Wang, X. P., Mu, X. Y., and Li, C. H. (2013). Effects of low-light stress on Male and female flower development and pollination and fructification ability of different maize (Zea mays l.) genotypes. *Acta Agron. Sin.* 39 (11), 2065–2073. doi: 10.3724/SP.J.1006.2013.02065

Wen, Z. R. (2020). *Effects of post-silking heat and drought stress on grain development of waxy maize* (Yangzhou, China: Yangzhou Univ).

frontiers | Frontiers in Plant Science

TYPE Original Research
PUBLISHED 16 February 2023
DOI 10.3389/fpls.2023.1128780

OPEN ACCESS

EDITED BY
Xuecai Zhang,
International Maize and Wheat Improvement Center, Mexico

REVIEWED BY
Mingnan Qu,
Shanghai Institutes for Biological Sciences (CAS), China
Jiban Shrestha,
Nepal Agricultural Research Council, Nepal

*CORRESPONDENCE
Xuemei Zhong
zhongxuemei@syau.edu.cn

SPECIALTY SECTION
This article was submitted to Plant Abiotic Stress, a section of the journal Frontiers in Plant Science

RECEIVED 21 December 2022
ACCEPTED 03 February 2023
PUBLISHED 16 February 2023

CITATION
Fu J, Li L, Wang S, Yu N, Shan H, Shi Z, Li F and Zhong X (2023) Effect of gibberellic acid on photosynthesis and oxidative stress response in maize under weak light conditions.
Front. Plant Sci. 14:1128780.
doi: 10.3389/fpls.2023.1128780

Effect of gibberellic acid on photosynthesis and oxidative stress response in maize under weak light conditions

Jianjun Fu[1], Linlin Li[1], Shuang Wang[1], Na Yu[1], Hong Shan[2], Zhensheng Shi[1], Fenghai Li[1] and Xuemei Zhong[1*]

[1]Special Corn Institute, Shenyang Agricultural University, Shenyang, China, [2]Liaoning Dongya Seed Co., Ltd., Shenyang, China

Gibberellin (GA) is an important endogenous hormone involved in plant responses to abiotic stresses. Experiments were conducted at the Research and Education Center of Agronomy, Shenyang Agricultural University (Shenyang, China) in 2021.We used a pair of near-isogenic inbred maize lines comprising, SN98A (light-sensitive inbred line) and SN98B (light-insensitive inbred line) to study the effects of exogenous gibberellin A3 (GA_3) application on different light-sensitive inbred lines under weak light conditions. The concentration of GA_3 was selected as 20, 40 and 60 mg L^{-1}. After shade treatment, the photosynthetic physiological indexes of SN98A were always lower than SN98B, and the net photosynthetic rate of SN98A was 10.12% lower than SN98B on the 20th day after shade treatment. GA_3 treatments significantly reduced the barren stalk ratios in SN98A and improved its seed setting rates by increasing the net photosynthetic rate (Pn), transpiration rate (Tr), stomatal conductance (Gs), photosynthetic pigment contents, photochemical efficiency of photosystem II (PS II) (Fv/Fm), photochemical quenching coefficient (qP), effective quantum yield of PSII photochemistry (Φ_{PSII}), and antioxidant enzyme activities, where the most effective treatment was 60 mg $L^{-1}GA_3$. Compared with CK group, the seed setting rate increased by 33.87%. GA_3 treatment also regulated the metabolism of reactive oxygen species (ROS) and reduced the superoxide anion (O_2^-) production rate, H_2O_2 content, and malondialdehyde content. The superoxide anion (O_2^-) production rate, H_2O_2 content and malondialdehyde content of SN98A sprayed with 60 mg L^{-1} GA_3 decreased by 17.32%,10.44% and 50.33% compared with CK group, respectively. Compared with the control, GA_3 treatment significantly ($P < 0.05$) increased the expression levels of *APX* and *GR* in SN98A, and *APX*, *Fe-SOD*, and *GR* in SN98B. Weak light stress decreased the expression of *GA20ox2*, which was related to gibberellin synthesis, and the endogenous gibberellin synthesis of SN98A. Weak light stress accelerated leaf senescence, and exogenous GA_3 application inhibited the ROS levels in the leaves and maintained normal physiological functions in the leaves. These results indicate that exogenous GA_3 enhances the adaptability of plants to low light stress by regulating photosynthesis, ROS metabolism and protection mechanisms, as well as the expression of key genes, which may be an economical and environmentally friendly method to solve the low light stress problem in maize production.

KEYWORDS

maize, low light stress, GA3, barren stalk, photosynthesis

Introduction

Under suitable cultivation conditions, the productivity of different crops is strongly related to the amount of light radiation intercepted in the crop canopy (Slattery and Ort, 2021), where excessive or insufficient amounts of light energy will have adverse effects on photosynthesis by crops (Ferrante and Mariani, 2018). Maize (*Zea mays* L.) is a light-loving and light-sensitive crop (Wang et al., 2016; Xue et al., 2019), but due to frequent extreme weather events in recent years, maize plants have experienced continuous low-temperature and rainy weather in the booting stage. These conditions can severely affect ear development and grain formation in maize, thereby resulting in large areas which high proportions of hollow straw and severe bald tip in some varieties (Huang et al., 2022), which are extremely unfavorable for agricultural production. Light is necessary for photosynthesis and it is the basis of plant life. Insufficient light will lead to decreases in the net photosynthetic rate (Pn) and partial chlorophyll fluorescence parameters in leaves (Qu et al., 2017; Wegrzyn and Mazur, 2020; Feng et al., 2021; Zahra et al., 2022). During this process, plant leaf cells undergo complex changes in physiological processes and cell metabolism, such as chloroplast decomposition, loss of photosynthetic activity, decomposition of chlorophyll and macromolecular compounds, and programmed cell death (Asad et al., 2019). These changes are associated with increases in intracellular reactive oxygen species (ROS) (Ramel et al., 2009). Insufficient light will accelerate leaf senescence and result in the excessive accumulation of ROS, oxidative damage to proteins, nucleic acids, and membrane lipids (Jbir-Koubaa et al., 2015), and decreases or losses of the activities of various enzymes (Mittler, 2002; Gill and Tuteja, 2010). As a consequence, the integrity of the cell membrane can be disrupted (Benlloch-Gonzalez et al., 2015), and the normal functions of chloroplast and mesophyll cells are eventually damaged, with decreased photosynthetic electron transport efficiency (Feng et al., 2021). Plants have a complete protective system of antioxidant enzymes that remove excessive ROS to protect the photosynthetic system and enhance adaptation to stress (Li et al., 2020).These enzymes include superoxide dismutase (SOD), and peroxidase (POD) (Dvorak et al., 2021). Thus, the antioxidant enzyme activity is an important indicator for evaluating whether the redox balance of plant cells is disrupted under adverse conditions (Gill et al., 2013).

The changes in the dependence of plant growth and development on light are regulated by plant hormones (Zhong et al., 2012). The changes in levels of plant hormones under shading are active responses by plants to adverse environments, and they provide the physiological basis that allows plants to make better use of assimilation products (Jiang et al., 2021). Gibberellin (GA) is necessary for the shade avoidance response in plants (Djakovic-Petrovic et al., 2007). In a previous study, we measured the changes in the contents of various hormones in two different light-sensitive inbred lines under shade treatment and in a control group without shade. According to the activities of the hormones, we found that the change in the gibberellin A_3 (GA_3) content was the most important. GA_3 is a type of tetracyclic diterpene plant hormone that can regulate many plant growth and development processes (e.g., seed germination, stem elongation, pollen maturation and fruit development), and one of its important functions is regulating the flowering time (Vicente and Plasencia, 2011). Previous studies of *Arabidopsis* showed that endogenous GA was necessary for flowering under non-induced conditions, and the flowering time was generally delayed in a GA synthesis defect mutant and GA signal transduction mutant (Rood et al., 1989; Ni and Bradford, 1993; Magome et al., 2004). Exogenous GA application can also promote flowering in *Arabidopsis thaliana* (Ezura and Harberd, 1995; Sauret-Gueto et al., 2012; Bao et al., 2020). It should also be noted GA is an excellent antioxidant that can enhance the tolerance of various biological and abiotic stresses by plants (Yamaguchi et al., 2014; Khan et al., 2015). GA_3 can also increase the number of cell divisions by activating the intermediate meristems to promote cell division (Mcatee et al., 2013). Guo et al. (2022) showed that spraying GA_3 could improve photosynthesis and the antioxidant defenses to increase the yield in salted wood pea. The exogenous application of GA_3 can delay the degradation of chlorophyll and protein, reduce the malondialdehyde (MDA) content, and delay plant senescence (Yu et al., 2009; Wang et al., 2015). Under low light stress, the abscisic acid (ABA) and zeatin (ZT) contents of soybean leaves decreased, whereas the indole acetic acid (IAA) and gibberellin (GA_3) contents increased. Similar results were obtained in previous studies of maize leaves under low light conditions, thereby suggesting that the response of this hormone to low light is an active stress response that allows plants to adapt to low light environments. Therefore, it is of great theoretical and practical significance to study the regulatory effects of exogenous GA_3 on different light-sensitive inbred maize lines under low light condition.

During the breeding of inbred maize lines over numerous years, we found and bred two inbred maize lines called SN98A and SN98B with extreme differences in their culms. In particular, the distinction, SN98A is called the "ear differentiation and sensitive to low light intensity inbred line"(ESL) and SN98B is called the "ear differentiation and insensitive to low light intensity near isogenic line" (EISL-NIL). Under low light stress condition, the hollowing rate in SN98A was 98% and that in SN98B was 0. Thus, in the present study, we used these weak light sensitive near-isogenic lines as experimental materials. By applying GA_3 to leaves, the regulation effect of exogenous GA_3 on empty stalk of maize under low light condition was analyzed. Through the analysis of photosynthetic response, antioxidant enzyme activity and other indexes, the purpose was to find out which physiological indexes of maize were affected by low light stress to induce maize stalk emptying. The regulatory effect of exogenous GA_3 on maize hollows under low light conditions and its regulatory mechanism were discussed, so as to provide solutions for poor maize yield under bad weather conditions.

Materials and methods

Plant materials and experimental design

The maize varieties used in this study were SN98A and SN98B, which are inbred maize lines with extreme differences in the frequency of hollow culms. Under certain low light conditions, the hollow culm rate in SN98A is as high as 98%, whereas SN98B exhibits a normal ear setting. A field experiment was conducted at the South Experimental Base of Shenyang Agricultural University (41°48′N, 123°34′E) in July 2021. The normal light intensity from late July to

early August in the Northern Test Field at Shenyang Agricultural University was usually between 1100– 1500 μmol m^{-2} s^{-1}, with an average light intensity of about 1300 μmol m^{-2} s^{-1}. Soil characteristics for temperate subhumid continental climate, the climate belongs to the temperate monsoon climate. A split block design was applied in the experiment. The concentration of GA_3 was the main influence factor and the inbred line was the secondary influence factor. The length of the plot was 5 m, the row spacing was 0.6 m, and each plot had 15 rows. In the first three days of the tasseling period, 38% shading was applied with a black shade net, and different concentrations of GA_3 were applied by spraying (Beijing Merida Technology Co., Ltd, China), 20mg L^{-1}, 40mg L^{-1}, and 60mg L^{-1} or water as the control. Samples were taken at five, 10, 15, and 20 days after shading, which were frozen in liquid nitrogen and then stored at -80°C. Each treatment was repeated three times.

Phenotypic evaluations

The number of plants, number of bearing plants (with more than 20 grains), and the number of plants with empty stems under each treatment determined during the harvest period. The seed setting rate (%) and empty stalk rate (%) were calculated. Seed setting rate (%) = number of seeds/total number of plants *100%. Empty stalk rate (%) = number of empty culms/total number of plants *100%.

Gas-exchange parameters

Net photosynthetic rate, stomatal conductance, transpiration rate and intercellular carbon dioxide concentration of panicle leaves under different treatments were measured by Li-6400 (US-COR) portable photosynthesometer at 5, 10, 15 and 20 days after shading (Zhou et al., 2022). The measuring time was 9:00-11:00 a.m. The measured environment was 400mol (CO_2) mol^{-1} and 50% relative humidity. Ten replicates per process.

Photosynthetic pigment contents

To determine the photosynthetic pigment contents (chlorophyll a (Chl a) and chlorophyll b (Chl b)), 0.1g of fresh leaves were crushed, soaked in 10 mL of acetone, and kept in the dark for 48 h. Chl was extracted and analyzed according to the methods reported by Lichtenthaler and Wellburn (1983). The absorbance values were then recorded at 645 and 663 nm by using a spectrophotometer (Multiskan GO, Thermo Fisher Science, USA), with acetone as a blank control. The following formulae were used to calculate the photosynthetic pigment contents:

Chl a [mg g^{-1} (FM)] = (12.7 × OD663–2.69 × OD645) ×V/M (1000×M)

Chl b [mg g^{-1} (FM)] = (22.9 × OD645–4.68 × OD663) × V/M (1000×M)

Chl (a+b) [mg g^{-1}(FM)] = Chl a + Chl b

where OD645 and OD663 represent the absorbance values for Chl a/b at the corresponding wavelengths, V represents the total volume of the extract, and M represents the mass of the sample. Each treatment was repeated three times.

Determination of chlorophyll fluorescence parameters

The panicle leaves were removed 20cm from the tip, placed in wet gauze, and stored for 30 min under certain humidity in the dark and away from light. The FluorCam (Czech PSI) chlorophyll fluorescence imaging system was used to determine the photochemical efficiency of photosystem II (PS II) (Fv/Fm). Chlorophyll fluorescence parameters were determined comprising the photochemical quenching coefficient (qP) and non-photochemical quenching coefficient (NPQ) and images were collected. Each treatment was repeated three times.

Determination of H_2O_2 content and antioxidant enzyme activities

POD (extinction coefficient = 25.2 mm^{-1} cm^{-1}) was determined at 470 nm in a 1.0 mL reaction mixture containing 100 mM potassium phosphate buffer (pH 6.0), 16 mM guaiacol, 5 μL 10% (v/v) H_2O_2, and enzyme extract. The SOD activity was measured based on its capacity to inhibit blue light in the chemical reduction of nitrotetrazolium, which was monitored at 560 nm (Abedi and Pakniyat, 2010). Three biological replicates were tested for each sample.

Determination of MDA and superoxide radical contents

The MDA content was determined by using the thiobarbituric acid method to evaluate the level of lipid peroxidation. Leaf tissue (0.5 g) was homogenized in 5.0 mL of 10% trichloroacetic acid and centrifuged at 4°C and 10,000×*g* for 10 min. The supernatant was assessed as described by Hodges et al. (1999). According to the method of Xia et al. (2009), with some modifications. The panicle leaves were sampled, cleaned with distilled water, and sucked dry. They were then placed in 50 mL 0.5 mg mL–1 NBT reaction solution (potassium phosphate buffer, pH 7.8) and incubated in darkness at 25°C for 2 h to detect O_2^-. Three biological replicates were tested for each sample.

Real-time fluorescence quantitative PCR detection of expressed of target genes

The *ZmActin* gene in maize was used as the internal reference gene and SYBR Green Real-time PCR Master Mix was used as the fluorescent dye. The samples were tested after shading for 15 days. The template comprised cDNA diluted 20 times and it was repeated three times. The total reaction system volume was 20 μL and the reaction conditions comprised: 95°CC for 30 s, and 45 cycles at 60°CC for 30 s and 72°CC for 30s (Xu et al., 2023). After PCR, the dissolution curve was analyzed. The primers used are shown in Tables 1, 2.

TABLE 1 Primers used real-time fluorescence quantitative PCR.

Primer name	Primer (5′-3′)
ZmActin	F:GTTAAAGATTGCGCCACCT.R:GCCTGACGTACCATGTCGAAC
APX	F:CGCGCATTTCCAGATCTTTG.R:GATCGATGCGAGATCAGGGG
Fe-SOD	F:CGACTGTCCCTTCTCACAAA.R:ATCCGGTAAGGGACCTTCTT
GR	F:TTGGCAATGAACCTACCAAA.R:CAATTGCCTGCTCCTCAGTA

TABLE 2 Primers used real-time fluorescence quantitative PCR.

Primer name	Primer(5′-3′)
DELLA1	F:GCAAATCAAGCCATCCTC. R:AGCAAACGGCACTCTAACT
DELLA2	F:CAGGCGGTCCTCCTTCATTCC.R:GCTATCGCTTCTGGTTCCTCGTCGG
DELLA3	F:CAGCAACAGCAAGCCACA.R:CCACTTCTTCCACGCAATAC
GID1C1	F:CCCAATGGGAATGATCTCAA.R:ACAATTAGAACTCACAAAACCCTT
GID1C2	F:TCAACCCCACCCGAATCC.R:AGGTCGCCGTTGCATGTT
GID1C3	F:CAATTCACCCAATTCTAACC.R:AAATGCCTTCCAATACCAA
GA20ox2	F:CCCTCACCATTCTCCAACA.R:CCCGGACCACCTTATCTTC
KAO1	F:TTTGAAGGCAAGAAAGACG.R:TGTGATATGACCCGAAGAT
KAO2	F:ATGATTGACTTCTTGTGGTGCTT.R:TTAGACATCGCCGTAACCCCTT

Statistical analysis

DPS (version 9.01) was used for multiple comparative analysis between treatments, the confidence level was 0.05, and one-way ANOVA was used. Data are expressed as mean standard deviation. Chart using Origin 2021 software.

Results

Seed setting rate and hollow stalk rate

Figure 1A shows that after spraying GA_3, the seed setting rate increased in the two inbred lines and the hollow stalk rate decreased. The seed setting rates were highest in the 60 mg L^{-1} GA_3 treatment groups, where those in SN98A and SN98B were 23.56% and 14.68% higher than that in the control group sprayed with water, respectively (Fig 1A).Treatment with GA_3 at 60 mg L^{-1} obtained the lowest hollowing rates, where the rates were 14.25% and 12.34% lower in SN98A and SN98B than the controls, respectively (Figure 1B).

Photosynthetic parameters

Figure 2 shows that in the control group under low light weak light conditions, Pn continued to decrease in SN98A, whereas Pn in SN98B tended to decrease initially before then increasing. Among the two inbred lines, Pn was always higher in SN98B than SN98A. After GA_3 treatment, Pn and the transpiration rate (Tr) were significantly higher in SN98A compared with the control. After shading for 20 days, the mean Pn and Tr values in the three treatment groups were 10.88% and 68.43% higher than those in the control, respectively. Thus, GA_3 treatment had a positive regulatory effect on Pn in the low light-sensitive inbred line SN98A. Treatment with 40 mg L^{-1} GA_3 had the greatest effect but the difference between the treatments was not significant (Figure 2). After GA_3 treatment, the stomatal conductance (Gs) was generally higher in the two inbred lines than the control, and the external application of 60 mg L^{-1} GA_3 had the greatest effect. The intercellular CO_2 concentrations in the two inbred lines were also lowest at this concentration. Thus, the external application of GA_3 under low light conditions increased Gs for the maize leaves and enhanced the photosynthetic activity of the mesophyll cells according to the Pn results. Pn increased under low light conditions in SN98A.

Chlorophyll fluorescence parameters

After shading treatment, Fv/Fm, the effective quantum yield of PSII photochemistry (Φ_{PSII}), and qP were significantly lower in the SN98A control group than SN98B, whereas the NPQ values were significantly higher compared with SN98B. Compared with the control, GA_3 significantly improved the PSII photosynthetic characteristics of maize leaves, where treatment with 60 mg L^{-1} GA_3 had the greatest effect, and SN98A had the highest Fv/Fm, Φ_{PSII} and qP values. On day 20 under 60 mg L^{-1} GA_3 treatment, the Fv/Fm, Φ_{PSII}, and qP values in SN98A were 6.9%, 16.39%, and 14.75% higher, respectively, compared with those in the control, and the NPQ value was 22.89% lower compared with the control (Figure 3). The effect of GA_3 treatment on SN98B was not significant, but the photosynthetic activity of PSII was higher than that in SN98A, thereby indicating that GA_3 was involved in the shading reaction by maize leaves and it had a positive role in maintaining the photosynthetic efficiency of maize leaves under low light stress.

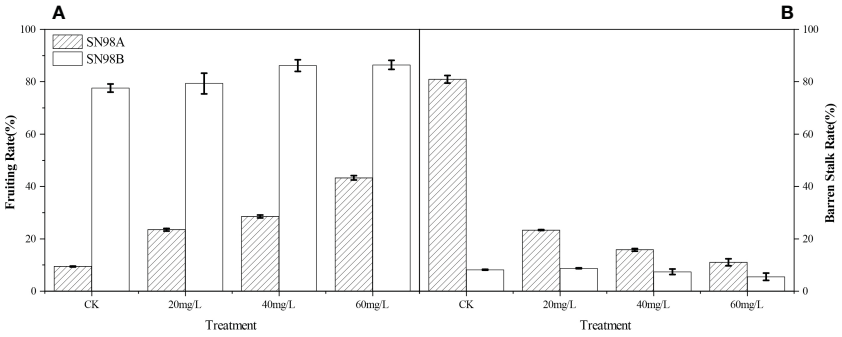

FIGURE 1
Effects of exogenous GA_3 on seed setting rate and hollow stalk rate in different light-sensitive inbred maize lines under low light-stress. **(A)** Seed setting rates in different light-sensitive inbred maize lines sprayed with different concentrations of GA_3 and water. **(B)** Hollow stalk rates in different light-sensitive inbred maize lines sprayed with different concentrations of GA_3 and water. CK is the control water spraying treatment under shade. The numbers 20, 40, and 60 denote GA_3 concentrations of 20 mg L^{-1}, 40 mg L^{-1}, and 60 mg L^{-1}, respectively. SN98A is the shade intolerant line and SN98B is the shade tolerant line. Values are expressed as mean ± SD of three replicates. Lower-case letters indicate the mean difference of different treatments in the same period, which is statistically significant (P<0.05).

Chlorophyll contents

Figure 4 shows that under shading treatment, the Chl a, Chl b and Chl (a+b) contents in the SN98A control group tended to increase initially and then decrease, whereas the Chl content in SN98B did not significantly and it was always higher than that in SN98A. Compared with the control, GA_3 had a significant positive regulatory effect on the photosynthetic pigment contents of the low light-sensitive inbred line SN98A, and the Chl a, Chl b and Chl (a+b) contents increased under all three GA_3 treatments. The effect of treatment with 60 mg L^{-1} GA_3 was most obvious, and the photosynthetic pigment contents increased on days 5, 10, 15, and 20 after treatment, where the Chl (a+b) contents increased by 25.7%, 19.6%, 2.9% and 17.3%, respectively. The photosynthetic pigment content of SN98B was the same as that of the control and it was always higher than that of SN98A, where the content was significantly higher in SN98B on day 10 after treatment with 60 mg L^{-1} GA_3.

ROS contents and membrane lipid peroxidation

Under shading, the H_2O_2 and O_2^- contents increased initially and then decreased in the SN98B control group, whereas the H_2O_2 and O_2^- contents continued to increase in the hollowing line SN98A and the contents were always higher than those in SN98B (Figure 5). After GA_3 treatment, the H_2O_2 and O_2^- contents of the two inbred lines were lower compared with those in the control group. After shading for 15days, treatment with 60 mg $L^{-1}GA_3$ significantly reduced the O_2^- production rate and H_2O_2 content of SN98A by 17.3% and 10.4%, respectively. In the control and treatment groups, the H_2O_2 and O_2^- contents were always higher in SN98A than SN98B, and the ROS contents were always lower in SN98B. The changes in the ROS contents (H_2O_2 and O_2^-) were basically the same. GA_3 treatment significantly reduced the MDA contents of the two inbred lines under low light. The MDA contents were higher in SN98A than SN98B in both the control and treatment groups (Figure 6). The effects of short-term shading were similar under the three treatments, but the effect of treatment with 20 mg L^{-1} GA_3 decreased as the shading period continued. In conclusion, the application of GA_3 could have reduced the peroxidation of membrane lipids caused by the accumulation of ROS in maize leaves to delay leaf senescence and enhance the tolerance of shading in maize. Treatments with 40 mg L^{-1} and 60 mg L^{-1} GA_3 were most effective.

Antioxidant enzyme activities

After shading and treatment with different concentrations of GA_3, the SOD and POD activities increased initially and then decreased in the SN98A control group, where the activities were highest after shading for 10 days. The POD activities continued to increase in SN98B and did not peak until 20 days. During short-term shading the antioxidant system was activated to remove ROS and maintain crop growth. Crops can avoid damage caused by short-term adverse conditions by activating their stress response mechanisms, but they cannot prevent damage under long-term adverse conditions. After treatment with GA_3 at different concentrations, the antioxidant enzyme activities were significantly higher in SN98A than the control (Figure 7), where treatment with 60 mg L^{-1} GA_3 had the most significant effect. After shading for 20 days, the SOD and POD enzyme activities in SN98A were 17% and 31.7% higher compared with the control, respectively, and the difference was significant (Figures 7A, C).

Antioxidant-related genes

Real-time fluorescence quantitative PCR analysis was performed to quantify the expression levels of three genes related to antioxidant stress, and the results are shown in Figure 8. Compared with the control, after GA_3 treatment, the expression levels of *APX* (Figure 8A) and *GR* (Figure 8C) were significantly higher in SN98A under treatment with different GA_3 concentrations, where the expression levels were highest under treatment with 60 mg L^{-1} GA_3, i.e., 6.73 and 2.75 times than those in the control, respectively. The expression levels of *APX* and *GR* under treatment with 40 mg L^{-1} GA_3 were 5.41 times and 1.93 times those in the control, respectively. The expression of *Fe-SOD* (Figure 8B) did not increase significantly in SN98A, where

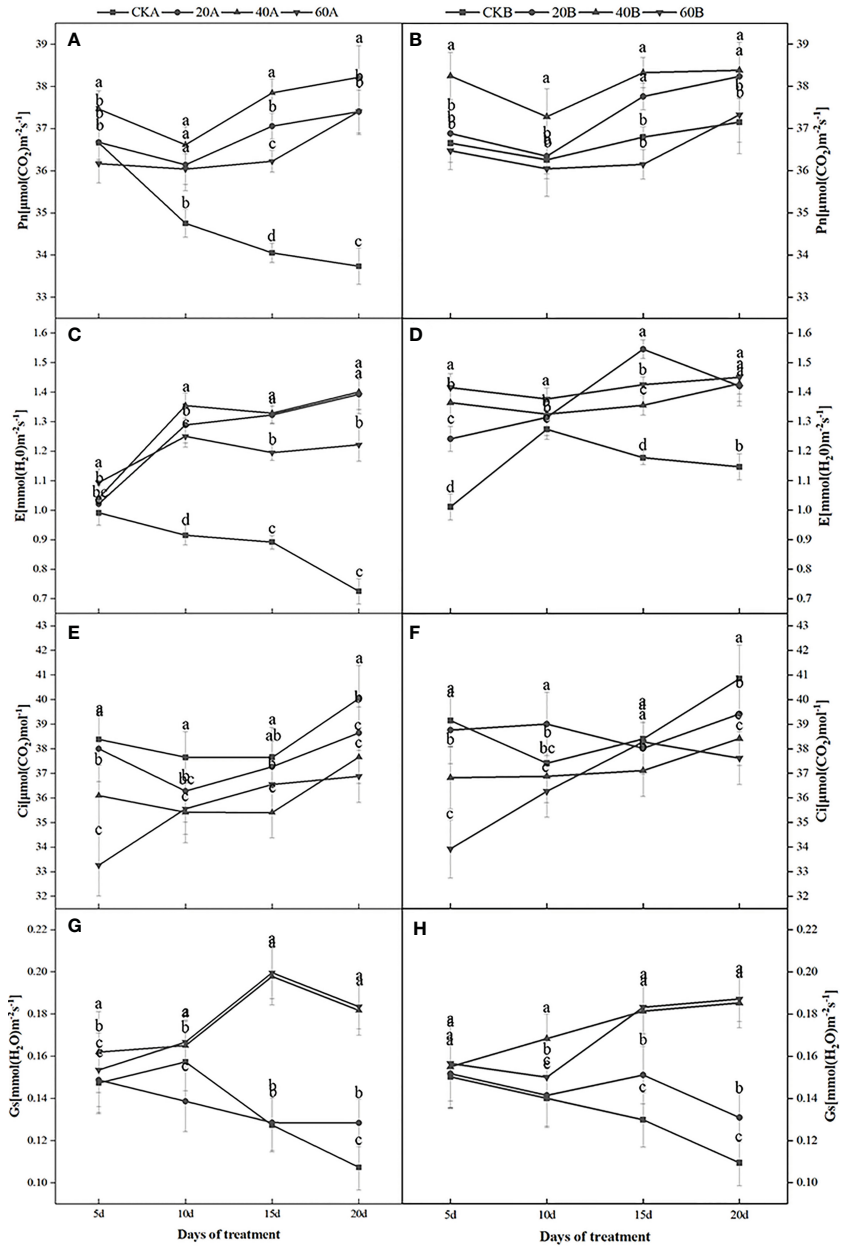

FIGURE 2
Effects of GA_3 on net photosynthetic rate (Pn), transpiration rate (Tr), intercellular CO_2 concentration, and stomatal conductance (Gs) in different light-sensitive inbred maize lines under low light stress. **(A, B)** show the Pn values; **(C, D)** show the Tr values; **(E, F)** show the intercellular carbon dioxide concentrations; and **(G, H)** show the Gs values. In the figure panels, 20A, 40A, and 60A denote SN98A sprayed with 20 mg L^{-1},40 mg L^{-1}, and 60 mg L^{-1} GA_3, respectively, and 20B, 40B, and 60B denote SN98B sprayed with 20 mg L^{-1},40 mg L^{-1},and 60 mg L^{-1} GA_3.CKA denotes the SN98A control group sprayed with water and CKB denotes the SN98B control group sprayed with water. Values are expressed as mean ± SD of three replicates. Lower-case letters indicate the mean difference of different treatments in the same period, which is statistically significant ($P<0.05$).

the expression level was highest under treatment with 40 mg L^{-1} GA_3 i.e., 1.62 times that in the control. All three genes responded positively to exogenous GA_3 in SN98B, whereas only *APX* and *GR* responded positively in SN98A.

GA-related gene

In this experiment, the relative expressions of gibberellin receptors *GID1C1*, *GID1C2* and *GID1C3* decreased after exogenous GA_3 treatment, and the relative expressions of *GA20ox*, *KAO1* and *KA02* genes related to gibberellin synthesis and degradation decreased in plants (Figure 9). The expression levels of signal transduction related genes *DELLA1*, *DELLA2* and *DELLA3* were not significantly changed. These results indicated that exogenous GA_3 could inhibit the synthesis of endogenous gibberellin in maize.

Discussion

Northeast China is the most important maize-producing area in China, where the maize output in this region account for more than

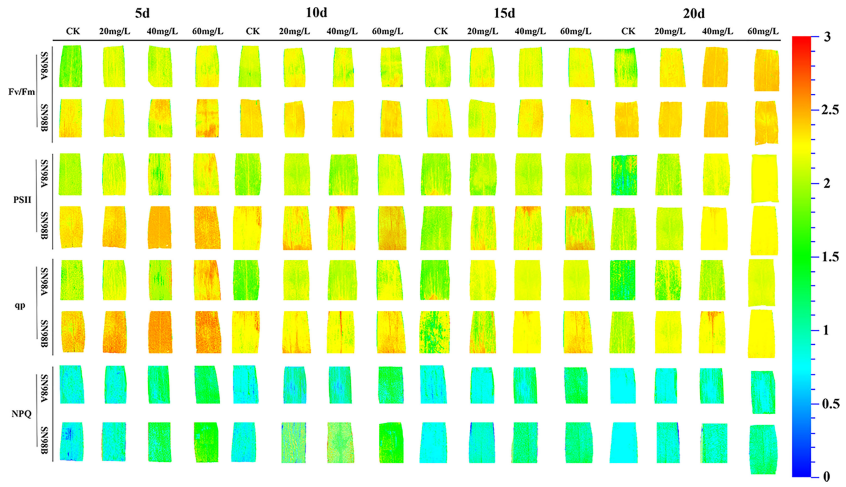

FIGURE 3
Effects of GA_3 application on chlorophyll fluorescence according to *in situ* imaging of inbred maize lines with differences in light sensitivity under low light stress conditions. In the figure panels, 5d, 10d, 15d, and 20d denote the number of days under shading treatment; 20, 40, and 60mg L^{-1} denote the GA_3 concentrations applied; and CK denotes the water control treatment.

30% of the national maize output. In this region, light, heat, and water resources are generally abundant in the growing period. However due to global climate change, extreme weather events have become more frequent during the maize growing season, The frequency of overcast weather with high rain and low radiation during the withering and silking stage has recently increased each year (Yang et al., 2020), thereby adversely affecting the stability of the maize yield in Northeast China. Light is essential for photosynthesis by plants and the basis for plant growth and development (Jiang et al., 2021). Maize is a light-loving crop with no obvious light saturation point and it is very sensitive to changes in the light intensity. A lack of light during tasseling will inhibit the normal physiological activities, decrease photosynthesis in the leaves, and cause cell metabolism disorders and REDOX homeostasis damage, thereby leading to problems such as ear bald tip, yield reductions, and even hollow stalks. Low light stress can accelerate the excessive accumulation of ROS in maize leaves and cause the peroxidation of membrane lipids. Colebrook et al. (2014) indicated that hormones can effectively help plants to cope with abiotic stress, where stress responses are regulated mainly by activating specific hormones *via* signal transduction and crosstalk in different developmental environments (Verma et al., 2016). Therefore, how to increase the yield and reduce the empty stalk rate under the condition of insufficient light has become an important problem.

GA_3 is a plant growth regulator and it is involved in the response to many abiotic stresses in plants, with positive regulatory effects on plant growth and development (Bao et al., 2020). Exogenous GA_3 application can reduce the effects of nickel stress (Wiszniewska et al., 2018) and increase the plant cell length independent of biosynthesis (Rizza et al., 2017). In addition, GA and photoperiod pathways have been shown to synergistically regulate crop flowering under long sunshine conditions (Fukuda et al., 2012; Wang et al., 2016). In the present study, GA_3 treatment reduced the hollow stem rate in maize by regulating the flowering interval between male and female ears, where treatment with 60 mg L^{-1} GA_3 had the greatest effect, followed by treatment with 40 mg L^{-1} GA_3 and 20 mg $L^{-1}GA_3$. Under shading treatment, the H_2O_2 and O_2^- contents continued to increase in the SN98A control group, and the contents were always higher than those in SN98B. After GA_3 spraying treatment, the O_2^- production rate and H_2O_2 contents still increased in SN98A and SN98B, but the increases were significantly smaller than those in the control group, and the O_2^- production rate and H_2O_2 contents were always lower in SN98B than SN98A due to the photoprotective capacity of the shade-tolerant inbred line SN98B. Low light stress can induce oxidative stress in maize, but GA_3 treatment can enhance the ability of maize to resist low light stress and reduce the oxidative pressure caused by insufficient light. Numerous studies have shown that membrane lipid peroxidation leads to the accumulation of MDA. Low light stress can disrupt the dynamic equilibrium between ROS production and scavenging in plants, thereby resulting in the accumulation of ROS and increased membrane permeability. As a consequence, membrane lipid peroxidation lead to the accumulation of MDA and exacerbates maize aging (Wang et al., 2021). In this study, GA_3 treatment significantly reduced the MDA contents of the two inbred lines under low light. The MDA contents were higher in SN98A than SN98B in both the control and treatment groups. The antioxidant enzyme system in plants protects against the toxic effects of ROS. SOD and POD are important antioxidant enzymes in the plant defense mechanism. GA_3 may have reduced the ROS contents in maize by enhancing the activities of POD and SOD in the light-sensitive inbred line SN98A, as also suggested by Ali et al. (2021). *APX*, *Fe-SOD* and *GR* are important genes related to the activities of antioxidant enzymes (Lee et al., 2007). Studies have shown that the overexpression of *APX*, *Fe-SOD*, and *GR* significantly improved the tolerance of abiotic stresses by transgenic tall fescue plants. In the present study, we found that exogenous GA_3 treatment significantly upregulated the expression levels of *APX* and *GR* in SN98A and SN98B compared with the control group, thereby indicating that exogenous GA_3 could enhance the activities of antioxidant enzymes to resist external abiotic stress by increasing the expression of antioxidant-related genes. Therefore, exogenous GA_3 may improve the tolerance of stress in plants by regulating antioxidant metabolism and reducing the lipid peroxidation of cell membranes (Gilroy and

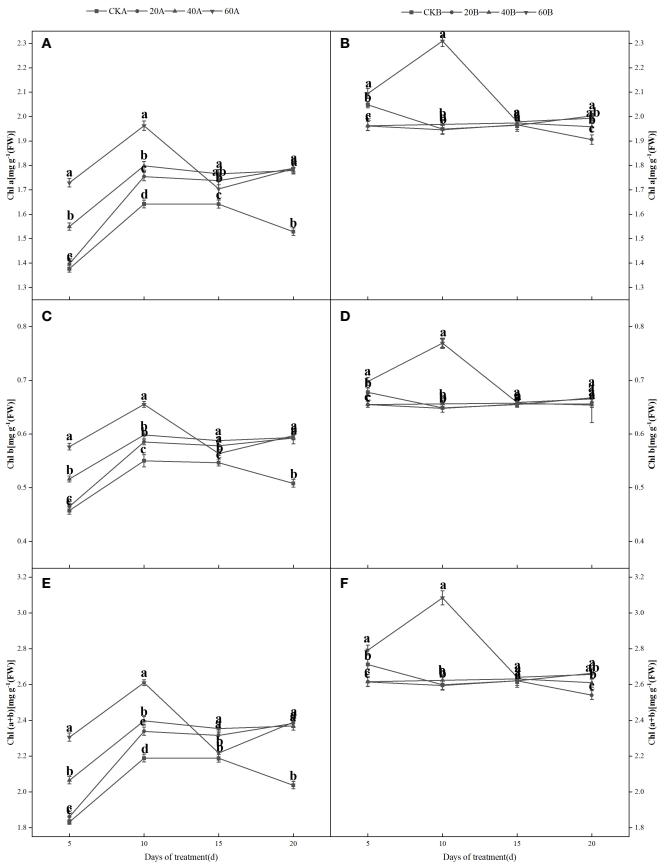

FIGURE 4
Effects of GA_3 application on the Chl a **(A, B)**, Chl b **(C, D)**, and Chl a+b **(E, F)** contents of different light-sensitive inbred maize lines under low light stress. Values are expressed as mean ± SD of three replicates. Lower-case letters indicate the mean difference of different treatments in the same period, which is statistically significant (P<0.05).

Jones, 1992; Jiang and Huang, 2001) to decrease the damage due to low light stress in plants. According to the expression level of GA-related genes, the gene pathway of gibberellin signaling is GA-GID1-DELLA signaling pathway. When gibberellin is at a high level, GID1 can sense the GA signal and combine with it to form GA-GID1. Then it binds to DELLA protein to form GID1-GA-DELLA complex trimer (Zentella et al., 2007), so that ubiquitin ligase SCF in F-Box protein can bind to DELLA protein GRAS region (Fleet and Sun, 2005). The rapid degradation of DELLA protein through ubiquitin proteomic channels resulted in the release of its repression and normal gibberellin response in plants. Therefore, the reduction of gibberellin receptor GID1 may also affect the degradation of DELLA protein at the protein level. After exogenous GA_3 was applied, the expression of *GA20ox2*, a gene related to gibberellin synthesis, decreased (FIG 9G). *GA20ox2* plays an important role in the synthesis of gibberellin in higher plants, and the decreased expression of *GA20ox* gene may decrease the production of endogenous gibberellin. In CK group, the expression level of gibberellin-synthesis-related genes in SN98A was lower than that in SN98B, and CKA of degradation-related genes was higher than that in CKB. Therefore, low light stress inhibited the synthesis of gibberellin by decreasing the expression of genes related to gibberellin synthesis and enhancing the expression of genes related to degradation, resulting in empty culms.

The responses of photosynthetic organs to low light stress and the associated mechanisms are important for understanding the adaptation of crops to different light environments. Thus, many studies have investigated the self-regulation mechanism and light energy conversion process in maize under low light conditions (Zivcak et al., 2014; Hazrati et al., 2016; Yamori, 2016). Chloroplasts are the site of photosynthesis in plants. Weak light stress can significantly damage the anatomical structure of plants to directly affect normal photosynthetic electron transport and the photosynthetic rate (P_n) (Du et al., 2011; Feng et al., 2021). Under low light, the oxidative pressure is intensified in maize leaves and the accumulation of large amounts of ROS leads to changes in the spatial configurations of various enzymes in chloroplasts, thereby adversely affecting their function, decreasing the chlorophyll content, and inhibiting photosynthesis. In the present study, under shading treatment, the Chl a, Chl b and chlorophyll (a+b) contents, tended to increase initially and then decrease in SN98A, whereas the Chl contents did not change greatly in SN98B and they were always higher than those in SN98A. After GA_3 treatment, the photosynthetic pigment contents increased significantly in SN98, and the Pn, Tr, and Gs values were also significantly higher compared with those in the control. PSII is one of the primary sites in photosynthetic organs damaged by stress, and it plays important roles in the light energy conversion and electron transport processes. (Zhang et al., 2020). The

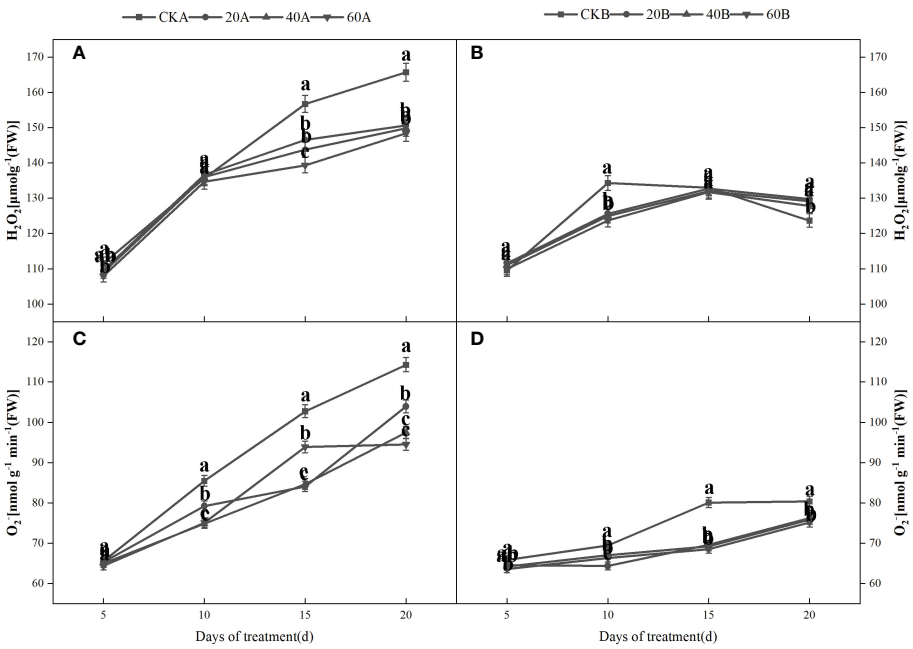

FIGURE 5
Effects of GA_3 on H_2O_2 contents and O_2^- production rate in light-sensitive inbred maize lines after different periods under low light stress. In the figure panels, 20A, 40A, and 60A denote SN98A sprayed with 20 mg L^{-1}, 40 mg L^{-1}, and 60 mg L^{-1} GA_3, respectively, and 20B, 40B, and 60B denote SN98B sprayed with 20 mg L^{-1}, 40 mg L^{-1}, and 60 mg L^{-1} GA_3. CKA denotes the SN98A control group sprayed with water and CKB denotes the SN98B control group sprayed with water. In the figure, **(A, C)** represent the changes of H_2O_2 and O_2^- after SN98A is treated with GA_3. **(B, D)** are the changes of H_2O_2 and O_2^- after SN98B is treated with GA_3. Values are expressed as mean ± SD of three replicates. Lower-case letters indicate the mean difference of different treatments in the same period, which is statistically significant (P<0.05).

photoreaction requires coordination of the photosynthetic system in order to complete the normal linear electron transfer and provide the homogeneity for the fixation and reduction of CO_2 in the dark reaction. (Qian et al., 2017). In the present study, Pn, qP, and Φ_{PSII} continued to decrease during shading in SN98A, whereas they tended to increase initially and then decrease in SN98B, but the values were always higher than those in SN98A, thereby indicating that the normal photosynthetic physiological process was maintained in SN98B. GA_3 treatment could have increased the stomatal conductivity of the maize leaves, enhanced the photosynthetic activity of mesophyll cells, and improved the photosynthetic capacity of maize leaves (Verma et al., 2016), where 60 mg L^{-1} GA_3 treatment had the greatest effect, and thus GA_3 may be involved in the shade protection response process in maize leaves. GA_3 had a positive effect on the photosynthetic efficiency of maize leaves under low light stress.

Plant photosynthesis is an extremely complex physiological process and it is negatively affected by both biological and abiotic

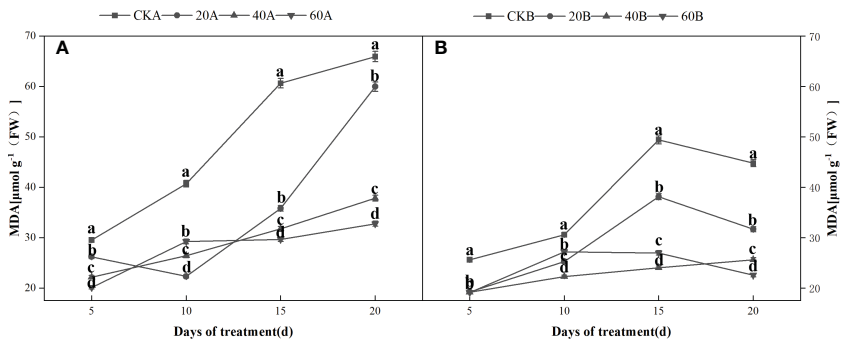

FIGURE 6
Effects of GA_3 on MDA content of light-sensitive maize inbred lines at different periods under low light stress. In the figure panels, 20A, 40A, and 60A denote SN98A sprayed with 20 mg L^{-1}, 40 mg L^{-1}, and 60 mg L^{-1} GA_3, respectively, and 20B, 40B, and 60B denote SN98B sprayed with 20 mg L^{-1}, 40 mg L^{-1}, and 60 mg L^{-1} GA_3. CKA denotes the SN98A control group sprayed with water and CKB denotes the SN98B control group sprayed with water. In the figure, **(A)** is the change of MDA in SN98A after GA_3 treatment, and **(B)** is the change of MDA in SN98B after GA_3 treatment. Values are expressed as mean ± SD of three replicates. Lower-case letters indicate the mean difference of different treatments in the same period, which is statistically significant (P<0.05).

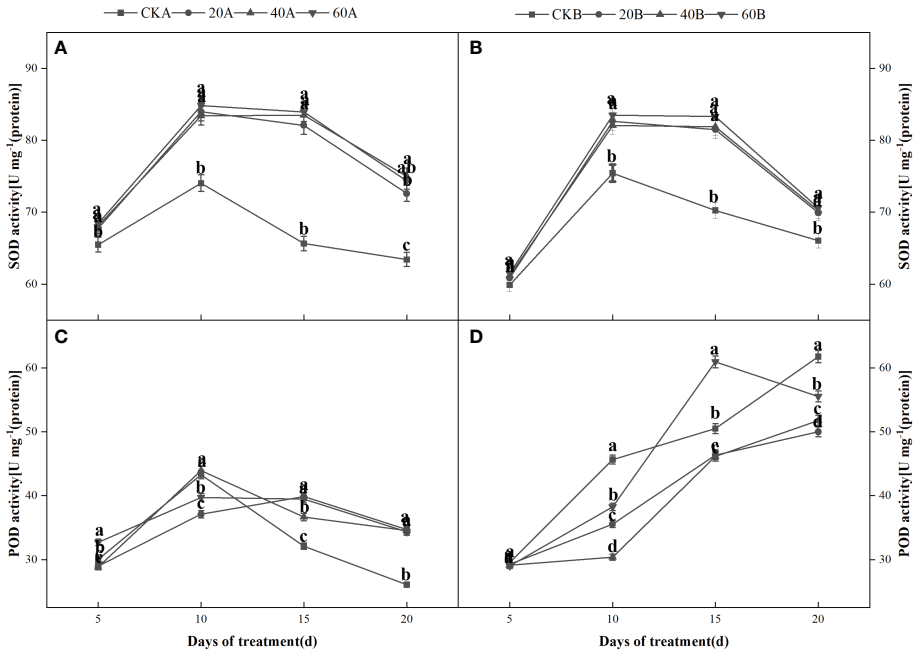

FIGURE 7
Effects of GA_3 on antioxidant enzymes contents in different light-sensitive inbred maize lines after different periods under low light stress. In the figure panels, 20A, 40A, and 60A denote SN98A sprayed with 20 mg L^{-1}, 40 mg L^{-1}, and 60 mg L^{-1} GA_3, respectively, and 20B, 40B, and 60B denote SN98B sprayed with 20 mg L^{-1}, 40 mg L^{-1}, and 60 mg L^{-1} GA_3. CKA denotes the SN98A control group sprayed with water and CKB denotes the SN98B control group sprayed with water. In the figure, **(A, C)** represent the changes of H_2O_2 and O_2^- after SN98A is treated with GA_3. **(B, D)** are the changes of H_2O_2 and O_2^- after SN98B is treated with GA_3. Values are expressed as mean ± SD of three replicates. Lower-case letters indicate the mean difference of different treatments in the same period, which is statistically significant (P<0.05).

stresses. The main limiting factors for photosynthesis are light and carbon dioxide (Smith, 1938). Under low light stress, photosynthesis is inhibited in crops and yields are reduced (Liu et al., 2020). In the present study, under low light stress, Pn, Tr, and Gs all decreased with time during shading, in the SN98A control group and the intercellular carbon dioxide concentration increased. Applying GA_3 improved Pn, Tr, and Gs in SN98A and reduced the intercellular carbon dioxide concentration, where the effect of 60 mg L^{-1} GA_3 was most significant. Low light stress also reduced Pn, Tr, and Gs in the leaves in the SN98B control group, and increased the intercellular carbon dioxide concentration, but the normal physiological activities were generally maintained.

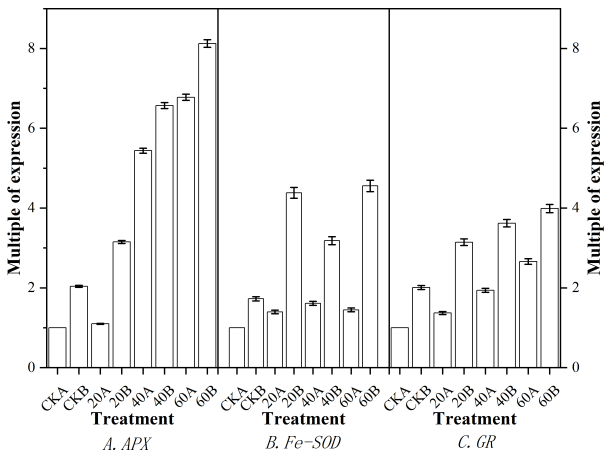

FIGURE 8
Effects of GA_3 application under low light stress on the expression levels of antioxidant-related genes in different light-sensitive inbred maize lines after shading for 15 days. **(A)** *APX*; **(B)** *Fe-SOD*; **(C)** *GR*. Values are expressed as mean ± SD of three replicates. Lower-case letters indicate the mean difference of different treatments in the same period, which is statistically significant (P<0.05).

Conclusion

In the present study, maize inbred lines SN98A and SN98B with differences in their light sensitivity were subjected to shading in the maize tasseling stage (Figure 10). We found that low light treatment reduced the photosynthetic capacity of the maize leaves and inhibited the transport of photosynthetic products to other organs, thereby resulting in plant growth inhibition and leaf senescence. The adverse effects of shading were significantly greater in the weak light-sensitive inbred line SN98A than SN98B, mainly because SN98A had a significantly higher hollow stem rate than SN98B after shading. GA is an excellent antioxidant that can improve the tolerance of various biological and abiotic stresses in plants. These findings help us to understand the physiological mechanisms in maize inbred lines with differences in photosensitivity that mediate the response to low light stress under treatment with exogenous GA. The photosynthetic performance parameters of plants, i.e., Pn, Tr, Gs, photosynthetic pigment contents, (Fv/Fm), qP, and Φ_{PSII}, improved after applying GA_3 (20 mg L^{-1}, 40 mg L^{-1},

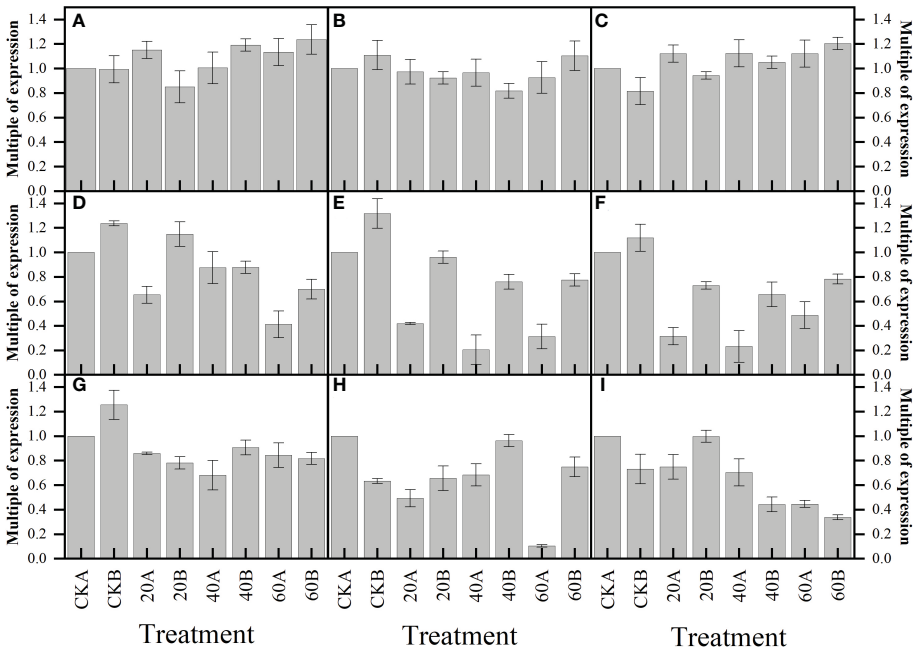

FIGURE 9
Effects of GA_3 application under low light stress on GA-related gene expression levels of different photosensitive inbred lines after shade for 15 days. **(A)** DELLA1; **(B)** DELLA2; **(C)** DELLA3; **(D)** GID1C1; **(E)** GID1C2; **(F)** GID1C3; **(G)** GA20ox2; **(H)** KAO1; **(I)**KAO2. Values are expressed as mean ± SD of three replicates.

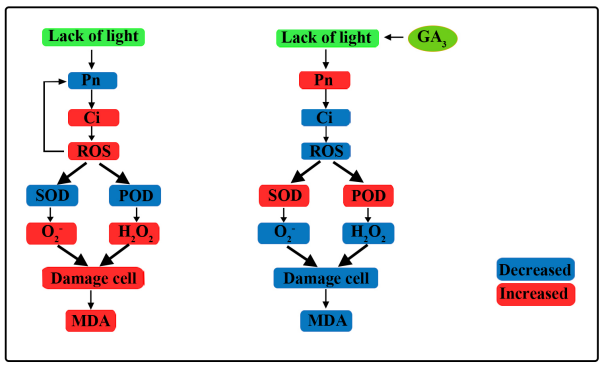

FIGURE 10
Overview of effects of exogenous GA_3 on plant photosynthetic physiology and reactive oxygen species (ROS) scavenging pathways. Under low light, the net photosynthetic rate (Pn) decreased, the intercellular carbon dioxide concentration increased, and the ROS content increased, which further affected Pn. Under low light, the activities of antioxidant enzymes decreased and the ROS scavenging rate decreased, thereby leading to cell damage and MDA was produced increase the degree of membrane lipid peroxidation. After the application of GA_3, Pn improved, the activities of antioxidant enzymes increased, ROS scavenging was enhanced, cell damage was reduced, and the MDA content decreased.

and 60 mg L^{-1}) to the leaves, including 60 mg L^{-1} GA_3 works best. Thus, the foliar application of GA_3 to SN98A and SN98B will be beneficial for their growth and development under lower light conditions.

Data availability statement

The original contributions presented in the study are included in the article/Supplementary Material. Further inquiries can be directed to the corresponding author.

Author contributions

JF: investigation, data curation, validation, and writing—original draft; LL: review and editing; SW: data curation, methodology, formal analysis, and software; NY: formal analysis and editing; HS: investigation and formal analysis; ZS: resources and funding acquisition; FL: writing—review and editing; XZ: conceptualization, writing—review, editing and funding acquisition. All authors contributed to the article and approved the submitted version.

Funding

This work was supported by National Natural Science Foundation of China (31901460) and Basic Scientific Research Project of Education Department of Liaoning Province (LJKMZ20221018).

Conflict of interest

Author HS is employed by Liaoning Dongya Seed Co.

The remaining authors declare that the research was conducted in the absence of any commercial or financial relationships that could be construed as a potential conflict of interest.

Publisher's note

Supplementary material

The Supplementary Material for this article can be found online at: https://www.frontiersin.org/articles/10.3389/fpls.2023.1128780/full#supplementary-material

References

Abedi, T., and Pakniyat, H. (2010). Antioxidant enzyme changes in response to drought stress in ten cultivars of oilseed rape (Brassica napus l.). *Czech J. Genet. Plant Breed.* 46 (1), 27–34. doi: 10.17221/67/2009-CJGPB

Ali, M., Kamran, M., Abbasi, G. H., Saleem, M. H., Ahmad, S., Parveen, A., et al. (2021). Melatonin-induced salinity tolerance by ameliorating osmotic and oxidative stress in the seedlings of two tomato (*Solanum lycopersicum* l.) cultivars. *J. Plant Growth Regul.* 40, 2236–2248. doi: 10.1007/s00344-020-10273-3

Asad, M., Zakari, S. A., Zhao, Q., Zhou, L., Ye, Y., and Cheng, F. (2019). Abiotic stresses intervene with ABA signaling to induce destructive metabolic pathways leading to death: Premature leaf senescence in plants. *Int. J. Mol. Sci.* 20 (2), 256. doi: 10.3390/ijms20020256

Bao, S. J., Hua, C. M., Shen, L. S., and Yu, H. (2020). New insights into gibberellin signaling in regulating flowering in arabidopsis. *J. Integr. Plant Biol.* 62, 118–131. doi: 10.1111/jipb.12892

Benlloch-Gonzalez, M., Quintero, J. M., Garcia-Mateo, M. J., Fourniera, J. M., and Benllocha, M. (2015). Effect of water stress and subsequent re-watering on k+ and water flows in sunflower roots. A possible mechanism to tolerate water stress. *Environ. Exp. Bot.* 118, 78–84. doi: 10.1016/j.envexpbot.2015.06.008

Colebrook, E. H., Thomas, S. G., Phillips, A. L., and Hedden, P. (2014). The role of gibberellin signalling in plant responses to abiotic stress. *J. Exp. Biol.* 217, 67–75. doi: 10.1242/jeb.089938

Djakovic-Petrovic, T., De Wit, M., Voesenek, L., and Pierik, R. (2007). DELLA protein function in growth responses to canopy signals. *Plant J. Cell Mol. Biol.* 51, 117–126. doi: 10.1111/j.1365-313X.2007.03122.x

Du, C., Li, C., Liu, T., and Zhao, Y. (2011). Response of anatomical structure and photosynthetic characteristics to low light stress in leaves of different maize genotypes. *Acta Ecologica Sinica.* 21, 6633–6640.

Dvorak, P., Krasylenko, Y., Zeiner, A., Samaj, J., and Takac, T. (2021). Signaling toward reactive oxygen species-scavenging enzymes in plants. *Front. Plant Sci.* 11. doi: 10.3389/fpls.2020.618835

Ezura, H., and Harberd, N. P. (1995). Endogenous gibberellin levels influence *in-vitro* shoot regeneration in arabidopsis thaliana (L.) heynh. *Planta* 197, 301–305. doi: 10.1007/BF00202651

Feng, Y., Cui, X., Shan, H., Shi, Z. S., Li, F. H., Wang, H. W., et al. (2021). Effects of solar radiation on photosynthetic physiology of barren stalk differentiation in maize. *Plant Sci.* 312. doi: 10.1016/j.plantsci.2021.111046

Ferrante, A., and Mariani, L. (2018). Agronomic management for enhancing plant tolerance to abiotic stresses: High and low values of temperature, light intensity, and relative humidity. *Horticulturae* 4. doi: 10.3390/horticulturae4030021

Fleet, C. M., and Sun, T.-P. (2005). A DELLAcate balance: the role of gibberellin in plant morphogenesis. *Curr. Opin. Plant Biol.* 8, 77–85. doi: 10.1016/j.pbi.2004.11.015

Fukuda, N., Yoshida, T., Olsen, J. E., Senaha, C., Jikumaru, Y., and Yuji, K. (2012). "Short main shoot length and inhibition of floral bud development under red light can be recovered by application of gibberellin and cytokinin," in *7th international symposium on light in horticultural systems. Acta Hortic.* 956 (956), 215–222. doi: 10.17660/ActaHortic.2012.956.23

Gill, S. S., Anjum, N. A., Hasanuzzaman, M., Gill, R., Trivedi, D. K., Ahmad, I., et al. (2013). Glutathione and glutathione reductase: A boon in disguise for plant abiotic stress defense operations. *Plant Physiol. Biochem.* 70, 204–212. doi: 10.1016/j.plaphy.2013.05.032

Gill, S. S., and Tuteja, N. (2010). Reactive oxygen species and antioxidant machinery in abiotic stress tolerance in crop plants. *Plant Physiol. Biochem.* 48, 909–930. doi: 10.1016/j.plaphy.2010.08.016

Gilroy, S., and Jones, R. L. (1992). Gibberellic acid and abscisic acid coordinately regulate cytoplasmic calcium and secretory activity in barley aleurone protoplasts. *Proc. Natl. Acad. Sci. United States America* 89, 3591–3595. doi: 10.1073/pnas.89.8.3591

Guo, X. Q., Wu, Q. D., Zhu, G. L., Ibrahim, M. E. H., and Zhou, G. S. (2022). Gibberellin increased yield of sesbania pea grown under saline soils by improving antioxidant enzyme activities and photosynthesis. *Agronomy-Basel* 12. doi: 10.3390/agronomy12081855

Hazrati, S., Tahmasebi-Sarvestani, Z., Modarres-Sanavy, S., Mokhtassi-Bidgoli, A., and Nicola, S. (2016). Effects of water stress and light intensity on chlorophyll fluorescence parameters and pigments of aloe vera l. *Plant Physiol. Biochem.* 106, 141–148. doi: 10.1016/j.plaphy.2016.04.046

Hodges, D. M., Delong, J. M., Forney, C. F., and Prange, R. K. (1999). Improving the thiobarbituric acid-reactive-substances assay for estimating lipid peroxidation in plant tissues containing anthocyanin and other interfering compounds. *Planta* 207, 604–611. doi: 10.1007/s004250050524

Huang, C., Gao, Y., Qin, A. Z., Liu, Z. G., Zhao, B., Ning, D. F., et al. (2022). Effects of waterlogging at different stages and durations on maize growth and grain yields. *Agric. Water Manage.* 261. doi: 10.1016/j.agwat.2021.107334

Jbir-Koubaa, R., Charfeddine, S., Ellouz, W., Saidi, M. N., Drira, N., Gargouri-Bouzid, R., et al. (2015). Investigation of the response to salinity and to oxidative stress of interspecific potato somatic hybrids grown in a greenhouse. *Plant Cell Tissue Organ Culture* 120, 933–947. doi: 10.1007/s11240-014-0648-4

Jiang, Y. P., Ding, X. T., Wang, J. Y., Zou, J., and Nie, W. F. (2021). Decreased low-light regulates plant morphogenesis through the manipulation of hormone biosynthesis in solanum lycopersicum. *Environ. Exp. Bot.* 52 (355), 341–9. doi: 10.1016/j.envexpbot.2021.104409

Jiang, Y., and Huang, B. (2001). Effects of calcium on antioxidant activities and water relations associated with heat tolerance in two cool-season grasses. *J. Exp. Bot.* 52 (355), 341–349. doi: 10.1093/jexbot/52.355.341

Khan, A. L., Hussain, J., Al-Harrasi, A., Al-Rawahi, A., and Lee, I. J. (2015). Endophytic fungi: resource for gibberellins and crop abiotic stress resistance. *Crit. Rev. Biotechnol.* 35, 62–74. doi: 10.3109/07388551.2013.800018

Lee, S.-H., Ahsan, N., Lee, K.-W., Kim, D.-H., Lee, D.-G., Kwak, S.-S., et al. (2007). Simultaneous overexpression of both CuZn superoxide dismutase and ascorbate peroxidase in transgenic tall fescue plants confers increased tolerance to a wide range of abiotic stresses. *J. Plant Physiol.* 164, 1626–1638. doi: 10.1016/j.jplph.2007.01.003

Li, J. K., Essemine, J., Shang, C., Zhang, H. L., Zhu, X. C., Yu, J. L., et al. (2020). Combined proteomics and metabolism analysis unravels prominent roles of antioxidant system in the prevention of alfalfa (*Medicago sativa* l.) against salt stress. *Int. J. Mol. Sci.* 21 (3), 909. doi: 10.3390/ijms21030909

Lichtenthaler, H. K., and Wellburn, A. R. (1983). Determinations of total carotenoids and chlorophylls a and b of leaf extracts in different solvents. *Analysis* 11, 591–592. doi: 10.1007/s004250050524

Liu, Y. X., Pan, T., Tang, Y. Y., Zhuang, Y., Liu, Z. J., Li, P. H., et al. (2020). Proteomic analysis of rice subjected to low light stress and overexpression of OsGAPB increases the stress tolerance. *Rice* 13. doi: 10.1186/s12284-020-00390-8

Magome, H., Yamaguchi, S., Hanada, A., Kamiya, Y., and Oda, K. (2004). Dwarf and delayed-flowering 1, a novel arabidopsis mutant deficient in gibberellin biosynthesis because of overexpression of a putative AP2 transcription factor. *Plant J. Cell Mol. Biol.* 37, 720–729. doi: 10.1111/j.1365-313X.2003.01998.x

Mcatee, P., Karim, S., Schaffer, R., and David, K. (2013). A dynamic interplay between phytohormones is required for fruit development, maturation, and ripening. *Front. Plant Sci.* 4. doi: 10.3389/fpls.2013.00079

Mittler, R. (2002). Oxidative stress, antioxidants and stress tolerance. *Trends Plant Sci.* 7, 405–410. doi: 10.1016/s1360-1385(02)02312-9

Ni, B. R., and Bradford, K. J. (1993). Germination and dormancy of abscisic acid- and gibberellin-deficient mutant tomato (*Lycopersicon esculentum*) seeds (Sensitivity of

germination to abscisic acid, gibberellin, and water potential). *Plant Physiol.* 101, 607–617. doi: 10.1104/pp.101.2.607

Qian, C. J., Zhang, W., Zhong, X. M., Li, F. H., and Shi, Z. S. (2017). Comparative studies on the photosynthetic characteristics of two maize (Zea mays l.) near-isogenic lines differing in their susceptibility to low light intensity. *Emirates J. Food Agric.* 29, 300–311. doi: 10.9755/ejfa.2016-07-839

Qu, M. N., Zheng, G. Y., Hamdani, S., Essemine, J., Song, Q. F., Wang, H. R., et al. (2017). Leaf photosynthetic parameters related to biomass accumulation in a global rice diversity survey. *Plant Physiol.* 175, 248–258. doi: 10.1104/pp.17.00332

Ramel, F., Sulmon, C., Bogard, M., Couee, I., and Gouesbet, G. (2009). Differential patterns of reactive oxygen species and antioxidative mechanisms during atrazine injury and sucrose-induced tolerance in arabidopsis thaliana plantlets. *BMC Plant Biol.* 9. doi: 10.1186/1471-2229-9-28

Rizza, A., Walia, A., Lanquar, V., Frommer, W. B., and Jones, A. M. (2017). *In vivo* gibberellin gradients visualized in rapidly elongating tissues. *Nat. Plants* 3, 803–813. doi: 10.1038/s41477-017-0021-9

Rood, S. B., Mandel, R., and Pharis, R. P. (1989). Endogenous gibberellins and shoot growth and development in brassica napus. *Plant Physiol.* 89, 269–273. doi: 10.1104/pp.89.1.269

Sauret-Gueto, S., Calder, G., and Harberd, N. P. (2012). Transient gibberellin application promotes arabidopsis thaliana hypocotyl cell elongation without maintaining transverse orientation of microtubules on the outer tangential wall of epidermal cells. *Plant J.* 69, 628–639. doi: 10.1111/j.1365-313X.2011.04817.x

Slattery, R. A., and Ort, D. R. (2021). Perspectives on improving light distribution and light use efficiency in crop canopies. *Plant Physiol.* 185, 34–48. doi: 10.1093/plphys/kiaa006

Smith, E. L. (1938). LIMITING FACTORS IN PHOTOSYNTHESIS: LIGHT AND CARBON DIOXIDE. *J. Gen. Physiol.* 22, 21–35. doi: 10.1085/jgp.22.1.21

Verma, V., Ravindran, P., and Kumar, P. P. (2016). Plant hormone-mediated regulation of stress responses. *BMC Plant Biol.* 16. doi: 10.1186/s12870-016-0771-y

Vicente, M. R. S., and Plasencia, J. (2011). Salicylic acid beyond defence: its role in plant growth and development. *J. Exp. Bot.* 62, 3321–3338. doi: 10.1093/jxb/err031

Wang, H. P., Pan, J. J., Li, Y., Lou, D. J., Hu, Y. R., and Yu, D. Q. (2016). The DELLA-CONSTANS transcription factor cascade integrates gibberellic acid and photoperiod signaling to regulate flowering. *Plant Physiol.* 172, 479–488. doi: 10.1104/pp.16.00891

Wang, J., Wang, D., Zhu, M., and Li, F. (2021). Exogenous 6-benzyladenine improves waterlogging tolerance in maize seedlings by mitigating oxidative stress and upregulating the ascorbate-glutathione cycle. *Front. Plant Sci.* 12. doi: 10.3389/fpls.2021.680376

Wang, X., Xu, C., Cang, J., Zeng, Y., Yu, J., Liu, L., et al. (2015). Effects of exogenous GA (3) on wheat cold tolerance. *J. Agric. Sci. Technol.* 17 (4), 921–934.

Wegrzyn, A., and Mazur, R. (2020). Regulatory mechanisms of photosynthesis light reactions in higher plants. *Postepy biochemii* 66, 134–142. doi: 10.18388/pb.2020_325

Wiszniewska, A., Muszynska, E., Hanus-Fajerska, E., Dziurka, K., and Dziurka, M. (2018). Evaluation of the protective role of exogenous growth regulators against Ni toxicity in woody shrub Daphne jasminea. *Planta* 248, 1365–1381. doi: 10.1007/s00425-018-2979-6

Xia, X.-J., Wang, Y.-J., Zhou, Y.-H., Tao, Y., Mao, W.-H., et al. (2009). Reactive oxygen species are involved in brassinosteroid-induced stress tolerance in cucumber. *Plant Physiol.* 150, 801–814. doi: 10.1104/pp.109.138230

Xu, Z., Zhang, J., Wang, X., Essemine, J., Jin, J., Qu, M., et al. (2023). Cold-induced inhibition of photosynthesis-related genes integrated by a TOP6 complex in rice mesophyll cells. *Nucleic Acids Res.* doi: 10.1093/nar/gkac1275

Xue, J., Li, T., Wang, S., Xue, Y., Liu, X., et al. (2019). Defoliation and gibberellin synergistically induce tree peony flowering with non-structural carbohydrates as intermedia. *J. Plant Physiol.* 233, 31–41. doi: 10.1016/j.jplph.2018.12.004

Yamaguchi, N., Winter, C. M., Wu, M. F., Kanno, Y., Yamaguchi, A., Seo, M., et al. (2014). Gibberellin acts positively then negatively to control onset of flower formation in arabidopsis. *Science* 344, 638–641. doi: 10.1126/science.1250498

Yamori, W. (2016). Photosynthetic response to fluctuating environments and photoprotective strategies under abiotic stress. *J. Plant Res.* 129, 379–395. doi: 10.1007/s10265-016-0816-1

Yang, Y. S., Guo, X. X., Hou, P., Xue, J., Liu, G. Z., Liu, W. M., et al. (2020). Quantitative effects of solar radiation on maize lodging resistance mechanical properties. *Field Crops Res.* 255. doi: 10.1016/j.fcr.2020.107906

Yu, K., Wang, Y., Wei, J., Ma, Q., Yu, D., and Li, J. R. (2009). Improving rhizome yield and quality of Paris polyphylla through gibberellic acid-induced retardation of senescence of aerial parts. *Plant Signaling Behav.* 4, 413–415. doi: 10.4161/psb.4.5.8268

Zahra, N., Al Hinai, M. S., Hafeez, M. B., Rehman, A., Wahid, A., Siddique, K. H. M., et al. (2022). Regulation of photosynthesis under salt stress and associated tolerance mechanisms. *Plant Physiol. Biochem. PPB* 178, 55–69. doi: 10.1016/j.plaphy.2022.03.003

Zentella, R., Zhang, Z.-L., Park, M., Thomas, S. G., Endo, A., Murase, K., et al. (2007). Global analysis of della direct targets in early gibberellin signaling in arabidopsis. *Plant Cell* 19, 3037–3057. doi: 10.1105/tpc.107.054999

Zhang, H. H., Wang, Y., Li, X., He, G. Q., Che, Y. H., Teng, Z. Y., et al. (2020). Chlorophyll synthesis and the photoprotective mechanism in leaves of mulberry (Mores alba l.) seedlings under NaCl and NaHCO3 stress revealed by TMT-based proteomics analyses. *Ecotoxicology Environ. Saf.* 190. doi: 10.1016/j.ecoenv.2020.110164

Zhong, S. W., Shi, H., Xue, C., Wang, L., Xi, Y. P., Li, J. G., et al. (2012). A molecular framework of light-controlled phytohormone action in arabidopsis. *Curr. Biol.* 22, 1530–1535. doi: 10.1016/j.cub.2012.06.039

Zhou, S., He, L., Lin, W., Su, Y., Liu, Q., Qu, M., et al. (2022). Integrative analysis of transcriptome and metabolism reveals potential roles of carbon fixation and photorespiratory metabolism in response to drought in shanlan upland rice. *BMC Genomics* 23, 862. doi: 10.1186/s12864-022-09094-3

Zivcak, M., Brestic, M., Kalaji, H. M., and Govindjee, (2014). Photosynthetic responses of sun- and shade-grown barley leaves to high light: is the lower PSII connectivity in shade leaves associated with protection against excess of light? *Photosynthesis Res.* 119, 339–354. doi: 10.1007/s11120-014-9969-8

frontiers | Frontiers in Plant Science

TYPE Original Research
PUBLISHED 17 March 2023
DOI 10.3389/fpls.2023.1133206

OPEN ACCESS

EDITED BY
Jiwang Zhang,
Shandong Agricultural University, China

REVIEWED BY
Tie Cai,
Northwest A&F University, China
Liu Zhandong,
Farmland Irrigation Research Institute (CAAS), China

*CORRESPONDENCE
Yongjun Wang
yongjunwang2004@126.com
Lin Ma
malin@caas.cn

SPECIALTY SECTION
This article was submitted to Crop and Product Physiology, a section of the journal Frontiers in Plant Science

RECEIVED 28 December 2022
ACCEPTED 28 February 2023
PUBLISHED 17 March 2023

CITATION
Wu Y, Yao F, Wang Y, Ma L and Li X (2023) Association of maize (*Zea mays* L.) senescence with water and nitrogen utilization under different drip irrigation systems.
Front. Plant Sci. 14:1133206.
doi: 10.3389/fpls.2023.1133206

Association of maize (*Zea mays* L.) senescence with water and nitrogen utilization under different drip irrigation systems

Yang Wu[1], Fanyun Yao[2], Yongjun Wang[2]*, Lin Ma[3]* and Xiangnan Li[4,5]

[1]Institute of Jiangxi Oil-tea Camellia, Jiujiang University, Jiujiang, China, [2]Institute of Agricultural Resource and Environment, Jilin Academy of Agricultural Sciences, Changchun, China, [3]Institute of Animal Science, Chinese Academy of Agricultural Sciences, Beijing, China, [4]Northeast Institute of Geography and Agroecology, Chinese Academy of Sciences, Changchun, China, [5]College of Advanced Agricultural Sciences, University of Chinese Academy of Sciences, Beijing, China

Introduction: Drip irrigation is an efficient water-saving system used to improve crop production worldwide. However, we still lack a comprehensive understanding of maize plant senescence and its association with yield, soil water, and nitrogen (N) utilization under this system.

Methods: A 3-year field experiment in the northeast plains of China was used to assess four drip irrigation systems: (1) drip irrigation under plastic film mulch (PI); (2) drip irrigation under biodegradable film mulch (BI); (3) drip irrigation incorporating straw returning (SI); and (4) drip irrigation with the tape buried at a shallow soil depth (OI), and furrow irrigation (FI) was used as the control. The plant senescence characteristic based on the dynamic process of green leaf area (GLA) and live root length density (LRLD) during the reproductive stage, and its correlation with leaf N components, water use efficiency (WUE), and N use efficiency (NUE) was investigated.

Results: PI followed by BI achieved the highest integral GLA and LRLD, grain filling rate, and leaf and root senescence rate after silking. Greater yield, WUE, and NUE were positively associated with higher N translocation efficiency of leaf protein responding for photosynthesis, respiration, and structure under PI and BI; whereas, no significant differences were found in yield, WUE, and NUE between PI and BI. SI effectively promoted LRLD in the deeper 20- to 100-cm soil layers, prolonged the GLA and LRLD persistent durations, and reduced the leaf and root senescence rates. The remobilization of non-protein storage N was stimulated by SI, FI, and OI, which made up for the relative inadequacy of leaf N.

Discussion: Instead of persistent GLA and LRLD durations and high translocation efficiency of non-protein storage N, fast and large protein N translocation from leaves to grains under PI and BI was found to facilitate maize yield, WUE, and NUE in the sole cropping semi-arid region, and BI was recommend considering that it can reduce plastic pollution.

KEYWORDS

leaf nitrogen, live root, green leaf area, water use efficiency, nitrogen use efficiency, drip irrigation

Introduction

Maize (*Zea mays* L.) is a major cereal crop that widely cultivated globally for grain, forage, and industrial raw material. The northeast plain of China (NEP) accounts for 34% maize production in the country. However, extreme weather events are increasing along with global climate changes, and drought disasters have been a growing threat to maize production. It is therefore imperative to implement water-saving agricultural practices (Lobell et al., 2014). Drip irrigation is one of the most water-efficient irrigation strategies, capable of prominently increasing crop yields and alleviating soil salinization in areas affected by drought. Meanwhile, drip irrigation coupled with plastic film mulching (PI) has become popular strategies used in NEP maize production since 2012 to help manage the impacts of increasing droughts by inhibiting excess evaporation (Zhang et al., 2018). Numerous studies have demonstrated that PI is effective in promoting crop growth, water use efficiency (WUE), and nitrogen use efficiency (NUE) by improving soil hydrothermal conditions, especially in arid or semi-arid regions with low annual average temperatures (Qin et al., 2016; Xue et al., 2017; Wang et al., 2021; Zhang et al., 2022). More recently, drip irrigation combined with biodegradable film mulching (BI) or straw returning to field (SI) as wells as drip irrigation with the tape buried to a shallow soil depth (OI) are methods employed to prevent plastic film pollution and achieve both economic and environmental benefits.

For annual crops, senescence is the last phase of the plant life cycle, comprising the reproductive phase and post-fertilization grain filling. Over 80 years ago, it was discovered that most of the diversity in crop yield is a consequence of variation in the leaf area duration rather than the photosynthesis rate (Heath and Gregory, 1938). Root senescence is strongly linked with leaf senescence *via* nutrient translocation and hormone signaling (Glanz-Idan et al., 2020; Zhu et al., 2021). Previous studies mostly focused on leaf senescence and indicated that stay-green genotypes with lagging senescence exhibit higher nitrogen (N) uptake and grain production than non–stay-green genotypes, especially under drought or low N stresses (Borrell et al., 2000; Gregersen et al., 2013; Kamal et al., 2018; Liu et al, 2021). Except for genetic background, plant senescence is also affected by agronomic management In addition to genetic background, plant senescence is also affected by agronomic management. Appropriate irrigation scheduling will prolong the leaf photosynthetic duration and increase crop yields by alleviating drought stresses (Si et al., 2023). Acciaresi et al. (2014) found that delayed leaf senescence at lower canopy levels was not associated with an increase in post-silking carbon (C) accumulation and may therefore be unproductive for maize under non-stressing conditions. In contrast, Li et al. (2022) found that high-density maize planting was associated with increased N uptake, C assimilation, root function, and yield, owing to the delayed post-silking senescence in lower leaves. Furthermore, plant senescence is directly associated with large N translocation from leaf to grains. Leaf N allocation has great importance in the photosynthetic capacity and the balance of N and C (Liu et al., 2018a; Evans and Clarke, 2019; Mu and Chen, 2021), and it can be classified in detail by function as photosynthetic N, structural N, respiration N, and storage N (Xu et al., 2012; Ali et al., 2016). However, the response of leaf N components to plant senescence process is still unclear.

Film mulching, or film mulching combined with irrigation, can greatly facilitate N utilization (Gu et al., 2021; Liao et al., 2022). Some research studies have suggested that high soil temperature under PI-limited root activity decreases N supply to the canopy and thus accelerates plant senescence (Yang et al., 2016). However, we still lack a comprehensive understanding of leaf and root senescence patterns under varied water-saving irrigation systems as well as the impact of plant senescence on yield, soil water, and N utilization. To address these knowledge gaps, we conducted a 3-year field experiment in NEP consisting of four water-saving drip irrigation treatments (PI, BI, SI, and OI) applied to maize planting. The purpose of this study was to identify the plant senescence characteristic based on the dynamic process of green leaf area (GLA) and live root length density (LRLD) during the reproductive stage, as well as its association with leaf N components, grain filling, yield, WUE, and NUE. The study contributes vital information to improve evaluation of maize productivity under different drip irrigation systems in a semi-arid region.

Material and methods

Site description

The experiment was conducted during 2016–2018 at the Taonan farm research station (45° 20′N, 122° 47′E), Jilin Province, China. In the 0- to 100-cm soil layer, the soil was clay loam with a mean bulk density of 1.5 g cm^{-3}, a field capacity of 22.7% (weight %), and a wilting coefficient of 11.8% (weight %). The organic matter content and the available N, P, and K were 8.8, 50.4, 20.0, and 90.5 mg kg^{-1}, respectively, which was determined according to Arif et al. (2017). Over the last 35 years, the annual mean sunshine duration was 2,817.2 h, the annual mean pan evaporation was 1,928 mm, the frost-free season was 140 days, the annual mean temperature was 6.0°C, and the annual mean precipitation was 419.7 mm. The precipitation and air temperature distributions during the experimental period are shown in Supplementary Figure 1 and Supplementary Table 1.

Experimental design

Four treatments were set as follows: (1) drip irrigation under plastic film mulch (PI), (2) drip irrigation under biodegradable film mulch (BI), (3) drip irrigation incorporating straw returning (SI), and (4) drip irrigation with the tape buried at a shallow soil depth (OI). In addition, traditional furrow irrigation (FI) was used as the control. The experiment employed a completely randomized design with three replicates, and each plot area measured 255 m^2 (8.5 × 30 m). Plastic film (polyethylene clear film, 0.9 m wide × 0.008 mm thick; produced by Jilin Difu Agricultural Technology Co. Ltd., Jilin, China) and biodegradable film (polylactic clear film, 0.9 m wide × 0.008 mm thick; produced by Jilin Difu Agricultural Technology

Co. Ltd., Jilin, China) were used to cover the surface of the planting ridges. Varying levels of damage to the biodegradable film were observed in August, and the film was completely degraded after crop harvest. The planting schematic diagram for the different treatments is shown in Supplementary Figure 2. Maize cultivar "Fumin 985" (dent type) was sown at a rate of 77,000 plants ha^{-1} based on the local planting density.

Under SI treatment, maize straw produced in the identical plot areas (9,000 kg ha^{-1}) was cut to lengths of ~10 cm and scattered over the ground evenly. Then, the straw was returned into a 20-cm deep soil layer by using a 110-horsepower tractor after harvest (ca. October 1~10). Except for SI, the straw under other treatments was completely removed from the previous season. In the OI and SI treatments, drip tape was buried at a soil depth of 5–10 cm to prevent evaporation of soil water. Film mulching, drip tape laying, fertilizer application, and seed sowing were performed synchronously by using a multi-functional machine equipped with a 60-horsepower tractor. The drip tape was taken away after harvest by using a recovery machine equipped with a 15-horsepower tractor. All the machines were provided by Jilin Province Kangda Agricultural Machinery Co. Ltd. in Jilin, China.

Fertilizer consisted of N (210 kg ha^{-1}), phosphorus pentoxide (105 kg ha^{-1}), and potassium oxide (90 kg ha^{-1}) applied one time before sowing for each treatment. Supplemental irrigation at critical water demand periods was considered the most efficient way to meet the soil water deficit and is a method that can be easily adopted by local farmers (Gao et al., 2017; Yang et al., 2022). The soil was very dry before sowing in the experimental region (about 50% of the field capacity in the 0- to 20-cm soil layer). To guarantee seed germination and seedling growth, 55 mm of irrigation water was applied on 02 May, 30 April, and 04 May, in the 2016, 2017, and 2018 planting seasons, respectively. Another 40, 30, and 20 mm of irrigation water was applied for each treatment at the jointing, tasseling, and filling stages, respectively. The irrigation amount was determined as the difference between crop water demand (ET_C) and effective precipitation during the past 6 years (Wu et al., 2019). ET_C determination was based on the Food and Agriculture Organization (FAO) Penman–Monteith equation (Allen et al., 1998). The effective precipitation was the fraction of the precipitation excluding surface runoff, deep percolation, or evaporation, and it was calculated by using the method of Döll and Siebert (2002). The specific irrigation time and precipitation amount between each irrigation event is described in Supplementary Table 2. The drip irrigation tape was placed in the middle of planting rows, and the spacing distance was 130 cm (Supplementary Figure 2). The tape was 16 mm in diameter with an emitter spacing of 30 cm, and the flow rate of the emitter was 3 L h^{-1} at a working pressure of 0.1 MPa. The irrigation rate was recorded using a precise water meter. The maize seeds were sown on 04 May, 01 May, and 06 May in the 2016, 2017, and 2018, respectively. Growth and developmental progress for each treatment are listed in Table 1.

Grain weight, yield, and NUE

Fifty ears that silked on the same day with uniform growth were tagged for each plot. Three tagged ears from each plot were sampled at 10-day intervals from the beginning of the first treatment entered the silking stage. The total number of grains was determined, and the grains were oven-dried at 65°C until constant weight. The 100-kernel weight was calculated until maturity for each treatment. At harvest, four representative, undamaged lines were selected from each plot, and 15 random plants in each line were harvested. The numbers of seeds per ear and the seed weight (14% standard water content) were determined to estimate the yield.

Three maize plants in each plot were sampled to measure biomass and N uptake at silking and maturity stages. Thereinto, roots were sampled every 10 cm in the 0- to 40-cm soil layer, and every 20 cm in the 40- to 100-cm soil layer. The root sampling position was determined on the basis of root distribution area: 65 × 20 × 100 cm (Supplementary Figure 2), using a 100/50-mm-diameter steel core-sampling drill. Root samples were carefully washed, and any non-root impurities were carefully removed. Plant samples (roots and aboveground parts) were then oven-dried to constant weights at 65°C to calculate the dry weights. After weighing, the dry samples were ground and passed through a 1-mm sieve, and the N concentration was measured using the micro-Kjeldahl method (CN61M/KDY-9820; Beijing, China) (Li et al., 2017a). Plant N uptake was calculated as the product of plant N concentration and dry matter weight. N translocation amount was calculated as the difference of N uptake between silking and maturity. In addition, N translocation efficiency was defined as the N translocation amount divided by N uptake at silking. The NUE was calculated as the ratio of yield relative to N uptake amount of the whole plant at maturity (Fu et al., 2017).

TABLE 1 Developmental progress with different drip irrigation treatments (date, days after sowing).

Stage	Treatments [a]	2016	2017	2018
Silking	PI	7/17 (74)	7/13 (73)	7/18 (73)
	BI	7/21 (78)	7/18 (78)	7/22 (77)
	SI/OI/FI	7/26 (83)	7/25 (85)	7/28 (83)
Maturity	PI	9/20 (139)	9/16 (138)	9/18 (135)
	BI	9/23 (142)	9/19 (141)	9/20 (137)
	SI/OI/FI	9/27 (146)	9/24 (146)	9/27 (144)

[a]PI and BI represent drip irrigation under plastic film mulch and biodegradable film mulch, respectively; SI, drip irrigation incorporating straw returning; OI, drip irrigation with the tape buried at a shallow soil depth; FI, furrow irrigation.

Soil water and WUE

Soil was sampled to a depth of 100 cm, following previous studies conducted in the similar semi-arid irrigation regions (Li et al., 2017b; Wang et al., 2019). Soil was sampled every 10 cm in the 0- to 40-cm soil layer, and every 20 cm in the 40- to 100-cm soil layer. According to the root distribution area, soil was sampled at three positions (Supplementary Figure 2). The average value of the three horizontal position samples was used to analyze the soil water profile. Soil water was measured by drying the soil to a constant weight at 105°C and then weighing. The field evapotranspiration (*ET*) value was calculated using the soil water balance equation described in Wu et al. (2021). Briefly, *ET* (mm) was equivalent to the sum of precipitation, irrigation, and the difference in soil water storage during a certain growth period. WUE was calculated as the ratio of the grain yield relative to ET during the entire growth period (Payero et al., 2008).

Live root length density and green leaf area

Fifteen representative plants per plot were tagged to measure the total leaf area every 10 days, starting when the first treatment entered into silking. Individual leaf area was calculated as the product of leaf length and width multiplied by 0.75. Subsequently, GLA was estimated visually until the canopy of all the plants fully turned yellow (Lisanti et al., 2013). Three maize plants per plot were sampled to measure the dynamics of LRLD every 20 days, from the beginning of the first treatment that entered into silking until the last treatment reached maturity. The same root sampling method was used as previously described (Supplementary Figure 2). Functional live roots can be distinguished by staining red using 2,3,5-triphenyltetrazolium chloride (TTC). The detail procedure referred to Stūrīte et al. (2005) is as follows: first, fresh roots were quickly incubated in breakers containing 0.6% (w/v) TTC, 0.06 M phosphate buffer, and 0.05% (v/v) Tween 20, at 24°C for 20 h; then, the roots were scanned with an Epson Perfection scanner, and the live root lengths were analyzed with Win RHIZO (Regent Instruments, Inc., Canada) pixel color classification method. LRLD was calculated by dividing the live root length by the sampling core volume for each of the soil layers.

Leaf N components

Leaf N components were measured at 20-day intervals once the first treatment entered the silking stage. On the basis of Ali et al. (2016), leaf N components were divided by function as photosynthetic N (N_{pn}), respiration N (N_{resp}), structural N (N_{stru}), and storage N (N_{store}). Maize is a C4 plant, and thus, we divided N_{pn} into five parts: ribulose-1,5-bisphosphate carboxylase (Rubisco) N, phosphoenolpyruvate carboxylase (PEPC) N, pyruvate orthophosphate dikinase (PPDK) N, electron transport/bioenergetics N (N_{et}, proteins involved in electron transport and light phosphorylated), and light harvesting N (N_{lh}, proteins for light capture in PSI, PSII, and other light-harvesting pigment protein complexes).

To extract water soluble proteins (N_w) and sodium dodecyl sulfate soluble proteins (N_{SDS}), frozen leaves were homogenized in extraction buffer and centrifuged following the method of Takashima et al. (2004). Rubisco, PEPC, and PPDK contents were separated using SDS-polyacrylamide gel electrophoresis, resulting in 52 and 15 kDa for Rubisco (Makino et al., 2003), 99 kDa for PEPC (Uedan and Sugiyama, 1976), and 94 kDa for PPDK (Sugiyama, 1973). Coomassie Brilliant Blue R-250–stained bands were washed off with formamide and then detected spectrophotometrically. N content in Rubisco ($N_{Rubisco}$), PEPC (N_{PECP}), and PPDK (N_{PPDK}) was estimated assuming 16% N in proteins. The sodium dodecyl sulfate insoluble protein N used to build cell walls was identified as structural N (N_{stru}) according to Takashima et al. (2004). Total leaf N content (N_T) and N content in N_{SDS} and N_{stru} fractions were also measured using the micro-Kjeldahl method.

N_{et}, N_{rep}, and N_{lh} were proportional to the maximum electron transport, total respiration rate, and chlorophyll concentration, respectively, and the specific calculation that we used has been described by Liu et al. (2018a). The maximum electron transport rate and total respiration rate (photorespiration rate can be ignored for maize) were measured using the A_n-C_i curve fitting calculation, according to the mechanistic model developed by Ye et al. (2013). Chlorophyll was extracted using a mixed reagent of acetone and ethyl alcohol in a ratio of 1:1. The concentrations of chlorophyll a and chlorophyll b were measured at 663 and 645 nm, respectively, using a spectrophotometer (Perkinelmer, UK) and were calculated according Arnon (1949).

Apart from N_{pn}, N_{resp}, and N_{stru}, the remaining N can be considered as N_{store}. Moreover, N_{store} included water-soluble protein storage N (N_{ow}), SDS-soluble protein storage N (N_{os}), and non-protein storage N (N_{nop}), where N_{ow} was calculated as N_w minus $N_{Rubisco}$, N_{PECP}, N_{PPDK}, and N_{rep}; N_{os} was calculated as N_{SDS} minus N_{et} and N_{lh}; and N_{nop} was calculated as N_T minus N_w, N_{SDS}, and N_{stru} (Liu et al., 2018a).

Estimation of senescence and filling traits

Leaf and root senescence dynamics were estimated from a differential logistic function (Equation 1) (van Oosterom et al., 1996) fitted to total plant GLA (GLA_T) and total LRLD in the sampling zone ($LRLD_T$) per plant, respectively.

$$y = ae^{b-ct}/(1 + e^{b-ct}) \quad \text{Eq. 1}$$

where y is GLA_T or $LRLD_T$; t is the number of days after silking; and a, b, and c are constants (a is the maximum y-value in potential, b is related to the onset and terminal of senescence, and c is related to senescence rate and duration).

The equation of the Richards function (Equation 2) fitted to the 100-kernel weight was adopted to describe filling dynamics.

$$y = a/(1 + be^{-ct})^{1/d} \quad \text{Eq. 2}$$

where y is 100-kernel weight; t is the number of days after silking; and a, b, c, and d are constants (a is the maximum y-value in potential, and b, c, and d codetermine the onset, terminal, and rate of filling, respectively).

The specific senescence and filling traits are described in Table 2.

Statistical analyses

One-way analysis of variance was performed using a general linear model (GLM) of SPSS 19.0 (SPSS, Inc., Chicago, IL, USA). The data from each sampling event for all irrigation treatments were tested using the Duncan's multiple range tests and different letters at a 0.05 level of probability. Non-linear regression model for the estimation of senescence and filling traits as well as Pearson correlation coefficients were also calculated using SPSS.

Results

Yield, WUE, and NUE

Film mulching followed by straw returning significantly improved maize yield and WUE under drip irrigation system (Figure 1; Supplementary Table 3). PI, BI, SI, and OI increased the average yield by 37.48%, 28.93%, 10.27%, and 2.23%, respectively, and increased the average WUE by 28.77%, 26.17%, 14.82%, and 3.08%, respectively, compared with and FI. PI and BI favored N translocation efficiencies for aboveground plant part as well as root and effectively improved NUE compared with other treatments. Whereas, no significant differences were found among SI, OI, and FI for N translocation efficiencies and NUE in different years ($P > 0.05$).

LRLD distribution

PI improved $LRLD_T$ at silking contributed to the large LRLD in the 0- to 20-cm soil layers (Figure 2). SI followed by BI effectively improved LRLD in the deeper 20- to 60-cm and 60- to 100-cm soil layers. There were no significant differences between FI and OI in LRLD in the 0- to 20-cm and 60- to 100-cm soil layers. However, FI significantly increased LRLD in the 20- to 60-cm soil layers in contrast to OI ($P< 0.05$).

Leaf N components and their translocation efficiencies

At earlier filling stage, N_{pn} ($N_{Rubisco}$, N_{PEPC}, N_{PPDK}, N_{et}, and N_{lc}), N_{stru}, N_{resp}, N_{ow}, and N_{os} ranked as follows: PI > BI > SI > OI,

TABLE 2 Abbreviations and descriptions of senescence and filling traits estimated from Equations 3 and 4, respectively.

Abbreviations	Traits	Description
GLA_T	Total green leaf area	Green leaf area of total plant
$LRLD_T$	Total live root length density	Live root length density in total growth zone (65 × 20 × 100 cm)
GLA_{max}	The maximum GLA_T	The maximum green leaf area of total plant
$LRLD_{max}$	The maximum $LRLD_T$	The maximum live root length density in total growth zone (65 × 20 × 100 cm)
LT_o	Onset of leaf senescence	Time at 95% of the maximum GLA_T in potential
RT_o	Onset of root senescence	Time at 95% of the maximum $LRLD_T$ in potential
GT_o	Onset of active grain filling period	Time at 5% of the maximum 100-kernel weight in potential
LT_e	Terminal of leaf senescence	Time at 1% of the maximum GLA_T in potential
RT_e	Terminal of root senescence	Time at 1% of the maximum $LRLD_T$ in potential
GT_e	Terminal of active grain filling period	Time at 95% of the maximum 100-kernel weight in potential
D_{leaf}	Green leaf duration	Period from onset to terminal of leaf senescence
D_{root}	Live root duration	Period from onset to terminal of root senescence
$D_{filling}$	Active grain filling duration	Period from onset to terminal of grain filling
LV_{max}	Maximum leaf senescence rate	Maximum descent rate of GLA_T
RV_{max}	Maximum root senescence rate	Maximum descent rate of $LRLD_T$
GV_{max}	Maximum grain filling rate	Maximum increase rate of 100-kernel weight
LV_a	Average leaf senescence rate	Average descent rate of GLA_T during D_{leaf}
RV_a	Average root senescence rate	Average descent rate of $LRLD_T$ during D_{root}
GV_a	Average grain filling rate	Average increase rate of 100-kernel weight during $D_{filling}$
I_{leaf}	Green leaf integral	Cumulative GLA_T from silking to maturity
I_{root}	Live root integral	Cumulative $LRLD_T$ from silking to maturity
GWA	Grain weight increment during active filling period	Accumulation of 100-kernel weight at $D_{filling}$

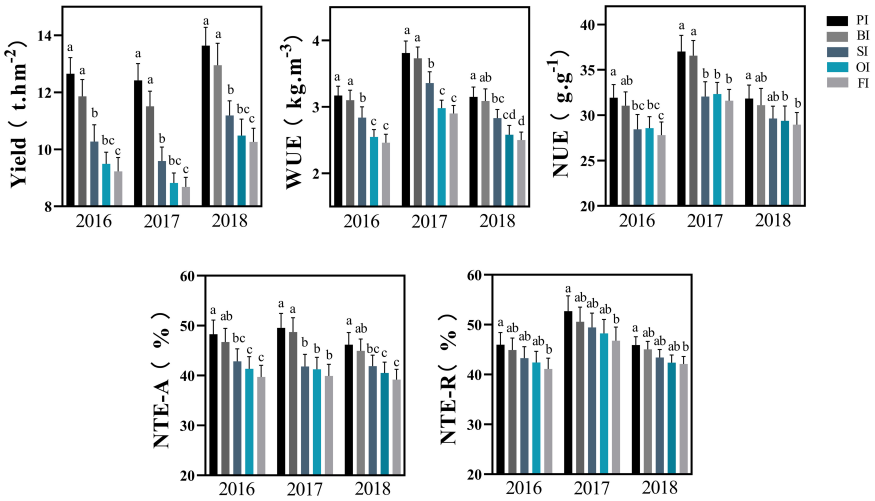

FIGURE 1
Yield, water, and N use efficiency with the different irrigation treatments. PI and BI represent drip irrigation under plastic film mulch and biodegradable film mulch, respectively; SI, drip irrigation incorporating straw returning; OI, drip irrigation with the tape buried at a shallow soil depth; FI, furrow irrigation. WUE, soil water use efficiency; NTE-A, N translocation efficiency for above ground parts; NTE-R, N translocation efficiency for roots; NUE, N use efficiency. The error bars represent standard deviations. Different lowercase letters indicate significant differences at $P < 0.05$. The data in this figure are presented in Table S2 for further interpretation.

FI (Figures 3–5). With the filling progress, the improvements for N_{pn}, N_{stru}, N_{resp}, N_{ow}, and N_{os} with PI and BI were weakened due to the protein degradation and higher translocation efficiencies of N_{pn}, N_{stru}, and N_{resp} (Figure 6). Instead, there was an increasement in N_{nop} under PI and BI during the late reproductive stage, and SI achieved higher N_{pn}, N_{stru}, N_{resp}, N_{ow}, and N_{os} during the late reproductive stage. In contrast to film mulching and straw returning treatments, OI and FI significantly increased the translocation efficiencies of N_{store} ($P< 0.05$).

Leaf senescence

PI followed by BI achieved the highest I_{leaf} associated to the large GLA_{max}, and the GLA_T value at the beginning of reproductive stage (Figure 7). Then, the GLA_T under PI and BI was gradually decreased and even lower than the other treatments considering the fast rate of leaf senescence (LV_{max} and LV_a) (Table 3). PI delayed the onset time of leaf senescence (LT_o) and simultaneously advanced the terminal time of leaf senescence (LT_e) and then resulted in a short GLA

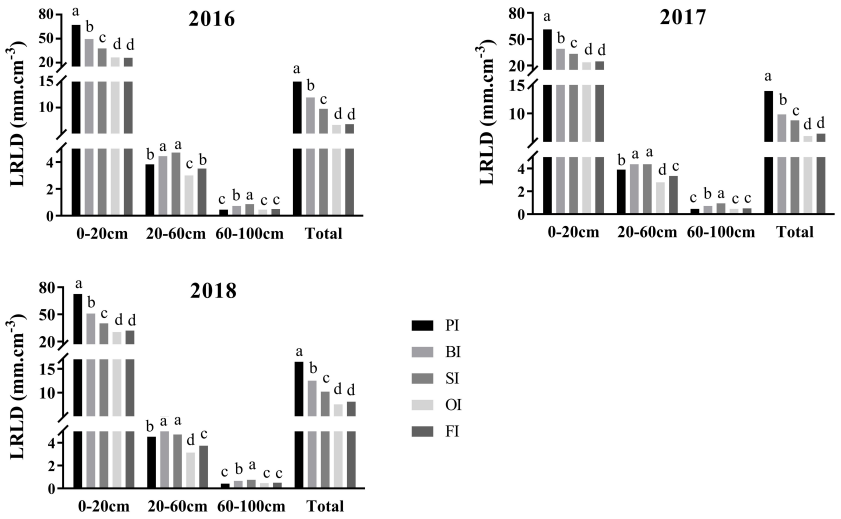

FIGURE 2
Live root length density (LRLD) distribution at silking in different soil layers. PI and BI represent drip irrigation under plastic film mulch and biodegradable film mulch, respectively; SI, drip irrigation incorporating straw returning; OI, drip irrigation with the tape buried at a shallow soil depth; FI, furrow irrigation. Different lowercase letters indicate significant differences at $P < 0.05$.

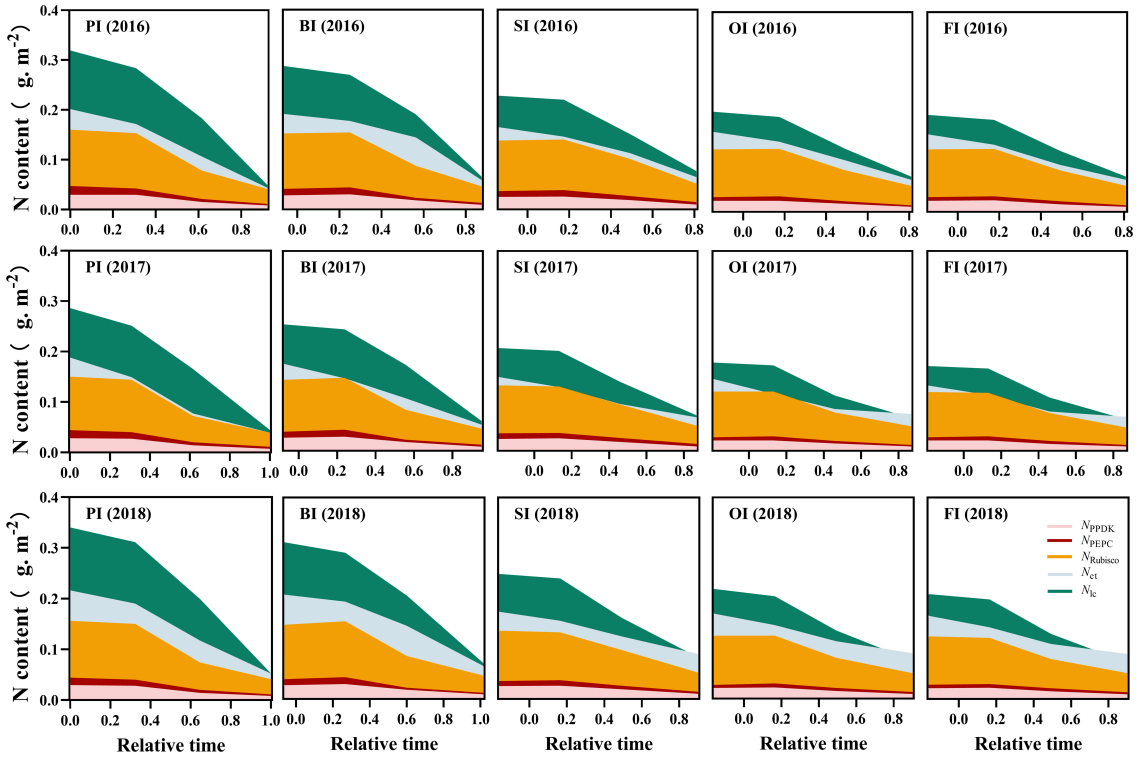

FIGURE 3
Leaf photosynthetic N dynamics during the reproductive period. PI and BI represent drip irrigation under plastic film mulch and biodegradable film mulch, respectively; SI, drip irrigation incorporating straw returning; OI, drip irrigation with the tape buried to a shallow soil depth; FI, furrow irrigation. Relative time is the ratio of days after silking to the duration from silking to maturity. N_{PPDK}, N_{PECP}, and $N_{Rubisco}$ represent N content in PPDK, PEPC, and Rubisco protein, respectively. N_{lh}, protein N responsible for light harvesting system. N_{et}, protein N responsible for electron transport/ bioenergetics. The data in this figure are presented in Table S4 for further interpretation.

duration (D_{leaf}). SI averagely prolonged D_{leaf} by 12, 8, 4, and 7 days compared with PI, BI, OI, and FI, respectively, which maintained a higher GLA_T value at the late of reproductive stage.

Root senescence

PI followed by BI maintained a higher $LRLD_{max}$, $LRLD_T$ before maturity (Figure 7), and resulted in an increased I_{root} compared with other treatments (Table 4). Although PI accelerated maize growth and development progress as well as root senescence rate (RV_{max} and RV_a), the onset time of root senescence (RT_o) with PI was only advanced in the drought year of 2017, and it was delayed in both 2016 and 2018 compared with other treatments. The shortened D_{root} under PI was mainly due to the advanced terminal time of root senescence (RT_e). SI maintained the longest D_{root}, which postponed the root senescence in contrast to PI. OI significantly delayed RT_e compared with FI, but no significant differences were found in the other root senescence traits between OI and FI ($P > 0.05$).

Grain filling characteristics

The grain weight during the reproductive stage ranked as follows: PI > BI > SI > OI > FI (Figure 7). PI obtained the highest GW_{max} and grain filling rate (GV_{max} and GV_a). Moreover, PI obviously advanced the onset time of active grain filling period (GT_o) and the terminal time of active grain filling period (GT_e) and then shortened the active grain filling duration ($D_{filling}$) compared with other treatments. SI gained higher GWA during active grain filling stage compared with OI and FI, attributed to the higher GV_{max}, GV_a, and $D_{filling}$ (Table 5).

Senescence parameters related to yield, WUE, and NUE

High GWA, GV_a, yield, WUE, and NUE were highly positively related to fast senescence rate of source organs (RV_a and LV_a), large I_{leaf} and I_{root}, and high translocation efficiency of leaf protein N (N_{pn}, N_{stru}, and N_{resp}) ($P< 0.05$) (Figure 8). D_{root} and D_{leaf} did not play a significant role in determining $D_{filling}$ significantly ($P > 0.05$), which negatively related to yield, WUE, and NUE ($P< 0.05$). The high translocation efficiency of N_{store} was not positively associated with yield, WUE, and NUE.

Discussion

Drip irrigation combined with film mulching improved *GLA*, *LRLD*, and yield

Previous studies have been proved that film mulching combined with irrigation can obviously promote maize leaf area, root size, and

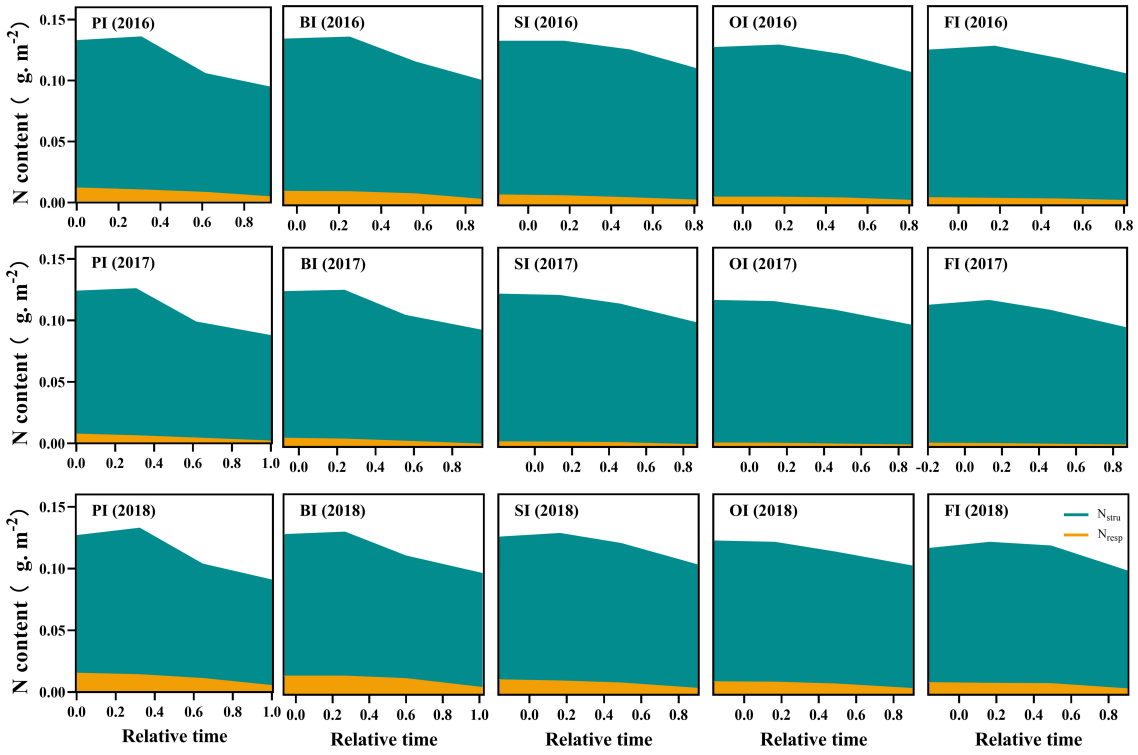

FIGURE 4
Leaf respiration protein N (N_{resp}) and structural protein N (N_{stru}) dynamics during the reproductive period. PI and BI represent drip irrigation under plastic film mulch and biodegradable film mulch, respectively; SI, drip irrigation incorporating straw returning; OI, drip irrigation with the tape buried to a shallow soil depth; FI, furrow irrigation. Relative time is the ratio of days after silking to the duration from silking to maturity. The data in this figure are presented in Table S4 for further interpretation.

biomass accumulation (Qin et al., 2016; Xue et al., 2017; Wang et al., 2021). Whereas, activated source organs, e.g., GLA and LRLD, during the reproductive stage essentially determine C assimilation, soil water, inorganic nutrient absorption, and thus ultimate grain yield formation. Drip irrigation combined with film mulching achieved the highest GLA_T and $LRLD_T$ at the silking stage due to better soil water and temperature conditions (Bu et al., 2013; Wu et al., 2021). In present study, roots were mainly distributed in the 0- to 20-cm soil layers considering the heavy clay soil (Wang et al., 2009; Sampathkumar et al., 2012; Sharma et al., 2017). PI significantly improved LRLD in the 0- to 20-cm soil layers due to the better soil hydrothermal environment during the vegetative stage (Supplementary Figures 3, 4). In addition, it facilitates plant growth and contributed to higher GLA_T and $LRLD_T$ values compared with other treatments. However, PI decreased LRLD in the deeper 20- to 100-cm soil layers accompanied with lower soil water content, in contrast to BI. SI was particularly beneficial to increase LRLD in the 60- to 100-cm soil layers, which can be explained that straw returning to the field was beneficial to improve soil water and soil structure in the deep soil layers (Wu et al., 2021). FI got higher LRLD than OI in the 20- to 60-cm soil layers, due to more irrigation water percolated to the deeper soil layers (Hassanli et al., 2009). PI and BI showed relatively low GLA_T and $LRLD_T$ only during the late filling stage (around R_5 stage) compared with other treatments and then maintained high I_{leaf} and I_{root} values during the entire reproductive stage.

Yang et al. (2016) found that drip irrigation with plastic film mulching accelerated plant senescence owing to the decreased N supply to canopy, considering the constrictive root architecture and higher soil temperature during the reproductive stage. While some studies pointed out that large root was not required for high yielding potential in high input cropping systems (Sharma et al., 2017). The present study also found that drip irrigation combined with film mulching system, especially PI, improved leaf and root senescence rates with a more constrictive LRLD distribution and higher soil temperature during the reproductive stage compared to other treatments (Supplementary Figure 4). We agreed with Christopher et al. (2016) that the higher I_{leaf} and I_{root} under drip irrigation combined with film mulching system led to a greater grain yield. I_{leaf} and I_{root} had the highest correlation to maize yield in different water environments, which were the most useful indicator to describe plant stay-green trait.

Drip irrigation combined with film mulching accelerated plant senescence accompanied with large amount of leaf protein N translocation

Maize root stops growing at anthesis when senescence started. We further found that root senescence precedes leaf senescence by 7-10 days averagely with different treatments, which was similar

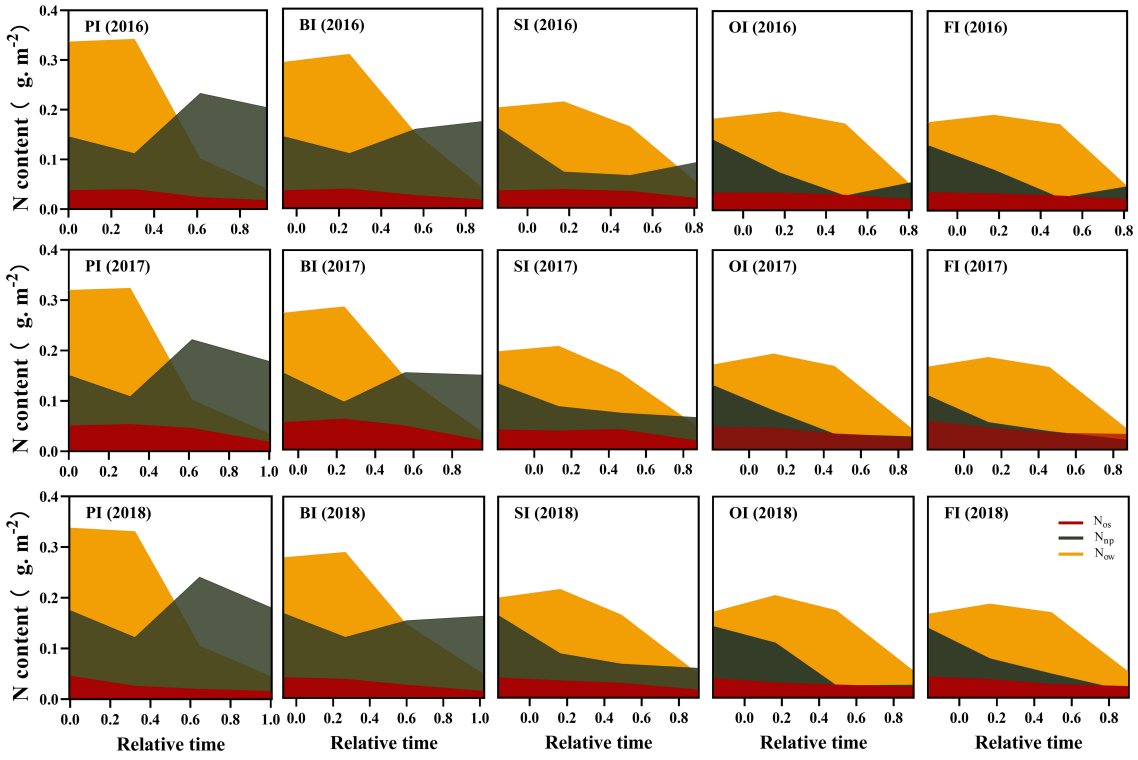

FIGURE 5
Leaf storage N dynamics during the reproductive period. PI and BI represent drip irrigation under plastic film mulch and biodegradable film mulch, respectively; SI, drip irrigation incorporating straw returning; OI, drip irrigation with the tape buried to a shallow soil depth; FI, furrow irrigation. Relative time is the ratio of days after silking to the duration from silking to maturity. N_{os}, SDS-soluble protein storage N. N_{ow}, water-soluble protein storage N. N_{nop}, non-protein storage N. The data in this figure are presented in Table S4 for further interpretation.

with the result obtained by Lisanti et al. (2013). Root activity depends on C supply from the leaves. While leaf senescence could also be induced by the ageing root, in terms of deficit N/water supply, cytokinin signal molecule, and decreased root respiration (Glanz-Idan et al., 2020; Liu et al., 2018b; Tang et al., 2019). However, in contrast to nature programmed cell death, nucleus and mitochondria remain active for a long time during the senescence process (Roberts et al., 2012), the communications between photosynthesizing leaves and roots still need more investigation during the crop reproductive stage. Drought or low N input could accelerate the senescence process (Pommel et al., 2006; Wang et al., 2013; Christopher et al., 2016). In present study, plant senescence was not induced by drought or low N stresses considering the supplemental irrigation and sufficient fertilizer supply in each treatment. The time of anthesis is a highly variable character and can strongly confound the effect of senescence on productivity (Bogard et al., 2011; Naruoka et al., 2012). PI advanced maize anthesis, but vigorous plant growth at the early filling stage delayed leaf and root senescence onset. In addition, only the advanced root senescence onset time under PI was observed during the year of 2017. Fast senescence under PI followed by BI can be also triggered by the large grain sink and greater nutrient requirement that enhanced N mobilization from source organs to grains (Aubry et al., 2008; Distelfeld et al., 2014; Ma and Dwyer, 1998; Rajcan and Tollenaar, 1999). As a consequence, the leaf protein N contents fell rapidly after silking. The delayed onset

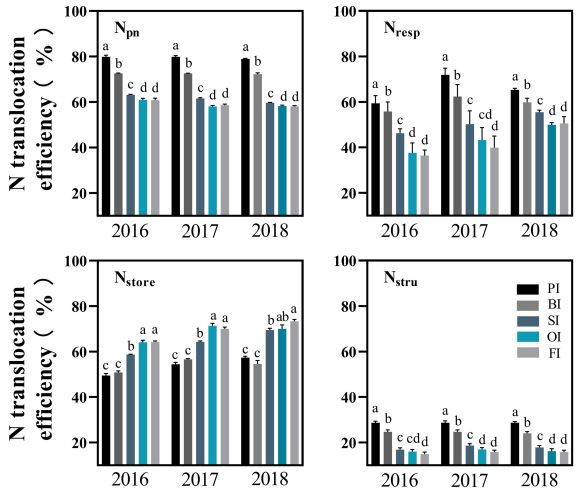

FIGURE 6
Translocation efficiency of different leaf N components. PI and BI represent drip irrigation under plastic film mulch and biodegradable film mulch, respectively; SI, drip irrigation incorporating straw returning; OI, drip irrigation with the tape buried to a shallow soil depth; FI, furrow irrigation. N_{pn}, photosynthetic protein N. N_{resp}, respiration protein N. N_{stru}, structural protein N. N_{store}, storage N. The error bars represent standard deviations. Different lowercase letters indicate significant differences at $P < 0.05$.

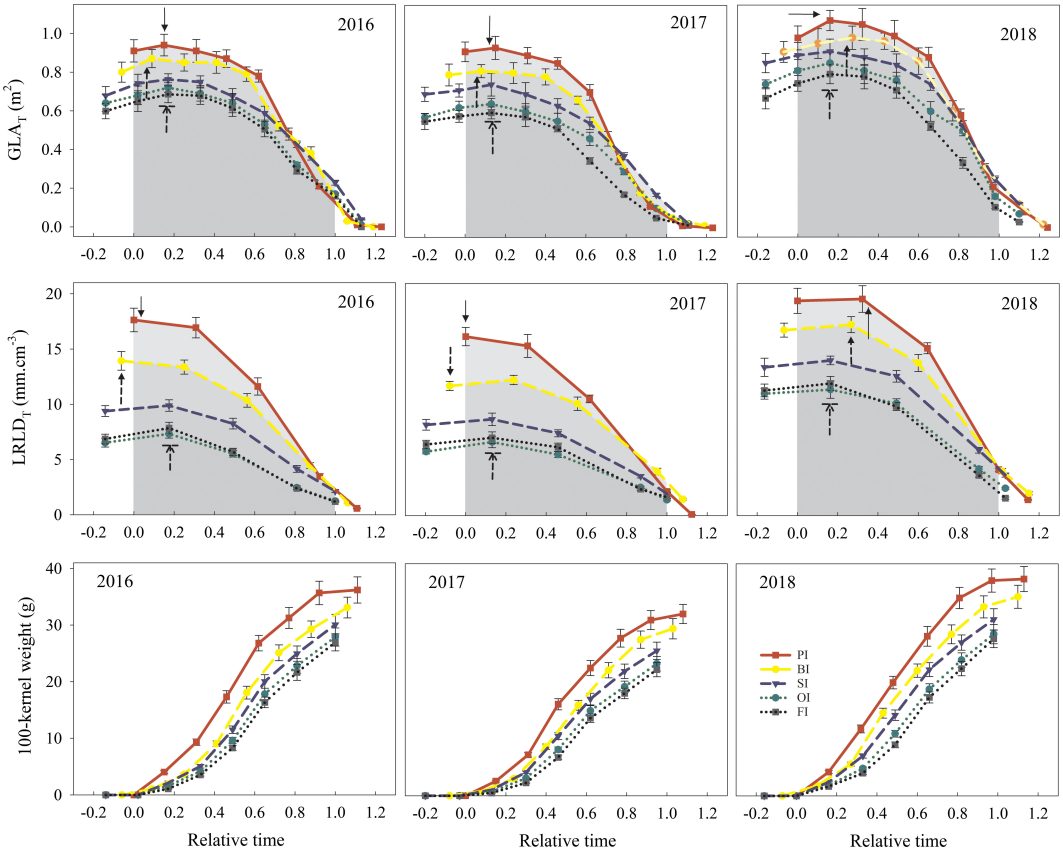

FIGURE 7
Total green leaf area per plant (GLA_T), total live root length density per plant ($LRLD_T$), and 100-kernel weight dynamics during the reproductive period. PI and BI represent drip irrigation under plastic film mulch and biodegradable film mulch, respectively; SI, drip irrigation incorporating straw returning; OI, drip irrigation with the tape buried to a shallow soil depth; FI, furrow irrigation. Relative time is the ratio of days after silking to the duration from silking to maturity. Gray area indicates the integral value of GLAT and LRLDT from silking (relative time = 0) to maturity (relative time = 1). Solid arrow for PI, dotted arrow for BI, and dotted arrow for SI; OI and FI with a line indicate the GLAmax or LRLDmax. The error bars represent standard deviations.

TABLE 3 Leaf senescence traits with the different drip irrigation treatments.

Year	Treatments [a]	LT_o [b] (DS)	LT_e (DS)	D_{leaf} (d)	LV_{max} (m^2. d^{-1})	LV_a (m^2. d^{-1})	I_{leaf} (m^2. d)
2016	PI	30.97 a [c]	81.65 d	50.68 d	0.034 a	0.017 a	46.12 a
	BI	30.38 a	85.18 c	54.81 c	0.029 b	0.015 b	42.98 b
	SI	28.74 b	93.09 a	64.35 a	0.022 c	0.011 c	38.32 c
	OI	27.56 c	87.57 c	60.01 b	0.022 c	0.011 c	33.94 d
	FI	27.62 c	85.86 c	58.24 b	0.021 c	0.011 c	32.26 d
2017	PI	28.96 a	75.67 c	46.71 c	0.037 a	0.018 a	42.66 a
	BI	26.04 b	78.29 b	52.25 b	0.029 b	0.014 b	36.91 b
	SI	23.97 b	85.91 a	61.93 a	0.022 c	0.011 c	33.05 c
	OI	25.45 b	80.16 b	54.71 b	0.021 c	0.010 c	27.81 d
	FI	20.96 c	73.40 d	52.44 b	0.021 c	0.010 c	23.75 e
2018	PI	32.54 a	81.19 cd	48.66 c	0.040 a	0.020 a	52.06 a
	BI	29.58 b	82.93 c	53.35 b	0.034 b	0.017 b	46.88 b

(Continued)

10.3389/fpls.2023.1133206

TABLE 3 Continued

Year	Treatments [a]	LT_o [b] (DS)	LT_e (DS)	D_{leaf} (d)	LV_{max} (m^2. d^{-1})	LV_a (m^2. d^{-1})	I_{leaf} (m^2. d)
	SI	30.33 b	88.06 a	57.73 a	0.029 c	0.014 c	44.82 bc
	OI	30.18 b	85.06 b	54.88 ab	0.027 c	0.014 c	39.80 cd
	FI	27.04 c	79.47 d	52.44 b	0.027 c	0.013 c	34.93 d

[a]PI and BI represent drip irrigation under plastic film mulch and biodegradable film mulch, respectively; SI, drip irrigation incorporating straw returning; OI, drip irrigation with the tape buried at a shallow soil depth; FI, furrow irrigation.
[b]LT_o, onset of leaf senescence; LT_e, terminal of leaf senescence; D_{leaf}, green leaf duration; LV_{max}, maximum leaf senescence rate; LV_a, average leaf senescence rate; I_{leaf}, green leaf integral; DS, days after silking.
[c]Values are estimated from the Equation 3 fitted to the total green leaf area per plant, and the determination coefficient (R^2) of the regression equations with different treatments were >0.978. Different lowercase letters indicate significant differences at $P < 0.05$.

TABLE 4 Root senescence traits with the different drip irrigation treatments.

Year	Treatments [a]	RT_o [b] (DS)	RT_e (DS)	D_{root} (d)	RV_{max} ($mm.cm^{-3}$. d^{-1})	RV_a ($mm.cm^{-3}$. d^{-1})	I_{root} ($mm.cm^{-3}$. d)
2016	PI	18.86 a [c]	88.30 d	69.43 b	0.484 a	0.242 a	801.01 a
	BI	17.66 a	93.21 b	75.55 a	0.348 b	0.174 b	635.78 b
	SI	17.87 a	96.34 a	78.47 a	0.235 c	0.117 c	452.42 c
	OI	15.11 b	92.40 b	77.30 a	0.171 d	0.085 d	306.28 d
	FI	14.45 b	90.09 c	75.64 a	0.185 d	0.092 d	317.46 d
2017	PI	18.73 b	87.75 c	69.02 b	0.445 a	0.222 a	728.51 a
	BI	24.65 a	95.05 a	70.41 a	0.324 b	0.161 b	598.09 b
	SI	19.72 b	95.58 a	75.86 a	0.211 c	0.105 c	396.50 c
	OI	21.68 ab	92.97 ab	71.29 a	0.164 d	0.082 d	292.37 d
	FI	20.91 ab	91.55 b	70.64 a	0.182 d	0.091 cd	315.47 d
2018	PI	25.43 a	89.32 c	63.90 b	0.583 a	0.291 a	957.32 a
	BI	21.73 ab	93.19 b	71.45 a	0.456 b	0.227 b	811.34 b
	SI	23.64 ab	97.42 a	73.78 a	0.356 c	0.178 c	679.78 c
	OI	22.78 ab	93.65 b	70.88 a	0.301 d	0.150 d	539.93 d
	FI	19.43 b	89.72 c	70.29 a	0.314 d	0.157 d	528.92 d

[a]PI and BI represent drip irrigation under plastic film mulch and biodegradable film mulch, respectively; SI, drip irrigation incorporating straw returning; OI, drip irrigation with the tape buried at a shallow soil depth; FI, furrow irrigation.
[b]RT_o, onset of root senescence; RT_e, terminal of root senescence; D_{root}, live root duration; RV_{max}, maximum root senescence rate; RV_a, average root senescence rate; I_{root}, live root integral; DS, days after silking.
[c]Values are estimated from the Equation 3 fitted to the total live root length density per plant, and the determination coefficient (R^2) of the regression equations with different treatments were >0.975. Different lowercase letters indicate significant differences at $P < 0.05$.

TABLE 5 Grain filling traits with the different drip irrigation treatments.

Year	Treatments [a]	GT_o [b] (DS)	GT_e (DS)	$D_{filling}$ (d)	GV_{max} (g. d^{-1})	GV_a (g. d^{-1})	GWA (g)
2016	PI	5.04 d [c]	64.29 c	59.25 b	0.920 a	0.621 a	33.83 a
	BI	10.74 c	71.34 b	60.61 ab	0.841b	0.567 b	31.56 b
	SI	11.15 c	73.74 ab	62.59 a	0.777 c	0.524 c	30.15 c
	OI	12.65 b	74.25 ab	61.60 ab	0.737 c	0.498 c	28.16 d
	FI	14.69 a	77.35 a	62.66 a	0.721 c	0.486 c	27.93 d

(Continued)

TABLE 5 Continued

Year	Treatments [a]	GT_o [b] (DS)	GT_e (DS)	$D_{filling}$ (d)	GV_{max} (g. d^{-1})	GV_a (g. d^{-1})	GWA (g)
2017	PI	8.39 d	68.90 c	60.51 b	0.823 a	0.548 a	30.46 a
	BI	10.14 c	73.08 b	62.93 ab	0.755 b	0.507 b	29.31 b
	SI	10.69 c	76.25 a	65.56 a	0.681 c	0.449 c	27.02 c
	OI	12.47 b	77.09 a	64.61 a	0.632 c	0.419 c	24.88 d
	FI	14.70 d	76.89 a	62.19 ab	0.631 c	0.419 c	23.93 d
2018	PI	5.36 d	68.42 c	63.06 b	0.953 a	0.636 a	36.86 a
	BI	7.68 c	73.00 b	65.31 ab	0.870 b	0.575 b	34.49 b
	SI	8.70 c	76.09 a	67.39 a	0.782 c	0.520 c	32.22 c
	OI	10.72 b	77.19 a	66.48 a	0.734 c	0.493 c	30.15 d
	FI	12.12 a	77.65 a	65.53 ab	0.730 c	0.493 c	29.65 d

[a]PI and BI represent drip irrigation under plastic film mulch and biodegradable film mulch, respectively; SI, drip irrigation incorporating straw returning; OI, drip irrigation with the tape buried at a shallow soil depth; FI, furrow irrigation.

[b]GT_o, onset of active grain filling period; GT_e, terminal of active grain filling period; $D_{filling}$, active grain filling duration; GV_{max}, maximum grain filling rate; GV_a, average grain filling rate; GWA, grain weight increment during active filling period; DS, days after silking.

[c]Values are estimated from the Equation 4 fitted to the 100-kernel weight, and the determination coefficient (R^2) of the regression equations with different treatments were >0.998. Different lowercase letters indicate significant differences at P < 0. 05.

time as well as the advanced terminal time of senescence resulted in a short duration of GLA and LRLD under PI and BI. No significant differences were found between OI and FI in senescence rates, GLA and LRLD durations, or filling dynamics due to the approximate soil environment and plant growth process.

Many genetic studies have suggested that the stay-green trait (referred to as a delay in the onset of leaf senescence, or a longer green area duration) correlates with high yield for cereal crops. The previous results also suggested that stay-green cultivars enhanced root absorption capacity for soil water and N nutrient by ensuring the supply of photosynthetic C assimilate (Ma and Dwyer, 1998; Hoang and Kobata, 2009; Bogard et al., 2011; Gaju et al., 2011; Gregersen et al., 2013; Zhang et al., 2013; Liu et al., 2021). However, the relationship between senescence and crop productivity is complex. More recent works showed that there was no consistent advantage of the delayed senescence hybrids on crop production, and stay-green trait could be only necessary for higher yield under terminal drought or low N stresses (Borrell et al., 2000; Acciaresi et al., 2014; Antonietta et al., 2014; Christopher et al., 2016). Moreover, the average temperature at the late filling stage (September) was only 16.8°C, which limited photosynthetic C and N assimilation and slowed the export of nutrients to grains (temperatures between 22-24°C are optimal for maize filling) (Christopher et al., 2016). Therefore, longer GLA and LRLD durations under SI treatment did not contribute to higher yield. We agreed with Xie et al. (2016); Yang and Udvardi (2018) and Zhang et al. (2019) that faster senescence led to better utilization of photosynthetic C and N assimilation for larger grains. Thus, filling rate, grain weight increment, yield, WUE, and NUE were positively associated with senescence rates of leaf and root, but negatively associated with GLA and LRLD durations. We also found that a larger biomass translocation amount and a higher biomass translocation efficiency (Supplementary Figure 5) were necessary for high-yield formation under PI and BI during the fast senescence process. In addition to leaf protein N, PI showed a higher biomass translocation amount/efficiency in contrast to BI, which lead to a higher grain weight.

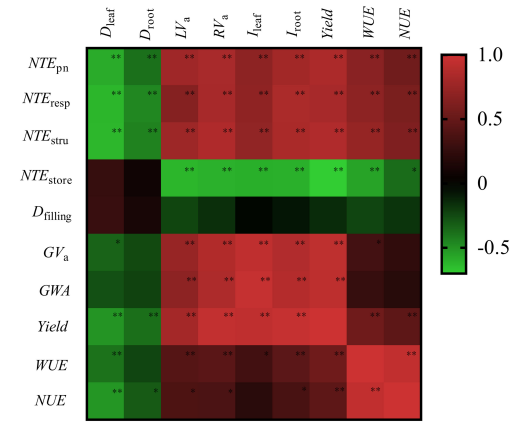

FIGURE 8
Heatmap of correlation coefficients between senescence traits, filling traits, yield, water, and N use efficiency. D_{leaf}, green leaf duration; D_{root}, live root duration; LV_a, average leaf senescence rate; RV_a, average root senescence rate; I_{leaf}, green leaf integral; I_{root}, live root integral; $D_{filling}$, grain filling duration; GV_a, average grain filling rate; *GWA*, grain weight growth during filling. WUE, water use efficiency. NUE, N use efficiency. NUE_{pn}, NTE_{resp}, NTE_{stru}, and NTE_{store} are the translocation efficiency of photosynthetic N, respiration N, structure N and storage N, respectively. * $P < 0.05$ and ** $P < 0.01$.

Higher leaf storage N transport efficiency did not attribute to high yield, WUE, and NUE

CO_2 assimilation capacity is positively regulated by leaf N, which is the main component of chlorophyll and photosynthetic proteins. The distribution of different leaf N fractions determines leaf growth and photosynthesis capacity, thus affecting N utilization. A decrease in photosynthetic rate is mainly due to the degradation of photosynthetic enzymes. Our results showed that different leaf N components decreased along with a reduction of GLA during the reproductive stage. Considering the vigorous vegetative growth, higher $N_{Rubisco}$, N_{PEPC}, N_{PPDK}, N_{et}, N_{lc}, N_{stru}, N_{resp}, N_{ow}, and N_{os} were obtained by PI and BI at the earlier filling stage. The transfer of leaf N after anthesis has an important effect on photosynthesis. In addition, degraded leaf proteins provided an enormous source of N for kernel development (Masclaux-Daubresse et al., 2010). Mu et al. (2018) found that photosynthetic proteins, i.e., Rubisco, PEPC, and PPDK, had great transfer potential in maize, and their transfer efficiencies were enhanced by low N treatment. Storage N in the forms of nitrate, amino acid, and protein is important for plant to prevent from adversity (Xu et al., 2012; Liu et al., 2018a). However, the regulation effect of storage N on crop production during the senescence period is still lack of research. Our results further showed that the highest translocation efficiency was found in N_{pn}, whereas the lowest was found in N_{stru}. In contrast to PI, SI improved soil water and achieved higher LRLD in the deep soil layer, which was beneficial to root absorption capacity, therefore allowing leaves to retain photosynthetic capacity with less N mobilization during the reproductive period, and led to a higher leaf N content during the late reproductive stage. PI followed by BI had the highest translocation efficiency in N_{pn}, N_{resp}, and N_{stru}, which were positively associated with senescence rate (LV_a and RV_a), NUE, WUE, and yield and were negatively correlated with D_{leaf} and D_{root}. Meanwhile, non-protein storage N accumulated only under PI and BI treatments during the late reproductive stage. PI and BI showed a low translocation efficiency of N_{store} compared with SI, OI, and FI. Thus, it can be concluded that higher remobilization of non-protein storage N was improved by SI, FI, and OI to make up for the relative inadequacy of leaf N. Faster and larger translocation of protein N from leaves to grains ensured a high WUE and NUE under drip irrigation combined with film mulching system (Figure 9).

Conclusions

Drip irrigation combined with a film mulching system achieved the highest grain yield, WUE, and NUE, by increasing the cumulative GLA and LRLD, biomass, and leaf protein N transportation efficiency during the reproductive period. Drip irrigation combined with biodegradable film mulching had no significant differences in yield, WUE, and NUE compared to that with plastic film mulching, and it is the recommended practice to reduce overall use of plastic and creation of plastic waste. Under drip irrigation combined with returning straw into soil, root growth was effectively promoted in the deeper soil layer, and the duration of GLA and LRLD was prolonged. However, the delayed senescence under this system did not contribute to higher yield, considering the limited C and N assimilation capacity associated with low air temperature during the late reproductive stage in the northeast plain of China. Larger remobilization of leaf non-protein storage N

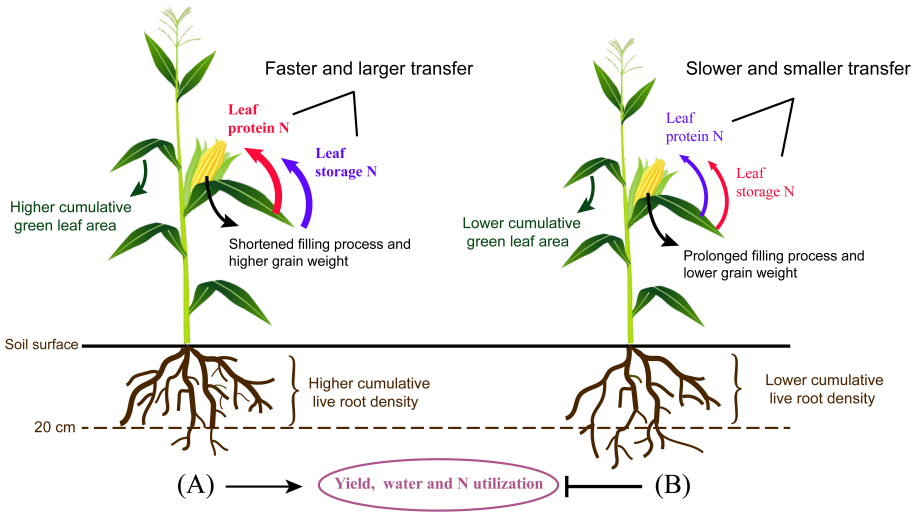

FIGURE 9
The comparison of drip irrigation under film mulch **(A)** and drip irrigation incorporating straw returning **(B)** during the reproductive stage of maize. In contrast to **(B)**, **(A)** showed a higher cumulative green leaf area and live root density in the top 0- to 20-cm soil layers, but a lower cumulative live root density in the deeper soil layers. In addition, larger N was fast transferred from leaves to grains, accompanied with a shortened filling process and higher grain weight, which contributed to the improvement of yield, water, and N utilization for **(A)**. Non-protein storage N transfer was stimulated by **(B)** to make up for the relative inadequacy of leaf N. In the comparison between **(A, B)**, the red and bule font represent higher and lower translocation efficiency for different N components, respectively.

could not contribute to a high yield, WUE, or NUE under drip irrigation combined with straw returning, drip irrigation with the tape buried at a shallow soil depth, and furrow irrigation systems. Whereas, the hormone signals and molecular regulation mechanisms of the protein N translocation from leaves to grains are worthy of further exploration in the future under different cropping systems.

Data availability statement

The raw data supporting the conclusions of this article will be made available by the authors, without undue reservation.

Author contributions

YW and YJW designed the study. YW, FYY, and XNL performed the measurements. LM performed the data analysis and wrote the first draft of the manuscript, which was extensively edited by all authors. All authors contributed to the article and approved the submitted version.

Funding

This work was supported by National Natural Science Foundation of China (U19A2035); the Science and Technology Project of Education Department of Jiangxi Province, China (GJJ2201901); China Agricultural Research System (CARS-34); Jilin Province Key Technology R&D Program (20220302004NC); and the Strategic Priority Research Program of the Chinese Academy of Sciences (XDA28020400).

Conflict of interest

The reviewer LZ declared a shared parent affiliation with authors MA, FY and YW to the handling editor at the time of review. The authors declare that the research was conducted in the absence of any commercial or financial relationships that could be construed as a potential conflict of interest.

Publisher's note

Supplementary material

The Supplementary Material for this article can be found online at: https://www.frontiersin.org/articles/10.3389/fpls.2023.1133206/full#supplementary-material

References

Acciaresi, H. A., Tambussi, E. A., Antonietta, M., Zuluaga, M. S., Andrade, F. H., and Guiamét, J. (2014). Carbon assimilation, leaf area dynamics, and grain yield in contemporary earlier- and later-senescing maize hybrids. *Eur. J. Agron.* 59, 29–38. doi: 10.1016/j.eja.2014.05.007

Ali, A. A., Xu, C., Rogers, A., Fisher, R. A., Wullschleger, S. D., Massoud, E. C., et al. (2016). A global scale mechanistic model of photosynthetic capacity (LUNA V1. 0). *Geosci. Model. Deve.* 9, 587–606. doi: 10.5194/gmdd-8-6217-2015

Allen, R. G., Pereira, L. S., Raes, D., and Smith, M. (1998). Crop evapotranspiration *Guidelines for computing crop water requirements, irrigation and drainage paper 56* (Rome: FAO), 300.

Antonietta, M., Fanello, D., Acciaressi, H., and Guiamet, J. J. (2014). Senescence and yield responses to plant density in stay green and earlier-senescing maize hybrids from Argentina. *Field Crop Res.* 155, 111–119. doi: 10.1016/j.fcr.2013.09.016

Arif, M., Ilyas, M., Riaz, M., Ali, K., Shah, K., Haq, I. U., et al. (2017). Biochar improves phosphorus use efficiency of organic-inorganic fertilizers, maize-wheat productivity and soil quality in a low fertility alkaline soil. *Field Crop Res.* 214, 25–37. doi: 10.1016/j.fcr.2017.08.018

Arnon, D. I. (1949). Copper enzymes in isolated chloroplasts polyphenoloxidase in beta vulgaris. *Plant Physiol.* 24, 1–15. doi: 10.1104/pp.24.1.1

Aubry, S., Mani, J., and Hörtensteiner, S. (2008). Stay-green protein, defective in mendel's green cotyledon mutant, acts independent and upstream of pheophorbide a oxygenase in the chlorophyll catabolic pathway. *Plant Mol. Biol.* 67, 243–256. doi: 10.1007/s11103-008-9314-8

Bogard, M., Jourdan, M., Allard, V., Martre, P., Perretant, M. R., Ravel, C., et al. (2011). Anthesis date mainly explained correlations between post-anthesis leaf senescence, grain yield, and grain protein concentration in a winter wheat population segregating for flowering time QTLs. *J. Exp. Bot.* 62, 3621–3636. doi: 10.1093/jxb/err061

Borrell, A. K., Hammer, G. L., and Douglas, A. C. L. (2000). Does maintaining green leaf area in sorghum improve yield under drought? i. leaf growth and senescence. *Crop Sci.* 40, 1026–1037. doi: 10.2135/cropsci2000.4041026x

Bu, L. D., Liu, J. L., Zhu, L., Luo, S. S., Chen, X. P., Li, S. Q., et al. (2013). The effects of mulching on maize growth, yield and water use in a semi-arid region. *Agric. Water Manage.* 123, 71–78. doi: 10.1016/j.agwat.2013.03.015

Christopher, J. T., Christopher, M. J., Borrell, A. K., Fletcher, S., and Chenu, K. (2016). Stay-green traits to improve wheat adaptation in well-watered and water-limited environments. *J. Exp. Bot.* 67, 5159–5172. doi: 10.1093/jxb/erw276

Distelfeld, A., Avni, R., and Fischer, A. M. (2014). Senescence, nutrient remobilization, and yield in wheat and barley. *J. Exp. Bot.* 65, 3783–3798. doi: 10.1093/jxb/ert477

Döll, P., and Siebert, S. (2002). Global modeling of irrigation water requirements. *Water Resour. Res.* 38, 8–1-8-10. doi: 10.1029/2001WR000355

Evans, J. R., and Clarke, V. C. (2019). The nitrogen cost of photosynthesis. *J. Exp. Bot.* 70, 7–15. doi: 10.1093/jxb/ery366

Fu, F. B., Li, F. S., and Kang, S. Z. (2017). Alternate partial root-zone drip irrigation improves water and nitrogen use efficiencies of sweet-waxy maize with nitrogen fertigation. *Sci. Rep-UK.* 7, 1–10. doi: 10.1038/s41598-017-17560-2

Gaju, O., Allard, V., Martre, P., Snape, J. W., Heumez, E., LeGouis, J., et al. (2011). Identification of traits to improve the nitrogen-use efficiency of wheat genotypes. *Field Crop Res.* 123, 139–152. doi: 10.1016/j.fcr.2011.05.010

Gao, Z., Liang, X. G., Lin, S., Zhao, X., Zhang, L., Zhou, L. L., et al. (2017). Supplemental irrigation at tasseling optimizes water and nitrogen distribution for high-yield production in spring maize. *Field Crop Res.* 209, 120–128. doi: 10.1016/j.fcr.2017.04.015

Glanz-Idan, N., Tarkowski, P., Turečková, V., and Wolf, S. (2020). Root-shoot communication in tomato plants: cytokinin as a signal molecule modulating leaf photosynthetic activity. *J. Exp. Bot.* 71, 247–257. doi: 10.1093/jxb/erz399

Gregersen, P. L., Culetic, A., Boschian, L., and Krupinska, K. (2013). Plant senescence and crop productivity. *Plant Mol. Biol.* 82, 603–622. doi: 10.1007/s11103-013-0013-8

Gu, X. B., Cai, H. J., Chen, P. P., Li, Y. P., Fang, H., and Li, Y. N. (2021). Ridge-furrow film mulching improves water and nitrogen use efficiencies under reduced irrigation and nitrogen applications in wheat field. *Field Crop Res.* 270, 108214. doi: 10.1016/j.fcr.2021.108214

Hassanli, A. M., Ebrahimizadeh, M. A., and Beecham, S. (2009). The effects of irrigation methods with effluent and irrigation scheduling on water use efficiency and corn yields in an and region. *Agric. Water Manage.* 96, 93–99. doi: 10.1016/j.fcr.2017.04.015

Heath, O. V. S., and Gregory, F. G. (1938). The constancy of the mean net assimilation rate and its ecological importance. *Ann. Bot-London.* 2, 811–818. doi: 10.1093/oxfordjournals.aob.a084036

Hoang, T. B., and Kobata, T. (2009). Root contribution to stay-green in rice (*Oryza sativa* l.) subjected to desiccated soils in the post-anthesis period. *Root Res.* 18, 5–13. doi: 10.3117/rootres.18.5

Kamal, N. M., Gorafi, Y. S., Tsujimoto, H., and Ghanim, A. M. (2018). Stay-green QTLs response in adaptation to post-flowering drought depends on the drought severity. *BioMed. Res. Int.* 1, 1–15. doi: 10.1155/2018/7082095

Li, R. F., Hu, D. D., Ren, H., Yang, Q. L., Dong, S. T., Zhang, J. W., et al. (2022). How delaying post-silking senescence in lower leaves of maize plants increases carbon and nitrogen accumulation and grain yield. *Crop J.* 10, 853–863. doi: 10.1016/j.cj.2021.11.006

Li, X. Y., Šimůnek, J., Shi, H. B., Yan, J. W., Peng, Z. Y., and Gong, X. W. (2017b). Spatial distribution of soil water, soil temperature, and plant roots in a drip-irrigated intercropping field with plastic mulch. *Eur. J. Agron.* 83, 47–56. doi: 10.1016/j.eja.2016.10.015

Li, G. H., Zhao, B., Dong, S. T., Zhang, J. W., Liu, P., and Vyn, T. J. (2017a). Impact of controlled release urea on maize yield and nitrogen use efficiency under different water conditions. *PLoS One* 12, e0181774. doi: 10.1371/journal.pone.0181774

Liao, Z. Q., Zeng, H. L., Fan, J. L., Lai, Z. L., Zhang, C., Zhang, F. C., et al. (2022). Effects of plant density, nitrogen rate and supplemental irrigation on photosynthesis, root growth, seed yield and water-nitrogen use efficiency of soybean under ridge-furrow plastic mulching. *Agr. Water Manage.* 268, 107688. doi: 10.1016/j.agwat.2022.107688

Lisanti, S., Hall, A. J., and Chimenti, C. A. (2013). Influence of water deficit and canopy senescence pattern on *Helianthus annuus* (L.) root functionality during the grain-filling phase. *Field Crop Res.* 154, 1–11. doi: 10.1016/j.fcr.2013.08.009

Liu, Z., Hu, C., Wang, Y., Sha, Y., Hao, Z., Chen, F., et al. (2021). Nitrogen allocation and remobilization contributing to low-nitrogen tolerance in stay-green maize. *Field Crop Res.* 263, 108078. doi: 10.1016/j.fcr.2021.108078

Liu, T., Ren, T., White, P. J., Cong, R., and Lu, J. W. (2018a). Storage nitrogen co-ordinates leaf expansion and photosynthetic capacity in winter oilseed rape. *J. Exp. Bot.* 69, 2995–3007. doi: 10.1093/jxb/ery134

Liu, H. Y., Wang, W. Q., He, A., and Nie, L. X. (2018b). Correlation of leaf and root senescence during ripening in dry seeded and transplanted rice. *Rice Sci.* 25, 279–285. doi: 10.1016/j.rsci.2018.04.005

Lobell, D. B., Roberts, M. J., Schlenker, W., Braun, N., Little, B. B., Rejesus, R. M., et al. (2014). Greater sensitivity to drought accompanies maize yield increase in the US Midwest. *Science* 344, 516–519. doi: 10.1126/science.1251423

Ma, B. L., and Dwyer, L. M. (1998). Nitrogen uptake and use of two contrasting maize hybrids differing in leaf senescence. *Plant Soil* 199, 283–291. doi: 10.1023/A:1004397219723

Makino, A., Sakuma, H., Sudo, E., and Mae, T. (2003). Differences between maize and rice in n-use efficiency for photosynthesis and protein allocation. *Plant Cell Physiol.* 44, 952–956. doi: 10.1093/pcp/pcg113

Masclaux-Daubresse, C., Daniel-Vedele, F., Dechorgnat, J., Chardon, F., Gaufichon, L., and Suzuki, A. (2010). Nitrogen uptake, assimilation and remobilization in plants: challenges for sustainable and productive agriculture. *Ann. Bot.* 105, 1141–1157. doi: 10.1093/aob/mcq028

Mu, X., and Chen, Y. (2021). The physiological response of photosynthesis to nitrogen deficiency. *Plant Physiol. Bioch.* 158, 76–82. doi: 10.1016/j.plaphy.2020.11.019

Mu, X., Chen, Q., Chen, F., Yuan, L., and Mi, G. (2018). Dynamic remobilization of leaf nitrogen components in relation to photosynthetic rate during grain filling in maize. *Plant Physiol. Bioch.* 129, 27–34. doi: 10.1016/j.plaphy.2018.05.020

Naruoka, Y., Sherman, J. D., Lanning, S. P., Blake, N. K., Martin, J. M., and Talbert, L. E. (2012). Genetic analysis of green leaf duration in spring wheat. *Crop Sci.* 52, 99–109. doi: 10.2135/cropsci2011.05.0269

Payero, J. O., Tarkalson, D. D., Irmak, S., Davison, D., and Petersen, J. L. (2008). Effect of irrigation amounts applied with subsurface drip irrigation on corn evapotranspiration, yield, water use efficiency, and dry matter production in a semiarid climate. *Agric. Water Manage.* 95, 895–908. doi: 10.1016/j.agwat.2008.02.015

Pommel, B., Gallais, A., Coque, M., Quilleré, I., Hirel, B., Prioul, J.L., et al. (2006). Carbon and nitrogen allocation and grain filling in three maize hybrids differing in leaf senescence. *Eur. J. Agron.* 24, 203–211. doi: 10.1016/j.eja.2005.10.001

Qin, S. J., Li, S. E., Kang, S. Z., Du, D. S., Tong, L., and Ding, R. S. (2016). Can the drip irrigation under film mulch reduce crop evapotranspiration and save water under the sufficient irrigation condition? *Agric. Water Manage.* 177, 128–137. doi: 10.1016/j.agwat.2016.06.022

Rajcan, I., and Tollenaar, M. (1999). Source-sink ratio and leaf senescence in maize: II. nitrogen metabolism during grain filling. *Field Crop Res.* 60, 255–265. doi: 10.1016/S0378-4290(98)00143-9

Roberts, I. N., Caputo, C., Criado, M. V., and Funk, C. (2012). Senescence-associated proteases in plants. *Physiol. Plantarum.* 145, 130–139. doi: 10.1111/j.1399-3054.2012.01574.x

Sampathkumar, T., Pandian, B. J., and Mahimairaja, S. (2012). Soil moisture distribution and root characters as influenced by deficit irrigation through drip system in cotton-maize cropping sequence. *Agric. Water Manage.* 103, 43–53. doi: 10.1016/j.agwat.2011.10.016

Sharma, S. P., Leskovar, D. I., Crosby, K. M., and Volder, A. (2017). Root growth dynamics and fruit yield of melon (*Cucumis melo* l.) genotypes at two locations with sandy loam and clay soils. *Soil Till. Res.* 168, 50–62. doi: 10.1016/j.still.2016.12.006

Si, Z., Qin, A., Liang, Y., Duan, A., and Gao, Y. (2023). A review on regulation of irrigation management on wheat physiology, grain yield, and quality. *Plants* 12, 692. doi: 10.3390/plants12040692

Stūrīte, I., Henriksen, T. M., and Breland, T. A. (2005). Distinguishing between metabolically active and inactive roots by combined staining with 2,3,5-triphenyltetrazolium chloride and image colour analysis. *Plant Soil* 271, 75–82. doi: 10.1007/s11104-004-2027-0

Sugiyama, T. (1973). Purification, molecular, and catalytic properties of pyruvate phosphate dikinase from the maize leaf. *Biochemistry* 12, 2862–2868. doi: 10.1021/bi00739a014

Takashima, T., Hikosaka, K., and Hirose, T. (2004). Photosynthesis or persistence: nitrogen allocation in leaves of evergreen and deciduous *Quercus* species. *Plant Cell Environ.* 27, 1047–1054. doi: 10.1111/j.1365-3040.2004.01209.x

Tang, G. L., Li, X. Y., Lin, L. S., Gu, Z. Y., and Zeng, F. J. (2019). Leaf senescence can be induced by inhibition of root respiration. *J. Plant Growth Regul.* 38, 980–991. doi: 10.1007/s00344-018-09907-4

Uedan, K., and Sugiyama, T. (1976). Purification and characterization of phosphoenolpyruvate carboxylase from maize leaves. *Plant Physiol.* 57, 906–910. doi: 10.1104/pp.57.6.906

van Oosterom, E. J., Jayachandran, R., and Bidinger, F. R. (1996). Diallel analysis of the stay-green trait and its components in sorghum. *Crop Sci.* 36, 549–555. doi: 10.2135/cropsci1996.0011183X003600030002x

Wang, J. T., Du, G. F., Tian, J. S., Jiang, C. D., Zhang, Y. L., and Zhang, W. F. (2021). Mulched drip irrigation increases cotton yield and water use efficiency *via* improving fine root plasticity. *Agr. Water Manage.* 255, 106992. doi: 10.1016/j.agwat.2021.106992

Wang, F. X., Feng, S. Y., Hou, X. Y., Kang, S. Z., and Han, J. J. (2009). Potato growth with and without plastic mulch in two typical regions of northern China. *Field Crop Res.* 110, 0–129. doi: 10.1016/j.fcr.2008.07.014

Wang, Z., Wu, Q., Fan, B., Zhang, J., Li, W., Zheng, X., et al. (2019). Testing biodegradable films as alternatives to plastic films in enhancing cotton (*Gossypium hirsutum* l.) yield under mulched drip irrigation. *Soil Till. Res.* 192, 196–205. doi: 10.1016/j.still.2019.05.004

Wang, D., Yu, Z. W., and White, P. J. (2013). The effect of supplemental irrigation after jointing on leaf senescence and grain filling in wheat. *Field Crop Res.* 151, 35–44. doi: 10.1016/j.fcr.2013.07.009

Wu, Y., Bian, S., Liu, Z., Wang, L., Wang, Y., Xu, W., et al. (2021). Drip irrigation incorporating water conservation measures: Effects on soil water–nitrogen utilization, root traits and grain production of spring maize in semi-arid areas. *J. Integr. Agr.* 20, 3127–3142. doi: 10.1016/S2095-3119(20)63314-7

Wu, D., Fang, S. B., Li, X., He, D., Zhu, Y. C., Yang, Z. Q., et al. (2019). Spatial-temporal variation in irrigation water requirement for the winter wheat-summer maize rotation system since the 1980s on the north China plain. *Agric. Water Manage.* 214, 78–86. doi: 10.1016/j.agwat.2019.01.004

Xie, Q., Mayes, S., and Sparkes, D. L. (2016). Early anthesis and delayed but fast leaf senescence contribute to individual grain dry matter and water accumulation in wheat. *Field Crop Res.* 187, 24–34. doi: 10.1016/j.fcr.2015.12.009

Xu, C., Fisher, R., Wullschleger, S. D., Wilson, C. J., Cai, M., and McDowell, N. G. (2012). Toward a mechanistic modeling of nitrogen limitation on vegetation dynamics. *PLoS One* 7, e37914. doi: 10.1371/journal.pone.0037914

Xue, X. X., Mai, W. X., Zhao, Z. Y., Zhang, K., and Tian, C. Y. (2017). Optimized nitrogen fertilizer application enhances absorption of soil nitrogen and yield of castor with drip irrigation under mulch film. *Ind. Crop Prod.* 95, 156–162. doi: 10.1016/j.indcrop.2016.09.049

Yang, W., Parsons, D., and Mao, X. (2022). Exploring limiting factors for maize growth in northeast China and potential coping strategies. *Irrig. Sci.*, 1–15. doi: 10.1007/s00271-022-00813-y

Yang, R., Tian, C. Y., and Mai, W. X. (2016). Characteristics of root development in cotton suffering presenility under drip irrigation and film mulch in xinjiang autonomous region. *J. Plant Nutri. Fert.* 22, 1384–1392. doi: 10.11674/zwyf.15321

Yang, J., and Udvardi, M. (2018). Senescence and nitrogen use efficiency in perennial grasses for forage and biofuel production. *J. Exp. Bot.* 69, 855–865. doi: 10.1093/jxb/erx241

Ye, Z. P., Suggett, D. J., Robakowski, P., and Kang, H. J. (2013). A mechanistic model for the photosynthesis–light response based on the photosynthetic electron transport of photosystem II in C3 and C4 species. *New Phytol.* 199, 110–120. doi: 10.1111/nph.12242

Zhang, W. Q., Dong, A., Liu, F. L., Niu, W. Q., and Siddique, K. H. M. (2022). Effect of film mulching on crop yield and water use efficiency in drip irrigation systems: A meta-analysis. *Soil Till. Res.* 221, 105392. doi: 10.1016/j.still.2022.105392

Zhang, Y. Q., Wang, J. D., Gong, S. H., Xu, D., Sui, J., Wu, Z. D., et al. (2018). Effects of film mulching on evapotranspiration, yield and water use efficiency of a maize field with drip irrigation in northeastern China. *Agric. Water Manage.* 205, 90–99. doi: 10.1016/j.agwat.2018.04.029

Zhang, Y. J., Yang, Q. Y., Lee, D. W., Goldstein, G., and Cao, K. F. (2013). Extended leaf senescence promotes carbon gain and nutrient resorption: importance of maintaining winter photosynthesis in subtropical forests. *Oecologia* 173, 721–730. doi: 10.1007/s00442-013-2672-1

Zhang, L., Zhou, X., Fan, Y., Fu, J., Hou, P., Yang, H., et al. (2019). Post-silking nitrogen accumulation and remobilization are associated with green leaf persistence and plant density in maize. *J. Integr. Agr.* 18, 1882–1892. doi: 10.1016/S2095-3119(18)62087-8

Zhu, L. X., Liu, L. T., Sun, H. C., Zhang, Y. J., Zhu, J. J., Zhang, K., et al. (2021). Physiological and comparative transcriptomic analysis provide insight into cotton (*Gossypium hirsutum* l.) root senescence in response. *Front. Plant Sci.* 12. doi: 10.3389/fpls.2021.748715

frontiers | Frontiers in Plant Science

TYPE Original Research
PUBLISHED 20 March 2023
DOI 10.3389/fpls.2023.1110727

OPEN ACCESS

EDITED BY
Baizhao Ren,
Shandong Agricultural University, China

REVIEWED BY
Aziz Khan Khan,
Guangxi University, China
Yin Wang,
Peking University, China
Fangmin Zhang,
Nanjing University of Information Science and Technology, China

*CORRESPONDENCE
Fu Cai
caifu@iaesy.cn
Yushu Zhang
zhangyushu@iaesy.cn

SPECIALTY SECTION
This article was submitted to Plant Abiotic Stress, a section of the journal Frontiers in Plant Science

RECEIVED 29 November 2022
ACCEPTED 06 March 2023
PUBLISHED 20 March 2023

CITATION
Cai F, Mi N, Ming H, Zhang Y, Zhang H, Zhang S, Zhao X and Zhang B (2023) Responses of dry matter accumulation and partitioning to drought and subsequent rewatering at different growth stages of maize in Northeast China. *Front. Plant Sci.* 14:1110727. doi: 10.3389/fpls.2023.1110727

Responses of dry matter accumulation and partitioning to drought and subsequent rewatering at different growth stages of maize in Northeast China

Fu Cai[1,2]*, Na Mi[1,2], Huiqing Ming[3], Yushu Zhang[1,2]*, Hui Zhang[4], Shujie Zhang[1,2], Xianli Zhao[1] and Bingbing Zhang[4]

[1]Institute of Atmospheric Environment, China Meteorological Administration, Shenyang, China, [2]Key Laboratory of Agrometeorological Disasters, Liaoning, Shenyang, China, [3]Liaoning Province Meteorological Service Center, Shenyang, China, [4]Jinzhou Ecology and Agriculture Meteorological Center, Jinzhou, China

Introduction: Dry matter accumulation (DMA) and dry matter partitioning (DMP) are important physiological processes determining crop yield formation. Deep understanding of the DMA and DMP processes and their responses to drought are limited by difficulty in acquiring total root biomass.

Methods: Pot experiments with treatments quitting and ceasing ear growth (QC) and controlling soil water (WC) during vegetative (VP) and reproductive (RP) growth stages of maize (Zea mays) were conducted in Jinzhou in 2019 and 2020 to investigate the effects of drought and rewatering on DMW and DMP of different organs.

Results: The response of DMW of reproductive organ to drought was more sensitive than those of vegetative organs, and was maintained after rehydration. Drought during VP (VPWC) reduced more sharply DMW of stalk than of leaves, and that during RP (RPWC) decreased more substantially leaves DMW. The effect of drought on DMPR was inconsistent with that on DMW for each organ. The DMP patterns of maize in different growth stages have adaptability to some level of water stress, and their responses increased with drought severity. Drought increased significantly DMP rates (DMPRs) of vegetative organs and reduced the ear DMPR and harvest index (HI), attributing to the suppressed photosynthates partitioning into ear and dry matter redistribution (DMRD) of vegetative organs, especially for stalk DMRD decreasing 26%. The persistence of drought impact was related to its occurrence stage and degree as well as the duration during rewatering to maturity. The aftereffect of drought during different growth periods on DMP were various, and that of VPWC enlarged and drastically induced the reduction of HI, also was larger than that of RPWC which demonstrated obvious alleviation in the previous responses of DMP and HI. Root-shoot ratio (RSR) increased under VPWC and RPWC and subsequent rehydration.

Discussion: The DMWs of stalk, roots and leaves were affected by VPWC in order from large to small, and were close to or larger than the controls after rehydration, indicating the compensation effect of rewatering after drought. The DMPRs, RSR AND HI are the important parameters in agricultural production, and are often used as the constants, but in fact they vary with plant growth. In addition, the interannual differences in ear and stalk DMPRs in response to drought were probably caused by the difference in degree and occurrence stage of drought, further reflecting the variation in response of allometry growth among organs to the environment. Besides, the persistence of drought impact was related to the occurrence stage and degree of drought, which is also associated with the duration during rewatering to maturity. Notably, the effect of drought on DMW was inconsistent with that on DMPR for each organ meaning that the two variables should be discussed separately. The QC did not affect total DMW but increased RSR, changed and intensified the effect and aftereffect of RPWC on DMP, respectively, indicating that the DMP pattern and its response to drought occur change under the condition of QC.

KEYWORDS

maize, dry matter partitioning, drought response, total root biomass, root-shoot ratio

1 Introduction

Dry matter accumulation (DMA) and dry matter partitioning (DMP) are important physiological processes determining crop yield formation (Kumar et al., 2006). In agro-ecosystems, crop yield is not only dependent on DMA, but also closely related to efficient allocation of dry matter to harvested organs (Zhang et al., 2019). The total amount of photosynthates stored in various organs at different growth stages of plants is determined by DMP and is affected by factors such as nutrition, temperature, radiation and soil moisture status (Steinfort et al., 2017; Lizaso et al., 2018). Generally, DMP refers to transport of accumulated photosynthates by leaves to different organs, which can be expressed as instantaneous values at a certain moment and cumulative values over a period of time (Poorter et al., 2012). According to the functional balance hypothesis, this allocation is characterized by preferential allocation of photosynthates to resource-constrained organs (Ma, 2017). In addition, when crops enter the reproductive period (RP), photosynthates mainly supply the growth of reproductive organs, while vegetative organs transfer a portion of dry matter to reproductive organs through dry matter redistribution (DMRD) to maintain a higher growth rate for the latter, with the redistribution rate of stalks being the largest, up to 35% of its dry weight (Weiner, 2004; Cai et al., 2022). Often, DMP is studied in plants such as crops and fruit trees whose reproductive organs are dominant (Andrews et al., 2001; Marcelis and Heuvelink, 2007). The ratio of DMP of photosynthates to each part of plant is usually calculated by measuring the change of dry matter weight (DMW) of each organ during a period of time. In crop models, aboveground and belowground biomass are often separated and the proportion of aboveground biomass occupied by each organ is then determined (Hijmans et al., 1994). In addition, root-shoot ratio (RSR) and harvest index (HI) are important parameters to reflect the DMP pattern among plant organs (Borras and Vitantonio, 2018), playing an important role in crop yield estimation and model construction.

Drought is one of the most vital constraints to crop yield and is an important factor affecting DMP (Li et al., 2019). On the one hand, it reduces dry matter quality by inhibiting photosynthesis (Gao et al., 2015) and, on the other hand, affects root and leaf growth by shifting DMP pattern (Berendse and Möller, 2009), thus affecting physiological processes such as nutrient absorption and photosynthesis (Djaman et al., 2013). Additionally, DMRD is inhibited by the ripening effect of drought (Turc and Tardieu, 2018). Overall, combination of the above effects leads to a decline in production. Studies on DMP have concentrated on the effects of such factors as planting density (Liu et al., 2011), sowing date (Dou et al., 2017), cultivation type (Wang et al., 2015; Cai et al., 2021) and soil fertilizer (Dai et al., 2008; Wei et al., 2017). There have also been some studies on the effects of drought on DMP (Jiang et al., 2018; Mi et al., 2018; Tan et al., 2019), but these have not generally considered roots, especially total root biomass, thus restricting in-depth understanding of relevant mechanisms.

Moreover, the response strategies of existing mainstream crop models to DMP under drought conditions all have defects of varying degrees, making it difficult to accurately simulate drought stress. In the AquaCrop model, allocation of photosynthates to different organs is not considered (Toumi et al., 2016). For the WOFOST model, the distribution of photosynthates to roots, stems and leaves is set to a fixed value only related to the development stage, and water stress would increase the proportion of roots, without considering DMRD (Hijmans et al., 1994). In the DSSAT model, the increase of DMW of leaves and stalks is proportional

and not affected by environmental stress, and the proportion of DMRD at maturity is a fixed empirical parameter, without considering the effect of environmental stress (Lizaso et al., 2011). In the EPICphase model, water stress is considered, but DMP is empirically expressed and lacks a mechanism (Cavero et al., 2000). Therefore, deep investigation of the drought response mechanism of DMP and improving its parameter scheme are crucial to improve the ability of crop models to reproduce the drought process (Anothai et al., 2013).

Maize (*Zea mays*) is one of the three major food crops in the world, has the largest planting area and yield in recent years, and plays an important role in guaranteeing world food security and economic development (FAO, 2019). Northeast China is the main production area of spring maize in China, has the second largest maize belt in the world and plays a crucial role in grain production (Cheng et al., 2016). Maize is sensitive to its major growth constraint, drought, during the whole growth period (Mi et al., 2017; Huang et al., 2019; Zhou et al., 2020). Considering the limitation in understanding the response of crop DMP to drought duo to minor field experiment especially for scarce root measurement and the importance of maize in crop, we carried out 2-year pot experiment for maize suffering drought in order to integrally obtain DMWs of all organs and figure out how to be partitioned for maize photosynthate under drought and when the growth of maize ear is limited, which will offer abundant information about maize DMP pattern and further make up the shortage of the existing studies. Specifically, the objective of this study is to reveal (1) the variation characteristics of DMA, DMP and DMRD of different organs of maize at various growth stages under normal water supply; (2) their responses to drought and subsequent rehydration; and (3) the responses to QC treatment (quitting and ceasing ear growth during the RP), QC combined with drought, and subsequent rewatering. This study will enhance understanding of the disaster-causing process for maize under drought conditions, and promote improved parameter schemes in crop models, providing a scientific basis for accurately assessing the impact of drought and reasonably guiding disaster prevention and reduction for maize production.

2 Data and methods

2.1 Site description

The water control experiment for maize in present study was conducted at the Jinzhou Agricultural Meteorological Experimental Station in Liaoning Province, which has a temperate monsoon continental climate with average temperature and precipitation during 1981–2010 of 9.9°C and 568 mm, respectively. The study area has a typical brown soil with a pH 6.3 and nutritional composition including soil organic matter content of 15.24 $g{\cdot}kg^{-1}$, nitrogen of 1.04 $g{\cdot}kg^{-1}$, phosphorus of 0.50 $g{\cdot}kg^{-1}$ and potassium of 22.62 $g{\cdot}kg^{-1}$. The average field capacity, the wilting point and bulk density for the top 50 cm soil layer are 22.64%, 5.64% and 1.426 $g{\cdot}cm^{-3}$, respectively.

2.2 Experimental design

The experiment pots with sealed bases were made of PVC pipe with diameter 40 cm and height 100 cm, and were closely fixed row by row on the aboveground with a homemade metal fence, which formed a row and column interval of 40 cm among the plant. In the autumn before the experiment year, surface soil (0–20 cm) was evenly mixed, weighed and loaded into the pots. The soil water content was measured, and dry soil weight in pots was calculated. The maize variety was 'Xianyu 335'. Three seeds were manually planted into the pots at the soil depth of 5 cm and a strong plant was remained when the corn had its fifth leaf. This research consisted of different experiments reflecting respectively the real-time and prolonged effects of drought. The experimental treatments and their abbreviations are shown in Table 1.

The real-time effect experiment of drought included VPWC, RPWC and QCWC, as well as their corresponding control treatments: VPCK, RPCK and QCCK. More specifically, each treatment had six replicate pots. Natural precipitation was allowed before jointing, and appropriate amounts of water were added when precipitation was insufficient to ensure normal growth of maize plants. At jointing stage, six samples were selected to

TABLE 1 Abbreviations used to denote each parameter and treatment.

Abbreviation	Description
DM	Dry matter
DMA	Dry matter accumulation
DMP	Dry matter partitioning
DMW	Dry matter weight
RSR	Root-shoot ratio
HI	Harvest index
DMPR	Dry matter partitioning rate
DMRD	Dry matter redistribution
WC	Water control treatment
VP	Vegetative period of maize
RP	Reproductive period of maize
QC	The treatment of quitting and ceasing ear growth during RP
CK	The control treatment
VPWC,VPCK	WC during VP and its CK
RPWC, RPCK	WC during RP and its CK
QCWC, QCCK	WC based on QC and its CK
VPAWC, RPAWC	VPWC and RPWC irrigated until maturity
CKA	The CK for VPAWC and RPAWC
QCAWC, QCACK	QCWC irrigated until maturity, and its CK
VPA, RPA, QCA	The corresponding referent treatments of VPAWC, RPAWC and QCAWC

determine soil moisture: the average relative moisture of the soil column was 39.1 ± 4.0% and 49.4 ± 3.8% in 2019 and 2020, respectively. Then, water was replenished according to the difference between the measured and the optimum water content, i.e. relative soil moisture of 75%. After entering jointing stage, a large mobile waterproof shelter was used to prevent natural precipitation reaching the ground (Mi et al., 2018). According to the growth stage, weather and soil water conditions, the control treatment was irrigated with appropriate water to ensure the normal growth of maize. Treatments VPWC and RPWC reduced water supply from jointing to silking stage and from tasseling to milk ripening stage, respectively, to build drought episodes. Based on RPWC treatment, QCWC was conducted by wrapping female panicles in plastic bags to limit pollination and then to inhibit grain growth, in order to analyze the response of DMP in different organs under inhibited ear growth. Specifically, the DMWs of different organs of maize for each treatment were measured at the end of VPWC, RPWC and QCWC.

The prolonged effects of drought were reflected with comparisons of DMWs and DMPs of different organs after rewatering between drought and control treatments, and the experiment was designed as follows. After the end of drought process, some treatments for VPWC, RPWC and QCWC adopted the same irrigation measures as the control treatment until maturity, and were defined as VPAWC, RPAWC, and QCAWC, respectively, with the corresponding control treatments of VPAWC and RPAWC named CKA, and that of QCAWC named QCACK. Similarly, each treatment had six replicate pots.

Tables 2, 3 show the dates of growth periods of maize and irrigation regimes for the different treatments. In 2019, for the VPWC, water supplementation was not conducted on June 27, and was half of the amount of CKA from June 27 to July 15, and was the same as that of CKA after July 20. The DMWs for VPWC were observed on July 16. For the RPWC, water supplementation was not conducted on July 20, and was half of that of CKA from July 22 to August 14, and was the same as that of CKA after August 22. The DMWs for RPWC were observed on 15 August and harvesting was conducted on 15 September. In 2020, the water supplementation of VPWC was one-third of CKA for July 9–15, half of CKA on July 20 and consistent with CKA from July 24. The DMWs for VPWC were observed on July 21. For the RPWC, water supplementation was half of CKA from July 24 to August 11, and consistent with CKA after August 20. The DMWs for RPWC were observed on August 20 and harvesting was conducted on September 18.

2.3 Methods

2.3.1 Soil water content measurement

Soil water content was calculated as follows:

$$\theta_{rm} = \frac{\sum_i^n (\frac{\theta_i}{\theta_f})}{n} \quad (1)$$

where θ_{rm} is soil relative moisture; θ_i and θ_f are soil weight water content and field capacity, respectively; and n is the number of replicates (i.e. n = 6).

Soil moisture status in pots at the end of different treatments in each year is shown in Figure 1. Soil moisture of the CK treatments was higher than those of the WC treatments after drought in 2019, but failed to reach the appropriate level, i.e. soil water content of 60%, due to deficient water supply. After rehydration, soil moisture of VPAWC, QCACK and QCAWC still did not reach 60%. Conversely, soil moisture of the CK treatment in 2020 reached the appropriate level after drought and rehydration, while soil moisture for QCAWC and QCACK was below 60% likely due to experimental errors. It is worth noting that soil moisture of RPAWC and QCAWC was higher than for the corresponding CK treatments in both years. The reason was that the physiological functions of plants were disrupted due to RP drought, and the plants withered after rewatering, which decreased the water consumption of transpiration. In addition, the measured soil samples were in the outer layer of the soil column, and were drier than those in the inside of the soil column, resulting in a lower value relative to the real condition.

TABLE 2 Dates (month/day) of maize growth periods and sampling in 2019 and 2020.

Growth/Sampling period	2019			2020		
	CKA	VPWC	RPWC	CKA	VPWC	RPWC
Sowing	4/30	4/30	4/30	5/10	5/10	5/10
Emergence	5/6	5/6	5/6	5/17	5/17	5/17
Jointing	6/15	6/15	6/15	6/20	6/20	6/20
Tasseling	7/10	7/12	7/10	7/16	7/16	7/16
Silking	7/15	7/17	7/15	7/21	7/27	7/21
Milk	8/6	8/6	8/6	8/18	8/18	8/18
Maturity	9/15	9/15	9/15	9/18	9/18	9/18
Sampling for VPWC	7/16			7/21		
Sampling for RPWC	8/15			8/20		

TABLE 3 Irrigation regimes for the different experimental treatments in 2019 and 2020.

Water supply amount (mm)	2019				2020			
	Dates (m/d)	CKA	VPWC	RPWC	Dates (m/d)	CKA	VPWC	RPWC
Precipitation	5/3-6/21	285.2	285.2	285.2	5/10-6/13	185.9	185.9	185.9
Irrigation	6/26	56.6	56.6	56.6	6/22	56.6	56.6	56.6
	6/27	28.3	0	28.3	6/25	5.7	5.7	5.7
	7/2	56.6	28.3	56.6	6/26	5.4	5.4	5.4
	7/5	56.6	28.3	56.6	6/29	85	85	85
	7/10	84.9	42.5	84.9	7/9	85	28.3	85
	7/15	56.6	28.3	56.6	7/15	85	28.3	85
	7/20	56.6	56.6	0	7/20	56.6	28.3	56.6
	7/22	56.6	56.6	28.3	7/24	56.6	56.6	28.3
	7/25	56.6	56.6	28.3	7/30	113.2	113.2	56.6
	7/29	28.3	28.3	28.3	8/3	113.2	113.2	56.6
	7/30	84.9	84.9	28.3	8/8	113.2	113.2	56.6
	8/1	56.6	56.6	28.3	8/11	113.2	113.2	56.6
	8/7	28.3	28.3	28.3	8/20	56.6	56.6	56.6
	8/14	56.6	56.6	28.3				
	8/22	56.6	56.6	56.6				
Total amount		1105.9	950.3	879.5		1131.2	989.5	876.5

2.3.2 Sampling and measurement

The height, stalk diameter and leaf area of maize plants were measured at the end of every treatment. The stalk diameter was presented with the maximum width of the second stem node from ground surface. Maximum length and width were measured for each leaf of the maize plant, and computation formulas of total leaf area per plant (LA) are as follows:

$$LA = \sum_{i=1}^{n}(L_i \times W_i \times 0.75) \quad (2)$$

Where i is the number of leaves on the plant, L_i is the maximum leaf length, W_i is the maximum leaf width, and 0.75 is a factor used conventionally.

Plants from each treatment were cut at the ground level and separated into the stalk, leaves, bracts and ear. It should be noted that the ear was divided into kernel and cob to measure in 2019, but not in 2020. Roots were obtained with washing method. Specifically, the experiment pot was cut open to gain an intact soil pillar, and then the soil pillar was splitted into segments in an interval of 10 cm, and was soaked in water for a period of time. At last, all roots were gained with washing. All the samples were oven-dried at 105°C for 30 min, and weighed after drying at 70°C to constant weight (Mi et al., 2018).

2.3.3 Calculations of DMPR, RSR and HI

In order to reflect the relationship of DMP among different organs and their responses to drought, the variation characteristics of DMPRs, RSRs and HIs were studied.

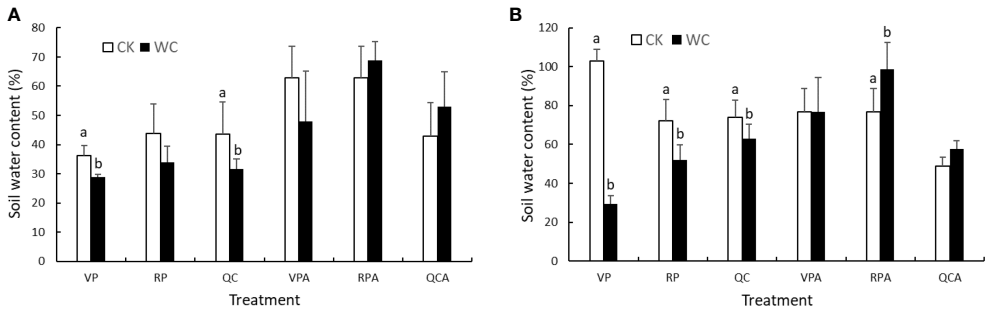

FIGURE 1
Soil moisture of WC and CK for different treatments in 2019 **(A)** and 2020 **(B)**.

DMPR is expressed as follows:

$$DMPR_i = DM_i/DM_t \quad (3)$$

$$DM_t = DM_r + DM_s + DM_l + DM_e + DM_b,$$

where DM_i is the DMW of organ i; DM_r, DM_s, DM_l, DM_e and DM_b are the DMWs of roots, stalks, leaves, ears and bracts, respectively and $DMPR_i$ is the DMPR of organ i.

RSR is expressed as follows:

$$RSR = DM_r/DM_{ab}, \quad (4)$$

where DM_{ab} is aboveground DMW, i.e. the sum of DMWs of stalks, leaves, ears and bracts.

HI is expressed as follows:

$$HI = DM_g/DM_{ab}. \quad (5)$$

DM_g is the DMW of grain i.e. the DM_e substracts the DMW of maize cob. The ratio of DM_g to DM_e for RPWC, RPCK, VPAWC, RPAWC and CKA in 2019 were 0.82, 0.85, 0.82, 0.84 and 0.87, and were used to calculate corresponding DM_g in 2020.

2.4 Data statistics

The observation data each year were statistically analyzed using SPSS 20.0 software (SPSS Inc., Chicago, IL, USA, URL:(https://www.ibm.com/cn-zh/spss?lnk=flatitem)) separately. The differences among experimental treatments were calculated using Duncan's multiple comparison test and a one-way ANOVA at the 0.05 significance levels.

3 Results

3.1 Drought response of maize morphological characteristics

Figure 2 shows the green leaf area per plant, plant height and stalk diameter for WC and CK after different treatments. Different letters represent significance level ($P < 0.05$) of differences of the variables between WC and CK treatments; no letter indicates insignificant difference; also applies in the other figures. The green leaf area of RPWC in 2020 was 0 because the leaves were all dry and not green. In

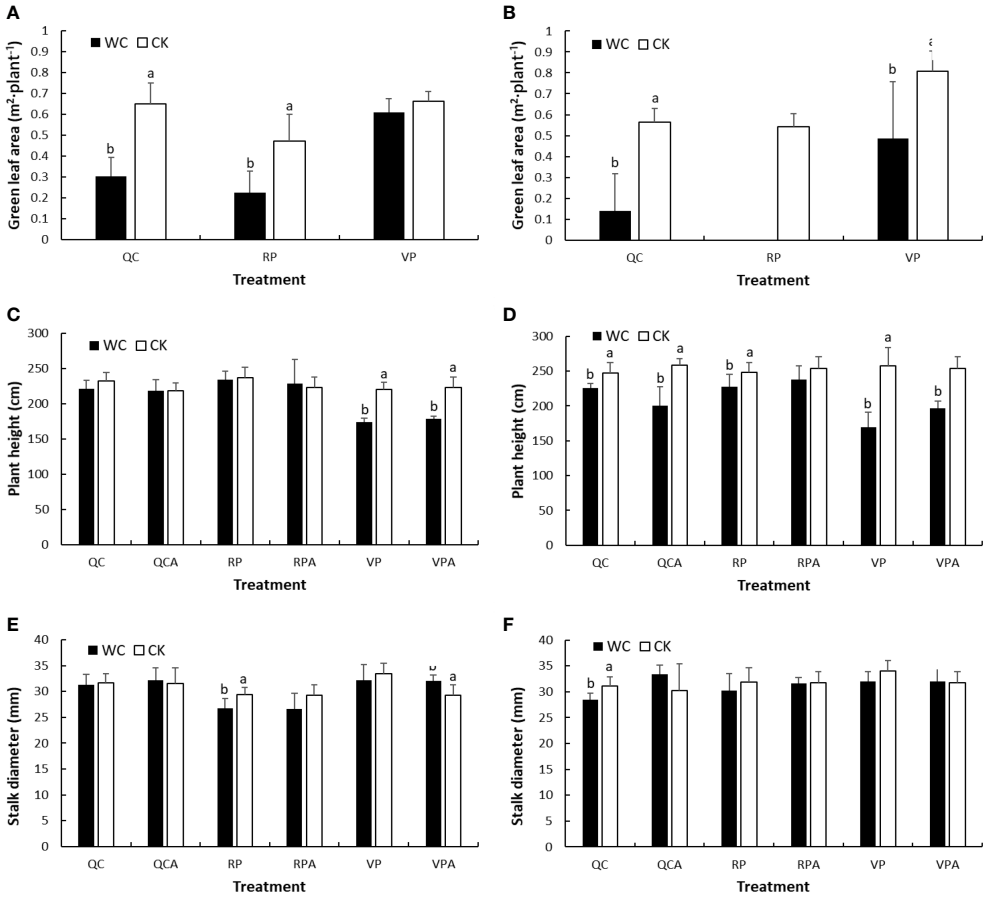

FIGURE 2
Green leaf area **(A, B)**, plant height **(C, D)** and stalk diameter **(E, F)** for WC and CK of different treatments in 2019 and 2020.

2019 and 2020, the leaf areas of most WC treatments were significantly smaller than those of the controls except that of VPWC in 2019.

For plant height, there were no significant differences between WC and CK for RP, RPA, QC and QCA treatments in 2019, while those for VP and VPA were significant. In 2020, RPWC resulted in a significant small reduction in plant height, and rewatering narrowed the difference at later growth stages. The QCWC significantly decreased plant height, and its effect increased in later growth stages. Both VPWC and VPAWC induced significant and sharp decreases in plant height.

In 2019, stalk diameter was insignificantly reduced after VPWC, and significantly increased after rewatering. The RPWC significantly reduced stalk diameter, but the reduction was insignificant after rewatering. There were no significant variations in stalk diameter after QCWC and following rehydration. In 2020, stalk diameter was insignificantly affected by VPWC and RPWC, and reduced significantly after QCWC, but insignificantly increased for QCAWC.

3.2 Responses of maize DMWs to drought

3.2.1 Responses of belowground, aboveground and total DMWs to drought

The aboveground and total DMWs of maize for different drought treatments in 2019 and 2020 were nearly all significantly lower than the corresponding control values (Figure 3). They increased significantly from the end of VPWC to maturity, and the differences in DMWs of all treatments between WC and CK in 2020 were greater than in 2019. The roots DMWs of CK showed a decreasing trend from the end of VPWC and RPWC to maturity. The roots DMWs of VPWC and VPAWC were slightly smaller and significantly greater than the controls in 2019, respectively, and correspondingly were significantly and insignificantly smaller in 2020. The roots DMWs of RPWC and RPAWC were unaffected and insignificantly smaller than the control in 2019, respectively, and correspondingly significantly smaller and not significantly different in 2020. Under normal water supply, there was no significant difference in total DMW between QC and non-QC treatments in 2019 and 2020, belowground and aboveground DMWs of QC treatment were higher than and similar to those of non-QC treatment, respectively. The belowground DMWs of QCWC and QCAWC were slightly and significantly smaller than the controls in 2019, respectively, but both significantly smaller in 2020.

3.2.2 Responses of DMWs of aboveground organs to drought

The leaf DMWs of different control treatments in the 2 years were lower at maturity than after drought (Figure 4), indicating that they decreased with development progress of maize in the natural

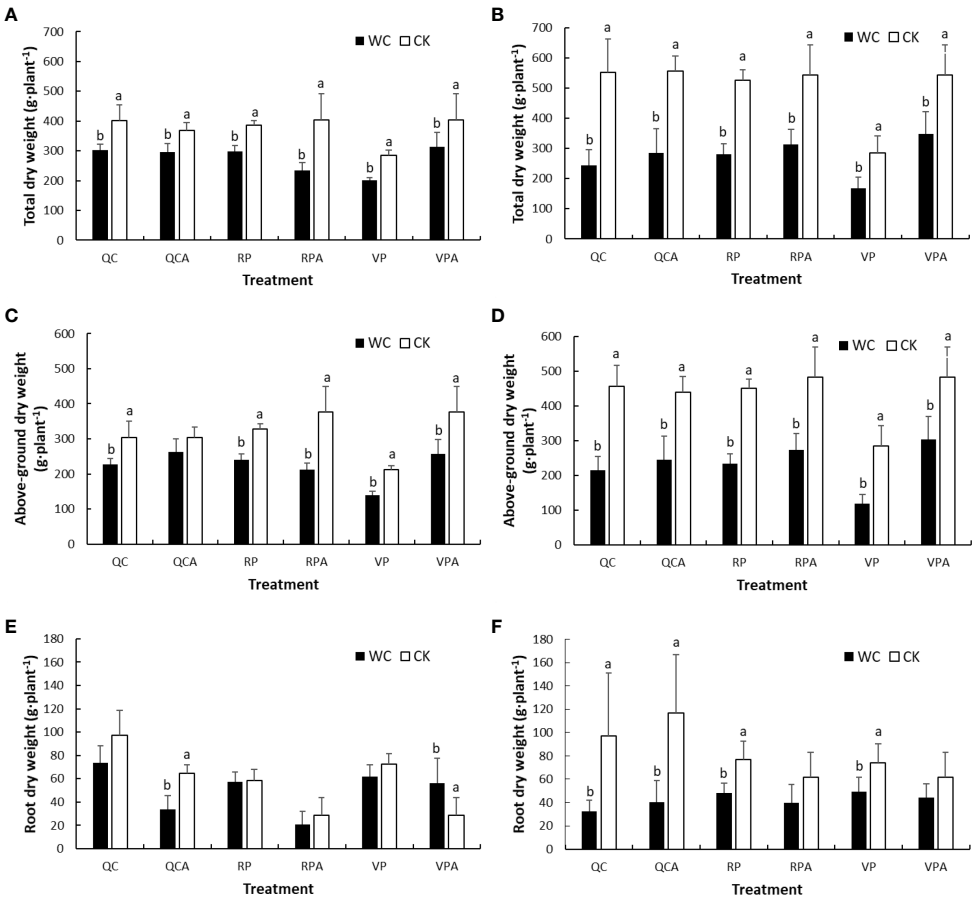

FIGURE 3
Comparisons of total **(A, B)**, aboveground **(C, D)** and root **(E, F)** DMWs of maize between WC and CK for different treatments in 2019 and 2020.

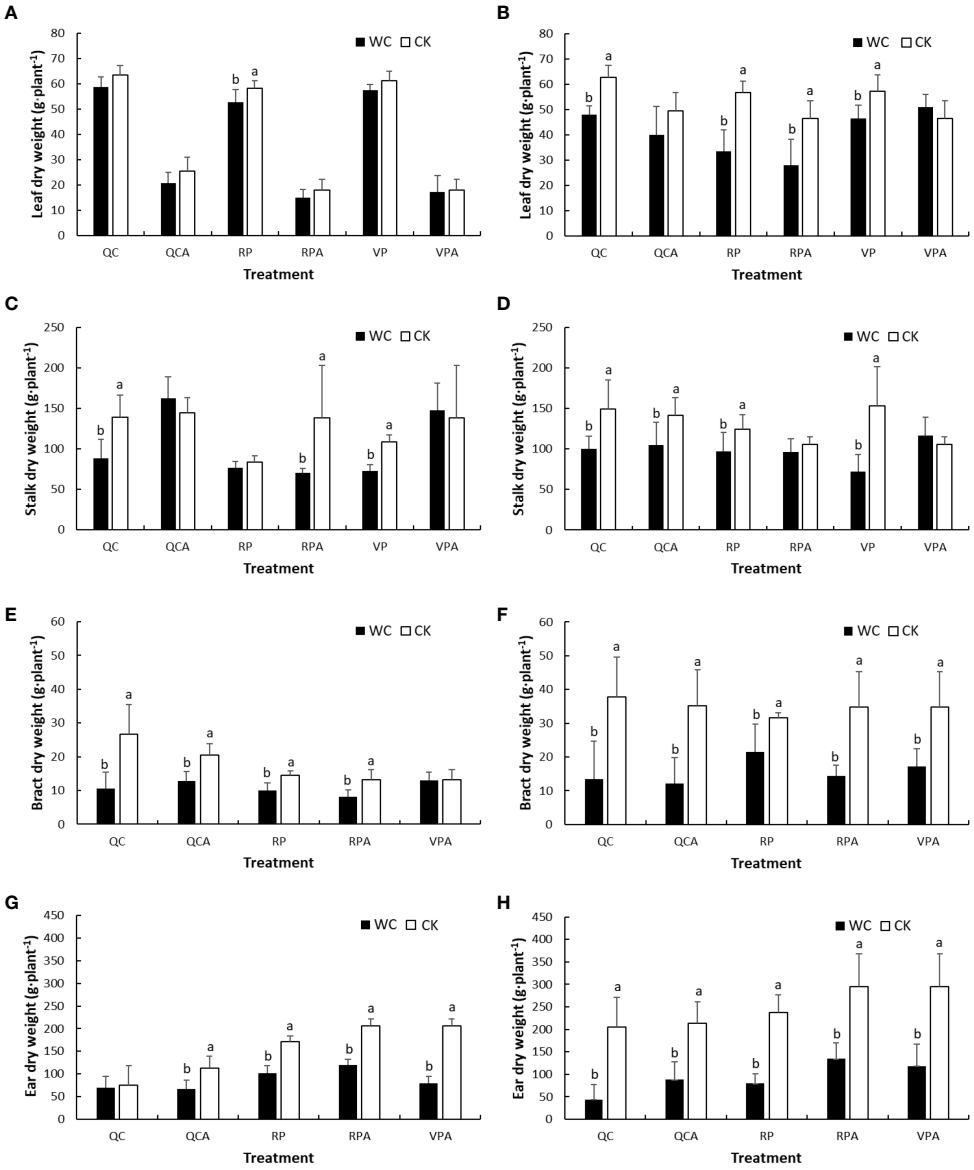

FIGURE 4
Comparisons of DMWs of aboveground organs of maize i.e. leaf **(A, B)**, stalk **(C, D)**, bract **(E, F)** and ear **(G, H)** between WC and CK for different treatments in 2019 and 2020.

state, and the decline was significantly greater in 2019 than 2020. From the perspective of drought effect, in 2019, the leaves DMW of RPWC decreased significantly, while those of the other WCs were slightly and insignificantly smaller than the control. In 2020, the leaves DMWs of most WCs were significantly smaller and that of VPAWC was insignificantly larger than the control. Stalk DMW, in 2019, was significantly lower for VPWC and QCWC and slightly larger for VPAWC and QCAWC under drought than the control values. There was little difference in stalk DMW between RPWC and RPCK, but the stalk DMW of RPAWC decreased significantly. In 2020, the stalk DMWs of most WCs except for RPAWC and VPAWC decreased significantly relative to the control. For bracts, most WCs except for VPAWC in 2019 significantly reduced DMWs in both years. The controls in 2019 were all smaller than those in 2020, and the decrease ranges of bracts DMWs for WCs in 2020 were significantly greater than those in 2019. The maize ear DMW for VP was not analyzed because the ear was not formed after VP. Specifically, the maize ears of most WCs except for QCWC in 2019 were significantly lower than the controls in both years, and with obviously greater reductions in 2020 than 2019. Notably, under normal conditions, the ear DMW of QCCK was lower than that of RPCK, demonstrating that QC inhibited the growth of ears.

3.3 Responses of RSR and HI to drought

The RSRs of VPWC and VPAWC were significantly 32% and 132% higher than those of CKs in 2019, respectively,

and correspondingly in 2020 were insignificantly higher by 12% and 13% (Figure 5). The RSR of RPWC increased significantly by 33% and insignificantly by 22%, while those of RPAWC varied slightly and significantly increased by 14% compared with the control in 2019 and 2020, respectively. However, the RSRs of QCCK were 82% and 20% larger than those of RPCK in 2019 and 2020, respectively. The RSRs of QCACK were 125% and 112% larger than those of CKA in 2019 and 2020, respectively. Whereas, the RSRs of QCWC and QCAWC were very similar and significantly 37% smaller compared with the controls in 2019, respectively, and correspondingly insignificantly 31% and 40% less in 2020.

The DMWs of grain for different treatments in 2020 were calculated with the ratio of grain to ear DMWs from the experiment in 2019 based on small variability for these ratios, and further HIs in 2020 were obtained. Comparing HIs between WCs and CKs showed that those for VPAWC and RPWC were significantly lower than the controls in 2019 and 2020. The HIs of RPAWC in 2019 and 2020 were insignificantly and significantly lower than the controls, respectively. The reduction of HIs in descending order was VPAWC, RPWC and RPAWC for both years.

3.4 Effect of drought on maize DMP

At the end of VPWC, maize was at silking stage in 2019 and 2020. The ear, leaves, stalk and roots DMPRs of VPCK in 2019 were 15%, 21%, 38% and 25%, respectively, and the leaves, stalk and roots DMPRs of VPCK in 2020 were 21%, 52% and 27%, respectively, when the ear and stalk DMWs were considered together as stalk DMW (Figure 6). After VPWC, the roots and leaves DMPRs significantly increased by 21% and 33%, respectively, the ear DMPR decreased significantly by 70%, and the change of stalk DMPR was not obvious in 2019; the leaves and stalk DMPRs increased and decreased significantly by 38% and 20%, respectively, and the root DMPR increased insignificantly by 10% in 2020. We speculate that the decrease of stalk DMPR in 2020 was mainly due to the reduction of ear DMW.

At the end of RPWC, the maize was at 16 and 2 days after milk ripening in 2019 and 2020, respectively. The DMPR of each maize organ for RPCK was 4% in bracts, 44% in ear, 15% in leaves, 22% in stalk and 15% in roots in 2019, and correspondingly 6%, 45%, 11%, 24% and 14% in 2020. The DMPRs of most of maize organs were significantly changed by drought stress. Specifically, ear DMPR significantly decreased by 24% and 36% in 2019 and 2020, respectively, and leaves, stalk and roots DMPRs increased by 17%, 19% and 27% in 2019, respectively, and by 27%, 69% and 37% in 2020; the increase in leaves DMPR in 2020 was insignificant. In addition, bracts DMPR was unaltered in 2019 and increased significantly by 42% in 2020 relative to the control.

Comparing the DMPR between QCCK and RPCK treatments showed that QC significantly reduced ear DMPR in 2019, but significantly increased the bracts, stalk and roots DMPRs. In 2020, the reduction in ear DMPR of QCCK relative to RPCK was less than that in 2019, and the DMPRs of other organs increased slightly. The DMPR of ear increased slightly for QCWC compared with QCCK, that of stalk decreased insignificantly, that of roots did not change, that of bracts significantly decreased and that of leaves significantly increased in 2019. The DMPRs of bracts and ear

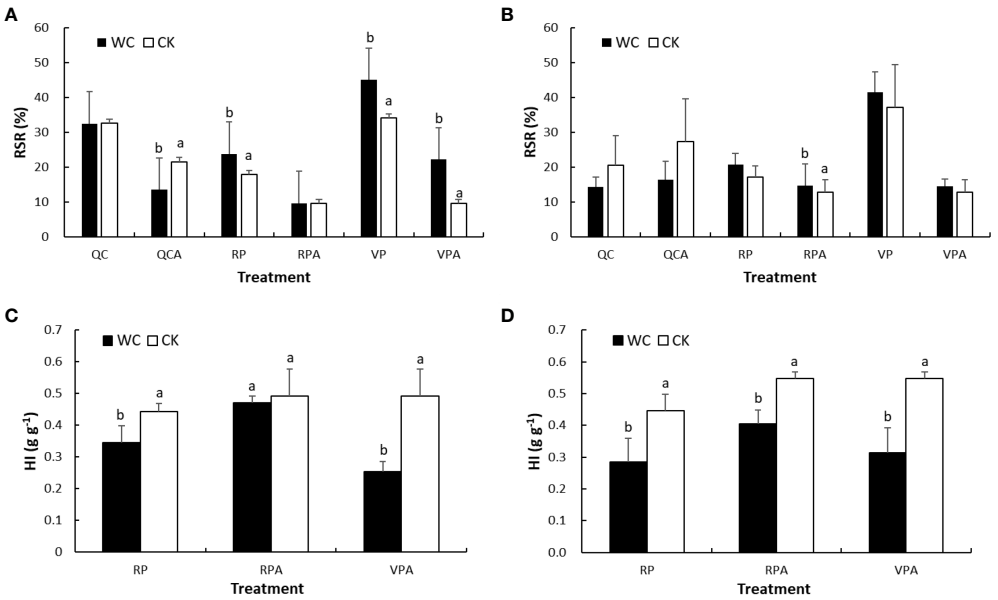

FIGURE 5
Comparisons of RSR **(A, B)** and HI **(C, D)** between WC and CK for different treatments in 2019 and 2020.

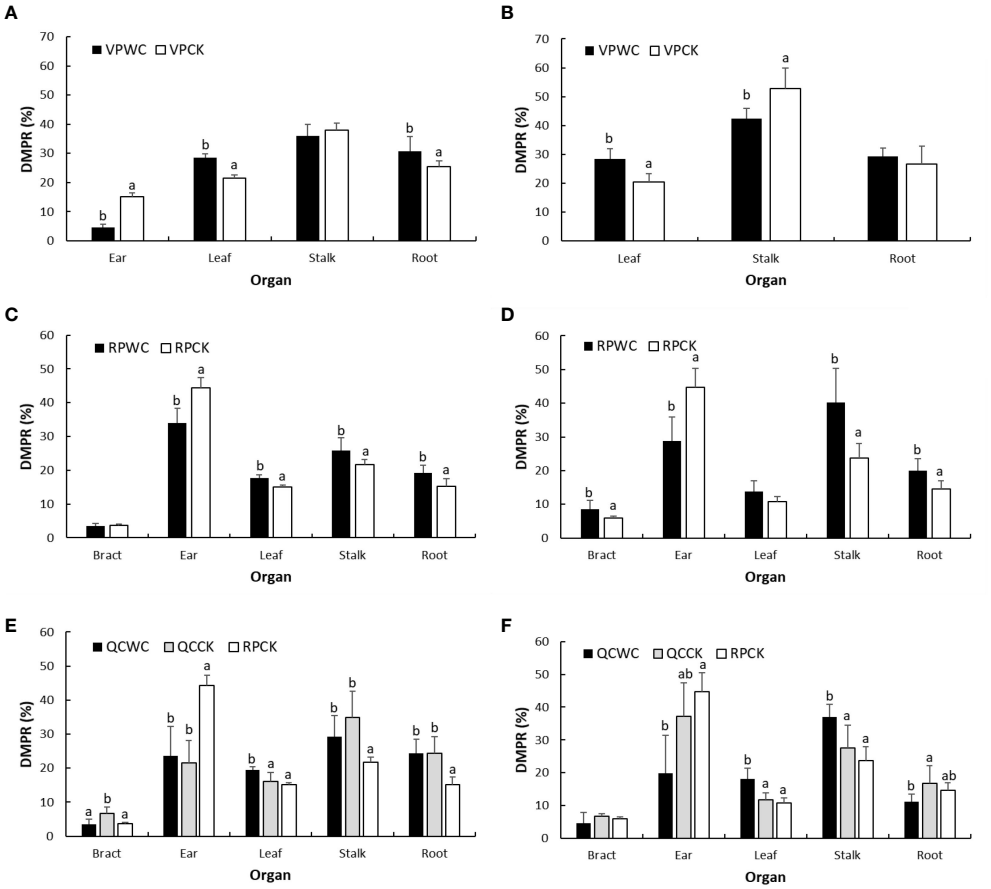

FIGURE 6
Comparisons of DMPRs of maize organs of different treatments for VP **(A, B)**, RP **(C, D)**, and QC **(E, F)** between WCs and CKs in 2019 and 2020.

decreased insignificantly, that of roots decreased significantly and those of leaves and stalk increased significantly in 2020.

3.5 Continuity of drought effect on maize DMP

The effect of previous drought on following maize growth can be shown by comparing the DMPRs of each organ between WC and CK at maturity. For VPAWC, the DMPR of ear decreased significantly, of stalk and roots increased significantly, and of bracts and leaves did not change significantly relative to the control in 2019 (Figure 7). In 2020, the DMPR of ear decreased, those of leaves and stalk increased significantly and that of roots was almost unchanged relative to the controls. Compared with the effects of VPWC, the difference between VPAWC and CKA in leaves DMPR decreased, while those in the DMPRs of other organs increased obviously in 2019. In 2020, the differences in DMPRs for ear and stalk increased, and those of other organs were unchanged.

For RPAWC, there was no significant difference in the DMPR of maize organs between WC and CK in 2019, and the DMPRs of ear, stalk and other organs were significantly smaller, larger and unchanged relative to the controls in 2020, respectively. Compared with the effects of RPWC, in 2019, the differences in DMPRs of each organ between RPAWC and CKA were obviously reduced. In 2020, the differences in bracts and roots DMPRs obviously decreased, and were unchanged for ear, leaves and stalk DMPRs.

In terms of QCACK, compared with CKA, the DMPRs of bracts, leaves and roots increased significantly, that of stalk increased insignificantly and that of ear significantly decreased in 2019. The DMPRs of bracts and leaves did not change, of ear decreased significantly, of stalk increased insignificantly and of roots increased significantly in 2020. Compared with QCACK, the DMPRs of bracts and leaves for QCAWC had no significant change, of ear and roots significantly decreased and of stalk significantly increased in 2019. The DMPRs of bracts and roots significantly decreased, of ear decreased insignificantly and of leaves and stalks significantly increased in 2020.

Relative to difference between RPAWC and CKA, the differences in the DMPRs of ear, stalk and roots between QCAWC and QCACK increased in 2019. However, the differences in the DMPRs of bracts, leaves and roots increased in 2020. Compared with the effects of QCWC, the differences between QCAWC and QCACK in the DMPRs of ear and roots changed from being inconspicuous to significantly decreasing, that of stalk changed from decreasing to significantly increasing, and those of leaves and bracts changed from

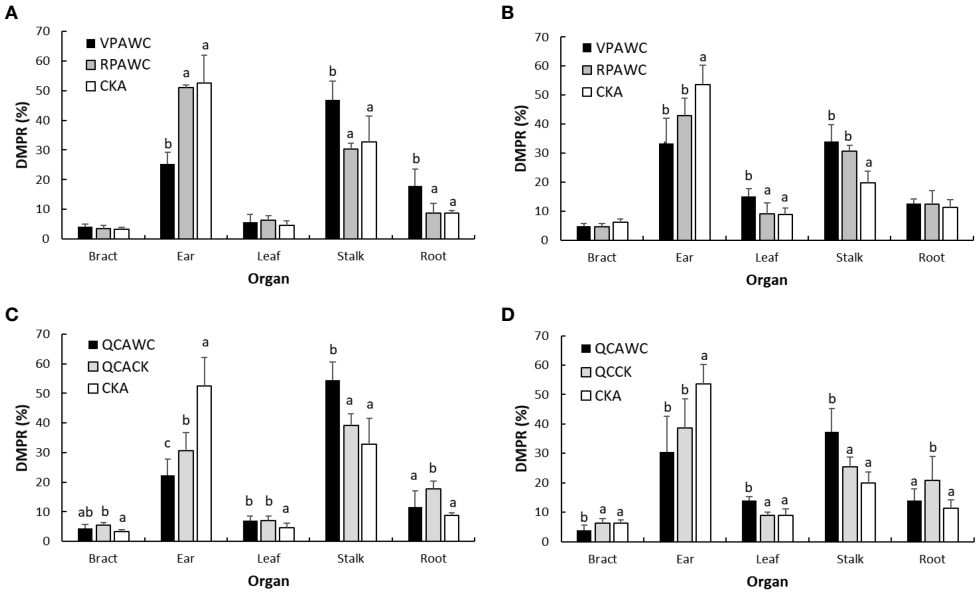

FIGURE 7
DMPRs of maize organs at the end of growth for WC **(A, B)** and QC **(C, D)** treatments in 2019 and 2020.

significantly increasing and decreasing, respectively, to no significant difference in 2019. The differences in the DMPRs of different organs in 2020 were invariable.

3.6 Drought response to DMRD process

3.6.1 Potential DMRD capacity of maize vegetative organs

Because there was no one-to-one correspondence between the sample plants at the end of drought and growth, the subtraction of the mean value of six samples at the two times was used to express the increment of DMW without the sample variance. It is well-known that vegetative organs including stalk, leaves and roots of maize reach their maxima at tasseling and silking stage, after which some dry matter is transferred to ear through a redistribution process. Notably, total DMW of maize plant of CK was sharply smaller in 2019 than 2020, indicating that the maize of CK in 2019 was also subjected to water stress in part of the period. As a result, the analysis was only conducted considering the situation in 2020. Under normal water supply, the decreased DMW of each vegetative organ was approximately equal to the DMRD amount during tasseling to maturity (from July 21 to September 18). The DMRD rates of different vegetative organs are shown in Table 4. About 35%, 41%, 24% and 27% of DMWs in total vegetative organs, stalk, leaves and roots were redistributed to ear, respectively, accounting for 31%, 21%, 4% and 6% of the increment of ear DMW. The contributions of stalk, leaves and roots were 65%, 13% and 22%, respectively.

3.6.2 Drought response of DMRD capacity of maize vegetative organs

The DMRDs for RPWC and RPCK from August 20 to September 18 are shown in Table 5. Under RPCK, during this period, 27% of stalk, 20% of leaves, 32% of roots and 27% of total vegetative organ DMWs were redistributed into ear. The ratios of DMRD from stalk, leaves and roots to increment of ear DMW were 34%, 11% and 23% accounting for 51%, 16% and 33% of DMRD of total vegetative organs, respectively. Under RPWC, 9% of DMW of total vegetative organs consisting of 1% of stalk, 20% of leaves and 22% of roots DMWs, accounting for 32%, 2%, 12% and 18% of increment of ears DMW, respectively, was redistributed into ear. The contributions of stalk, leaves and roots were about 7%, 36% and 57%, respectively. The proportions of stalk and roots DMRDs

TABLE 4 Potential percentage and contribution of maize vegetative organs to DMRD.

Parameters	Stalk	Leaves	Roots	Total
Percentage of organs DMW for redistribution (%)	41	24	27	35
Proportion of organ redistribution accounting for the increment of ears DMW (%)	21	4	6	31
Contribution of organ redistribution to the increment of ears DMW (%)	65	13	22	100

'Total' stands for total amount of DMRD of vegetative organs i.e. stalk, leaves and roots.

TABLE 5 Proportion and contribution of DMRD in maize organs.

Treatment	Parameters	Stalk	Leaves	Roots	Total
RPCK	Percentage of vegetative organs DMRD (%)	27	20	32	27
	Proportion of organ DMRD accounting for the increment of ears DMW (%)	34	11	23	68
	Contribution of organ DMRD to the increment of ears DMW (%)	51	16	33	100
RPWC	Percentage of vegetative organs DMRD (%)	1	20	22	9
	Proportion of organ DMRD accounting for the increment of ears DMW (%)	2	12	18	32
	Contribution of organ DMRD to the increment of ears DMW (%)	7	36	57	100

decreased to varying degrees due to drought, and the decrease for stalk was the largest, reflecting that drought seriously affected dry matter transfer from stalk to ear. The VPWC severely inhibited the redistribution from vegetative organs from tasseling to maturity. Specifically, the drought-induced limitation in DMA led to increases of stalk and leaves DMWs due to a compensatory effect during this period, and then their DMWs at maturity were significantly higher than those at tasseling stage and so their DMRDs could not be quantitatively determined.

4 Discussion

As an important concept in the fields of ecology and agriculture, DMP varies with changes in the environmental situation (Borras and Vitantonio, 2018). Although DMPR is the key parameter in crop models, existing models fail to determine the relationship between DMPR and environmental factors, which directly affects the simulation accuracy of biomass for different plant organs (Cai et al., 2022). In this paper, the biomasses of aboveground and belowground organs of maize were collected in a pot experiment under drought stress, and the drought response of DMP of each organ and compensation effect of following rehydration were investigated.

4.1 Responses of main morphological characteristics of maize to drought and rewatering

The change of morphological characteristics is the most direct manifestation of maize affected by drought (Welcker et al., 2011), which lowers the physiological function of leaves and further influences crop growth and yield (Chaves et al., 2009; Lobell et al., 2014). Droughts during different periods of maize growth affected green leaf area. As the plant growth center was transferred to the reproductive organ and the leaves gradually senesced, RPWC accelerated senescence of leaves and decreased green leaf area sharply compared to VPWC, related to decreasing photosynthesis capacity with the progress of growth (Song et al., 2018). In addition, drought affected two aspects of stalk growth: plant height and stalk diameter. Specifically, plant height was mainly influenced by drought in VP (Song et al., 2018). After rewatering, stalk growth was compensated by increasing diameter, reflecting that the plant adapted to environmental stress through varying its morphology (Lamers et al., 2020). RPWC slightly affected plant height, but significantly decreased stalk diameter (Figure 2), resulting in a decrease in stalk DMW (Figure 4).

4.2 Responses of DMWs of maize organs to drought

Drought induces the change in the DMP pattern, which is conducive to drought resistance (Shipley and Meziane, 2002). Studies on dry matter have mostly focused on plant aboveground parts, with very limited attention to total DMW due to the difficulty in acquiring whole roots (Mccormack et al., 2015; Julia et al., 2016; Komainda et al., 2016). In this study, the drought regime was artificially manufactured based on an experiment conducted throughout the whole growth process of maize using large experimental pots to allow whole roots sampling. The aboveground and total DMWs decreased significantly due to drought in different periods, and the DMWs of the various organs decreased to different degrees, reflecting differences in response to drought. The DMWs of stalk, roots and leaves were affected by VPWC in order from large to small, and were close to or larger than the controls after rehydration, indicating the compensation effect of rewatering after drought (Zhen and Wang, 2018). The effects of RPWC in descending order were leaves, roots and stalk, and the compensative growth of each organ to rehydration was not obvious, which was related to the short duration from rehydration to maturity and the gradual senescence. Notably, there was no significant difference between QC and non-QC treatments in total DMW, indicating that QC had no effect on total maize biomass. The DMWs of roots, stalk, leaves and bracts under QCCK were significantly higher than those under non-QC treatment, especially for roots and stalk, indicating that inhibition of ear growth could increase DMWs of vegetative organs. For QCWC, the DMW of each organ was significantly lower than the control, with rehydration playing a limited role in decreasing drought influence.

4.3 Drought responses of RSR and HI at different growth stages

The DMPs of different plant organs vary with growth stage and environment (Yin et al., 2016; Hu et al., 2022). In this study, VPWC and RPWC both increased RSR, an important indicator of crop yield (Liu et al., 2017), showing that drought promoted DMP to roots, consistent with the functional balance theory (Shipley and Meziane, 2002). The RSRs of QCCK and QCACK were larger than of RPCK and CKA, respectively (Figure 5), meaning that the dry matter originally allocated to ear would be allocated to other organs, especially roots, and the response of DMP to drought would be different from non-QC treatment, that is, the RSR decreased instead of increased. The HI, also known as reproductive effort in ecology, is an important parameter to measure crop productivity in agricultural production, and is often used as a constant to estimate yield by multiplication with aboveground DMW (Maddonni, 2012), but in fact it varies with plant growth (Bonelli et al., 2016). The RPWC reduced HI in different degrees, and rehydration had a recovery effect on HI. The HI of VPAWC was smaller than that of RPAWC, meaning that VPWC had a greater aftereffect on HI than RPWC.

4.4 Drought responses of DMP in maize at different growth stages

Further study showed that mild water stress had a limited effect on the DMP pattern of maize during VP, reflecting that DMP of maize has adaptability to some level of water stress. When VPWC was aggravated, the DMPRs of roots and leaves increased, DMP of ear was inhibited (Yu et al., 2009). For RPCK, there was also good interannual consistency in the DMP pattern, but drought reduced the DMPR of ear, and increased the DMPRs of other organs because, on one hand, drought suppressed photosynthates partitioning into ear and, on the other hand, DMRD from vegetative organ was inhibited (Dang et al., 2014). In addition, the interannual differences in ear and stalk DMPRs in response to drought were probably caused by the difference in degree and occurrence stage of drought (Wang et al., 2016), further reflecting the variation in response of allometry growth among organs to the environment (Zhang et al., 2019). The DMP for QCCK showed that the dry matter originally allocated into ear will be allocated to stalk and roots. QC also changed the effect of drought during RP on DMP pattern. Specifically, QCWC significantly increased leaf DMP, and affected the DMPs of other organs differently due to the difference of the extent of ear inhibition between years.

4.5 Continuity of drought effect on DMP in maize at different growth stages

Deep understanding of the aftereffect of previous drought on maize growth has an important role in drought impact prediction (Luo et al., 2016). The previous drought during different growth periods had various significant aftereffects on DMP of maize after rewatering. The aftereffect of VPWC had temporal difference among maize organs and varied with the growth process in different years (Mi et al., 2017). However, rehydration alleviated the response of DMP of each organ to RPWC. Thus, the persistence of drought impact was related to the occurrence stage (Cai et al., 2020) and degree of drought (Alam et al., 2014; Cai et al., 2022), and was weaker in RP than in VP, which is also associated with the duration during rewatering to maturity. Regrettably, soil water content was not continuously measured and so the influence of drought degree could not be evaluated in this study. Furthermore, rehydration after QCWC caused remarkable reduction in DMPR of ear and roots and increased stalk DMPR. Besides, the QC intensified the aftereffect of drought in RP on the DMP. Notably, the effect of drought on DMW was inconsistent with that on DMPR for each organ (Shi et al., 2021), meaning that the two variables should be discussed separately.

4.6 Drought response of maize DMRD

The DMRD of vegetative organ is an important source of DMA of reproductive organ during late maize growth period (Weiner et al., 2009). Potential DMRD is the key parameter in the DMP process of crop models, and plays a crucial role in accurately estimating crop yield (Dang et al., 2014). Ma and Zhou (2016) set the redistribution potential of stalk, leaves and roots as 30%, 10% and 10%, respectively, while those in this study were relatively higher. The DMRD potential of stalk was significantly higher than those of leaves and roots, and the latter two were similar to each other. Under normal growth conditions, from tasseling to maturity, the contributions to ear DMA were in descending order of stalk, roots and leaves. Whereas, the DMRDs of stalk and roots decreased sharply and slightly under drought, respectively, probably due to plant senescence and leaf abscission, indicating that drought had an inhibitory effect on the DMRD of stalk and roots. Liu et al. (2006) found that the DMPRs of maize roots and leaves at maturity significantly decreased by more than 1 times relative to those in silking stage, which is consistent with results in this study.

5 Conclusions

In this study, the effects of drought on DMA and DMP of maize organs during VP and RP were studied based on an experiment using large capacity pots. The responses to drought and following rehydration for the DMAs, DMPRs, redistribution potential, RSRs and HIs of different organs were deeply analyzed with some conclusions obtained as follows.

The DMAs of maize organs declined under drought in different growth periods. The VPWC had larger effect on the DMW of stalk than of leaves, and rehydration resulted in compensatory growth of stalk, leaves and roots. The RPWC affected green leaf area and leaves DMW more significantly than did VPWC. The effects of VPWC and RPWC and following rehydrations on roots DMWs were very similar. Bracts and ear DMWs were sensitive to drought

during different periods, and their reductions were greater than those of vegetative organs. The QCCK did not affect total DMW of maize plants, leading to more dry matter transfer to roots. Whereas, QCWC and QCAWC reduced significantly DMW of each organ relative to QCCK. The DMP pattern and RSR of maize organs in different growth stages maintained certain stability under normal water supply or mild drought, and varied and increased with aggravation of drought, respectively. The RSR of QC was larger than that of non-QC under normal conditions, and declined under drought, which is opposite to the effect of non-QC drought. Rewatering increased (decreased) the responses of RSR of QC (non-QC) to drought. The VPWC increased DMPRs of roots and leaves, and decreased ear DMPR and did not change stalk DMPR. After rewatering, HI was still dramatically smaller than the control, but the DMPR of stalk significantly increased. The RPWC reduced HI and ear DMPR and increased the DMPRs of vegetative organs. However, rehydration alleviated reductions of HI and the response of DMP of each organ to drought. The QC intensified the aftereffect of previous RPWC on the DMPRs. The potential of DMRD of stalk was larger than those of leaves and roots. The contribution of DMRD of vegetative organs to ear DMA during milk ripening to maturity in descending order were stalk, roots and leaves. Drought inhibited sharply and slightly the redistribution of stalk and roots, respectively.

Data availability statement

The raw data supporting the conclusions of this article will be made available by the authors, without undue reservation.

Author contributions

FC and YZ conceived and designed the experiments, and FC drafted the manuscript; HZ, BZ and XZ performed the experiments; NM, HM and SZ analyzed the data and prepared all figures. All authors contributed to the article and approved the submitted version.

Funding

This study was supported by the National Natural Science Foundation of China (Grant nos. 41775110, 41975149 and 42275202), National key research and development plan project subject (Grant no. 2022YFF0801304), the LiaoNing Revitalization Talents program (Grant no. XLYC1807262) and the foundation of China meteorological administration Shenyang institute of atmospheric environment (2022SYIAEJY12).

Acknowledgments

We thank International Science Editing for editing this manuscript (http://www.internationalscienceediting.com).

Conflict of interest

The authors declare that the research was conducted in the absence of any commercial or financial relationships that could be construed as a potential conflict of interest.

Publisher's note

All claims expressed in this article are solely those of the authors and do not necessarily represent those of their affiliated organizations, or those of the publisher, the editors and the reviewers. Any product that may be evaluated in this article, or claim that may be made by its manufacturer, is not guaranteed or endorsed by the publisher.

References

Alam, M. R., Nakasathien, S., Sarobol, E., and Vichukit, V. (2014). Responses of physiological traits of maize to water deficit induced at different phenological stages. *Nat. Sci.* 48, 183–196. Available at: https://www.mendeley.com/catalogue/22df67b5-8133-3786-a1f0-df731c972778/.

Andrews, M., Raven, J. A., and Sprent, J. I. (2001). Environmental effects on dry matter partitioning between shoot and root of crop plants: relations with growth and shoot protein concentration. *Ann. Appl. Biol.* 138, 57–68. doi: 10.1111/j.1744-7348.2001.tb00085.x

Anothai, J., Soler, C. M. T., and Green, A. (2013). Evaluation of two evapotranspiration approaches simulated with the CSM-CERES maize model under different irrigation strategies and the impact on maize growth, development and soil moisture content for semi-arid conditions. *Agric. For. Meteorol.* 176, 64–76. doi: 10.1016/j.agrformet.2013.03.001

Berendse, F., and Möller, F. (2009). Effects of competition on root-shoot allocation in plantago lanceolata l.: adaptive plasticity or ontogenetic drift? *Plant Ecol.* 201, 567–573. doi: 10.1007/s11258-008-9485-z

Bonelli, L. E., Monzon, J. P., Cerrudo, A., and Rizzalli, R. H. (2016). Maize grain yield components and source-sink relationship as affected by the delay in sowing date. *Field Crops Res.* 198, 215–225. doi: 10.1016/j.fcr.2016.09.003

Borras, L., and Vitantonio, M. L. N. (2018). Maize reproductive development and kernel set under limited plant growth environments. *J. Exp. Bot.* 69 (13), 3235–3243. doi: 10.1093/jxb/erx452

Cai, Q., Sun, Z. X., Zheng, J. M., Wang, W. B., Bai, W., Feng, L. S., et al. (2021). Dry matter accumulation, allocation, yield and productivity of maize soybean intercropping systems in the semi-arid region of Western liaoning province. *Sci. Agric. Sin.* 54 (5), 909–920. doi: 10.3864/j.issn.0578-1752.2021.05.004

Cai, F., Zhang, Y. C., Mi, N., Ming, H. Q., Zhang, S. J., Zhang, H., et al. (2020). Maize (Zea mays l.) physiological responses to drought and rewatering, and the associations with water stress degree. *Agric. Water Manage.* 241, 106479. doi: 10.1016/j.agwat.2020.106379

Cai, F., Zhang, Y. C., Mi, N., Ming, H. Q., Zhang, S. J., Zhang, H., et al. (2022). The effect of drought and sowing date on dry matter accumulation and partitioning in the above-ground organs of maize. *Atmosphere* 13, 677. doi: 10.3390/atmos13050677

Cavero, J., Farre, I., Debaeke, P., and Faci, J. M. (2000). Simulation of maize yield under water stress with the EPICphase and CROPWAT models. *Agron. J.* 92, 679–690. doi: 10.2134/agronj2000.924679x

Chaves, M. M., Flexas, J., and Pinheiro, C. (2009). Photosynthesis under drought and salt stress: regulation mechanisms from whole plant to cell. *Ann. Bot.* 103, 551–560. doi: 10.1093/aob/mcn125

Cheng, Z. Q., Meng, J. H., and Wang, Y. M. (2016). Improving spring maize yield estimation at field scale by assimilating time-series HJ-1 CCD data into the WOFOST model using a new method with fast algorithms. *Remote Sens.* 8, 303. doi: 10.3390/rs8040303

Dai, M. H., Tao, H. B., Wang, L. N., and Wang, P. (2008). Effects of different nitrogen managements on dry matter accumulation, partition and transportation of spring maize (Zea mays l.). *Acta Agric. Boreali-Sin.* 23 (1), 154–157. doi: 10.7668/hbnxb.2008.01.034

Dang, H. K., Li, W., Cao, C. Y., Zheng, C. L., Ma, J. Y., and Li, K. J. (2014). Effects of late milk irrigation on water use efficiency and dry matter distribution of maize. *Trans. Chin. Soc. Agric. Mach.* 45 (5), 131–138.

Djaman, K., Irmak, S., Rathje, W. R., Martin, D. L., and Eisenhauer, D. E. (2013). Maize evapotranspiration, yield production functions, biomass, grain yield, harvest index, and yield response factors under full and limited irrigation. *Trans. ASABE* 56, 373–393. doi: 10.13031/2013.42676

Dou, P., Li, X. D., Kong, F. L., Wang, X. L., Ma, X. J., Zhang, J. L., et al. (2017). Effect of sowing date on dry matter accumulation and yield of maize in hilly regions of sichuan province, China. *Chin. J. Eco-Agric.* 25 (2), 221229. doi: 10.13930/j.cnki.cjea.160631

FAO. (2019). *Faostat*. Available at: http://www.fao.org/faostat/en/#data.

Gao, J., Zhang, R. H., Wang, W. B., Li, Z. W., Xue, J. Q., and Aamp, N. (2015). Effects of drought stress on performance of photosystem II in maize seedling stage. *Chin. J. Appl. Ecol.* 26 (5), 1391–1396. doi: 10.13287/j.1001-9332.20150319.020

Hijmans, R. J., Guiking-lens, I. M., and Van Diepen, C. A. (1994). *WOFOST, user guide for the WOFOST 6.0 crop growth simulation model* (Wageningen: Technical Document, DLO Win and Staring Centre).

Hu, J., Ren, B. Z., Dong, S. T., Liu, P., Zhao, B., and Zhang, J. W. (2022). Poor development of spike differentiation triggered by lower photosynthesis and carbon partitioning reduces summer maize yield after waterlogging. *Crop J.* 10 (2), 478–489. doi: 10.1016/j.cj.2021.08.001

Huang, S., Wang, L., Wang, H., Huang, Q., Leng, W., Fang, W., et al. (2019). Spatiotemporal characteristics of drought structure across China using an integrated drought index. *Agric. Water Manage.* 218, 182–192. doi: 10.1016/j.agwat.2019.03.053

Jiang, P., Cai, F., Zhao, Z. Q., Meng, Y., Gao, L. Y., and Zhao, T. H. (2018). Physiological and dry matter characteristics of spring maize in northeast China under drought stress. *Water* 10 (11), 1561. doi: 10.3390/w10111561

Julia, C., Wissuwa, M., Kretzschmar, T., Jeong, K., and Rose, T. (2016). Phosphorus uptake, partitioning and redistribution during grain filling in rice. *Ann. Bot.* 118, 1151–1162. doi: 10.1093/aob/mcw164

Komainda, M., Taube, F., Klub, C., and Herrmann, A. (2016). Above-and belowground nitrogen uptake of winter catch crops sown after silage maize as affected by sowing date. *Eur. J. Agron.* 79, 31–42. doi: 10.1016/j.eja.2016.05.007

Kumar, R., Sarawgi, A. K., Ramos, C., Amarante, S. T., Ismail, A. M., and Wade, L. J. (2006). Partitioning of dry matter during drought stress in rainfed lowland rice. *Field Crops Res.* 96, 455–465. doi: 10.1016/j.fcr.2005.09.001

Lamers, J., van der Meer, T., and Testerink, C. (2020). How plants sense and respond to stressful environments. *Plant Physiol.* 182, 1624–1635. doi: 10.1104/pp.19.01464

Li, Y. B., Song, H., Zhou, L., Xu, Z. Z., and Zhou, G. S. (2019). Tracking chlorophyll fluorescence as an indicator of drought and rewatering across the entire leaf lifespan in a maize field. *Agric. Water Manage.* 211, 190–201. doi: 10.1016/j.agwat.2018.09.050

Liu, Y. H., Yang, Q., Yang, W. Y., Gao, Q., He, W. T., and Ke, G. H. (2006). Effect of soil drying-wetting alternation on dry biomass accumulation and reallocation at maize flowering stage. *Acta Agron. Sin.* 32 (11), 1723–1727. Available at: https://zwxb.chinacrops.org/CN/Y2006/V32/I11/1723.

Liu, W., Zhang, J. W., Peng, L., Yang, J. S., and Sun, Q. Q. (2011). Effect of plant density on grain yield dry matter accumulation and partitioning in summer maize cultivar denghai 661. *Acta Agron. Sin.* 37 (7), 1301–1307. doi: 10.3724/SP.J.1006.2011.01301

Liu, Z., Zhu, K., Dong, S., Liu, P., Zhao, B., and Zhang, J. (2017). Effects of integrated agronomic practices management on root growth and development of summer maize. *Eur. J. Agron.* 84, 140–151. doi: 10.1016/j.eja.2016.12.006

Lizaso, J., Boote, J. W., Jones, C. H., Porter, L. E., Westgate, M. E., and Sonohat, G. (2011). CSM-IXIM: A new maize simulation model for DSSAT version 4.5. *Agron. J.* 103, 766–779. doi: 10.2134/agronj2010.0423

Lizaso, J., Ruiz-Ramos, M., Rodríguez, L., Gabaldon-Leal, C., Oliveira, J., Lorite, I., et al. (2018). Impact of high temperatures in maize: phenology and yield components. *Field Crops Res.* 216, 129–140. doi: 10.1016/j.fcr.2017.11.013

Lobell, D. B., Roberts, M. J., Schlenker, W., Braun, N., Little, B. B., Rejesus, R. M., et al. (2014). Greater sensitivity to drought accompanies maize yield increase in the US Midwest. *Science* 344, 516–519. doi: 10.1126/science.1251423

Luo, H. H., Yong, H. H., Zhang, Y. L., and Zhang, W. F. (2016). Effects of water stress and rewatering on photosynthesis, root activity, and yield of cotton with drip irrigation under mulch. *Photosynthetica* 54 (1), 65–73. doi: 10.1007/s11099-015-0165-7

Ma, X. Y. (2017). *The occurrence and development of drought on summer maize and its quantitative research* (Beijing: Chinese Academy of Meteorological Sciences).

Ma, X. Y., and Zhou, G. S. (2016). Maize biomass simulation based on dynamic photosynthate allocation. *Chin. J. Appl. Ecol.* 27 (7), 2292–2300. doi: 10.13287/j.1001-9332.201607.026

Maddonni, G. A. (2012). Analysis of the climatic constraints to maize production in the current agricultural region of Argentina–a probabilistic approach. *Theor. Appl. Climatol.* 107, 325–345. doi: 10.1007/s00704-011-0478-9

Marcelis, L. F. M., and Heuvelink, E. (2007). "Concepts of modelling carbon allocation among plant organs," in *Functional-structural plant modelling in crop production*. Eds. J. Vos, L. F. M. Marcelis, P. H. B. de Visser, P. C. Struik and J. B. Evers (The Netherlands: Springer), 103–111.

Mccormack, L. M., Dickie, I. A., Eissenstat, D. M., Fahey, T. J., Fernandez, C. W., Guo, D. L., et al. (2015). Redefining fine roots improves understanding of below-ground contributions to terrestrial biosphere processes. *New Phytol.* 207 (3), 505–518. doi: 10.1111/nph.13363

Mi, N., Cai, F., Zhang, Y. S., Ji, R. P., Yu, W. Y., Zhang, S. J., et al. (2017). Effects of continuous drought during different growth stages on maize and its quantitative relationship with yield loss. *Chin. J. Appl. Ecol.* 28 (5), 1563–1570. doi: 10.13287/j.1001-9332.201705.025

Mi, N., Cai, F., Zhang, Y. S., Ji, R. P., Zhang, S. J., and Wang, Y. (2018). Differential responses of maize yield to drought at vegetative and reproductive stages. *Plant Soil Environ.* 64, 260–267. doi: 10.17221/141/2018-PSE

Poorter, H., Niklas, K. J., Reich, P. B., Oleksyn, J., Poot, P., and Mommer, L. (2012). Biomass allocation to leaves, stems and roots: Meta-analyses of interspecific variation and environmental control. *New Phycol.* 193 (1), 30–50. doi: 10.1111/j.1469-8137.2011.03952.x

Shi, R., Tong, L., Ding, R., Du, T., and Shukla, M. K. (2021). Modeling kernel weight of hybrid maize seed production with different water regimes. *Agric. Water Manage* 250, 106851. doi: 10.1016/j.agwat.2021.106851

Shipley, B., and Meziane, D. (2002). The balanced-growth hypothesis and the allometry of leaf and root biomass allocation. *Funct. Ecol.* 16, 326–331. doi: 10.1046/j.1365-2435.2002.00626.x

Song, H., Li, Y. B., Zhou, L., Xu, Z. Z., and Zhou, G. S. (2018). Maize leaf functional responses to drought episode and rewatering. *Agric. For. Meteorol.* 249, 57–70. doi: 10.1016/j.agrformet.2017.11.023

Steinfort, U., Trevaskis, B., Fukai, S., Bell, K. L., and Dreccer, M. F. (2017). Vernalisation and photoperiod sensitivity in wheat: impact on canopy development and yield components. *Field Crops Res.* 201, 108–121. doi: 10.1016/j.fcr.2016.10.012

Tan, F. Y., Li, H., Wang, J. L., and Wang, Z. W. (2019). Response of dry matter partitioning coefficient of summer maize to drought stress in north China. *Chin. J. Appl. Ecol.* 30 (1), 217–223. doi: 10.13287/j.1001-9332.201901.031

Toumi, J., Er-Raki, S., Ezzahar, J., and Khabba, S. (2016). Performance assessment of AquaCrop model for estimating evapotranspiration, soil water content and grain yield of winter wheat in tensift Al haouz (Morocco): Application to irrigation management. *Agric. Water Manage.* 163, 219–235. doi: 10.1016/j.agwat.2015.09.007

Turc, O., and Tardieu, F. (2018). Drought affects abortion of reproductive organs by exacerbating developmentally-driven processes, *via* expansive growth and hydraulics. *J. Exp. Bot.* 69, 3245–3254. doi: 10.1093/jxb/ery078

Wang, Y., Li, L., Zhou, D.-w., and Weiner, J. (2016). The allometry of reproductive allocation in a chloris virgata population in response to simulated atmospheric nitrogen deposition. *Basic Appl. Ecol.* 17, 388–395. doi: 10.1016/j.baae.2016.01.004

Wang, X. C., Yang, W. Y., Deng, X. Y., Zhang, Q., Yong, T. W., Liu, W. G., et al. (2015). Differences of dry matter accumulation and distribution of maize and their responses to nitrogen fertilization in maize/soybean and maize/sweet potato relay intercropping systems. *Plant Nutr. Fert. Sci.* 21 (1), 46–57. doi: 10.11674/zwyf.2015.0105

Wei, T. B., Hu, F. L., Zhao, C., Feng, F. X., Yu, A. Z., Liu, C., et al. (2017). Response of dry matter accumulation and yield components of maize under n-fertilizer postponing application in oasis irrigation areas. *Sci. Agric. Sin.* 50 (15), 2916–2927. doi: 10.3864/j.issn.0578-1752.2017.15.006

Weiner, J. (2004). Allocation, plasticity and allometry in plants. *Perspect. Plant Ecol. Evol. Syst.* 6, 207–215. doi: 10.1078/1433-8319-00083

Weiner, J., Campbell, L. G., Pino, J., and Echarte, L. (2009). The allometry of reproduction within plant populations. *J. Ecol.* 97, 1220–1233. doi: 10.1111/j.1365-2745.2009.01559.x

Welcker, C., Sadok, W., Dignat, G., Renault, M., Salvi, S., Chacosset, A., et al. (2011). A common genetic determinism for sensitivities to soil water deficit and evaporative demand: meta–analysis of quantitative trait loci and introgression lines of maize. *Plant Physiol.* 157 (2), 718–729. doi: 10.1104/pp.111.176479

Yin, W., Feng, F. X., Zhao, C., Yu, A. Z., Chai, Q., Hu, F. L., et al. (2016). Effects of wheat straw returning patterns on characteristics of dry matter accumulation, distribution and yield of rotation maize. *Acta Agron. Sin.* 42 (5), 751757. doi: 10.3724/SP.J.1006.2016.00751

Yu, Z. Q., Yu, W. W., Tan, X. S., Ye, B. X., and Bi, J. J. (2009). Effect of water stress on dry-matter partition of summer maize. *Acta Agric. Boreali-sin.* 24 (S2), 149–154. doi: 10.7668/hbnxb.2009.S2.033

Zhang, Z. X., Yu, K. L., Jin, X. L., Nan, Z. B., Wang, J. F., Niu, X. L., et al. (2019). Above- and belowground dry matter partitioning of four warm-season annual crops sown on different dates in a semiarid region. *Eur.J. Agron.* 109, 125918. doi: 10.1016/j.eja.2019.125918

Zhen, R. R., and Wang, X. L. (2018). Effects of root depth on compensatory growth of corn seedlings during post-drought re-watering. *Chin. J. Ecol.* 37 (11), 3291–33297. doi: 10.13292/j.1000-4890.201811.030

Zhou, Z., Shi, H. Y., Fu, Q., Li, T. X., Gan, T. Y., and Liu, S. N. (2020). Assessing spatiotemporal characteristics of drought and its effects on climate-induced yield of maize in northeast China. *J. Hydrol.* 588, 125097. doi: 10.1016/j.jhydrol.2020.125097

frontiers | Frontiers in Plant Science

TYPE Original Research
PUBLISHED 08 May 2023
DOI 10.3389/fpls.2023.1165582

OPEN ACCESS

EDITED BY
Jiwang Zhang,
Shandong Agricultural University, China

REVIEWED BY
Hengyou Zhang,
Northeast Institute of Geography and Agroecology (CAS), China
Reetika Mahajan,
University of Toledo, United States

*CORRESPONDENCE
Ao Zhang
zhangao7@syau.edu.cn
Yanye Ruan
yanyeruan@syau.edu.cn

RECEIVED 14 February 2023
ACCEPTED 24 March 2023
PUBLISHED 08 May 2023

CITATION
Chen S, Dang D, Liu Y, Ji S, Zheng H, Zhao C, Dong X, Li C, Guan Y, Zhang A and Ruan Y (2023) Genome-wide association study presents insights into the genetic architecture of drought tolerance in maize seedlings under field water-deficit conditions.
Front. Plant Sci. 14:1165582.
doi: 10.3389/fpls.2023.1165582

Genome-wide association study presents insights into the genetic architecture of drought tolerance in maize seedlings under field water-deficit conditions

Shan Chen[1], Dongdong Dang[1,2,3], Yubo Liu[2,3], Shuwen Ji[1], Hongjian Zheng[2,3], Chenghao Zhao[4], Xiaomei Dong[1], Cong Li[1], Yuan Guan[2,3], Ao Zhang[1]* and Yanye Ruan[1]*

[1]Shenyang City Key Laboratory of Maize Genomic Selection Breeding, College of Bioscience and Biotechnology, Shenyang Agricultural University, Shenyang, Liaoning, China, [2]CIMMYT-China Specialty Maize Research Center, Crop Breeding and Cultivation Research Institute, Shang-hai Academy of Agricultural Sciences, Shanghai, China, [3]International Maize and Wheat Improvement Center (CIMMYT), Texcoco, Mexico, [4]Dandong Academy of Agricultural Sciences, Fengcheng, Liaoning, China

Introduction: Drought stress is one of the most serious abiotic stresses leading to crop yield reduction. Due to the wide range of planting areas, the production of maize is particularly affected by global drought stress. The cultivation of drought-resistant maize varieties can achieve relatively high, stable yield in arid and semi-arid zones and in the erratic rainfall or occasional drought areas. Therefore, to a great degree, the adverse impact of drought on maize yield can be mitigated by developing drought-resistant or -tolerant varieties. However, the efficacy of traditional breeding solely relying on phenotypic selection is not adequate for the need of maize drought-resistant varieties. Revealing the genetic basis enables to guide the genetic improvement of maize drought tolerance.

Methods: We utilized a maize association panel of 379 inbred lines with tropical, subtropical and temperate backgrounds to analyze the genetic structure of maize drought tolerance at seedling stage. We obtained the high quality 7837 SNPs from DArT's and 91,003 SNPs from GBS, and a resultant combination of 97,862 SNPs of GBS with DArT's. The maize population presented the lower heritabilities of the seedling emergence rate (ER), seedling plant height (SPH) and grain yield (GY) under field drought conditions.

Results: GWAS analysis by MLM and BLINK models with the phenotypic data and 97862 SNPs revealed 15 variants that were significantly independent related to drought-resistant traits at the seedling stage above the threshold of $P < 1.02 \times 10\text{-}5$. We found 15 candidate genes for drought resistance at the seedling stage that may involve in (1) metabolism (*Zm00001d012176*, *Zm00001d012101*, *Zm00001d009488*); (2) programmed cell death (*Zm00001d053952*); (3) transcriptional regulation (*Zm00001d037771*, *Zm00001d053859*, *Zm00001d031861*, *Zm00001d038930*, *Zm00001d049400*, *Zm00001d045128*

and *Zm00001d043036*); (4) autophagy (*Zm00001d028417*); and (5) cell growth and development (*Zm00001d017495*). The most of them in B73 maize line were shown to change the expression pattern in response to drought stress. These results provide useful information for understanding the genetic basis of drought stress tolerance of maize at seedling stage.

KEYWORDS

maize (*Zea mays* L.), genome-wide association study, seedling stage, field drought tolerance, SNPs

1 Introduction

Maize (*Zea mays* L.) is a critical source of food, feed, and energy because of its high yield potential. Poor harvest of maize caused by environmental stresses will have a tremendous detrimental impact on human life. Any stage of maize vegetative and reproductive growth, such as germination, plant establishment, and flowering is threaten by globally water shortage (Lobell et al., 2014). The emergence rate, uniformity, and robustness of seedlings are crucial factors in determining the yield potential of maize, as they are directly influenced by the initial stages of maize development, namely seed germination and seedling establishment(Tian et al., 2014). However, in arid and semi-arid areas such as northern China, the sowing time of spring maize often encounters serious drought stress, which reduces the emergence rate, hinders the growth of seedlings and usually decreases the grain yield although sometimes the short and mild drought effect may be irreversible. Thus, improving the drought tolerance of maize during its early growth stages is crucial in enhancing both seedling establishment and subsequent growth.

The drought-resistant varieties of maize have a higher, more stable grain yield than drought-susceptible varieties do in both arid, semi-arid zones, and occasional drought areas because of the erratic rainfall. Thus, if the drought-resistant varieties are widely planted in the drought areas, the yield loss caused by drought can be mitigated to a large extent. The drought resistance of crops is a complicated quantitative trait that is controlled by multiple genes (Wang et al., 2019). In the traditional breeding, breeders select drought resistant lines only depending on their performance under drought stress. The characteristics of drought-resistant varieties bred are limited by the drought circumstances under which breeders select the varieties. The breeders will inevitably miss some drought associated genes that are not expressed under those drought circumstances. As a result, the breeders are not able to mine the drought resistance potential maize and to meet the requirements of drought-resistant varieties of maize. Dissecting the genetic structure of drought resistance and identifying the molecular markers will underlie the genetic modification of drought resistance in maize.

Genome-wide association study (GWAS) is an important foundation of molecular marker-assisted breeding technology, which can locate molecular markers related to plant target traits, thereby obtaining quantitative trait locus (QTL) available for breeding selection or for inferring candidate genes to analyze the genetic basis of complex quantitative traits (Aranzana et al., 2005; Wang et al., 2019; Liu et al., 2021b; Ren et al., 2021). Compared with traditional QTL mapping, GWAS has multiple advantages in identifying the genetic architecture of complex traits, which avoids the difficulty of screening large biparental mapping population (Dinka et al., 2007) and can verify gene function by fine mapping and cloning. For instance, a GWAS exploration, using the survival rate and high-quality SNPs of the associated population consisted of 367 maize lines, obtained genetic variations and identified candidate genes, of which the natural variation in *ZmVPP1* (encoding a vacuolar-type H^+ pyrophosphatase) contributes most significantly to the survival rate, and transgenic maize plants with *ZmVPP1* gene exhibited stronger drought tolerance (Wang et al., 2016). Yet the molecular mechanism of drought resistance of maize remains largely unknown.

The maize plant drought resistance is a quantitative trait with complicated phenotypes, which is difficult to be evaluated. The most evaluations of maize seedlings are usually conducted under osmotic stress caused by PEG solvents or simulated drought by controlling soil water content in the indoor cultivation pool. In this circumstance, the physiological indices such as survival rate and root correlated traits are commonly used to identify the drought resistance. The survival rate refers to the ability of plants to maintain their viability under drought stress and restore normal growth after they obtain sufficient water again. For example, Qin Feng's team (Liu et al., 2013; Mao et al., 2015; Wang et al., 2016) transferred the three-leaf stage maize seedlings in the cultivation pool without water for drought treatment. When all the seedlings were severely withered, they were rehydrated for a week then to be investigated the survival rates. The team found the survival rates of maize from different genetic resources manifesting a great genetic diversity under drought stress (Wang et al., 2016). Root traits such as root length, total root number, and root surface area can reflect the ability of plants to absorb water and nutrients under drought condition (Guo et al., 2020a). But such physiological indices are not suitable to measure in high throughput in the field condition. Leaf rolling is one of the main responses of maize plants to drought stress which can be scored visually in the field. However, the leaf scoring technique does not meet the high-throughput requirements for efficient phenotypic determination by breeders (Baret et al., 2018). The grain yield (GY) of maize under water shortage is an ultimate index to evaluate its drought tolerance. But, if only depending on this index to research the drought

resistance, we are not able to gain insight into the physiological changes that result in the yield declination under drought stress. When maize plants are subjected to drought stress during flowering stage, the development of female flower organs is inhibited more severely than that of male flower organs, and the silking time is delayed and the interval between anthesis and silking is enlarged, which leads to the pistil pollination failure and serious yield loss (Setter et al., 2010). Therefore, the anthesis -silking interval (ASI) is a desired method to evaluate the maize drought resistance under the field condition because it is yield-related, high throughput and cost-effective (Thirunavukkarasu et al., 2014; Farfan et al., 2015). However, so far there is no any index perfectly suitable to evaluate maize drought resistance at seedling stage under the field condition.

An ideal sequencing platform should be high throughput, high genome coverage, high repeatability, and low cost. Among various platforms, genotyping-by-sequencing (GBS) is one of the most extensively used sequencing technologies (Elshire et al., 2011; Guo et al., 2020b; Wang et al., 2020). DArT (Diversity Arrays Technology sequence) is a novel molecular marker identification technology based on gene chip (Kilian et al., 2012), and being used in molecular assisted selection of plants (dos Santos et al., 2016), however, its reliability in maize needs more exploration.

In this study, a maize association panel (NCCP) containing 379 inbred lines were planted in the arid region for 2 years. SNPs genotyped by GBS and DArT, and the combination of SNPs from GBS and DArT were used to conduct GWAS for seedling emergence rate (ER), seedling plant height (SPH) and grain yield (GY) under natural drought conditions. Fifteen common independent and significant SNPs were obtained by BLINK and MLM models, and 15 corresponding candidate genes were identified. The expressions of most of them in the reference inbred line B73 of maize were significantly responded to drought treatment.

2 Results

2.1 Phenotypic variation

According to our analysis, the drought resistance related traits in maize seedling in the NCCP panel exhibited extensive phenotypic variation. Normal distributions were observed for the 19SPH, 20SPH and SPH (from the across environment analysis); other traits, 19ER, 20ER, ER (from the across environment analysis), 19GY, 20GY and GY (from the across environment analysis) displayed slightly skewed normal distribution, which are consistent with the performance of quantitative traits (Supplementary Figure 1). When the phenotypic variances of traits in different environments were analyzed independently, significant differences were detected in emergence rate, seedling plant height and grain yield among the two environments (Figure 1). The median of 19ER was 0.86 and significantly higher than that of 20ER (0.70) and ER (0.77), and the variation range of the emergence rate in 2019 was also broader than that in 2020. The same trend was observed for plant height at seedling stage and grain yield at harvest (Figure 1). The phenotypic correlation between BLUE values of the three traits across two environments were positive and significant, as previously reported (Zhang et al., 2022). The results showed that yield trait could be used as the related trait of drought resistance in maize seedling stage, and could reflect the final impact of drought on maize seedling stage.

The broad-sense heritability (H^2) of the emergence rate ranged from 0.32 in the across environment analysis to 0.88 in the 2019 environment analysis. H^2 of plant height traits at seedling stage ranged from 0.26 in the across environment analysis to 0.82 in the 2019 environment analysis. For grain yield, H^2 was 0.85 in the 2019 environment analysis, and 0.33 in both the 2020 environment analysis and across environment analysis (Figure 2). The analysis

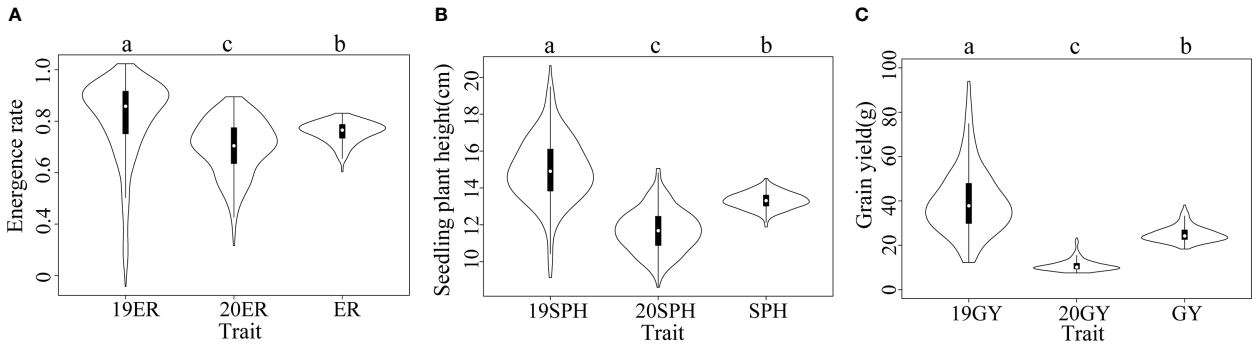

FIGURE 1
Violin plots of distributions of drought resistance related traits in maize seedlings. The horizontal axis represents different traits. In a violin plot, the inner black box represents the interquartile range. The central white dot represents the median value. The outer white shape on each side represents all measured data points and the thickness represents the probability density of the data. Analysis of variance (ANOVA) was applied to examine the difference of phenotypes among different environments. Different letters indicate statistically significant differences at $P \leq 0.05$. **(A)** 19ER, seedling emergence rate measured in Fuxin in 2019; 20ER, seedling emergence rate measured in Fuxin in 2020; ER, seedling emergence rate BLUE value calculated from two-year data; **(B)** 19SPH, seedling plant height measured in Fuxin in 2019; 20SPH, seedling plant height measured in Fuxin in 2020; SPH, BLUE value of seedling plant height calculated from two-year data; **(C)** 19GY, grain yield measured in Fuxin in 2019; 20GY, grain yield measured in Fuxin in 2020; GY, grain yield BLUE value calculated from two-year data.

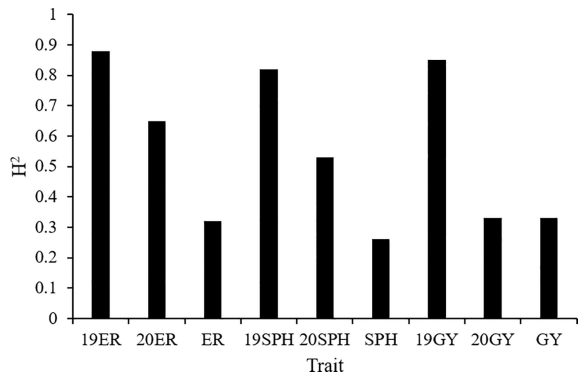

FIGURE 2
The broad-sense heritability (H^2) of drought resistance related traits in maize seedlings. 19ER, seedling emergence rate measured in Fuxin in 2019; 20ER, seedling emergence rate measured in Fuxin in 2020; ER, seedling emergence rate BLUE value calculated from two-year data; 19SPH, seedling plant height measured in Fuxin in 2019; 20SPH, seedling plant height measured in Fuxin in 2020; SPH, BLUE value of seedling plant height calculated from two-year data; 19GY, grain yield measured in Fuxin in 2019; 20GY, grain yield measured in Fuxin in 2020; GY, grain yield BLUE value calculated from two-year data.

of variance on drought resistance-related traits in maize seedlings showed that genotypic variance had a significant effect ($P< 0.01$) in all analyses. Additionally, the interaction between genotype and environment (G × E) and environmental variance were also highly significant ($P< 0.01$) across all environments analyzed (Zhang et al., 2022).

2.2 Population structure, kinship, and linkage disequilibrium (LD)

We obtained high-quality datasets after filtering, and the average missing rates were 0.073, 0.069, and 0.070 for SNPs from DArT, GBS and the combination of GBS and DArT (GBS - DArT) (Table 1). For inbred lines, heterozygosity was also an important index for marker filtering. In this research, the proportion heterozygous of the three marker datasets were less than 0.02 after filtering, which means our material was homozygous and implies the sequencing was accurate (Figure 3A). The principal component analysis using 97,862 SNPs of GBS-DArT revealed that there were significant differences among some inbred lines in the association population, and the panel had a strong population stratification structure. Meanwhile, the first three principal components explained 40% of the phenotypic variation rate (Figure 3A). A high genetic correlation among inbred lines in the population were shown in the heat map (Figure 3B).

A rapid LD decay pattern in the entire panel was observed. The LD decay distance across the 10 chromosomes ranged from 29.46 Kb (Chr5) to 96.67 Kb (Chr8), and the average LD decay distance was 80.18 Kb at an r^2 value of 0.1. The LD decay distance of 10 chromosomes ranged from 7.43Kb (Chr5) - 10.74Kb (Chr6), the average LD decay distance was 8.61Kb while $r^2 = 0.15$. When r2 = 0.2, the LD decay distance of 10 chromosomes was from 0.96Kb (Chr6) to 2.03Kb (Chr7), and the average LD decay distance was 1.09Kb (Figure 4). To ensure the accuracy of mapping, it is assumed that at least one SNP marker is in linkage disequilibrium with the QTL of the controlled trait. The minimum number of markers required for GWAS (minimum number of SNP markers = genome size/LD decay distance) are 27,438, 254,629 and 2,018,349 respectively when $r^2 = 0.1$, 0.15 and 0.2. Consequently, to assure that the markers have sufficient coverage in the whole genome, the LD decay distance of $r^2 = 0.1$ was selected in this study.

2.3 Genome-wide association analysis

To reduce the impact of environmental variability, phenotypic BLUE values across two environments (19FX, and 20FX) were also used for association study. The GWAS analysis was performed using 97,862 SNPs from the combination of GBS and DArT, with a threshold of $P< 1.02 \times 10^{-5}$, and the effects of population structure and kinship were considered. A total of 20 and 15 independently significant SNPs were found by applying BLINK (Supplementary Figures 2, 3 and Supplementary Table 1) and MLM models (Figures 5, 6 and Table 2), respectively. Among them, 15 SNPs obtained by the two methods are common (Table 2). This result indicates that these common SNPs have high reliability. Therefore, the subsequent analysis mainly focused on these 15 common SNPs.

For the emergence rate, there were five independent significant SNPs on chromosomes 1, 4, 6 and 8 above the threshold, accounting for 5.5-7.0% of the phenotypic variation, respectively (Figures 5A–C and Table 1). For the plant height trait at seedling stage, seven

TABLE 1 The number of materials and sites, proportion heterozygous and MAF for markers of DArT, GBS and GBS-DArT (combination of both) datasets after filtering.

	DArT	GBS	GBS_DArT
Number of Taxa	379	378	378
Number of Sites	7837	91003	97862
Proportion Missing	0.073	0.069	0.070
Proportion Heterozygous	0.020	0.018	0.018
Average Minor Allele Frequency	0.24	0.233	0.233

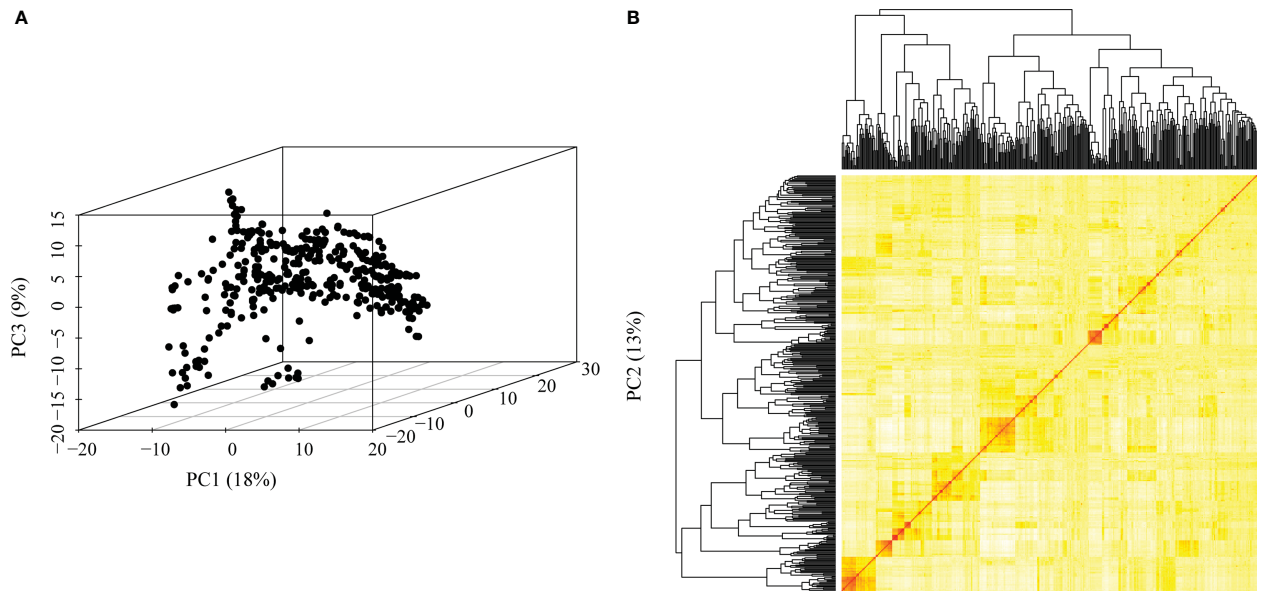

FIGURE 3
Genetic relatedness among the inbred lines visualized using the heat map, dendrogram of kinship matrix and principal component analysis (PCA) in the association panel. **(A)** Principal component analysis (PCA) in the association population using GBS-DArT dataset, including the first three principal components. The percentage of variation among lines explained by each principal component is displayed on both the x- (PC1), y- (PC2) and z- (PC3) axes. Points in the PCA plot denote individual line; **(B)** The lower right corner is the genetic distance heat map of paired lines, and the upper and left are the dendrogram of kinship matrix in the association panel using GBS-DArT dataset.

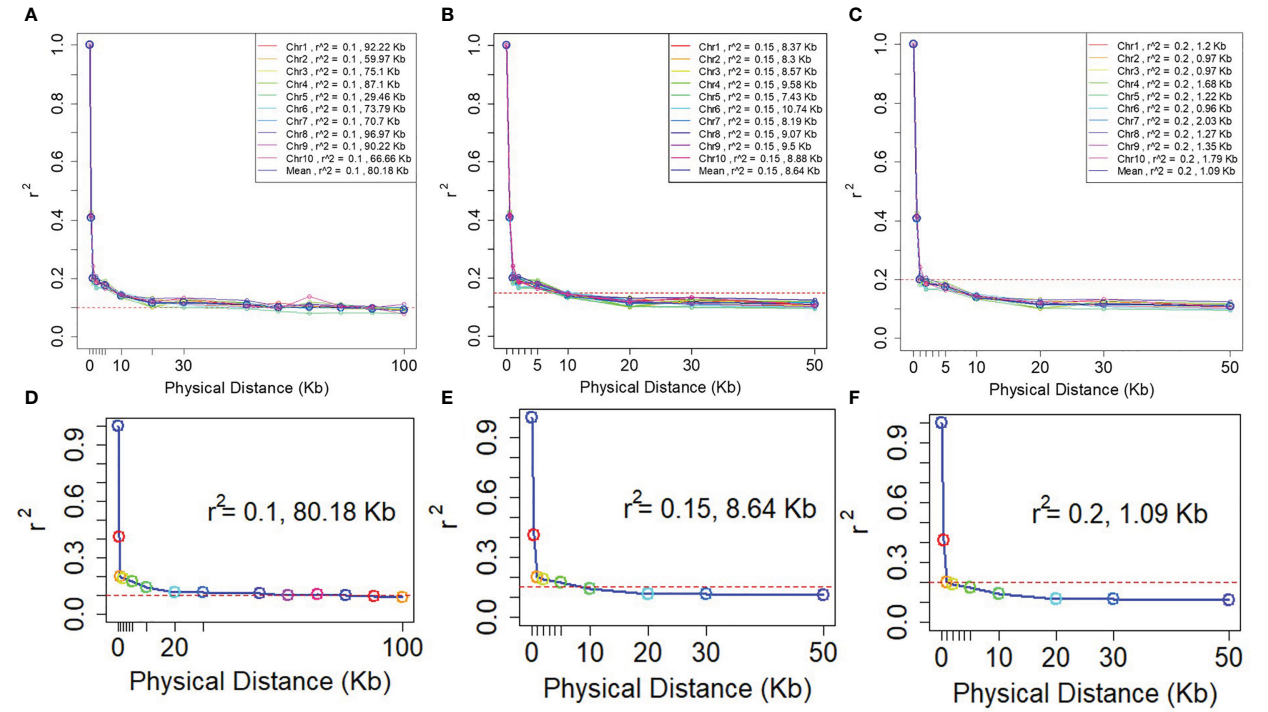

FIGURE 4
LD decay plots of the NCCP panel. The horizontal axe is the decay distance (Kb) of LD with different r^2. **(A–C)** are the LD decay for each chromosome; **(D–F)** are the average LD decay for all 10 chromosomes.

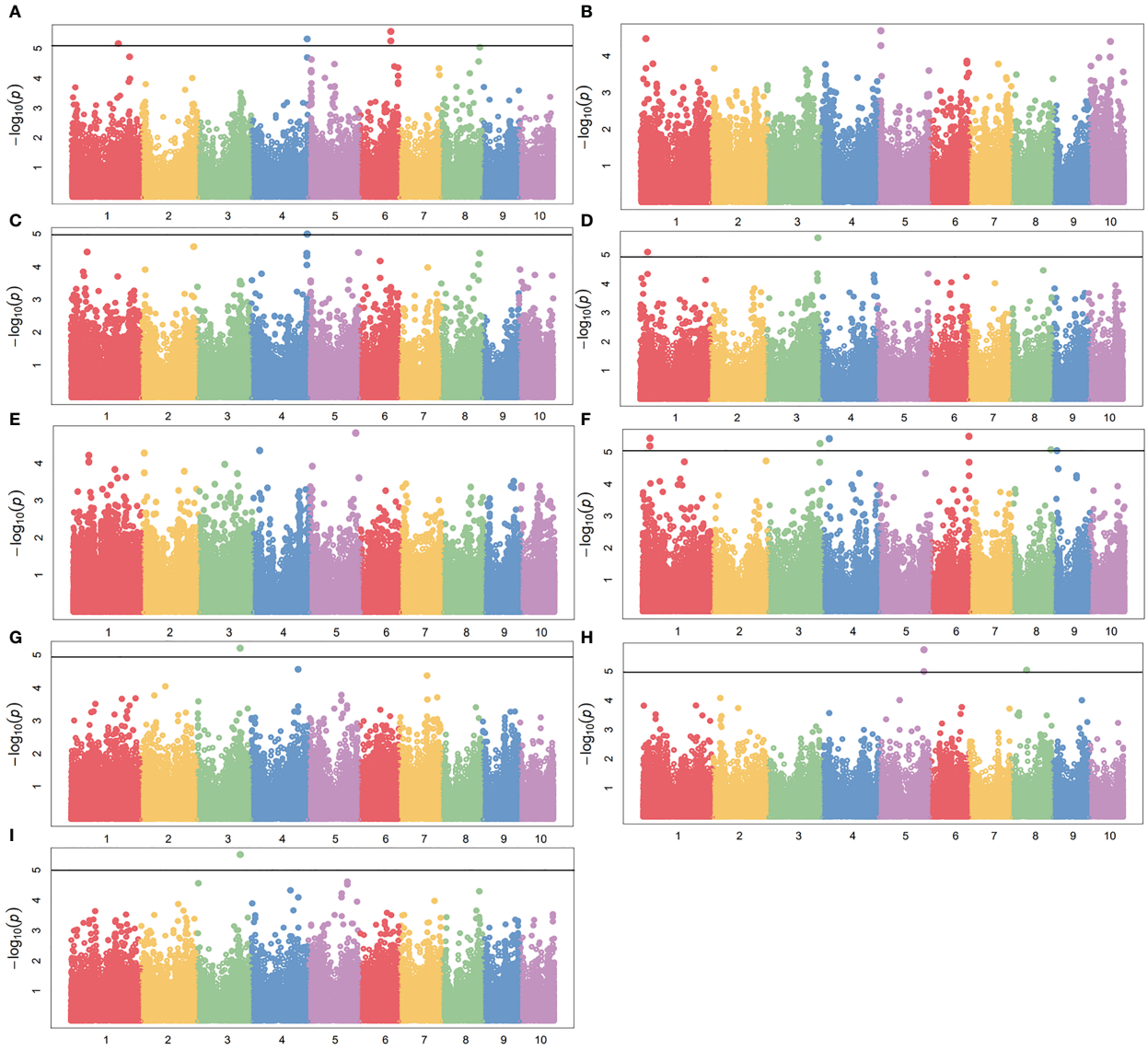

FIGURE 5
GWAS-derived Manhattan plots showing significant SNPs associated with maize drought resistance traits using MLM. Each dot represents a SNP. The horizontal dashed black line represents the Bonferroni-corrected significant threshold of 1.02×10^{-5}. **(A)** 19ER: seedling emergence rate (ER) was measured in 19FX (2019 Fuxin); **(B)** 20ER: seedling emergence rate (ER) was measured in 20FX (2020 Fuxin); **(C)** ER: BLUE of seedling emergence rate across two environments; **(D)** 19SPH: seedling plant height (SPH) was measured in 19FX (2019 Fuxin); **(E)** 20SPH: seedling plant height (SPH) was measured in 20FX (2020 Fuxin); **(F)** SPH: BLUE of seedling plant height across two environments; **(G)** 19GY: grain yield (GY) was measured in 19FX (2019 Fuxin); **(H)** 20GY: grain yield (GY) was measured in 20FX (2020 Fuxin); **(I)** GY: BLUE of grain yield across two environments.

independent significant SNPs on chromosomes 1, 3, 4, 6, 8 and 9 above the threshold, accounting for 6.2-7.5% of the phenotypic variation respectively (Figures 5D–F and Table 2). For the grain yield trait, three independent significant SNPs on chromosomes 3, 5 and 8 above the threshold had been discovered, accounting for 7.5-8.7% of the phenotypic variation, respectively (Figures 5G–I and Table 2). For these traits, the most significant SNP (2428947-36-C) from 20GY showed the largest phenotypic variation and higher reliability, which signified that the drought resistance in maize seedling stage was a complex quantitative trait controlled by multiple genes with minor effects.

2.4 Genotype effects of significant SNPs associated with drought resistance traits in maize seedlings

The allele effects of these 15 overlapping significant SNPs were also evaluated (Supplementary Figure 4). The phenotypic distribution differences for different traits between the major alleles and minor alleles were extremely significant for all 15 significant SNPs ($P< 0.01$). The allele effect of 2394080-64-C on chromosome 3 was the most significant for 19GY/GY phenotypic variation with P-value of 4.4×10^{-11} and 1.1×10^{-13}, which was

10.3389/fpls.2023.1165582

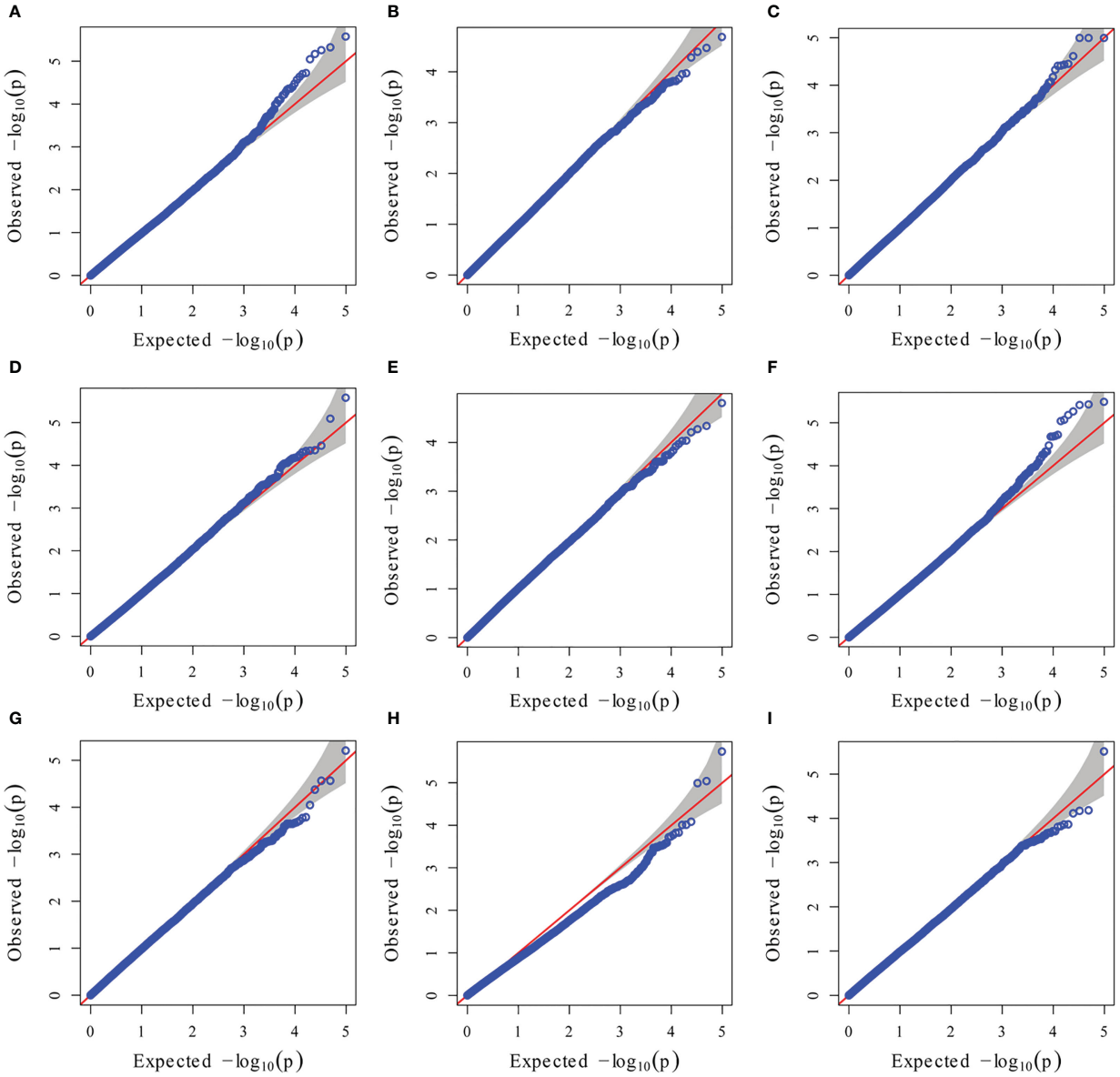

FIGURE 6
GWAS-derived QQ plots using MLM. **(A)** 19ER: seedling emergence rate (ER) was measured in 19FX (2019 Fuxin); **(B)** 20ER: seedling emergence rate (ER) was measured in 20FX (2020 Fuxin); **(C)** ER: BLUE of seedling emergence rate across two environments; **(D)** 19SPH: seedling plant height (SPH) was measured in 19FX (2019 Fuxin); **(E)** 20SPH: seedling plant height (SPH) was measured in 20FX (2020 Fuxin); **(F)** SPH: BLUE of seedling plant height across two environments; **(G)** 19GY: grain yield (GY) was measured in 19FX (2019 Fuxin); **(H)** 20GY: grain yield (GY) was measured in 20FX (2020 Fuxin); **(I)** GY: BLUE of grain yield across two environments.

consistent in MLM and BLINK methods (Supplementary Figure 4). This indicates that the significant locus identified by GWAS related to drought resistance traits in maize seedlings are reliable and can be utilized for further candidate genes determination. Through the above analysis, the drought susceptible and tolerant alleles of 15 independently significant SNPs were identified. Sequentially, the phenotypic values of 9 different scenarios were sorted from large to small, and the first 20 lines were selected to take the intersection, and 5 lines with a high degree of coincidence were discovered. As shown in Table 3, the distribution ratio of tolerant genes was 53.3%-86.7%, which indicates that the more tolerant genes contained in a maize inbred line, the stronger the resistance to drought.

The relationship between these significant SNPs and drought resistance in maize seedlings was further verified by searching for candidate genes at significant SNPs and confirming the gene function. During maize breeding, if breeders know drought-resistant SNPs, they can select drought resistant inbred lines or cross combinations and exclude ones without marker SNPs *via* molecular detection. This approach does not require field planting the breeding materials for identifying drought resistance, thus

TABLE 2 SNPs significantly associated with drought resistance related traits in maize seedling identified by GWAS using the MLM method.

Trait[a]	SNP	Chr	Pos(bp)	Allele	MAF[b]	P-value	R^2(%)[c]
19ER	Marker.553171	6	136921236	G/A	0.05	2.66×10^{-6}	6.2
	2387359-54-T	4	242397378	C/T	0.27	4.75×10^{-6}	5.9
	101239269-43-G	1	204458682	G/A	0.07	6.80×10^{-6}	5.7
	2405469-50-C	8	169559968	T/C	0.15	9.01×10^{-6}	5.5
ER	Marker.425514	4	244195583	C/A	0.1	1.01×10^{-5}	7.0
19SPH	2436908-21-A	3	224392713	G/A	0.06	2.61×10^{-6}	6.2
SPH	2432311-16-G	6	167215240	G/T	0.3	3.25×10^{-6}	7.5
	2461151-33-G	1	34541393	G/A	0.32	3.73×10^{-6}	7.4
	2450059-7-C	4	29282468	C/T	0.14	3.85×10^{-6}	7.4
	2428524-68-C	1	34223477	C/T	0.29	6.59×10^{-6}	7.0
	2484848-55-T	8	168277928	G/T	0.15	8.53×10^{-6}	6.8
	2427986-14-T	9	13708582	T/A	0.11	9.13×10^{-6}	6.8
20GY	2428947-36-C	5	197541412	C/A	0.25	1.84×10^{-6}	8.7
	2506549-24-A	8	67043226	A/G	0.05	9.12×10^{-6}	7.5
19GY/GY	2394080-64-C	3	187093184	C/G	0.15	3.07×10^{-6}	7.5

[a]19ER, seedling emergence rate measured in Fuxin in 2019; ER, seedling emergence rate BLUE value calculated from two-year data; 19SPH, seedling plant height measured in Fuxin in 2019; SPH, BLUE value of seedling plant height calculated from two-year data; 19GY, grain yield measured in Fuxin in 2019; 20GY, grain yield measured in Fuxin in 2020; GY, grain yield BLUE value calculated from two-year data.
[b]Minor Allele Frequency.
[c]Percentage of phenotypic variation explained by the additive effect of the single significant SNP.

TABLE 3 The drought tolerant alleles and genotype composition of drought-resistant lines of independently significant SNPs.

SNP	drought tolerant allele	NCCP037	NCCP228	NCCP305	NCCP310	NCCP327
Marker.553171	G	G	G	G	G	G
2387359-54-T	C	Y	C	T	C	C
101239269-43-G	G	G	G	G	G	G
2405469-50-C	T	T	T	T	T	T
Marker.425514	C	C	C	C	C	C
2436908-21-A	A	G	G	A	G	G
2432311-16-G	G	G	G	G	G	G
2461151-33-G	A	R	A	A	A	A
2450059-7-C	T	C	C	C	T	C
2428524-68-C	T	Y	T	T	T	T
2484848-55-T	T	K	G	G	T	G
2427986-14-T	T	T	T	T	T	T
2428947-36-C	A	A	A	C	A	A
2506549-24-A	G	A	A	A	A	A
2394080-64-C	C	C	C	C	C	C

saving a large amount of manpower, land, productive expenses, and time.

2.5 Candidate genes selection based on LD of significant SNPs

According to the B73 RefGen v4, nine significant SNPs (Marker.553171, 101239269-43-G, 2405469-50-C, 2432311-16-G, 242852468-C, 2484848-55-T, 2428947-36-C, 2436908-21-A and 2461151-33-G) were just located on the gene sequences, *Zm00001d037771*, *Zm00001d031861*, *Zm00001d012176*, *Zm00001d038930*, *Zm00001d028417*, *Zm00001d012101*, *Zm00001d017495*, *Zm00001d044291* and *Zm00001d028423*, which are directly regarded as candidate genes associated with drought resistance. For the other six significant SNPs, not located on the gene sequence, we perform the linkage disequilibrium (LD) decay within 80Kb (Supplementary Figure 5). For 2387359-54-T, 2450059-7-C, 2427986-14-T, 2506549-24-A and 2394080-64-C, the nearest gene is *Zm00001d053859*, *Zm00001d049400*, *Zm00001d045128*, *Zm00001d009488*, *Zm00001d043036*, respectively. In terms of location, the significant SNPs and these candidate genes are within the linkage regions (Table 4). For Marker.425514, according to the location and gene function, *Zm00001d053952* located upstream 26,466bp of the SNP was identified as a candidate gene. In this location, the LD decay was larger than 0.6 (Table 4 and Supplementary Figure 5).

2.6 Expression pattern of candidate gene under indoor drought conditions

All 15 SNPs significantly related to drought resistance traits in maize seedling were identified by GWAS, and 15 candidate genes significantly related to drought resistance traits in maize seedling were obtained (Table 4). The 15 candidate genes were divided into five functional types, gene expression regulation, metabolic, programmed cell death, cell growth and development and

TABLE 4 Candidate genes significantly associated with drought resistance related traits in maize seedling identified by GWAS using the MLM method.

Trait[a]	Gene	Chr	Gene interval (bp)	Distance from the related SNP to the edge of the gene (bp)[b]	Annotation	Pathway
19ER	*Zm00001d037771*	6	136915169.136922617	Located	Transcription factor bHLH133	gene expression regulation
	Zm00001d053859	4	242396086.242396676	-702	Ethylene-responsive transcription factor 3	gene expression regulation
	Zm00001d031861	1	204458557.204459636	Located	Dehydration-responsive element-binding protein 2G	gene expression regulation
	Zm00001d012176	8	169557355.169562468	Located	Beta-hexosaminidase	metabolic
ER	*Zm00001d053952*	4	244166895.244169117	-26466	Bax inhibitor 1	programmed cell death
19SPH	*Zm00001d044291*	3	224387800.224393287	Located	Unknown	Unknown
SPH	*Zm00001d038930*	6	167214153.167215654	Located	Transcription factor MYB36	gene expression regulation
	Zm00001d028423	1	34540138.34541979	Located	Unknown	Unknown
	Zm00001d049400	4	29282763.29284915	295	Transcription factor GTE7	gene expression regulation
	Zm00001d028417	1	34216191.34223589	Located	Autophagy-related protein 9	autophagy
	Zm00001d012101	8	168277736.168281863	Located	E3 ubiquitin-protein ligase RGLG1	metabolic
	Zm00001d045128	9	13703300.13708121	-461	DBP-transcription factor 3	gene expression regulation
20GY	*Zm00001d017495*	5	197539628.197541548	Located	Expansin-B4	cell growth and development
	Zm00001d009488	8	67043287.67046926	61	ATP synthase subunit beta	metabolic
19GY/GY	*Zm00001d043036*	3	187095368.187096814	2184	LBD-transcription factor 20	gene expression regulation

[a]19ER, seedling emergence rate measured in Fuxin in 2019; ER, seedling emergence rate BLUE value calculated from two-year data; 19SPH, seedling plant height measured in Fuxin in 2019; SPH, BLUE value of seedling plant height calculated from two-year data; 19GY, grain yield measured in Fuxin in 2019; 20GY, grain yield measured in Fuxin in 2020; GY, grain yield BLUE value calculated from two-year data.
[b]The positive (+) and negative (−) values represent related SNPs location in the 5′ and 3′ direction, respectively, of their candidate gene.

autophagy (Table 4). Tissue specific expression analysis showed that each gene was expressed in different tissues, especially in roots. Interestingly, three genes *Zm00001d017495*, *Zm00001d009488* and *Zm00001d043036* related to yield traits had high expression in differentiation zone, elongated internode and primary root (Figure 7A). To further determine whether these genes have functions in drought conditions, their expression patterns were analyzed using published RNA-Seq datasets from control and drought-stressed plants at the V5/V6 developmental stage (Forestan et al., 2016), including 10 days of drought treatment (T0) and 7 days of rehydration (T7) (Figure 7B). Compared with Control_T0, one gene is not expressed (*Zm00001d031861*), two are up-regulated (*Zm00001d044291*, *Zm00001d053859*), and the other genes are down regulated under Drought_T0. Compared with Drought_T0, the expressions of *Zm00001d028423*, *Zm00001d043036*, *Zm00001d053952*, *Zm00001d037771*, *Zm00001d038930* were up regulated after 7 days of rehydration and could basically return to Control_T7 level or even higher. Nevertheless, the expressions of the remaining genes were unchanged or even lower, which indicated that drought caused irreversible damage to the activation of these gene expression. In this study, we designed specific primers to verify the expression changes of 10 candidate genes under normal and drought condition at seedling stage (Supplementary Table 2 and Figure 8A). The real-time quantitative PCR indicated that all of 10 genes were sensitive for drought stress and their expression changed under drought conditions, especially *Zm00001d009488* (Figure 8B), indicating that these significant SNPs and candidate genes may be potential genetic markers and genes for drought tolerance at seedling stage or in grain yield formation. In this study, we did not detect the change in the expression of the other five candidate genes.

3 Discussions

3.1 Genetic dissection of drought tolerance in maize seedling

Drought tolerance is a complex and inherent characteristic of maize (Wang et al., 2016). Especially in the early development stage, maize seedlings are susceptible to drought stress and the adverse effects generated by severe drought stress on seedling growth are irreversible (Liu and Qin, 2021). Along with rising temperature and dramatically fluctuated rainfall patterns due to the aggravation of the global greenhouse effect in recent years, global maize production has already showed stagnation, especially in arid and semi-arid regions. Fuxin County of Liaoning Province locates in the semi-arid zone of northeast China and the high frequency of spring drought is its typical climate characteristic. In this region, we can conduct larger scale field drought experiments without the use of greenhouses. In our current study, ER, SPH and GY traits exhibited a wide range of phenotypic variations and followed a normal or skewed normal distribution in the NCCP panel (Figure 1 and Supplementary Figure 1). A phenotypic variation analysis uncovered significant differences among different environments,

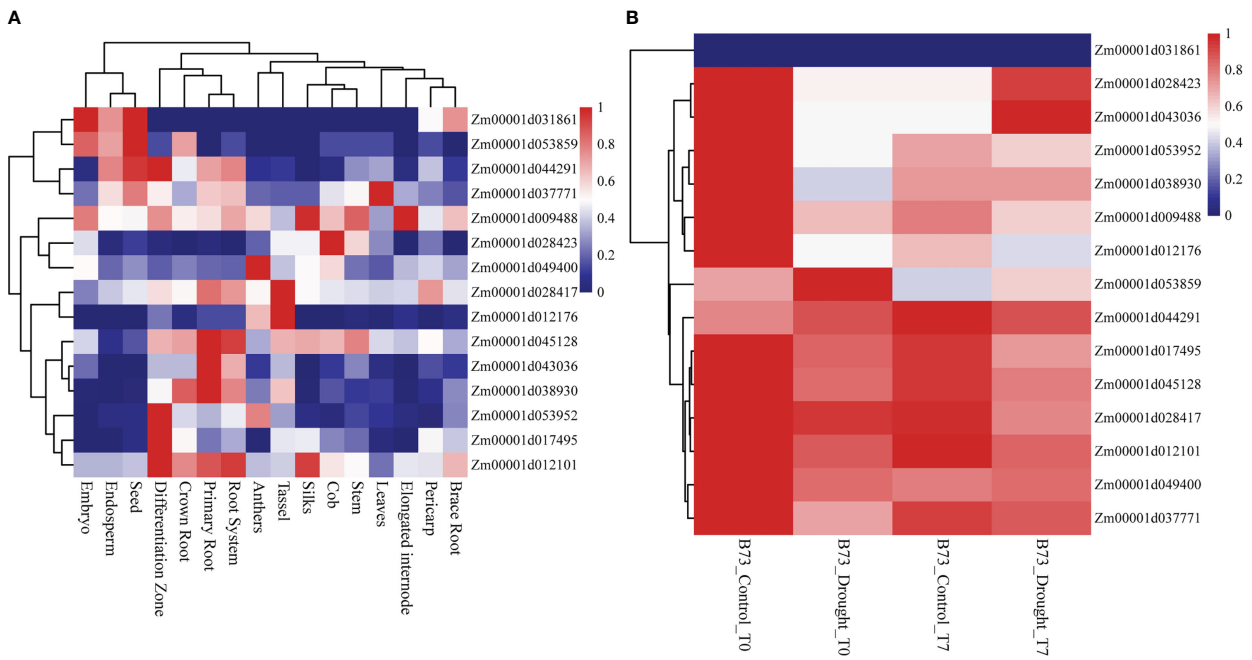

FIGURE 7
Heat map of expression patterns of candidate genes identified by GWAS in different tissues and different drought treatments. The values used in the figure were normalized TPM value by row. Columns and rows were ordered according to similarity (hierarchical cluster analysis at the top and left. The red and navy blue represented higher and lower expression level. **(A)** Expression of 15 genes in different tissues of maize. **(B)** Expression of 15 genes in different treatments. Drought_T0 is 10 days of drought, Drought_T7 represents 7 days of rehydration after drought and Control is the negative control.

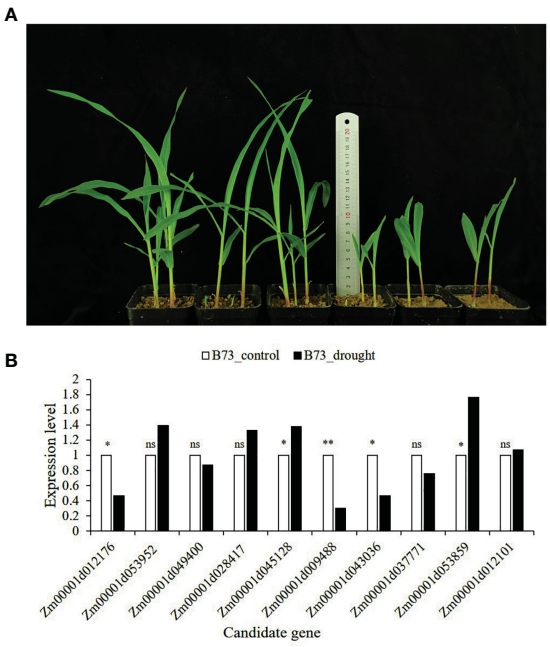

FIGURE 8
B73 growth plot under normal and drought conditions and the expression of candidate genes verified by qRT-PCR. **(A)** The left side is B73 maize under normal conditions (60% of the maximum water holding capacity), and the right side is B73 maize under drought conditions (30% of the maximum water holding capacity); **(B)** The expression level in the leaves of B73 seedlings under drought stress in laboratory. The value in the figure is $2^{-\Delta\Delta Ct}$. The statistical significance was determined *via* an Independent Samples t-test with $^{**}P \leq 0.01$, $^{*}P \leq 0.05$, and ns represent not statistically significant ($P > 0.05$).

which suggested that different environments could promote or diminish the effects of traits variance. Compared with 2019, 2020 has less precipitation and higher temperature at maize seedling stage, resulting in a smaller phenotypic value (Figure 9). According to our genetic analysis, the heritability of ER, SPH and GY were 0.32, 0.26 and 0.33 with a relatively low level, indicating that these traits were controlled by multiple small-effect genes (Figure 2). The genotype effects for ER, SPH and GY across two years were significant, indicating the involvement of gene action in the control of drought resistance related traits of maize seedlings (Zhang et al., 2022). The effect of G × E interaction on the traits was highly significant, consistent with the observed phenotypic variation in different years.

3.2 Significant SNP involved in drought resistance under field natural drought condition

The two major strategies, linkage mapping and GWAS, have been widely used to identify QTLs for drought resistance in maize, and result in the dissection of many agronomic traits related to drought resistance (Liu and Qin, 2021). In this study, we identified 15 common significant SNPs that contribute to 5.5-8.7% natural variation of drought tolerance in maize seedlings using the MLM and BLINK methods (Table 2 and Supplementary Table 1). There was a different distribution of these SNPs in inbred lines, ranged from 53.3% to 86.7% in 5 drought-resistant inbred lines detected (Table 3). For some significant SNPs, although not just located in gene sequences, they all were in the linkage interval (Table 4 and Supplementary Figure 5). These data are consistent with the fact that drought resistance is a complicated trait that may be controlled by multiple quantitative trait loci (QTLs).

3.3 Candidate genes and pathways involved in drought resistance under field natural drought condition

At maize seedling stage, the most research focus on the effect of artificial water control or stimulated drought under indoor condition. For instance, the functions of *ZmDREB2.7* (Liu et al., 2013), *ZmNAC111* (Mao et al., 2015) and *ZmVPP1* (Wang et al., 2016) genes in drought resistance have been investigated. However, the mechanism of drought tolerance of maize seedlings in natural field environment is unclear. In this study, the functional annotation revealed that 15 candidate genes could mainly be placed into a few functional groups, such as metabolic, transcriptional regulation, autophagy, cell growth and development, and programmed cell death (Table 4). Here, we will discuss how candidate genes may respond to external drought stress.

3.3.1 Transcription factor related candidate genes

Transcription factors (TFs) play an important role in signal transduction networks spanning the perception of a stress signal and the expression of corresponding stress-responsive genes. Multi-gene families (AP2/ERF, bZIP, MYB/MYC, NAC and WRKY) have been discussed in regulating plant drought responses *via* ABA-dependent and/or ABA-independent signaling (Yamaguchi-Shinozaki and Shinozaki, 2006; Hirayama and Shinozaki, 2010; Gahlaut et al., 2016; Hrmova and Hussain, 2021). TFs involved in water stress tolerance in plants may be utilized in future for developing drought-resistant varieties in maize and other crops.

The APETALA2/Ethylene-Responsive Factor (AP2/ERF) gene family constitutes one of the biggest gene families encoding plant-specific transcription factors. This superfamily is characterized by the presence of the AP2/ERF domain, which spans approximately 60 to 70 amino acids and mediates DNA binding. The subfamilies within this superfamily include AP2, RAV, DREB, ERF, and Soloist (Guo et al., 2016; Zhu et al., 2021). The TFs encoded by *Zm00001d031861*, *Zm00001d045128* and *Zm00001d053859* identified in this research belong to the DREB and ERF subfamilies and possess only one AP2/ERF structural domain. The candidate gene *Zm00001d031861* detected in 19ER, encodes dehydration responsive element binding protein 2G, which is a known drought responsive gene at maize seedling stage. Dehydration Responsive Element Binding proteins/C-repeat Binding Factors (DREBs/CBFs, referred as DREBs) are considered

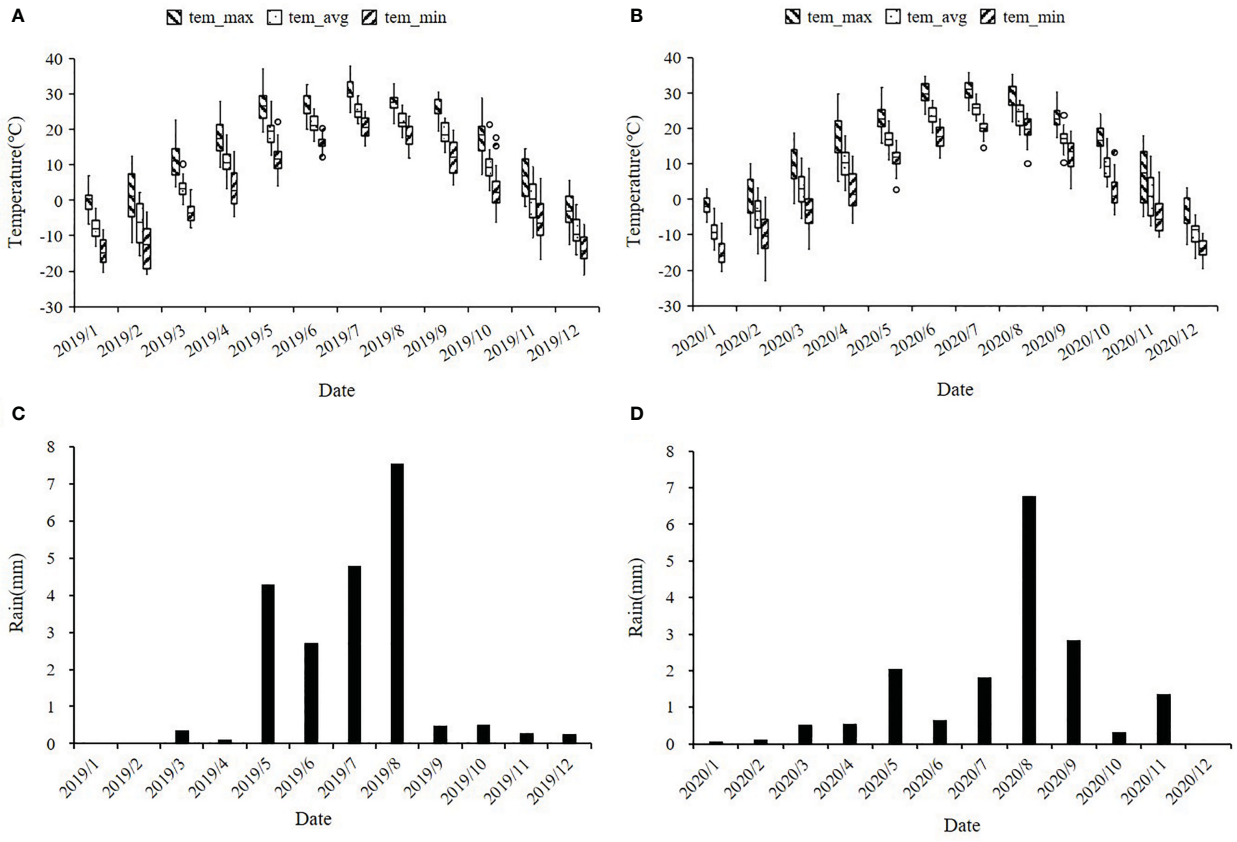

FIGURE 9
Distribution of temperature and rainfall in maize planting plots of Fuxin Mongolian Autonomous County in 2019 and 2020. **(A, B)** represent the monthly average temperatures (°C) for 2019 and 2020, including the monthly average maximum temperature, average temperature, and minimum temperature; **(C, D)** represent the monthly average rainfall in mm for 2019 and 2020.

to be the major TFs controlling the expression of stress-inducible genes in the ABA-independent pathway (Yamaguchi-Shinozaki and Shinozaki, 2006), and are able to bind a Dehydration Responsive Element (DRE, core motif: A/GCCGAC) in the promoter region of stress-inducible genes (Liu et al., 2013). Two *DREB* genes (*ZmDREB1A* and *ZmDREB2A*) of maize belonging to DREB1 and DREB2 subfamilies, respectively, were cloned and proved to be up-regulated in plants under drought, cold and heat stress (Qin et al., 2004; Qin et al., 2007). Liu (Liu et al., 2013) verified that the DNA polymorphism in the promoter region of *ZmDREB2.7* (*GRMZM2G028386*, B73 RefGen_v3; *Zm00001d031861*, B73 RefGen_v4) is related to drought tolerance of maize seedlings, and overexpression of *ZmDREB2.7* in Arabidopsis and maize showed enhanced tolerance to drought stress. *Zm00001d045128* related to SPH, encodes DBP-transcription factor 3. DNA binding protein phosphatase (DBP) factors are important regulators that participate in both transcriptional regulation and post-translational regulation (Jiao et al., 2020). *ZmDBP3* gene was isolated from maize seedlings and belongs to the A-1 subgroup of the DREBs subfamily. As a trans-acting factor, the ZmDBP3 protein is localized in the nucleus and activates genes containing C-repeat/dehydration-responsive elements (CRT/DRE) under normal growth conditions in transgenic Arabidopsis plants. Overexpression of *ZmDBP3* increased drought and cold resistance in transgenic Arabidopsis (Wang and Dong, 2009). Through transcriptional analysis, the *ZmDBP3* gene was identified as a potential marker for early selection of drought-tolerant maize lines (Marques et al., 2019). *Zm00001d053859*, detected in 19ER, encodes ethylene-responsive transcription factor3 (ERF3), which directly interacts with the GCC box (TAAGAGCCGCC) in the ethylene-responsive element that is necessary and sufficient for the regulation of transcription by ethylene. Transient transfection experiments in tobacco showed that ERFs were localized in the nucleus (Ohta et al., 2000). *Zm00001d053859* may thus regulate drought tolerance in maize by participating in ethylene signal transduction to change the physiological and biochemical reactions of maize seedlings.

The development of lateral roots may be affected by drought. *Zm00001d037771* identified from 19ER encodes bHLH133, pertaining to the basic helix-loop-helix (bHLH) family. The genome-wide analysis identified 208 putative bHLH family proteins in maize (Zhang et al., 2018). A study has indicated that bHLH133 determines the competence of the pericycle for lateral root initiation (Zhang et al., 2021), efficiently obtaining water and nutrients to resist water deficit. Similarly, LBD transcription factor 20 (LBD20) encoded by *Zm00001d043036*, whose Arabidopsis homologous gene *AT2G30340* (Lateral Organ Boundaries Domain

13, LBD13) is a transcription activator located in nuclear, controls the formation of lateral roots in Arabidopsis (Cho et al., 2019).

Zm00001d038930 encodes the transcription factor MYB36, belonging to the R2R3-MYB subfamily, which plays a central role in controlling plant-specific processes, including primary and secondary metabolism, development, and abiotic and biotic stress responses (Dubos et al., 2010). However, at present, only a few members of the R2R3-MYB family have been well described in maize. By analyzing the expression patterns of 46 *ZmMYB* genes under abiotic stress, researchers found that 13 *ZmMYB* genes responded to drought stress (20% PEG), and the relative expression of *ZmMYB36* was higher at 6 and 12 hours of 20% PEG osmotic stress (Chen et al., 2018). But the mechanism through which this gene can contribute to drought resistance needs further research. The candidate gene *Zm00001d049400* encodes global transcription factor group E7 (GTE7), and Arabidopsis homologous genes *AT5G65630* and *AT5G10550* encode GTE7 and GTE2, respectively. Arabidopsis GTE protein includes plant amphipathic domain (PAD), bromodomain (BRD), extra-terminal domain (ET) and transcriptional activation domains (TAD), which can interact with other TFs. In many cases, BRD can bind to acetylated lysine residues, forming a bridge between acetylated histones and TFs to activate transcription of target genes (Misra et al., 2018). Under drought stress in maize seedling stage, GTE protein may regulate gene expression and signal pathway by interacting with other proteins. But so far, little research has been done on maize GTE protein.

3.3.2 Candidate genes involved in plant cell developmental

The elongation and growth of plant cells will be inhibited under the condition of water scarcity, and the expression of related genes encoding expansins, aquaporins and XETs will also be affected (Wu et al., 2005; Liu et al., 2021a). *Zm00001d017495* identified from 20GY encodes Expansin-B4 (EXPB4). Expansins, driving turgor-driven cell enlargement by unlocking a network of wall polysaccharides (Cosgrove, 2000), are classified into α-expansins (EXPA) and β-expansins (EXPB) (Wu et al., 2001; Cosgrove, 2015). Maize was found to have a total of 88 *ZmEXPs* genes (Zhang et al., 2014). An association study revealed a significantly negative correlation between the level of *ZmEXPA4* expression and anthesis-silking interval (ASI), increasing ASI under drought will lead to low pollination rate and low yield. Furthermore, driving the expression of *ZmEXPA4* using a drought-inducible promoter can significantly reduce ASI under drought conditions (Liu et al., 2021a). Further studies on the function of maize EXPB are still necessary.

3.3.3 Candidate genes involved in cell signal transduction

Many signal molecules, such as intracellular Ca^{2+}, ABA, and reactive oxygen species (ROS), are very important for drought signal transduction. One of the first responses of plants to water deficit is the production of ROS. The moderate content of ROS is considered to mediate the induction of defense pathways and help plants adapt to the changing environment (Cruz de Carvalho, 2008). However, if stress continues to aggravate, the increase of ROS will lead to the damage of nucleic acids, proteins, lipids and other cellular components in plants, and causes programmed cell death (PCD) (Çakır and Tumer, 2015). The conserved cell death suppressor Bax inhibitor-1 (BI-1) encoded by *Zm00001d053952* plays a role in the downstream of PCD signaling and inhibits cell death. Studies have indicated that its Arabidopsis homologous gene *AtBI-1* (*AT5G47120*) encodes an endoplasmic reticulum (ER) membrane-associated protein, which modulates ER stress-induced PCD (Ruberti et al., 2018) by interacting with multiple partners to alter intracellular Ca^{2+} flux control (Ishikawa et al., 2011) and fatty acids metabolism (Nagano et al., 2012; Nagano et al., 2019). Simultaneously, the expression of *AtBI-1* cDNA from *Arabidopsis thaliana* in sugarcane, a C4 monocot species, might reduce the activation of cell death pathways initiated by hydric stress or chemical-induced ER stress (Ramiro et al., 2016). Therefore, suppressing the cell death of C4 grasses (including sorghum, maize, and other important crops) is an effective means to improve the long-term drought tolerance of crops. Moreover, ABA signal pathway is also the core of plant response to water deficiency, which has been clearly clarified by the identification of ABA receptors and other signal components. ABA binds to receptor PYRABACTIN RESISTANCE (PYR)/PYR-LIKE (PYL)/ REGULATORY COMPONENTS OF ABA RECEPTORS (RCAR), and then the ABA-receptor complex inhibits the activity of clade A type 2 C protein phosphatases (PP2Cs), resulting in the release of SNF1-related protein kinase 2s (SnRK2s) from PP2C-mediated inhibition, further phosphorylation or activation of downstream targets, ABA response transcription factors or ion channels (Danquah et al., 2014; Kumar et al., 2019; Chong et al., 2020; Lin et al., 2021). *Zm00001d012101* encodes E3 ubiquitin-protein ligase RGLG1, and its Arabidopsis homologous genes *AT3G01650* (RGLG1), *AT5G14420* (RGLG2) and *AT1G67800* (RGLG5) have been proved to mediate the signal pathway of drought stress. RGLG1 and RGLG5 interact with PP2Cs, a critical negative regulator of ABA signaling, accelerating PP2CA ubiquitination and degradation under the action of ABA, thereby promoting the activation of the ABA signaling (Wu et al., 2016). Meanwhile, mitogen activated protein kinase 18 (MAPKKK18) may be ubiquitinated at lysine residues K32 and K154 through RGLG1 and RGLG2. The deletion of RGLG1 and RGLG2 can stabilize MAPKKK18 and further enhance the drought resistance of MAPKKK18 overexpressing plants (Yu et al., 2021). Besides, RGLG1 and RGLG2 can also mediate AtERF53 protein degradation by ubiquitination, which has an adverse regulatory effect on drought tolerance (Cheng et al., 2011). Autophagy-related protein 9 (ATG9) encoded by *Zm00001d028417* is the only complete membrane protein in the core mechanism of autophagy and plays an essential role in mediating autophagosome formation (Lai et al., 2020). During a water shortage, autophagy proteins could selectively break down aquaporins to regulate water permeability

and damaged proteins to decrease their toxicity. Furthermore, autophagy might also degrade hormone signaling pathway regulators to promote a stress response (Tang and Bassham, 2022).

3.3.4 Candidate genes involved in biosynthesis

Zm00001d009488 encodes ATP synthase beta subunit, which is associated with the synthesis of ATP in photoreaction to drive carbon assimilation (Shi et al., 2014). Previous studies regarding the expression of ATP-related proteins in response to water deficit are contradictory. According to Tezara et al. (1999) and Valero-Galván et al. (2013), the expression of ATP synthase beta subunit reduces during drought. They suggested that since the cells require less energy during drought, the content of ATPase is likely to decrease in these plants. However, Kottapalli et al (2009); Zhou et al. (2015) and Cao et al. (2017b) observed the opposite, which higher expression of the ATP synthase beta subunit might enhance the energy supply to protect plants from damage under drought stress conditions (Rashid et al., 2022). *Zm00001d012176* encodes beta-hexosaminidase, a homologous gene of Arabidopsis beta-hexosaminidase 3 (hexo3), which can participate in the formation of paucimannosidic N-glycans (Liebminger et al., 2011), and Expression Pattern of Candidate Genes.

The specific high expression of different genes in the primary root and differentiation zone endows maize plants with resistance to water stress (Figure 7). At the same time, the three genes (*Zm00001d017495*, *Zm00001d009488* and *Zm00001d043036*) identified for grain yield are also highly expressed in primary tissues, which may play a crucial role in the drought resistance of maize seedlings. It also indicates that grain yield can be used as a drought resistance indicator of maize seedlings, reflecting the ultimate drought resistance of maize plants. In our qRT-PCR experiments, the results are basically consistent with Forestan (Forestan et al., 2016), but *Zm00001d045128* was up-regulated in the leaves of B73 seedlings under drought stress in laboratory, which may be caused by experimental differences (Figure 8). In particular, *Zm00001d009488* were down-regulated in the leaves of B73 seedlings under drought stress in laboratory, which is consistent with the results of Tezara (Tezara et al., 1999) and Valero-Galván (Valero-Galván et al., 2013). Kottapalli (Kottapalli et al., 2009) indicated that ATP synthase beta subunits are only highly induced in drought tolerant genotypes, but B73 is drought susceptible genotype.

4 Materials and methods

4.1 Association mapping panel

379 inbred lines, collected from China, America, Mexico, and other regions, among them, most from Northeast China, regarded as the northeast China core population (NCCP), were utilized to conduct GWAS in the current study. The heterosis group of the NCCP can be divided into 13 groups, including the Jidan, Longdan, NSS, SS, Huanglvxi, Lvxi, Reid, France, PA, Lvdahonggu, Tangsipingtou, Mixed and Unknown. The CML series from CIMMYT are tropical materials, and only two can be grown in Northeast China, here they were classified into the Mixed group. Some small groups and inbred lines from the multiple parent selection were classified as unknown group.

4.2 Field planting and phenotypic measurement

All 379 inbred lines of the association panel were planted in the Fuxin Mongolian autonomous county, Liaoning Province, China (42°06′N, 122°55′E) in 2019 (19FX) and 2020 (20FX), where drought occurs frequently and seriously in spring season. The seeds were sown on 12 May 2019 and 11 May 2020, respectively, and harvested on 7 October 2019 and 9 October 2020, respectively. During the 2019 maize growing season, the average temperature was 21°C and the average rainfall was 4 mm. In the 2020 maize growing season, the average temperature was 21°C and the average rainfall was 3 mm. During the maize seedling stage (May and June), maximum temperatures of 35°C across two years and average monthly precipitation of less than 5 mm caused severe drought stress at the seedling stage, maintaining three leaves throughout the growing season (Figure 9).

The maize field in our study were not irrigated, but seeds were sown before precipitation according to weather forecasts for germination. A completely randomized block design with three replications was used in each evaluation environment. Inbred lines were planted using one seed per hole on a single plot of 3 m length, with 10 cm spacing between plants and 60 cm spacing between rows. The target traits of seedling emergence (ER), seedling plant height (SPH) at the three-leaf stage and grain yield (GY) at the harvest stage were evaluated to represent the drought tolerance of the tested plant line. ER and SPH were measured at the seedling stage, i.e. 20 days after sowing. ER was measured as the ratio of surviving seedlings to the number of seeds sown. SPH was measured as the distance from the base of the plant to the highest point of the seedling. While GY was measured at the maturity stage, moisture content readings were taken by the LDS-1G Grain Moisture Meter. The average dry weight of five evenly grown ears was considered as the final yield of each inbred line.

4.3 Statistical analysis of phenotypes

The best linear unbiased prediction (BLUE) values and broad-sense heritability (H^2) of ER, SPH, and GY were calculated within and across environments using the META-R software version 6.04 (http://hdl.handle.net/11529/10201). The linear mixed models used in META-R are implemented in the LME4 R-package, functions of lmer () and REML were used to estimate the variance components.

$$Y_{ijk} = \mu + Gen_i + Env_j + Gen_i \times Env_j + Rep_k + \epsilon_{ijk}$$

Where Y_{ijk} is the trait of interest, μ is the overall mean, Gen_i, Env_j, and $Gen_i \times Env_j$ are the effects of the *i-th* genotype, *j-th* year, and *i-th* genotype by *j-th* year interation, respectively. Rep_k is the

effect of *k-th* replication.ϵ_{ijk} is the residual effect of the *i-th* genotype, *j-th* year, *k-th* replication. Genotype is considered as the fixed effect, whereas all other terms are declared as the random effects. Years with heritability below 0.05 were excluded from the across environment analysis.

Broad-sense heritability (H^2) based on the entry means within trials was estimated as follows:

$$H^2 = \frac{\sigma_g^2}{\sigma_g^2 + \frac{\sigma_{ge}^2}{nEnvs} + \frac{\sigma^2}{nEnvs \times nreps}}$$

Where σ_g^2, σ^2, and σ_{ge}^2 are the genotypic variance, error variance, and genotype-by-environment interaction variance, respectively, and *nreps* and *nEnvs* are the numbers of replications and environments, respectively.

4.4 Genotyping and quality control

Leaf samples were collected from each maize inbred line seedling for DNA extraction with a CTAB procedure, and genotyping was carried out by DArT and GBS platform. GBS was performed by the common protocol in maize in Wuhan Huada medical laboratory Co., Ltd (Elshire et al., 2011). The genomic DNA was digested with restriction enzyme *ApeKI*, and a DNA library was constructed in 96-plex and sequenced on Illumina-hiseq2500/4000 platform. Details in single nucleotide polymorphism (SNP) calling and imputation have been previously described (Cao et al., 2017a). Initially, 768,558 SNPs evenly distributed on maize chromosomes were called for each line; 760,831 of them were assigned to chromosomes 1-10, and 7,727 could not be anchored to any of the chromosomes.

DArT was completed in the SAGA sequencing platform established by Mexico DArT company and CIMMYT. It uses two enzymes (*PstI* and *HpaII*) to cut DNA samples to reduce the complexity of genome. After enzyme digestion, DNA from different samples was linked with barcodes of different base combinations and sequenced to construct a DNA simplified sequencing library. Combined with Illumina second-generation short fragment sequencing technology (150bp), the simplified sequencing DNA library of mixed samples was sequenced on a single sequencing lane (https://www.diversityarrays.com/) (Kilian et al., 2012). At first, 39,659 DArT SNPs were called for each line, of which 39112 were located on maize chromosomes 1-10, and 547 SNPs could not be anchored on any maize chromosomes.

In DArT and GBS datasets, TASSEL 5 (Bradbury et al., 2007) was used to filter out markers with minor allele frequency (MAF)< 0.05 and a missing rate > 20%. There were 379 lines and 7,837 markers remaining in DArT datasets, 378 lines and 91,003 SNPs remaining in GBS datasets. The remaining markers of the two sequencing platforms were combined and filtered again. Imputation approaches used the method of Cao (Cao et al., 2017a). Finally, we obtained 97,862 GBS-DArT SNPs of 378 lines for subsequent analysis.

4.5 Genome-wide association mapping and phenotypic variance contributions of significant loci

We used the trait values of single environment and BLUE in the Tab separator format and performed the GWAS analysis using a genotype with 97,862 SNP markers from GBS-DArT combination (MAF ≥ 0.05 and missing rate ≤ 20%). The mixed linear model (MLM) of GAPIT (Genomic Association and Prediction Integrated Tool) package was used to perform the association analysis for drought resistance related traits, and it is one of the most effective methods for controlling false positives in GWAS. This model simultaneously incorporates both population structure and kinship (Yu et al., 2006). The MLM model is described as follows:

$$y = X\beta + Qv + Zu + \epsilon$$

Where X is the SNP marker matrix, Q and Z represent the subpopulation membership matrix and kinship matrix respectively, β and v are the coefficient vectors of SNP markers and subpopulation membership respectively, u is the random genetic effect vector, and ϵ is the random error vector (Yu et al., 2006; Fan et al., 2016).

Simultaneously, association analysis for all the traits was also conducted with the model of Bayesian information criterion and Linkage-disequilibrium Iteratively Nested Keyway (BLINK) (Huang et al., 2019). The BLINK package can be downloaded from https://github.com/YaoZhou89/BLINK. The first three PCs were treated as covariates to perform GWAS. The principal component analysis (PCA) and kinship of 378 maize inbred lines were conducted using prcomp() and GAPIT.kinship.Zhang() function in R(v 4.1.1), separately.

The linkage disequilibrium (LD) of the entire panel was analyzed using TASSEL software (Bradbury et al., 2007), and LD decay plots were done using the LD decay Plot Tool written by Zhang Ao based on the base functions using the R language. The plotting script is available online on the webpage https://aozhangchina.github.io/R/LDdecay/LDdecayPlotTool.html. Then, we used the uniform Bonferroni-corrected threshold of $\alpha = 1$ for the mixed linear model's significance cutoff as reported in previous studies (Mao et al., 2015; Liu et al., 2022). Therefore, the suggested P-value was computed with 1/n (n = 97,862, total markers used), and we obtained a P-value threshold of 1.02×10^{-5} for GWAS.

4.6 Annotation of candidate genes

The most significant SNP was chosen to represent the locus in the same LD block (r^2< 0.2). The physical locations of the SNPs were determined in reference to the B73 RefGen_v4. LD, which was calculated for each independent significant SNP within its surrounding regions (80Kb). Candidate genes were identified by the presence of significant SNPs directly located within the gene sequence. Alternatively, genes residing within a corresponding LD region also were considered, and their biological functions were annotated using data from the MaizeGDB and UniProt website.

4.7 Heat map of candidate genes

The expression levels of candidate genes from different tissues and different drought treatments of B73 were downloaded from the MaizeGDB qTeller (https://qteller.maizegdb.org/). The values used for heat map construction were calculated as normalized TPM value by row.

4.8 RNA isolation and quantitative RT–PCR analysis

B73 seeds were sown in a cultivating pot (upper diameter 6.5cm, lower diameter 4.5cm, height 7.5cm). The test soil was clayey brown soil, collected from the northern experimental station of Shenyang Agricultural University in 2020 and baked at 120°C until the soil weight was no longer changed. Four seeds were sown in each small pot and repeated three times for two treatments. The soil water content of normal control was 60% of the maximum water holding capacity, and that of drought treatment was 30% of the maximum water holding capacity. Total RNA from maize leaves was extracted on the 12th day after sowing.

Total RNA was extracted using SteadyPure Plant RNA Extraction Kit (AG2109S) of Accurate Biotechnology from at least three seedlings of B73. Subsequently, the concentration of RNA was determined by BioDrop. cDNA was prepared using PrimerScriptTM RT reagent Kit with gDNA Eraser (Takara Biotechnology Dalian Co. Ltd.). The maize Ubi1 (UniProtKB/TrEMBL, Q42415) gene was used as an internal control to normalize the data, and the candidate gene primers were synthesized by Sangon Biotech company and purified by PAGE. qRT-PCR was performed on Bio-Rad CFX Connect Real-Time System (CA, USA) with a 10 µl reaction volume containing 4.6 µl of ddH2O, 3.6 µl of TB GreenTM Premix Ex TaqTM (Tli RNaseH Plus; TakKaRa), 0.4 µl of specific primers (10 µM) and 1 µl of cDNA. PCR conditions consisted of an initial denaturation step at 95°C for 40 seconds, followed by 39 cycles at 95°C for 5 seconds and 60°C for 1 minute, and a final stage of 60-95°C to determine melting curves of the amplified products. The quantification method ($2^{-\Delta\Delta Ct}$) was used and the variation in expression was estimated using three biological replicates.

5 Conclusions

In this study, we have explored the genetic basis of the performance of drought tolerance at seedling stage of maize natural population under natural field condition by applying GWAS approach. Drought resistance related traits manifested a relatively low heritability and a broad variation in the association panel. According to the GWAS, multiple genetic loci with small effects regulate the natural variation in ER, SPH and GY in maize under drought condition. 15 commonly significant SNPs were obtained by the MLM and BLINK method, and the phenotypic distribution of major and minor alleles in different traits showed extremely significant difference ($P< 0.01$). Simultaneously, the distribution ratio of tolerant genes was 53.3% - 86.7% in 5 drought-resistant inbred lines. We further found 15 candidate genes that may involve in plant cell developmental, cell signal transduction, and transcription factors. These candidate genes provide valuable resources for further investigation to dissect the molecular network to regulate drought resistance of maize seedlings to increase yield. In addition, the significantly associated SNPs found in this research will be helpful in facilitating marker-assisted selection of drought tolerance of maize seedlings in breeding programs.

Data availability statement

The original contributions presented in the study are publicly available. This data can be found here: https://www.ebi.ac.uk/eva/?eva-study=PRJEB61663.

Author contributions

AZ and YR initiated and designed the overall study. DD, SJ, CZ, and CL performed and coordinated the field experiments and phenotypic data collection. HZ, YL, XD, and YG carried out the data analysis. SC and AZ interpreted the results and wrote the manuscript. All authors contributed to the article and approved the submitted version.

Funding

This research was funded by Liaoning Provincial Department of Education Project for Youth Scientists (LJKZ0657).

Conflict of interest

The authors declare that the research was conducted in the absence of any commercial or financial relationships that could be construed as a potential conflict of interest.

Publisher's note

Supplementary material

The Supplementary Material for this article can be found online at: https://www.frontiersin.org/articles/10.3389/fpls.2023.1165582/full#supplementary-material

References

Aranzana, M. J., Kim, S., Zhao, K., Bakker, E., Horton, M., Jakob, K., et al. (2005). Genome-wide association mapping in arabidopsis identifies previously known flowering time and pathogen resistance genes. *PloS Genet.* 1 (5), e60. doi: 10.1371/journal.pgen.0010060

Baret, F., Madec, S., Irfan, K., Lopez, J., Comar, A., Hemmerlé, M., et al. (2018). Leaf-rolling in maize crops: from leaf scoring to canopy-level measurements for phenotyping. *J. Exp. Bot.* 69 (10), 2705–2716. doi: 10.1093/jxb/ery071

Bradbury, P. J., Zhang, Z., Kroon, D. E., Casstevens, T. M., Ramdoss, Y., and Buckler, E. S. (2007). TASSEL: software for association mapping of complex traits in diverse samples. *Bioinformatics* 23 (19), 2633–2635. doi: 10.1093/bioinformatics/btm308

Çakır, B., and Tumer, N. E. (2015). Arabidopsis bax inhibitor-1 inhibits cell death induced by pokeweed antiviral protein in saccharomyces cerevisiae. *Microb. Cell* 2 (2), 43–56. doi: 10.15698/mic2015.02.190

Cao, S., Loladze, A., Yuan, Y., Wu, Y., Zhang, A., Chen, J., et al. (2017a). Genome-wide analysis of tar spot complex resistance in maize using genotyping-by-Sequencing SNPs and whole-genome prediction. *Plant Genome* 10 (2), plantgenome2016.2010.0099. doi: 10.3835/plantgenome2016.10.0099

Cao, Y., Luo, Q., Tian, Y., and Meng, F. (2017b). Physiological and proteomic analyses of the drought stress response in amygdalus Mira (Koehne) yü et Lu roots. *BMC Plant Biol.* 17 (1), 53. doi: 10.1186/s12870-017-1000-z

Chen, Y. H., Cao, Y. Y., Wang, L. J., Li, L. M., Yang, J., and Zou, M. X. (2018). Identification of MYB transcription factor genes and their expression during abiotic stresses in maize. *Biol. Plantarum* 62 (2), 222–230. doi: 10.1007/s10535-017-0756-1

Cheng, M.-C., Hsieh, E.-J., Chen, J.-H., Chen, H.-Y., and Lin, T.-P. (2011). Arabidopsis RGLG2, functioning as a RING E3 ligase, interacts with AtERF53 and negatively regulates the plant drought stress response. *Plant Physiol.* 158 (1), 363–375. doi: 10.1104/pp.111.189738

Cho, C., Jeon, E., Pandey, S. K., Ha, S. H., and Kim, J. (2019). LBD13 positively regulates lateral root formation in arabidopsis. *Planta* 249 (4), 1251–1258. doi: 10.1007/s00425-018-03087-x

Chong, L., Guo, P., and Zhu, Y. (2020). Mediator complex: A pivotal regulator of ABA signaling pathway and abiotic stress response in plants. *Int. J. Mol. Sci.* 21 (20), 2–11. doi: 10.3390/ijms21207755

Cosgrove, D. (2000). Loosening of plant cell walls by expansins. *Nature* 407, 321–326. doi: 10.1038/35030000

Cosgrove, D. J. (2015). Plant expansins: diversity and interactions with plant cell walls. *Curr. Opin. Plant Biol.* 25, 162–172. doi: 10.1016/j.pbi.2015.05.014

Cruz de Carvalho, M. H. (2008). Drought stress and reactive oxygen species: Production, scavenging and signaling. *Plant Signal Behav.* 3 (3), 156–165. doi: 10.4161/psb.3.3.5536

Danquah, A., de Zelicourt, A., Colcombet, J., and Hirt, H. (2014). The role of ABA and MAPK signaling pathways in plant abiotic stress responses. *Biotechnol. Adv.* 32 (1), 40–52. doi: 10.1016/j.biotechadv.2013.09.006

Dinka, S. J., Campbell, M. A., Demers, T., and Raizada, M. N. (2007). Predicting the size of the progeny mapping population required to positionally clone a gene. *Genetics* 176 (4), 2035–2054. doi: 10.1534/genetics.107.074377

dos Santos, J. P. R., Pires, L. P. M., de Castro Vasconcellos, R. C., Pereira, G. S., Von Pinho, R. G., and Balestre, M. (2016). Genomic selection to resistance to stenocarpella maydis in maize lines using DArTseq markers. *BMC Genet.* 17 (1), 86. doi: 10.1186/s12863-016-0392-3

Dubos, C., Stracke, R., Grotewold, E., Weisshaar, B., Martin, C., and Lepiniec, L. (2010). MYB transcription factors in arabidopsis. *Trends Plant Sci.* 15 (10), 573–581. doi: 10.1016/j.tplants.2010.06.005

Elshire, R. J., Glaubitz, J. C., Sun, Q., Poland, J. A., Kawamoto, K., Buckler, E. S., et al. (2011). A robust, simple genotyping-by-sequencing (GBS) approach for high diversity species. *PloS One* 6 (5), e19379. doi: 10.1371/journal.pone.0019379

Fan, Y., Zhou, G., Shabala, S., Chen, Z. H., Cai, S., Li, C., et al. (2016). Genome-wide association study reveals a new QTL for salinity tolerance in barley (Hordeum vulgare l.). *Front. Plant Sci.* 7. doi: 10.3389/fpls.2016.00946

Farfan, I. D., de la Fuente, G. N., Murray, S. C., Isakeit, T., Huang, P. C., Warburton, M., et al. (2015). Genome wide association study for drought, aflatoxin resistance, and important agronomic traits of maize hybrids in the sub-tropics. *PloS One* 10 (2), e0117737. doi: 10.1371/journal.pone.0117737

Forestan, C., Aiese Cigliano, R., Farinati, S., Lunardon, A., Sanseverino, W., and Varotto, S. (2016). Stress-induced and epigenetic-mediated maize transcriptome regulation study by means of transcriptome reannotation and differential expression analysis. *Sci. Rep.* 6 (1), 30446. doi: 10.1038/srep30446

Gahlaut, V., Jaiswal, V., Kumar, A., and Gupta, P. K. (2016). Transcription factors involved in drought tolerance and their possible role in developing drought tolerant cultivars with emphasis on wheat (Triticum aestivum l.). *Theor. Appl. Genet.* 129 (11), 2019–2042. doi: 10.1007/s00122-016-2794-z

Guo, R., Dhliwayo, T., Mageto, E. K., Palacios-Rojas, N., Lee, M., Yu, D., et al. (2020b). Genomic prediction of kernel zinc concentration in multiple maize populations using genotyping-by-Sequencing and repeat amplification sequencing markers. *Front. Plant Sci.* 11. doi: 10.3389/fpls.2020.00534

Guo, J., Li, C., Zhang, X., Li, Y., Zhang, D., Shi, Y., et al. (2020a). Transcriptome and GWAS analyses reveal candidate gene for seminal root length of maize seedlings under drought stress. *Plant Sci.* 292, 110380. doi: 10.1016/j.plantsci.2019.110380

Guo, B., Wei, Y., Xu, R., Lin, S., Luan, H., Lv, C., et al. (2016). Genome-wide analysis of APETALA2/Ethylene-responsive factor (AP2/ERF) gene family in barley (Hordeum vulgare l.). *PloS One* 11 (9), e0161322. doi: 10.1371/journal.pone.0161322

Hirayama, T., and Shinozaki, K. (2010). Research on plant abiotic stress responses in the post-genome era: past, present and future. *Plant J.* 61 (6), 1041–1052. doi: 10.1111/j.1365-313X.2010.04124.x

Hrmova, M., and Hussain, S. S. (2021). Plant transcription factors involved in drought and associated stresses. *Int. J. Mol. Sci.* 22 (11), 1–29. doi: 10.3390/ijms22115662

Huang, M., Liu, X., Zhou, Y., Summers, R. M., and Zhang, Z. (2019). BLINK: a package for the next level of genome-wide association studies with both individuals and markers in the millions. *Gigascience* 8 (2), 1–12. doi: 10.1093/gigascience/giy154

Ishikawa, T., Watanabe, N., Nagano, M., Kawai-Yamada, M., and Lam, E. (2011). Bax inhibitor-1: a highly conserved endoplasmic reticulum-resident cell death suppressor. *Cell Death Differ* 18 (8), 1271–1278. doi: 10.1038/cdd.2011.59

Jiao, S., Zhou, J., Liu, Y., Zhai, H., and Bai, X. (2020). Phosphatase AtDBP1 negatively regulates drought and salt tolerance through altering leaf surface permeability in arabidopsis. *Mol. Biol. Rep.* 47 (5), 3585–3592. doi: 10.1007/s11033-020-05451-1

Kilian, A., Wenzl, P., Huttner, E., Carling, J., Xia, L., Blois, H., et al. (2012). Diversity arrays technology: a generic genome profiling technology on open platforms. *Methods Mol. Biol.* 888, 67–89. doi: 10.1007/978-1-61779-870-2_5

Kottapalli, K. R., Rakwal, R., Shibato, J., Burow, G., Tissue, D., Burke, J., et al. (2009). Physiology and proteomics of the water-deficit stress response in three contrasting peanut genotypes. *Plant Cell Environ.* 32 (4), 380–407. doi: 10.1111/j.1365-3040.2009.01933.x

Kumar, M., Kesawat, M. S., Ali, A., Lee, S. C., Gill, S. S., and Kim, A. H. U. (2019). Integration of abscisic acid signaling with other signaling pathways in plant stress responses and development. *Plants (Basel)* 8 (12), 592. doi: 10.3390/plants8120592

Lai, L. T. F., Yu, C., Wong, J. S. K., Lo, H. S., Benlekbir, S., Jiang, L., et al. (2020). Subnanometer resolution cryo-EM structure of arabidopsis thaliana ATG9. *Autophagy* 16 (3), 575–583. doi: 10.1080/15548627.2019.1639300

Liebminger, E., Veit, C., Pabst, M., Batoux, M., Zipfel, C., Altmann, F., et al. (2011). Beta-n-acetylhexosaminidases HEXO1 and HEXO3 are responsible for the formation of paucimannosidic n-glycans in arabidopsis thaliana. *J. Biol. Chem.* 286 (12), 10793–10802. doi: 10.1074/jbc.M110.178020

Lin, Z., Li, Y., Wang, Y., Liu, X., Ma, L., Zhang, Z., et al. (2021). Initiation and amplification of SnRK2 activation in abscisic acid signaling. *Nat. Commun.* 12 (1), 1–13. doi: 10.1038/s41467-021-22812-x

Liu, Y., Hu, G., Zhang, A., Loladze, A., Hu, Y., Wang, H., et al. (2021b). Genome-wide association study and genomic prediction of fusarium ear rot resistance in tropical maize germplasm. *Crop J.* 9 (2), 325–341. doi: 10.1016/j.cj.2020.08.008

Liu, S., and Qin, F. (2021). Genetic dissection of maize drought tolerance for trait improvement. *Mol. Breed.* 41 (2), 8. doi: 10.1007/s11032-020-01194-w

Liu, S., Wang, X., Wang, H., Xin, H., Yang, X., Yan, J., et al. (2013). Genome-wide analysis of ZmDREB genes and their association with natural variation in drought tolerance at seedling stage of zea mays l. *PloS Genet.* 9 (9), e1003790. doi: 10.1371/journal.pgen.1003790

Liu, B., Zhang, B., Yang, Z., Liu, Y., Yang, S., Shi, Y., et al. (2021a). Manipulating ZmEXPA4 expression ameliorates the drought-induced prolonged anthesis and silking interval in maize. *Plant Cell* 33 (6), 2058–2071. doi: 10.1093/plcell/koab083

Liu, M., Zhang, M., Yu, S., Li, X., Zhang, A., Cui, Z., et al. (2022). A genome-wide association study dissects the genetic architecture of the metaxylem vessel number in maize brace roots. *Front. Plant Sci.* 13. doi: 10.3389/fpls.2022.847234

Lobell, D. B., Roberts, M. J., Schlenker, W., Braun, N., Little, B. B., Rejesus, R. M., et al. (2014). Greater sensitivity to drought accompanies maize yield increase in the U.S. Midwest. *Science* 344 (6183), 516–519. doi: 10.1126/science.1251423

Mao, H., Wang, H., Liu, S., Li, Z., Yang, X., Yan, J., et al. (2015). A transposable element in a NAC gene is associated with drought tolerance in maize seedlings. *Nat. Commun.* 6 (1), 8326. doi: 10.1038/ncomms9326

Marques, T. L., Pinho, R. G. V., Pinho, D.V.D.R.V., Paniago, B. D. C., and Santos, H. O. D. (2019). Physiological analysis and gene expression analysis of ZmDBP3, ZmALDH9, ZmAN13, and ZmDREB2A in maize lines. *Acta Scientiarum Agron.* 42, e43479. doi: 10.4025/actasciagron.v42i1.43479

Misra, A., McKnight, T. D., and Mandadi, K. K. (2018). Bromodomain proteins GTE9 and GTE11 are essential for specific BT2-mediated sugar and ABA responses in arabidopsis thaliana. *Plant Mol. Biol.* 96 (4-5), 393–402. doi: 10.1007/s11103-018-0704-2

Nagano, M., Kakuta, C., Fukao, Y., Fujiwara, M., Uchimiya, H., and Kawai-Yamada, M. (2019). Arabidopsis bax inhibitor-1 interacts with enzymes related to very-long-chain fatty acid synthesis. *J. Plant Res.* 132 (1), 131–143. doi: 10.1007/s10265-018-01081-8

Nagano, M., Takahara, K., Fujimoto, M., Tsutsumi, N., Uchimiya, H., and Kawai-Yamada, M. (2012). Arabidopsis sphingolipid fatty acid 2-hydroxylases (AtFAH1 and AtFAH2) are functionally differentiated in fatty acid 2-hydroxylation and stress responses. *Plant Physiol.* 159 (3), 1138–1148. doi: 10.1104/pp.112.199547

Ohta, M., Ohme-Takagi, M., and Shinshi, H. (2000). Three ethylene-responsive transcription factors in tobacco with distinct transactivation functions. *Plant J.* 22 (1), 29–38. doi: 10.1046/j.1365-313x.2000.00709.x

Qin, F., Kakimoto, M., Sakuma, Y., Maruyama, K., Osakabe, Y., Tran, L. S., et al. (2007). Regulation and functional analysis of ZmDREB2A in response to drought and heat stresses in zea mays l. *Plant J.* 50 (1), 54–69. doi: 10.1111/j.1365-313X.2007.03034.x

Qin, F., Sakuma, Y., Li, J., Liu, Q., Li, Y. Q., Shinozaki, K., et al. (2004). Cloning and functional analysis of a novel DREB1/CBF transcription factor involved in cold-responsive gene expression in zea mays l. *Plant Cell Physiol.* 45 (8), 1042–1052. doi: 10.1093/pcp/pch118

Ramiro, D. A., Melotto-Passarin, D. M., Barbosa, M., Dos Santos, F., Gomez, S. G. P., Massola Júnior, N. S., et al. (2016). Expression of arabidopsis bax inhibitor-1 in transgenic sugarcane confers drought tolerance. *Plant Biotechnol. J.* 14 (9), 1826–1837. doi: 10.1111/pbi.12540

Rashid, U., Yasmin, H., Hassan, M. N., Naz, R., Nosheen, A., Sajjad, M., et al. (2022). Drought-tolerant bacillus megaterium isolated from semi-arid conditions induces systemic tolerance of wheat under drought conditions. *Plant Cell Rep.* 41 (3), 549–569. doi: 10.1007/s00299-020-02640-x

Ren, J., Li, Z., Wu, P., Zhang, A., Liu, Y., Hu, G., et al. (2021). Genetic dissection of quantitative resistance to common rust (Puccinia sorghi) in tropical maize (Zea mays l.) by combined genome-wide association study, linkage mapping, and genomic prediction. *Front. Plant Sci.* 12. doi: 10.3389/fpls.2021.692205

Ruberti, C., Lai, Y., and Brandizzi, F. (2018). Recovery from temporary endoplasmic reticulum stress in plants relies on the tissue-specific and largely independent roles of bZIP28 and bZIP60, as well as an antagonizing function of BAX-inhibitor 1 upon the pro-adaptive signaling mediated by bZIP28. *Plant J.* 93 (1), 155–165. doi: 10.1111/tpj.13768

Setter, T. L., Yan, J., Warburton, M., Ribaut, J.-M., Xu, Y., Sawkins, M., et al. (2010). Genetic association mapping identifies single nucleotide polymorphisms in genes that affect abscisic acid levels in maize floral tissues during drought. *J. Exp. Bot.* 62 (2), 701–716. doi: 10.1093/jxb/erq308

Shi, H., Ye, T., and Chan, Z. (2014). Comparative proteomic responses of two bermudagrass (Cynodon dactylon (L). pers.) varieties contrasting in drought stress resistance. *Plant Physiol. Biochem.* 82, 218–228. doi: 10.1016/j.plaphy.2014.06.006

Tang, J., and Bassham, D. C. (2022). Autophagy during drought: function, regulation, and potential application. *Plant J.* 109 (2), 390–401. doi: 10.1111/tpj.15481

Tezara, W., Mitchell, V. J., Driscoll, S. D., and Lawlor, D. W. (1999). Water stress inhibits plant photosynthesis by decreasing coupling factor and ATP. *Nature* 401 (6756), 914–917. doi: 10.1038/44842

Thirunavukkarasu, N., Hossain, F., Arora, K., Sharma, R., Shiriga, K., Mittal, S., et al. (2014). Functional mechanisms of drought tolerance in subtropical maize (Zea mays l.) identified using genome-wide association mapping. *BMC Genomics* 15 (1), 1182. doi: 10.1186/1471-2164-15-1182

Tian, Y., Guan, B., Zhou, D., Yu, J., Li, G., and Lou, Y. (2014). Responses of seed germination, seedling growth, and seed yield traits to seed pretreatment in maize (Zea mays l.). *ScientificWorldJournal* 2014, 834630. doi: 10.1155/2014/834630

Valero-Galván, J., González-Fernández, R., Navarro-Cerrillo, R. M., Gil-Pelegrín, E., and Jorrín-Novo, J. V. (2013). Physiological and proteomic analyses of drought stress response in Holm oak provenances. *J. Proteome Res.* 12 (11), 5110–5123. doi: 10.1021/pr400591n

Wang, C.-T., and Dong, Y.-M. (2009). Overexpression of maize ZmDBP3 enhances tolerance to drought and cold stress in transgenic arabidopsis plants. *Biologia* 64 (6), 1108. doi: 10.2478/s11756-009-0198-0

Wang, N., Liu, B., Liang, X., Zhou, Y., Song, J., Yang, J., et al. (2019). Genome-wide association study and genomic prediction analyses of drought stress tolerance in China in a collection of off-PVP maize inbred lines. *Mol. Breed.* 39 (8), 113. doi: 10.1007/s11032-019-1013-4

Wang, X., Wang, H., Liu, S., Ferjani, A., Li, J., Yan, J., et al. (2016). Genetic variation in ZmVPP1 contributes to drought tolerance in maize seedlings. *Nat. Genet.* 48 (10), 1233–1241. doi: 10.1038/ng.3636

Wang, N., Yuan, Y., Wang, H., Yu, D., Liu, Y., Zhang, A., et al. (2020). Applications of genotyping-by-sequencing (GBS) in maize genetics and breeding. *Sci. Rep.* 10 (1), 16308. doi: 10.1038/s41598-020-73321-8

Wu, Y., Jeong, B. R., Fry, S. C., and Boyer, J. S. (2005). Change in XET activities, cell wall extensibility and hypocotyl elongation of soybean seedlings at low water potential. *Planta* 220 (4), 593–601. doi: 10.1007/s00425-004-1369-4

Wu, Y., Meeley, R. B., and Cosgrove, D. J. (2001). Analysis and expression of the alpha-expansin and beta-expansin gene families in maize. *Plant Physiol.* 126 (1), 222–232. doi: 10.1104/pp.126.1.222

Wu, Q., Zhang, X., Peirats-Llobet, M., Belda-Palazon, B., Wang, X., Cui, S., et al. (2016). Ubiquitin ligases RGLG1 and RGLG5 regulate abscisic acid signaling by controlling the turnover of phosphatase PP2CA. *Plant Cell* 28 (9), 2178–2196. doi: 10.1105/tpc.16.00364

Yamaguchi-Shinozaki, K., and Shinozaki, K. (2006). Transcriptional regulatory networks in cellular responses and tolerance to dehydration and cold stresses. *Annu. Rev. Plant Biol.* 57, 781–803. doi: 10.1146/annurev.arplant.57.032905.105444

Yu, J., Kang, L., Li, Y., Wu, C., Zheng, C., Liu, P., et al. (2021). RING finger protein RGLG1 and RGLG2 negatively modulate MAPKKK18 mediated drought stress tolerance in arabidopsis. *J. Integr. Plant Biol.* 63 (3), 484–493. doi: 10.1111/jipb.13019

Yu, J., Pressoir, G., Briggs, W. H., Vroh Bi, I., Yamasaki, M., Doebley, J. F., et al. (2006). A unified mixed-model method for association mapping that accounts for multiple levels of relatedness. *Nat. Genet.* 38 (2), 203–208. doi: 10.1038/ng1702

Zhang, A., Chen, S., Cui, Z., Liu, Y., Guan, Y., Yang, S., et al. (2022). Genomic prediction of drought tolerance during seedling stage in maize using low-cost molecular markers. *Euphytica* 218 (11), 154. doi: 10.1007/s10681-022-03103-y

Zhang, T., Lv, W., Zhang, H., Ma, L., Li, P., Ge, L., et al. (2018). Genome-wide analysis of the basic helix-Loop-Helix (bHLH) transcription factor family in maize. *BMC Plant Biol.* 18 (1), 235. doi: 10.1186/s12870-018-1441-z

Zhang, Y., Mitsuda, N., Yoshizumi, T., Horii, Y., Oshima, Y., Ohme-Takagi, M., et al. (2021). Two types of bHLH transcription factor determine the competence of the pericycle for lateral root initiation. *Nat. Plants* 7 (5), 633–643. doi: 10.1038/s41477-021-00919-9

Zhang, W., Yan, H., Chen, W., Liu, J., Jiang, C., Jiang, H., et al. (2014). Genome-wide identification and characterization of maize expansin genes expressed in endosperm. *Mol. Genet. Genomics* 289 (6), 1061–1074. doi: 10.1007/s00438-014-0867-8

Zhou, S., Li, M., Guan, Q., Liu, F., Zhang, S., Chen, W., et al. (2015). Physiological and proteome analysis suggest critical roles for the photosynthetic system for high water-use efficiency under drought stress in malus. *Plant Sci.* 236, 44–60. doi: 10.1016/j.plantsci.2015.03.017

Zhu, Y., Liu, X., Gao, Y., Li, K., and Guo, W. (2021). Transcriptome-based identification of AP2/ERF family genes and their cold-regulated expression during the dormancy phase transition of Chinese cherry flower buds. *Scientia Hortic.* 275, 109666. doi: 10.1016/j.scienta.2020.109666

frontiers | Frontiers in Plant Science

TYPE Original Research
PUBLISHED 07 June 2023
DOI 10.3389/fpls.2023.1186921

OPEN ACCESS

EDITED BY
Baizhao Ren,
Shandong Agricultural University, China

REVIEWED BY
Haiwang Yue,
Hebei Academy of Agriculture and Forestry Sciences, China
Jialin Wang,
China Agricultural University, China

*CORRESPONDENCE
Wenchao Zhen
wenchao@hebau.edu.cn

†These authors have contributed equally to this work

RECEIVED 15 March 2023
ACCEPTED 28 March 2023
PUBLISHED 07 June 2023

CITATION
Liu P, Yin B, Gu L, Zhang S, Ren J, Wang Y, Duan W and Zhen W (2023) Heat stress affects tassel development and reduces the kernel number of summer maize. *Front. Plant Sci.* 14:1186921. doi: 10.3389/fpls.2023.1186921

Heat stress affects tassel development and reduces the kernel number of summer maize

Pan Liu[1,2†], Baozhong Yin[3†], Limin Gu[1,2†], Shaoyun Zhang[1,2], Jianhong Ren[1,2], Yandong Wang[1,2,4], Weiwei Duan[1,2,4] and Wenchao Zhen[1,2,4*]

[1]College of Agronomy, Hebei Agricultural University, Baoding, China, [2]Key Laboratory of North China Water saving Agriculture, Ministry of Agriculture and Rural Affairs, Baoding, China, [3]College of Plant Protection, Hebei Agricultural University, Baoding, China, [4]State Key Laboratory of North China Crop Improvement and Regulation, Baoding, China

Maize grain yield is drastically reduced by heat stress (HTS) during anthesis and early grain filling. However, the mechanism of HTS in reproductive organs and kernel numbers remains poorly understood. From 2018 to 2020, two maize varieties (ND372, heat tolerant; and XY335, heat sensitive) and two temperature regimens (HTS, heat stress; and CK, natural control) were evaluated, resulting in four treatments (372CK, 372HTS, 335CK, and 335HTS). HTS was applied from the nine-leaf stage (V9) to the anthesis stage. Various morphological traits and physiological activities of the tassels, anthers, and pollen from the two varieties were evaluated to determine their correlation with kernel count. The results showed that HTS reduced the number of florets, tassel volume, and tassel length, but increased the number of tassel branches. HTS accelerates tassel degradation and reduces pollen weight, quantity, and viability. Deformation and reduction in length and volume due to HTS were observed in both the Nongda 372 (ND372) and Xianyu 335 (XY335) varieties, with the average reductions being 22.9% and 35.2%, respectively. The morphology of the anthers changed more conspicuously in XY335 maize. The number of kernels per spike was reduced in the HTS group compared with the CK group, with the ND372 and XY335 varieties showing reductions of 47.3% and 59.3%, respectively. The main factors underlying the decrease in yield caused by HTS were reductions in pollen quantity and weight, tassel rachis, and branch length. HTS had a greater effect on the anther shape, pollen viability, and phenotype of XY335 than on those of ND372. HTS had a greater impact on anther morphology, pollen viability, and the phenotype of XY335 but had no influence on the appearance or dissemination of pollen from tassel.

KEYWORDS

heat stress, maize, tassel, kernel number per ear, anther

1 Introduction

Since 1880, the average global temperature has increased by around 0.8°C, with two-thirds of this increase occurring since 1975, at a rate of approximately 0.2°C per decade. By 2100, the global average surface temperature is expected to rise by 2–3°C (Apostolatos et al., 2010; Tian et al., 2018). The frequent occurrence of extreme heat in mid- and low-latitude regions has caused severe damage to crops, seriously affecting global food security (Tesfaye et al., 2016; Zandalinas et al., 2017; Libecap and Dinar, 2022). Pollination is an important aspect of the growth and development of higher plants and is significantly affected by unfavorable environments (Ali et al., 2018). Heat stress (HTS) is a typical environmental adversity that has a significant impact on both the physiological functions and phenotypic characteristics of plant reproductive organs and the pollination process (Hatfield and Prueger, 2015; Gabaldón-Leal et al., 2016). Brief HTS during the critical flowering stage can cause significant yield loss (Tian et al., 2018; Wang et al., 2022).

Maize (*Zea mays* L.), an annual plant belonging to the family Gramineae, is a highly valuable food and forage crop and is sensitive to heat (Yin et al., 2021; Wang et al., 2022). Maize yield is affected by HTS during all growth stages, with plants being most vulnerable during the flowering stage (Rattalino Edreira et al., 2011; Feng and Hao, 2020). The morphology and physiological functions of tassels, the reproductive organs for pollen production, are sensitive to HTS (Schoper et al., 1987). Pollen shedding is dramatically reduced at > 36°C owing to failed anther dehiscence, and pollen viability is greatly reduced at > 38°C because of the disturbed pollen structure and components in maize (Wang et al., 2019). Plants exposed to HTS from the nine-leaf stage (V9) to the tasseling stage (VT) show stunted tassel growth, disrupted anther structure, reduced pollen viability, and a shortened pollination period (Shao et al., 2021).

During the anthesis stage, HTS had a less pronounced effect on kernel weight than on kernel quantity (Suwa et al., 2010; Wang et al., 2019). Wang et al. (2019) found that the kernel weight of plants (including during the silking stage) exposed to high temperatures for 14 days [i.e., 40°C (day) and 30°C (night)] was comparable to that of plants exposed to slightly lower temperatures [i.e., 32°C (day) and 22°C (night. However, HTS significantly reduced the kernel per spike. Liu et al. (2022) reported that, under HTS, both before and after flowering, the number of kernels per spike decreased by 73%–98% on average. Similar results were obtained when the temperature was increased from the V9 to the VT. Studies have been conducted on the effects of HTS on kernel number and yield, as well as on the morphology and physiological functions of reproductive organs. However, the process by which HTS affects reproductive organ development and kernel formation is complex (Cairns et al., 2013; Lizaso et al., 2018) and is influenced not only by the timing of HTS coinciding with maize fertility, but also by factors such as the intensity and duration of HTS and varietal characteristics (Shao et al., 2021).

China is one of the world's leading maize-producing regions, accounting for over one-fifth of global maize production. The North China Plain (NCP) is China's primary maize-producing region and is responsible for approximately 40% of the country's total output (Li et al., 2022). The tasseling–anthesis stage of summer maize in NCP coincides with frequent HTS periods in the region (late July to mid-August), resulting in bad seed-setting and yield reduction (SHAO et al., 2021). Therefore, understanding the disaster mechanism of HTS is imperative to the development of a stress-resistant, high-yield cultivation technology system for maize in the NCP.

Using maize varieties with various heat sensitivities, a simulated HTS experiment was established in a greenhouse during tassel development over a 3-year period in the northern part of the NCP with the aims of (i) clarifying the effects of HTS on the phenotypic characteristics of tassels and anthers, pollen microstructure, and dispersal properties of summer maize, and (ii) determining if HTS reduces the number of kernels per ear, and its correlation with changes in tassel phenotype, pollen properties, and anther structure.

2 Materials and methods

2.1 Overview of test site

This study was performed at the Xinji Experimental Station of Hebei Agricultural University, north of the NCP (Mazhuang Village, Xinji City, Hebei Province, China, 115.22° E, 37.92° N, 43 m above sea level) throughout four summer maize-growing seasons (from mid to late June to early October, from 2018 to 2020). From 1981 to 2017, the average annual precipitation and temperature at this station were 470.3 mm and 12.9°C, respectively. The average annual precipitation and temperature during the summer seasons were 345.0 mm and 25.2°C, respectively. Daily precipitation as well as daily maximum, minimum, and average temperatures from 2018 to 2020 are shown in Figure 1A. At the experimental station, the topsoil was a neutral loam with a pH of 7.4. The organic matter content of the 0–20 cm soil layer was 18.5 g kg^{-1}, and the corresponding total nitrogen, alkali nitrogen, available phosphorus, and potassium contents were 1.0 g kg^{-1}, 91.6 mg kg^{-1}, 56.9 mg kg^{-1}, and 231.2 mg kg^{-1}, respectively. The 0–20 cm soil layer contained 18.5 g kg^{-1} organic matter, 1.0 g kg^{-1} total nitrogen, 91.6 mg kg^{-1} alkali nitrogen, 56.9 mg kg^{-1} available phosphorus, and 231.2 mg kg^{-1} potassium.

2.2 Experimental design and treatments

A two-factor split-zone design was adopted, and the main treatments were HTS and natural control (CK), with side treatments applied to maize varieties Xianyu 335 (XY335, a heat-sensitive variety) and Nongda 372 (ND372, a heat-tolerant variety). The four treatments (372CK, 372HTS, 335CK, and 335HTS) were repeated thrice. The CK group showed normal growth under natural conditions with an area of 66.6 m^2 per plot. A greenhouse heating system was used in the HTS treatment group, with an area of 18.0 m^2 (3.0 m width × 6.0 m length). The shed floor was 8.0 m wide, the heights of both sides were 2.75 m, the height of the middle was 3.75 m, and the length was 23.0 m. The top and surrounding areas of the shed were covered with a polyolefin (PO) plastic film (transmittance > 95%). There were 1.0-m-high ventilation

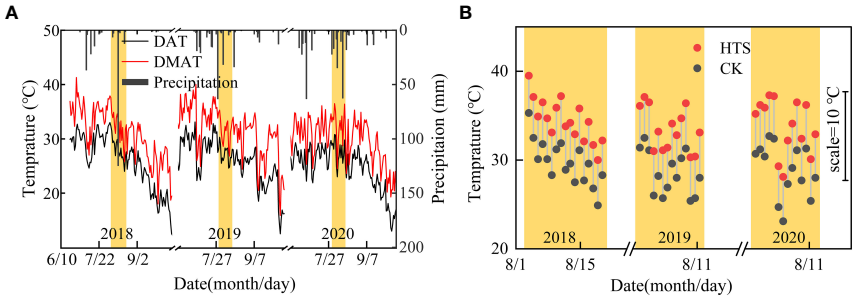

FIGURE 1
Daily temperature and precipitation during the experiment. **(A)** Daily average temprature (DAT) and daily maximum temprature (DMAT), and precipitation under natural conditions. **(B)** Average temperature between 8:00 and 16:00 in the greenhouse treated with HTS and the average temperature under natural conditions during the same time period.

belts on both sides of the shed. The airflow volume was varied by adjusting the height of the plastic film covered by the rotating shaft. To regulate the temperature inside the shed, exhaust systems were placed on both sides (Figures 2A, B).

The daily HTS treatment time was 8 h (8:00–16:00), and the HTS treatment began at V9 (recorded as DAT0) and continued until the end of the anthesis stage. The specific HTS process was as follows: all the PO plastic films were in place for HTS at 8:00, and the films were removed for cooling at 16:00. The greenhouse temperature was 5 ± 0.5°C higher than that in natural conditions during the HTS treatment period in the test (Figure 1B). The plastic film covering the shed was rolled up when the maize was in its natural growth stage outside the HTS phase. If rain occurred during the HTS period, the same volume of supplemental irrigation was applied after the cessation of the rain to maintain uniform soil moisture levels across all treatments. The seeds were sown on 21 June 2018, 16 June 2019, and 2020, with a row spacing of 60 cm and a planting density of 6,000 plants hm^{-2}. With the application of 112.5 kg N hm^{-2} at the bottom of seeding, P_2O_5 and K_2O at 150.0 kg hm^{-2} and 75.0 kg hm^{-2}, respectively, were applied as basal fertilizer. Furthermore, 112.5 kg N hm^{-2} as urea was applied together with the first irrigation in spring. Irrigation was maintained at 45 mm every year after sowing.

2.3 Phenotypic index of tassel

During the 2018–2020 growing season, 10 representative plants in each group were selected pre-V9 and labeled prior to HTS treatment and the extraction of tassels. On days 8 (DAT8), 12 (DAT12), 16 (DAT16), and 20 (DAT20) after HTS, the number of branches (TBN), main axis length (MAL), branch axis length (BAL), main axis and branch florets of the tassel (MFN and BFN, respectively), and tassel volume (TV_s) of the selected plants were measured. To avoid the impact of observation and growth determination, two groups of maize samples were selected alternately.

The total number of branches in a tassel is the sum of all branches with a branch length of less than 1.5 cm. Plants with dead limbs were excluded. The MAL (cm) of the tassel is the total distance between the lowest point of the main axis and the tip of the spike, and the BAL (cm) is the distance between the lowest point of the branch and the tip of the branch (Figure 3). MFN is the total number of florets along the main axis of the tassel, and BFN is the total number of florets along a single branch (count $plant^{-1}$). Three representative plants were selected for each treatment: the part above the base of the first branch of the tassel was cut off, and all branches and main axes were cut into 3- to 5-cm segments. The tassel volume (TV_s) (cm^3) per plant was measured using the displacement method.

2.4 Pollen dispersal quantity and pollen weight of tassel

During the 2018–2020 growing season, 10 plants were chosen as representatives for the daily monitoring of tassel extraction and floret opening. When the tassels and florets were about to open, the tassel was covered with a polyvinyl chloride (PVC) funnel [10 cm higher than the tassel, and the base was sealed with polytetrafluoroethylene (PTFE) tape] to cover the tassels and collect pollen daily at approximately 16:00 h. The pollen, anther microstructure, and pollen vitality were measured separately from the anthers and debris.

Before tassel extraction in the 2018–2020 growing season, 10 plants that underwent the same growth process and exhibited the same growth trends were selected for marking each time, and the progress of tassel extraction and floret opening was observed daily. When it was observed that the tassels and florets were about to open, a PVC funnel was used to cover the tassels (Wang et al., 2019); the top of the film was approximately 10 cm higher than the tassel top, and the base was sealed with PTFE tape (Figure 4). To avoid damaging the tassels and stems, two holes were made on each side of the top of the film, through which a rope was passed to fix the film. Pollen was collected daily from the funnel-shaped film at approximately 16:00 h, carefully separated from the anthers and debris, and then weighed.

2.5 Pollen, anther microstructure, and pollen vitality

Between 9:00 and 10:00 on days 3 and 4 after anthesis in 2018, five plants with uniform growth were selected from each treatment and their fresh anthers and pollen were collected. The length and volume of the anthers and pollen vitality were measured, and the ultrastructure of the pollen was observed (Begcy and Dresselhaus, 2017).

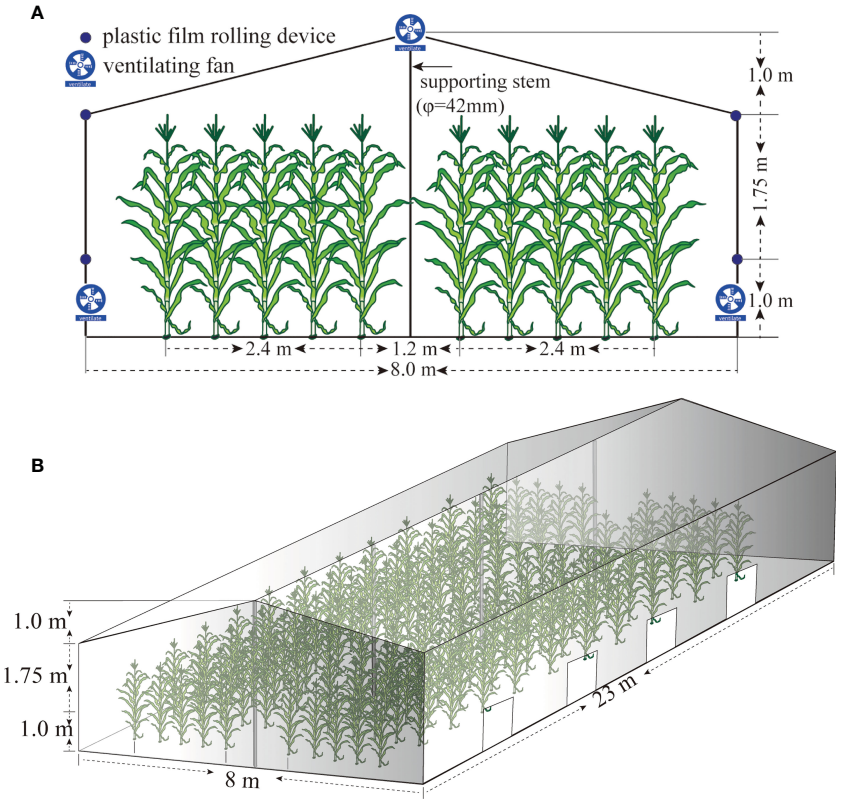

FIGURE 2
Simulated diagram of temperature increase in greenhouse maize. **(A)** Schematic diagram of the front elevation of the shed. **(B)** Schematic diagram of the 45° direction of the side elevation of the shed.

(1) Anther length (AL_s) and volume (AV_s). Anthers were of natural length (cm) from the base to the top. The anther volume was measured using the drainage method (cm^3).

(2) Anther microstructure. Anthers were placed overnight in Formalin-Aceto-Alcohol fixative soution (FAA) fixed solution for fixation, dehydrated with ethanol gradient, made xylene transparent, embedded in paraffin, and sliced to 8 μm thickness. The sealed film was made permanent and observed and photographed using an Olympus-DP71 optical microscope.

(3) Pollen vitality. The pollens were placed on a clean slide and stained with 0.5% triphenyl tetrazole chloride. After 10–15 min, the pollens were observed under a stereomicroscope to determine their color, and photographed. The pollens that

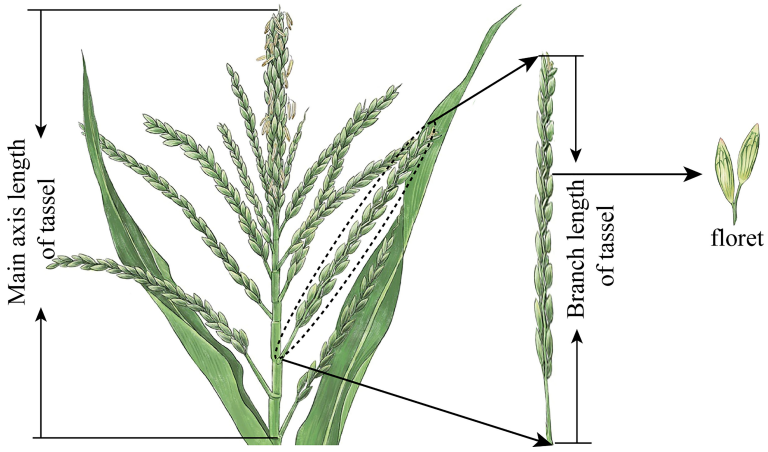

FIGURE 3
Measurement standard of main axis and branch length of maize tassels and schematic diagram of florets.

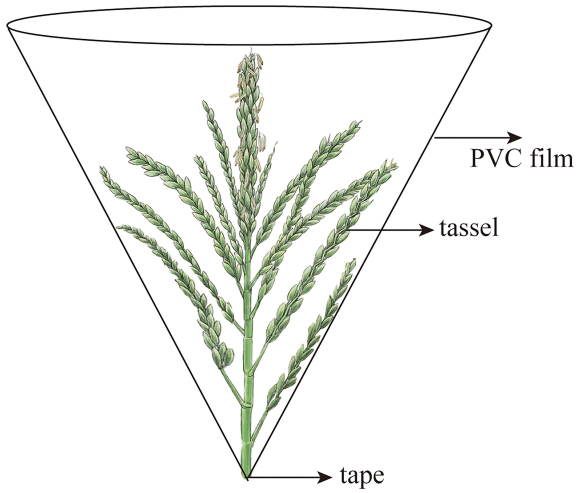

FIGURE 4
Maize pollen collection device.

were stained red were marked as active. The proportion of active pollens to the total number of pollens in each field was defined as the percentage pollen vitality (%) (Wang et al., 2021).

(4) Pollen microstructure. Pollens without anthers were collected, fixed with a 3% glutaraldehyde solution, rinsed with phosphoric acid buffer, dehydrated with an acetone gradient, placed on a sample table, vacuumed, sprayed with a gold coating, and observed using a KYKY-2800B scanning electron microscope (Wang et al., 2019).

2.6 Kernel number per ear

At the late stage of waxy ripening, sample sections with relatively consistent growth in each treatment were regularly collected from five plants to measure the kernel number of all ears.

2.7 Data processing and statistical analysis

Analysis of variance (ANOVA) was performed using SPSS 26.0 (IBM, NY, USA). Data are presented as means ± standard error (SE). One-way ANOVA was conducted, and a Student's *t*-test was used to compare treatment means at the 5% level. Pearson's correlation analysis was performed using SPSS software (version 26.0).

3 Results

3.1 Effect of HTS on effective branchs number and tassel volume

3.1.1 Branchs number of tassel

In addition to DAT8, HTS, variety, and year, the interaction between year and temperature significantly affected the number of branches in the tassel ($p < 0.05$). At DAT8–16, the number of effective spikelet branches of the two varieties in the CK group increased, whereas at DAT16–20, the number either remained unchanged or decreased (decaying branches were not counted). Under HTS, the tassel index showed a gradual increase at DAT8–12 and a gradual decrease at DAT12–20. Compared with the CK group, it was observed that tassel branching in the early stage was promoted in the two varieties under the HTS treatment at DAT8–12, whereas at DAT16, inhibition was observed. Compared with other varieties, the numbers of spikelets in the CK and HTS ND372 treatments were higher than that of the XY335 treatment (74% and 76% higher, respectively, 3-year average).

3.1.2 Tassel volume

Except for DAT12 and DAT16, there were significant differences between the years (Table 1). In addition, excluding DAT12, the effect of HTS on the TV_s was significant, whereas the influence of year (Y) × treatment (T) was negligible. With an increase in the number of HTS days, the volume of tassels increased rapidly at the DAT8–16 stage, whereas that at the DAT16–20 stage remained stable or slightly decreased. The TV_s of the ND372 variety peaked at DAT16, whereas that of the XY335 variety peaked at DAT12. HTS treatment increased the total volume of 337 varieties (DAT8–12 and XY335) but significantly decreased the total volume of 372 varieties (DAT16–20) and XY335 (DAT12–20). Compared with that of the XY335 variety, the TV_s of the ND372 variety was significantly greater under all conditions (21.2% higher on average over the 3 years) and 28.4% and 13.5% higher under natural and HTS conditions, respectively. In general, HTS increased the maximum TBNs by 9.8% and 30.0% relative to the CK treatment for the 372HTS and 335HTS varieties, respectively; however, HTS accelerated the decline of tassels. HTS also reduced the TV_s of the 372HTS and 335HTS varieties, by 32.0% and 15.1%, respectively, compared with their CK treatments.

3.2 Effect of HTS on tassel length

3.2.1 Main axis length of tassel

As shown in Table 2, short-term HTS treatment (DAT8) can accelerate tassel growth. The TVs of the XY335 and ND372 varieties

10.3389/fpls.2023.1186921

TABLE 1 Branch number and volume of tassels under treatments at different temperatures.

Year	Treatment	Days after treatment (d)							
		Branch number of tassel				Volume of tassel (cm^3 $plant^{-1}$)			
		8	12	16	20	8	12	16	20
2018	372CK	6.3 b	7.7 b	7.7 b	8.0 a	13.3 b	18.0 a	32.3 a	32.0 a
	372HTS	11.0 a	8.7 a	10 a	8.0 a	19.3 a	20.3 a	20.7 b	17.5 b
	335CK	2.7 c	3.7 d	3.7 c	4.0 a	13.0 b	20.7 a	20.7 b	16.7 b
	335HTS	5.3 b	6.0 c	4.3 c	4.3 a	13.3 b	19.3 a	16.3 b	15.8 b
2019	372CK	5.3 b	10.0 a	11.3 a	11.3 a	9.9 c	17.4 b	31.9 a	31.6 a
	372HTS	9.3 a	10.7 a	8.3 b	8.3 b	17.8 a	19 ab	24.0 b	22.5 b
	335CK	3.3 c	7.0 b	4.3 d	4.3 d	15.5 b	19.2 ab	19.0 c	15.4 c
	335HTS	5.7 b	7.0 b	5.7 c	5.7 c	18.5 a	20.4 a	16.7 d	16.0 c
2020	372CK	6.3 bc	11.7 a	9.7 a	9.7 a	9.2 d	15.8 b	33.5 a	31.1 a
	372HTS	10.0 a	13.0 a	10.3 a	10.3 a	14.6 a	22.4 a	21.8 b	19.4 b
	335CK	4.3 c	9.3 b	6.7 b	6.7 b	12.4 b	20.7 a	22.4 b	19.2 b
	335HTS	6.7 b	12.0 a	3.7 c	3.7 c	11.0 c	17.2 b	17.7 c	16.9 c
Year (Y)		NS	**	**	**	**	NS	NS	*
Treatment (T)		**	**	*	**	**	NS	**	**
Y × T		NS	*	**	**	NS	NS	NS	NS

**$P < 0.01$; *$P < 0.05$, NS, not statistically significant at $P < 0.05$. Different lowercase letters indicate significant differences between the treatments in the same year ($P < 0.05$).

were 5.8% and 5.5% higher than the CK treatment, respectively. The MAL of the tassels of the XY335 variety were higher than those of the ND372 variety: 13.6% and 13.9% higher under HTS and CK conditions, respectively (3-year average). From DAT8 to DAT12, tassel MAL was continuing to grow under CK conditions (26.8% on average over the 3 years) but modest under HTS conditions (9.4% mean over the 3 years). Except for 335HTS, the MAL continue to increase during DAT12-16. The MAL growth for the 372CK variety was the highest (11.4%), followed by the 372HTS (5.7%) and 335CK varieties (4.5%; 9.4% mean over the 3 years). By the end of the HTS treatment (DAT20), the MAL of the 372CK and 335CK variety were significantly higher than those of the respective HTS treatments (16.8% and 14.4% higher, respectively).

A comparison of the differences between the two cultivars further revealed that the MAL of the ND372 variety was 8.0% and 5.8% greater than that of the XY335 variety under CK and HTS conditions, respectively. Except for DAT16, there were significant or extremely significant differences between years and all treatments. However, the interaction between Y and T was significant only at DAT16.

3.2.2 Branch length of tassel

At the early stages of HTS treatment (DAT8), the BAL of the tassels of the 335CK and 372CK varieties showed no significant difference; however, the shorter HTS treatment period (8 d) accelerated the elongation of the tassel branches, and the tassel branches of the ND372 and XY335 varieties were 18.4% and 21.4% longer than those of plants subjected to the corresponding CK treatments (3-year average) (Table 2). With the extension of HTS time, the BAL growth rates of the 372CK and 372HTS varieties were significantly higher than that of the XY335 variety. By DAT16, the BAL of each treatments are basically stable. At this time, the BAL of the 372HTS and 335HTS groups decreased by 14.5% and 13.1% (3-year average), respectively, compared with their respective controls. By the end of the treatment, the BAL of the XY335 variety was lower than that of the ND372 variety, i.e., it was 20.5% and 19.1% lower under the CK and HTS treatments, respectively. By comparing the variation from different sources, it was observed that Y had a significant impact on BAL only at DAT12, while T and Y × T had a significant influence at all measuring times. Overall, HTS significantly reduced the MAL of the tassels by 14.4% (ND372) and 16.6% (XY335), respectively; and reduced the BAL of the tassels by 9.5% (ND372) and 9.8% (XY335), respectively.

3.3 Effect of HTS on the number of spikelets

3.3.1 Number of florets in main axis of tassel

With increasing HTS treatment time, the MFN in each treatment group first increased and then decreased, reaching a peak at DAT12. The MFN for each treatment followed the order 372CK > 372HTS > 335CK > 335HTS (Table 3). Under natural growth conditions, the MFN of the ND372 variety was significantly higher than that of the XY335 variety (3-year average of 33.6%). HTS significantly reduced the number of MFNs, and the numbers of

TABLE 2 Main axis and branch length of tassel under treatments at different temperatures.

Year	Treatment	Days after treatment (d)							
		Main axis length of tassel (cm)				Branch length of tassel (cm)			
		8	12	16	20	8	12	16	20
2018	372CK	17.1 b	21.4 a	26.1 a	30.6 a	35.5 b	66.1 a	70.5 a	76.0 a
	372HTS	17.6 b	20.4 a	25.1 a	25.1 c	45.5 a	56.3 b	62.7 a	62.7 b
	335CK	19.6 a	22.4 a	26.2 a	27.9 b	34.2 b	47.6 c	47.8 b	48.7 c
	335HTS	20.1 a	21.6 a	24.9 a	24.9 c	38.1 b	44.8 c	45.4 b	45.4 c
2019	372CK	16.8 c	24.2 a	29.2 a	30.9 a	37.0 bc	64.2 a	67.8 a	69.6 a
	372HTS	17.7 c	20.8 b	24.6 c	24.9 c	42.4 a	53.2 c	58.7 b	58.6 b
	335CK	19.3 b	23.7 a	27.0 b	28.4 b	34.2 c	57.1 b	57.9 b	58.8 b
	335HTS	21.1 a	21.4 b	25.2 c	25.5 c	38.3 b	44.9 d	49.3 c	49.0 c
2020	372CK	16.3 c	19.9 c	27.8 b	31.0 a	37.7 c	64.3 a	69.2 a	69.7 a
	372HTS	17.8 b	17.7 d	25.1 c	29.2 b	42.4 b	53.6 c	56.0 c	58.2 c
	335CK	18.3 b	24.3 a	28.8 a	29.4 b	32.5 d	59.0 b	62.3 b	62.8 b
	335HTS	19.2 a	22.0 b	24.3 d	24.5 c	45.7 a	49.9 d	50.3 d	50.4 d
Year (Y)		*	**	NS	**	NS	**	NS	NS
Treatment (T)		**	**	**	**	**	**	**	**
Y × T		NS	NS	*	NS	**	**	**	**

**$P < 0.01$; *$P < 0.05$, NS, not statistically significant at $P < 0.05$. Different lowercase letters indicate significant differences between the treatments in the same year ($P < 0.05$).

MFNs of the ND372 and XY335 varieties decreased by 13.4% and 32.5%, respectively, compared with those of the CK group. The number of small flowers on the main axis of the XY335 variety was significantly lower than that of the ND372 variety under both natural and high-temperature treatments. Further comparison of the differences between different sources showed that Y and T were the main sources of the difference in the number of small flowers on the main axis, whereas Y × T had a significant effect only at DAT8.

3.3.2 Number of florets in the branch of tassel

As shown in Table 3, the short-term high-temperature treatment (8 d) accelerated the differentiation rate of spikelet branches and florets, and the ND372 and XY335 varieties were 18.4% and 15.9% higher, respectively, than under the corresponding CK treatments (3-year average). When the high-temperature treatment time was increased, the BFN growth rates of the 372CK and 372HTS varieties were significantly higher than those of the XY335 variety. By DAT16, the BFN in each treatment group was stable. The BFN scores of the 372HTS and 335HTS varieties were 18.1% and 15.0% lower, respectively, than those of the corresponding controls (3-year averages). By the end of the treatment, the BFN of the tassels of the XY335 variety was less than that of the ND372 variety, specifically the BFN in the 335CK group was 11.5% less than in the 372CK group, and the BFN in the 335HTS group was 9.1% less than in the 372HTS group (3-year average). A comparison of the variation from different sources showed that Y, T, and Y × T had a significant effect on the BFN at all measurement times. In general, HTS significantly reduced the MFNs and BFNs of tassels in both the ND372 (by 13.5% and 18.2%, respectively) and XY335 groups (by 26.2% and 9.6%, respectively).

3.4 Effect of HTS on pollen fresh weight, number, and activity

3.4.1 Daily pollen weight

With an increase in the number of days of pollen dispersal, the fresh weight of pollen (PWs) produced showed a single peak trend, in which it first increased and then decreased, and the PW collected reached its peak on day 4. Under the CK conditions, there was a significant difference in PWs between the two varieties. Among them, the daily PWs of the ND372 and XY335 varieties were 0.04–1.18 g plant^{-1} and 0.04–0.79 g plant^{-1}, respectively, and the total PWs were 3.81 g/plant^{-1} and 2.68 g/plant^{-1}, respectively. The total and maximum daily PWs of the ND372 variety were 41.9% and 49.0% higher, respectively, than those of the XY335 variety. HTS significantly reduced the maximum PWs and total PWs during athesis period (by 37.0% and 41.0%, respectively). There was no significant difference between the two varieties in the reduction of PW and total PW under HTS conditions, but the daily PW and total PW of the ND372 variety under HTS conditions were significantly

10.3389/fpls.2023.1186921

TABLE 3 Main axis and branch florets of tassels under treatments at different temperatures.

Year	Treatment	Days after treatment (d)							
		Number of florets in main axis of tassel				Number of florets in branch of tassel (cm^3 $plant^{-1}$)			
		8	12	16	20	8	12	16	20
2018	372CK	244.7 a	295.6 a	246.8 a	242.7 a	149.1 b	184.6 b	239.1 a	227.4 a
	372HTS	208.2 b	227.5 b	206.1 b	205.3 b	156.4 a	168.7 c	185.3 c	190.8 c
	335CK	187.5 c	199.0 c	165.4 c	173.6 c	134.1 c	196.4 a	199.9 b	200.9 b
	335HTS	159.4 d	173.2 d	117.1 d	114.6 d	145.7 b	166.6 c	168.8 d	169.3 d
2019	372CK	233.6 a	287.2 a	255.0 a	254.7 a	160.2 b	240.9 a	228.6 a	226.4 a
	372HTS	205.1 b	240.5 b	217.1 b	219.6 b	192.9 a	200.1 d	203.3 c	204.0 b
	335CK	169.3 c	214.9 c	166.0 c	161.2 c	136.5 d	218.5 b	221.7 b	222.2 a
	335HTS	154.4 d	137.5 d	117.4 d	128.0 d	163.0 b	174.2 d	185.1 d	187.9 b
2020	372CK	228.9 a	284.9 a	233.4 a	214.3 a	148.1 c	228.8 a	230.0 a	234.9 a
	372HTS	183.2 c	237.3 b	212.5 b	206.4 ab	192.2 a	176.0 b	182.4 b	183.8 b
	335CK	206.3 b	240.0 b	206.43 b	204.3 b	130.9 d	181.3 b	186.9 b	185.6 b
	335HTS	158.2 d	172.8 c	126.63 c	117.5 c	156.4 b	157.4 c	162.8 c	168.8 c
Year (Y)		**	**	**	NS		**	**	**
Treatment (T)		**	**	**	**		**	**	**
Y × T		**	NS	NS	NS		**	**	**

**$P < 0.01$; NS = not statistically significant at $P < 0.05$. Different lowercase letters indicate significant differences between the treatments in the same year ($P < 0.05$).

higher than those of the XY335 variety (by 45.1% and 38.1%, respectively) (Figures 5A–C).

3.4.2 Daily pollen number

The change in the number of maize pollens (PNs) was similar to that of the fresh pollen weight. The daily PNs also showed a single peak trend, first increasing and then decreasing, and reached its peak on day 4. HTS and variety significantly affected the PNs ($p < 0.01$ or $p < 0.05$). The daily average PNs and maximum daily PNs of the two varieties were significantly reduced, by 43.4% and 32.8%, respectively, under the HTS treatment. Under the CK treatment, the daily average PNs and maximum daily PNs of the ND372 variety were 25.9% and 19.95% higher, respectively, than those of the XY335 variety. Under the HTS treatment, the daily average PNs of the two varieties decreased by 24.7%, but the daily average PNs and maximum daily PNs of the ND372 variety were 25.86% and 28.62% higher than those of the XY335 variety, respectively (Figures 5D–F). In general, HTS reduced PWs and PNs of maize, but there was no significant difference between the two varieties (the PWs of the ND372 and XY335 varieties decreased by 41.2% and 40.2%, respectively, and the PNs decreased by 32.3% and 35.9%, respectively, based on the 3-year average).

3.4.3 Daily pollen vitality

In the present study, the depth of pollen staining represented the level of pollen vitality (PVs). Under CK conditions, the pollen is deeply stained and is of regular size and shape. During observation, the viable pollens of the ND372 variety accounted for 94.3%, and the XY335 variety accounted for 90.0%. The vitality of the XY335 variety was slightly lower than that of the ND372 variety, but the difference was not significant (Figures 6A, B). After the HTS treatment, the degree of pollen staining differed significantly between the two varieties. Viable pollens of the ND372 variety accounted for 81.3% of the pollens, whereas that of the XY335 variety accounted for only 71.0% of the pollens. The PVs of the two varieties decreased by 13% and 19%, respectively, compared with those of the CK groups (Figures 6C, D). Further comparison of the two varieties subjected to the same HTS treatment revealed that the PVs of the 335HTS variety was 9.7% lower than that of the 372HTS variety. In general, HTS decreased PVs (both varieties decreased by an average of 16%), and the decrease was greater in the heat-sensitive varieties.

3.5 Effect of HTS on tassel pollen and anther microstructure

3.5.1 Anther microstructure and volume

At ambient temperature, the anthers of both varieties bulged without any evident deformation. Compared with the other varieties, the ALs and AVs of the ND372 variety under natural conditions were 6.3% and 14.7% higher, respectively, than those of the XY335 variety (Figures 7A, B). After HTS treatment, the anthers were deformed by bending, shrinking, and drying. The ALs of the ND372 and XY335 varieties decreased by 10.5% and 7.0% (Figures 7C, D), and their AVs decreased by 27.4% and 37.9%,

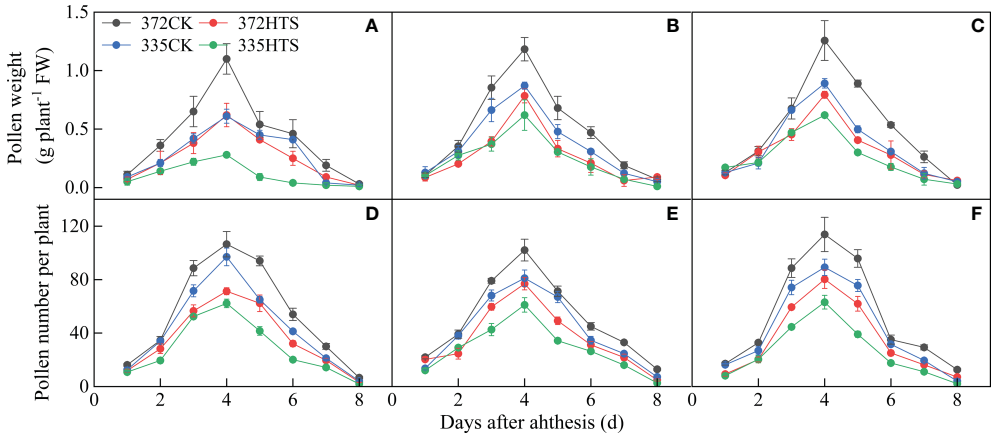

FIGURE 5
The quantity and weight of maize pollen per plant under different temperatures **(A–C)** depicts the fresh weight of pollen per plant in 2018, 2019, and 2020 respectively. **(D–F)** Number of pollen grains per plant in 2018, 2019, and 2020 respectively.

respectively, compared with those of the CK group. Further comparison of the phenotypic differences between the XY335 and ND372 varieties under the same HTS revealed that the ALs and AVs of the 335HTS treatment group were 18.3% and 32.5% lower, respectively, than those of the 372HTS group (Figure 7I). The cross-section of the anthers of the tassel of the two varieties (Figures 7E–H), resulted in high temperatures, causing the epidermal and middle layer cells of the anther wall to deform and arrange loosely, the tapetal cells to degenerate, the vascular bundle cells to arrange irregularly and become thinner, and the pollen grains in the flower chamber to scatter, and pollen to shrink, thereby clearly demonstrating the performance of the XY335 variety. Overall, HTS caused anther deformities and decreased ALs and AVs. The average of the two varieties decreased by 22.9% and 35.2% (3-year average), respectively, and the overall shape of the anthers of the heat-sensitive maize varieties changed.

3.5.2 Pollen microstructure

Under natural conditions, the pollen of the two varieties was of regular morphology and the surface was smooth and almost free of wrinkles (Figures 8A, B). After the HTS treatment, the number of reticulated grains on the pollen surface of the XY335 variety increased and thickened, forming serious folds. However, under the same HTS conditions, the pollen surface reticulation of the ND372 variety either did not change significantly or was slightly thickened, resulting in the formation of a slight fold, and the degree of pollen aperture was lower than that of the XY335 variety (Figures 8C, D). HTS changed the pollen diameter. Under natural conditions, the pollen diameter of the ND372 variety was larger than that of the XY335 variety; however, the difference between the varieties was not significant. After high-temperature treatment, there was a significant difference in pollen size between the two varieties, i.e., the pollen diameters of the ND372 and XY335 varieties decreased by 11.5% and 18.3%, respectively, compared with that of the control.

3.6 Effect of HTS on kernel number per ear and its correlation with tassels

Figure 9 shows that HTS can reduce the kernel number per ear, and the range of decrease of different varieties is large. Under natural conditions, there was no significant difference in kernel number per ear between the two varieties in 2018 and 2019, and the kernel number per ear of the XY335 variety was significantly lower than that of the ND372 variety in 2020 (a decrease of 14.7%). HTS significantly reduced the kernel number per ear, and in the 372HTS and 335HTS varieties were decreased by 47.3% and 59.3%, respectively, compared with the corresponding CK. Further comparison of the grain number per ear of the two varieties under HTS revealed that the average grain number per ear of the 372HTS variety was 39.3% higher than that of the 335HTS variety (3-year average). The analyses of Y, T, and Y × T as a source of variation of treatment effect showed that all three had a highly significant effect on the kernel number per ear ($p < 0.01$; Figure 9).

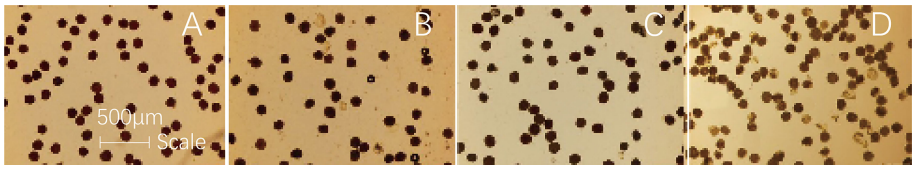

FIGURE 6
Maize pollen vitality under different temperatures. **(A, B)** are 372CK and 335CK, respectively; **(C, D)** are 372HTS and 335HTS, respectively.

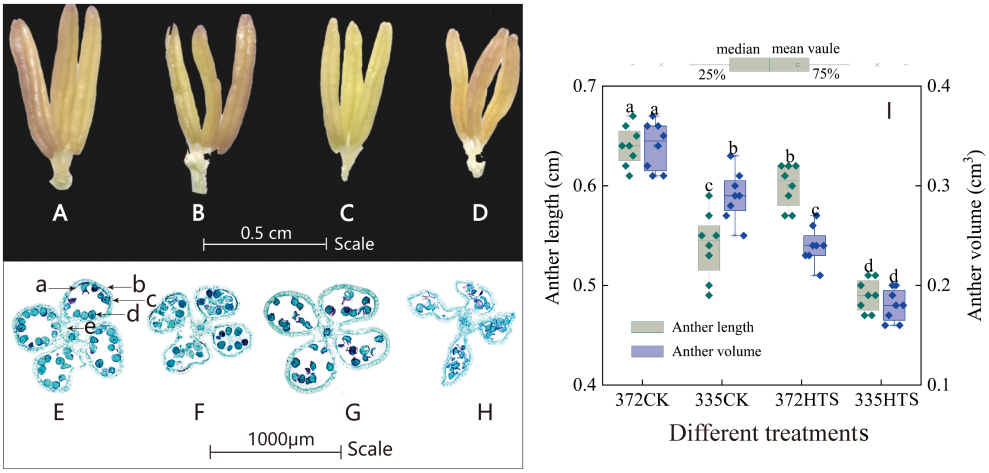

FIGURE 7
The shape, structure, length, and volume of maize anthers under different temperatures. **(A, E)** are 372CK, **(B, F)** are 335CK, **(C, G)** 372HTS, and **(D, H)** are 335HTS. **(I)** shows the difference in anther length and volume under different temperatures. Different lowercase letters in the data indicate significant differences between treatments of the same index (P<0.05).

The kernel number per ear is related to varying degrees of tassel shape, the number and weight of pollen, pollen vitality, and other phenotypic traits. Figure 10 shows that KN was significantly positively correlated with MAL, BAL, MFN, BFN, TVs, ALs, AVs, PWs, and vigor (PAs) ($p < 0.05$), and the correlation coefficient (r) was 0.72–0.94. Among them, the r of KN and PNs was the highest (0.94), followed by those of MAL, BFN, and PWs ($0.80 < r < 0.90$). The r-values for KN and ALs were the lowest (0.65). KN was weakly negatively correlated with TBN and PAs ($p > 0.05$). In general, the pollens number and weight, and MAL and BAL of the tassel had a significant effects on the KN per ear ($r = 0.86$), especially the pollens number ($r = 0.94$).

4 Discussion

4.1 Effect of HTS on the morphology and physiological characteristics of tassels

HTS thresholds exist at different stages of crop growth. If the threshold is exceeded, a series of morphological and physiological processes are affected, and eventually the yield is reduced (Cairns et al., 2012; Prasad et al., 2017). The tassel is one of the most important organs in maize plants. Tassel differentiation and development have a profound impact on yield, as they directly

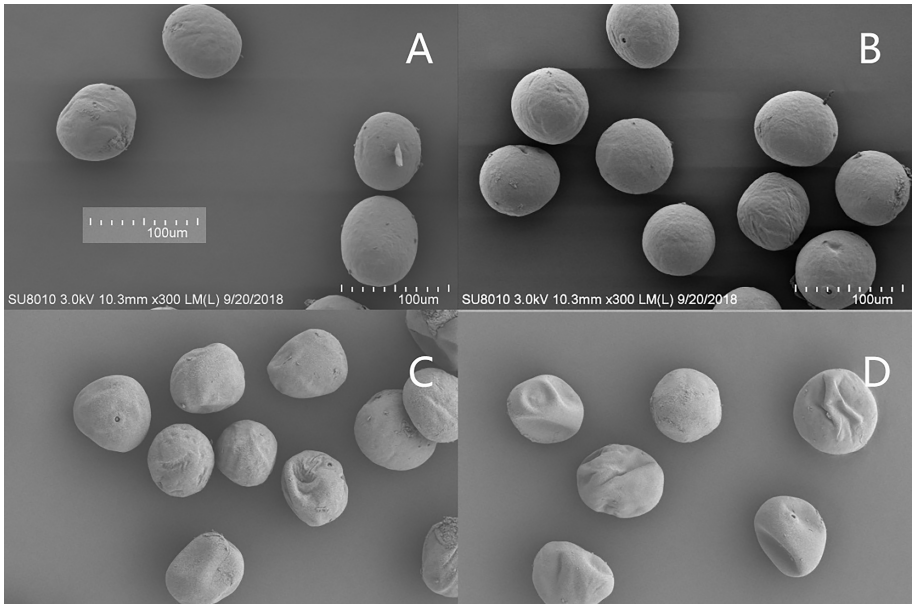

FIGURE 8
Surface ultrastructure of pollen at different temperatures (× 300). **(A, B)** are 372CK and 335CK, respectively; **(C, D)** are 372HTS and 335HTS, respectively.

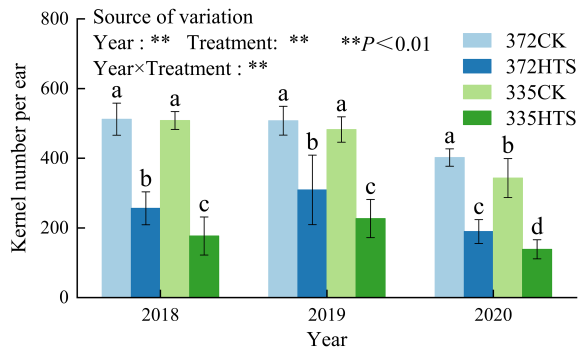

FIGURE 9
Kernel number per ear under different temperature. Different lowercase letters in the data indicate significant differences between different treatments in the same year (P<0.05).

determine the quantity and quality of pollen. Tassels begin to develop after the joining stage. At this time, the impact of HTS on tassels is serious, and damage, once it occurs, cannot be reversed (Hatfield and Prueger, 2015). Because the tassel is sensitive to high temperatures, some studies have suggested that the outer membranes of the anther are very thin, and therefore that the high temperatures of the external environment can be easily transmitted to the anther, leading to anther deformity and damage to physiological function (Sinsawat et al., 2004; Hussain et al., 2006). In the NCP, the temperature during the reproductive development in maize is often higher than the optimal temperature for the maximum differentiation of spikes (25–32°C). This further increases the risk to tassels under temperature stress (Shao et al., 2021).

This study found that HTS increased the maximum TBN to some extent (by 9.8% and 30.0% compared with the CK treatment for the 372HTS and 335HTS varieties, respectively) and decreased the volume of tassels, number of main axes and branch florets, and lengths of the main axis and branch. However, HTS also accelerated tassel decay. Therefore, we believe that a high temperature before the heading stage accelerated development and increased the number of branches, but decreased the total volume of the tassels. This is consistent with previous research results (Shao et al., 2021). In addition, the rapid development of tassels affected the differentiation of florets, resulting in a significant reduction in maize florets under the HTS treatment.

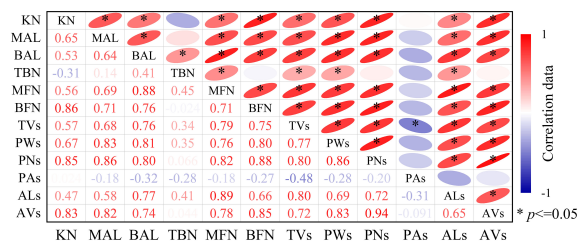

FIGURE 10
Correlation between the growth and development indexes of maize tassels and the kernel number per ear under different temperature. KN, kernel number per ear. In male spikes, MAL and BAL are the main axis and branch length, TBN is the number of branches, MFN and BFN are the number of main axis and branch florets, TVs is the volume, PWs and PNs are the total weight and number of pollen grains per plant, respectively, PAs is the average vitality of the pollen, and ALs and AVs are the length and volume of the anther, respectively. r is the Pearson correlation coefficient. *p < 0.05.

4.2 Effects of HTS on anther, pollen morphology, and pollen vitality

Most studies have shown that heat stress reduces the global yields of major crops to a greater extent than other environmental stresses (Deryng et al., 2014; Zhao et al., 2017). This effect is a result of frequent heat stress and coincides with sexual reproduction (Hedhly et al., 2009). Maize is a monoecious species, the plants of which bear a tassel at the top and a pistillate flower in the middle (Begcy and Dresselhaus, 2017). The synchronous flowering of the male and female reproductive organs and sufficient active pollen are critical determinants of successful pollination (Herrero, 2003). Research has shown that, in maize, male reproductive organs are more sensitive than female reproductive organs to HTS (Rattalino Edreira et al., 2011; Lizaso et al., 2018) (Rattalino Edreira et al., 2011). If pollen is exposed to a temperature above 32.5°C for a long period, its germination rate will significantly decline with the extension of exposure time, and may even approach zero (Hussain et al., 2006; Akbar et al., 2017). Other studies have also revealed that pollen number, pollen viability, kernel number, and grain yield are significantly reduced by increases in temperature from 36/26°C to 40/30°C approximately 2 weeks before and after silking (Begcy et al., 2019; Wang et al., 2019). However, current research results on the relationship between pollen morphology and vitality are inconsistent. Some studies have suggested that HTS causes pollen surface deformities that further affect pollen vitality. However, other studies have indicated that there is no relationship between pollen surface deformities and pollen vitality (Tsou et al., 2015).

This study showed that HTS reduced PWs and PNs in maize, but there was no significant difference between the two varieties (the PWs of the ND372 and XY335 varieties decreased by 41.2% and 40.2%, respectively, and PNs decreased by 32.3% and 35.9%, respectively, 3-year average). HTS also reduced pollen vitality (the two varieties decreased by an average of 16%), and the decrease in the heat-sensitive varieties was greater. These results support the findings of previous studies (Hussain et al., 2006; Begcy et al., 2019; Wang et al., 2019). HTS also leads to surface deformation and a reduction in pollen diameter. High temperatures caused further deformities, in addition to decreases in the length and volume. The average of the two varieties decreased by 22.9% and 35.2%, respectively (3-year average), and the overall shape of the anthers of the high temperature-sensitive varieties increased. Notably, under HTS, the difference in pollen quantity between the maize varieties with different heat tolerances was not significant. The main differences were in anther and pollen quality, especially in terms of pollen phenotypic structure and vitality. This is consistent with results reported for other crops (Djanaguiraman et al., 2017). In addition, this study confirmed the findings of a previous study

showing that the tassels of heat-sensitive varieties are more sensitive to high temperature (Wang et al., 2021).

4.3 Effect of HTS on kernel number per ear

The kernel number and weight are the determining factors of yield during the critical, approximately 30-day, period of silk formation (Cerrudo et al., 2020). However, the number of grains is not only determined after silking but also has a significant impact on the process of spike differentiation and pollination before silking. Therefore, some studies have indicated that temperatures during late vegetative growth and flowering greatly determine seed set (Wang et al., 2019). Many studies have shown that HTS at the flowering stage can significantly affect the number of kernels per ear, leading to a significant decline in the rate of seed setting (Alam et al., 2017; Prasad et al., 2017; Lizaso et al., 2018; Dong et al., 2021) and further affecting yield. This occurs after the V9 stage, when most of the male panicles are formed while the grains are still developing. HTS causes serious stress to both male and female reproductive organs, posing the hidden danger of a subsequent decline in kernel number per ear (Loussaert et al., 2017). Wang et al. (2019) reported that the kernel number per ear decreased by 77.6% in the group exposed to HTS compared with the conventional treatment group (temperatures were 40°C during the day and 30°C at night, and 32°C during the day and 22°C at night, respectively), 7 days before and after flowering. After HTS of the two heat-sensitive varieties, the bald tip length of the heat-sensitive variety (XY335) was significantly greater than that of the heat-resistant variety (ZD958), and the kernel number and yield per ear were significantly decreased (Shao et al., 2021).

This study showed that HTS significantly reduced the kernel number per ear, and in the ND372 and XY335 varieties it was decreased by 47.3% and 59.3%, respectively, compared with the CK of their respective varieties. Compared with the grain number per ear of the two varieties under HTS, the average grain number per ear of the 372HTS variety was 39.3% larger than that of the 335HTS variety (3-year average). The number and weight of pollen grains and the MAL and BAL of the tassel had significant effects on KN, particularly the number of pollen grains (r = 0.94). The effects of HTS on the shape of the tassel and the amount of pollen dispersed did not differ among the different varieties; however, HTS had significant effects on anther morphology, pollen vitality, and the phenotype of heat-sensitive varieties. In modern maize breeding, tassel reduction is a mainstream trend requiring the use of light energy and leading to reduced nutrient consumption in crop fields (Lu et al., 2015; Xu et al., 2017). However, a reduction of pollens number in the tassel leads to plants being incapable of coping with frequent HTS events in the future (Westgate et al., 2003).

5 Conclusion

HTS reduced the PNs, PWs, MAl and BAL of the tassel, which was the main reason for the reduced kernel number per ear. The effects of HTS on the shape of the tassel and the amount of loose pollen in maize did not differ among the different heat-sensitive maize varieties; however, the effects of high temperature on anther morphology, pollen vitality, and the phenotype of heat-sensitive maize varieties were significant.

Data availability statement

The original contributions presented in the study are included in the article/supplementary material. Further inquiries can be directed to the corresponding author.

Author contributions

WZ and LG conceived the project and set the scientific objectives. BY, SZ, and PL contributed to the preparation of field experiments and data acquisition. PL, BY, WD, JR, YW, and LG wrote the manuscript. All authors contributed to the article and approved the submitted version.

Funding

This research was funded by the National Key Research and Development Project (Grant No. 2017YFD0300900) and Key R&D projects in Hebei Province (Grant Nos. 20326407D and 21327001D).

Conflict of interest

The authors declare that the research was conducted in the absence of any commercial or financial relationships that could be construed as a potential conflict of interest.

Publisher's note

References

Akbar, M., Farooq, J., and Ashraf, Y. (2017). Genetic behavior for kernel yield and its physio-agronomic attributes in maize at normal and high temperature regimes. *Maydica* 62, 1–10.

Alam, M. A., Seetharam, K., Zaidi, P. H., Dinesh, A., Vinayan, M. T., and Nath, U. K. (2017). Dissecting heat stress tolerance in tropical maize (Zea mays l.). field. *Crop Res.* 204, 110–119. doi: 10.1016/j.fcr.2017.01.006

Ali, F., Waters, D. L. E., Ovenden, B., Bundock, P., Raymond, C. A., and Rose, T. J. (2018). Australian Rice varieties vary in grain yield response to heat stress during reproductive and grain filling stages. *J. Agro. Crop Sci.* 205, 179–187. doi: 10.1111/jac.12312

Apostolatos, H., Apostolatos, A., Vickers, T., Watson, J. E., Song, S., Vale, F., et al. (2010). Vitamin a metabolite, all-trans-retinoic acid, mediates alternative splicing of protein kinase c δVIII (PKCδVIII) isoform *via* splicing factor SC35. *J. Biol. Chem.* 285, 25987–25995. doi: 10.1074/jbc.m110.100735

Begcy, K., and Dresselhaus, T. (2017). Tracking maize pollen development by the leaf collar method. *Plant Reprod.* 30, 171–178. doi: 10.1007/s00497-017-0311-4

Begcy, K., Nosenko, T., Zhou, L.-Z., Fragner, L., Weckwerth, W., and Dresselhaus, T. (2019). Male Sterility in maize after transient heat stress during the tetrad stage of pollen development. *Plant Physiol.* 181, 683–700. doi: 10.1104/pp.19.00707

Cairns, J. E., Crossa, J., Zaidi, P. H., Grudloyma, P., Sanchez, C., Araus, J. L., et al. (2013). Identification of drought, heat, and combined drought and heat tolerant donors in maize. *Crop Sci.* 53, 1335–1346. doi: 10.2135/cropsci2012.09.0545

Cairns, J. E., Sonder, K., Zaidi, P. H., Verhulst, N., Mahuku, G., Babu, R., et al. (2012). Maize production in a changing climate. *Adv. Agron.* 14, 1–58. doi: 10.1016/b978-0-12-394275-3.00006-7

Cerrudo, D., Hernández, M., Tollenaar, M., Vega, C. R. C., and Echarte, L. (2020). Kernel number response to plant density in tropical, temperate, and tropical × temperate maize hybrids. *Crop Sci.* 60, 381–390. doi: 10.1002/csc2.20077

Deryng, D., Conway, D., Ramankutty, N., Price, J., and Warren, R. (2014). Global crop yield response to extreme heat stress under multiple climate change futures. *Environ. Res. Lett.* 9, 34011. doi: 10.1088/1748-9326/9/3/034011

Djanaguiraman, M., Perumal, R., Jagadish, S. V. K., Ciampitti, I. A., Welti, R., and Prasad, P. V. V. (2017). Sensitivity of sorghum pollen and pistil to high-temperature stress. *Plant Cell Environ.* 41, 1065–1082. doi: 10.1111/pce.13089

Dong, X., Guan, L., Zhang, P., Liu, X., Li, S., Fu, Z., et al. (2021). Responses of maize with different growth periods to heat stress around flowering and early grain filling. *Agric. For. Meteorol.* 303, 108378. doi: 10.1016/j.agrformet.2021.108378

Feng, S., and Hao, Z. (2020). Quantifying likelihoods of extreme occurrences causing maize yield reduction at the global scale. *Sci. Total. Environ.* 704, 135250. doi: 10.1016/j.scitotenv.2019.135250

Gabaldón-Leal, C., Webber, H., Otegui, M. E., Slafer, G. A., Ordóñez, R. A., Gaiser, T., et al. (2016). Modelling the impact of heat stress on maize yield formation. *Field Crop Res.* 198, 226–237. doi: 10.1016/j.fcr.2016.08.013

Hatfield, J. L., and Prueger, J. H. (2015). Temperature extremes: effect on plant growth and development. *Weather. Clim. Extrem.* 10, 4–10. doi: 10.1016/j.wace.2015.08.001

Hedhly, A., Hormaza, J. I., and Herrero, M. (2009). Global warming and sexual plant reproduction. *Trends. Plant Sci.* 14, 30–36. doi: 10.1016/j.tplants.2008.11.001

Herrero, M. (2003). Male And female synchrony and the regulation of mating in flowering plants. *Phil. Trans. R. Soc Lond. B* 358, 1019–1024. doi: 10.1098/rstb.2003.1285

Hussain, T., Khan, I., and Ali, Z. (2006). Breeding potential for high temperature tolerance in corn (*Zea mays*. L). *Pak. J. Bot*., 38(4): 1185–1195.

Li, T., Zhang, X., Liu, Q., Yan, P., Liu, J., Chen, Y., et al. (2022). Yield and yield stability of single cropping maize under different sowing dates and the corresponding changing trends of climatic variables. *Field Crop Res.* 285, 108589. doi: 10.1016/j.fcr.2022.108589

Libecap, G., and Dinar, A. (2022). *American Agriculture, water resources, and climate change* (Cambridge, MA: National Bureau of Economic Research). doi: 10.3386/w30290

Liu, M., Dong, X., Zhang, Y., Gu, M., Yu, Y., Xie, H., et al. (2022). Heat stress on maize with contrasting genetic background: differences in flowering and yield formation. *Agric. For. Meteorol.* 319, 108934. doi: 10.1016/j.agrformet.2022.108934

Lizaso, J. I., Ruiz-Ramos, M., Rodríguez, L., Gabaldon-Leal, C., Oliveira, J. A., Lorite, I. J., et al. (2018). Impact of high temperatures in maize: phenology and yield components. *Field Crop Res.* 216, 129–140. doi: 10.1016/j.fcr.2017.11.013

Loussaert, D., DeBruin, J., Pablo San Martin, J., Schussler, J., Pape, R., Clapp, J., et al. (2017). Genetic Male sterility (Ms44) increases maize grain yield. *Crop Sci.* 57, 2718–2728. doi: 10.2135/cropsci2016.08.0654

Lu, H., Cao, Z., Xiao, Y., Fang, Z., Zhu, Y., and Xian, K. (2015). Fine-grained maize tassel trait characterization with multi-view representations. *Comput. Electron. Agric.* 118, 143–158. doi: 10.1016/j.compag.2015.08.027

Prasad, P. V. V., Bheemanahalli, R., and Jagadish, S. V. K. (2017). Field crops and the fear of heat stress–opportunities, challenges and future directions. *Field Crop Res.* 200, 114–121. doi: 10.1016/j.fcr.2016.09.024

Rattalino Edreira, J. I., Budakli Carpici, E., Sammarro, D., and Otegui, M. E. (2011). Heat stress effects around flowering on kernel set of temperate and tropical maize hybrids. *Field Crop Res.* 123, 62–73. doi: 10.1016/j.fcr.2011.04.015

Schoper, J. B., Lambert, R. J., and Vasilas, B. L. (1987). Pollen viability, pollen shedding, and combining ability for tassel heat tolerance in maize. *Crop Sci.* 27, 27–31. doi: 10.2135/cropsci1987.0011183x002700010007x

Shao, R., Yu, K., Li, H., Jia, S., Yang, Q., Zhao, X., et al. (2021). The effect of elevating temperature on the growth and development of reproductive organs and yield of summer maize. *J. Integr. Agric.* 20, 1783–1795. doi: 10.1016/s2095-3119(20)63304-4

Sinsawat, V., Leipner, J., Stamp, P., and Fracheboud, Y. (2004). Effect of heat stress on the photosynthetic apparatus in maize (Zea mays l.) grown at control or high temperature. *Environ. Exp. Bot.* 52, 123–129. doi: 10.1016/j.envexpbot.2004.01.010

Suwa, R., Hakata, H., Hara, H., El-Shemy, H. A., Adu-Gyamfi, J. J., Nguyen, N. T., et al. (2010). High temperature effects on photosynthate partitioning and sugar metabolism during ear expansion in maize (Zea mays l.) genotypes. *Plant Physiol. Biochem.* 48, 124–130. doi: 10.1016/j.plaphy.2009.12.010

Tesfaye, K., Zaidi, P. H., Gbegbelegbe, S., Boeber, C., Rahut, D. B., Getaneh, F., et al. (2016). Climate change impacts and potential benefits of heat-tolerant maize in south Asia. *Theor. Appl. Climatol.* 130, 959–970. doi: 10.1007/s00704-016-1931-6

Tian, B., Zhu, J., Nie, Y., Xu, C., Meng, Q., and Wang, P. (2018). Mitigating heat and chilling stress by adjusting the sowing date of maize in the north China plain. *J. Agro. Crop Sci.* 205, 77–87. doi: 10.1111/jac.12299

Tsou, C.-H., Cheng, P.-C., Tseng, C.-M., Yen, H.-J., Fu, Y.-L., You, T.-R., et al. (2015). Anther development of maize (Zea mays) and longstamen rice (Oryza longistaminata) revealed by cryo-SEM, with foci on locular dehydration and pollen arrangement. *Plant Reprod.* 28, 47–60. doi: 10.1007/s00497-015-0257-3

Wang, Y., Liu, X., Hou, X., Sheng, D., Dong, X., Gao, Y., et al. (2021). Maximum lethal temperature for flowering and seed set in maize with contrasting male and female flower sensitivities. *J. Agro. Crop Sci.* 207, 679–689. doi: 10.1111/jac.12506

Wang, Y., Tao, H., Tian, B., Sheng, D., Xu, C., Zhou, H., et al. (2019). Flowering dynamics, pollen, and pistil contribution to grain yield in response to high temperature during maize flowering. *Environ. Exp. Bot.* 158, 80–88. doi: 10.1016/j.envexpbot.2018.11.007

Wang, T., Wang, F., Song, H., Zhou, S., Ru, X., and Zhang, H. (2022). Maize yield reduction and economic losses caused by ground-level ozone pollution with exposure- and flux-response relationships in the north China plain. *J. Environ. Manage.* 324, 116379. doi: 10.1016/j.jenvman.2022.116379

Westgate, M. E., Lizaso, J., and Batchelor, W. (2003). Quantitative relationships between pollen shed density and grain yield in maize. *Crop Sci.* 43, 934–942. doi: 10.2135/cropsci2003.9340

Xu, G., Wang, X., Huang, C., Xu, D., Li, D., Tian, J., et al. (2017). Complex genetic architecture underlies maize tassel domestication. *New Phytol.* 214, 852–864. doi: 10.1111/nph.14400

Yin, B., Hu, Z., Wang, Y., Zhao, J., Pan, Z., and Zhen, W. (2021). Effects of optimized subsoiling tillage on field water conservation and summer maize (Zea mays l.) yield in the north China plain. *Agric. Water Manage.* 247, 106732. doi: 10.1016/j.agwat.2020.106732

Zandalinas, S. I., Mittler, R., Balfagón, D., Arbona, V., and Gómez-Cadenas, A. (2017). Plant adaptations to the combination of drought and high temperatures. *Physiol. Plantarum* 162, 2–12. doi: 10.1111/ppl.12540

Zhao, C., Liu, B., Piao, S., Wang, X., Lobell, D. B., Huang, Y., et al. (2017). Temperature increase reduces global yields of major crops in four independent estimates. *Proc. Natl. Acad. Sci. U.S.A.* 114, 9326–9331. doi: 10.1073/pnas.1701762114

frontiers | Frontiers in Plant Science

TYPE Original Research
PUBLISHED 20 June 2023
DOI 10.3389/fpls.2023.1220827

OPEN ACCESS

EDITED BY
Baizhao Ren,
Shandong Agricultural University, China

REVIEWED BY
Gu Wanrong,
Northeast Agricultural University, China
Jiying Sun,
Inner Mongolia Agricultural University, China

*CORRESPONDENCE
Guanghao Li
guanghaoli@yzu.edu.cn
Dalei Lu
dllu@yzu.edu.cn

†These authors have contributed equally to this work

RECEIVED 11 May 2023
ACCEPTED 06 June 2023
PUBLISHED 20 June 2023

CITATION
Li G, Li W, Liang Y, Lu W and Lu D (2023) Spraying exogenous hormones alleviate impact of weak-light on yield by improving leaf carbon and nitrogen metabolism in fresh waxy maize.
Front. Plant Sci. 14:1220827.
doi: 10.3389/fpls.2023.1220827

Spraying exogenous hormones alleviate impact of weak-light on yield by improving leaf carbon and nitrogen metabolism in fresh waxy maize

Guanghao Li[1,2*†], Wei Li[1†], Yuwen Liang[1], Weiping Lu[1,2] and Dalei Lu[1,2*]

[1]Jiangsu Key Laboratory of Crop Genetics and Physiology, Jiangsu Key Laboratory of Crop Cultivation and Physiology, Jiangsu Co-Innovation Center for Modern Production Technology of Grain Crops, Yangzhou University, Yangzhou, China, [2]Joint International Research Laboratory of Agriculture and Agri-Product Safety, The Ministry of Education of China, Yangzhou University, Yangzhou, China

Insufficient light during the growth periods has become one of the main factors restricting maize yield with global climate change. Exogenous hormones application is a feasible measure to alleviate abiotic stresses on crop productivity. In this study, a field trial was conducted to investigate the effects of spraying exogenous hormones on yield, dry matter (DM) and nitrogen (N) accumulation, leaf carbon and N metabolism of fresh waxy maize under weak-light stress in 2021 and 2022. Five treatments including natural light (CK), weak-light after pollination (Z), spraying water (ZP1), exogenous Phytase Q9 (ZP2) and 6-benzyladenine (ZP3) under weak-light after pollination were set up using two hybrids suyunuo5 (SYN5) and jingkenuo2000 (JKN2000). Results showed that weak-light stress significantly reduced the average fresh ear yield (49.8%), fresh grain yield (47.9%), DM (53.3%) and N accumulation (59.9%), and increased grain moisture content. The net photosynthetic rate (Pn), transpiration rate (Tr) of ear leaf after pollination decreased under Z. Furthermore, weak-light decreased the activities of RuBPCase and PEPCase, nitrate reductase (NR), glutamine synthetase (GS), glutamate synthase (GOGAT), superoxide dismutase (SOD), catalase (CAT) and peroxidase (POD) in ear leaves, and increased malondialdehyde (MDA) accumulation. And the decrease was greater on JKN2000. While ZP2 and ZP3 treatments increased the fresh ear yield (17.8%, 25.3%), fresh grain yield (17.2%, 29.5%), DM (35.8%, 44.6%) and N (42.5%, 52.4%) accumulation, and decreased grain moisture content compared with Z. The Pn, Tr increased under ZP2 and ZP3. Moreover, the ZP2 and ZP3 treatments improved the activities of RuBPCase, PEPCase; NR, GS, GOGAT; SOD, CAT, POD in ear leaves, and decreased MDA content during grain filling stage. The results also showed the mitigative effect of ZP3 was greater than ZP2, and the improvement effect was more significant on JKN2000.

KEYWORDS

weak-light stress, yield, carbon and nitrogen metabolism, fresh waxy maize, exogenous hormones

Introduction

Light provides energy for the generation of plant assimilatory power and acts as a signal for photomorphogenesis (Kumar et al., 2016). Weak-light is a type of abiotic stress that seriously affects plant growth, development and production efficiency. Maize is a typical C_4 crop, and sufficient light is necessary to ensure its high and stable yield. However, over the past 50 years, global solar radiation has declined at an average rate of 1.4%–2.7% per decade (Stanhill and Cohen, 2001; Ramanathan and Feng, 2009), and the effective sunlight duration declined by 1.28% per decade in China (Che et al., 2005). Studies showed that maize yield reduced by 6%-7% when every 1 MJ/m^2 decrease in solar radiation (Chen et al., 2020). In southern China, the plum rain season from June and July overlaps with the grain-filling stage of spring maize. However, the grain-filling stage is the key period affecting the yield and quality of waxy maize (Lu et al., 2014). Weak-light stress during grain-filling stage led to yield reduction by reducing grain number and weight (Yang et al., 2016; Shi et al., 2018; Wen et al., 2019), which posed a serious threat to the production safety of maize. Fresh waxy maize is the special maize with the largest planting area in China. The grain starch is almost 100% composed of amylopectin, and the characteristics of high viscosity, low regeneration and easy digestion, made waxy maize the best edible maize. The development of fresh waxy maize plays an important role in promoting the adjustment of planting structure and increasing farmers' income in China. Therefore, it is of great significance to study how to alleviate the effect of weak-light stress on fresh waxy maize. Weak-light throughout the growth period led to slower growth and development of maize plants, sterility of tassel and ear, lower pollen viability and filament differentiation, and lower DM accumulation, which ultimately resulting in a reduced yield (Cui et al., 2015). Weak-light stress at different periods had different influences on maize, and more yield reduction occurred under weak-light at reproductive growth stage than vegetative growth stage (Yang et al., 2019). Weak-light stress occurred in the early stages has less effect on crop production (Deng et al., 2009), possibly because crop could be able to compensate for stress damage in middle and late stages (Kobata et al., 2000). However, grain number, weight and yield were significantly decreased under weak-light during the grain-filling stage (Deng et al., 2009). Maize grain yield primarily come from direct accumulation of photosynthates at post-silking and remobilization of the non-structural carbohydrate reserved from vegetative organs at pre-silking, and the direct accumulation of photosynthates at post-silking is essential for grain development (Tollenaar and Daynard, 1982; Farooq et al., 2011).

Weak-light stress at post-silking stage decreased chlorophyll content, damaged the ultrastructure of mesophyll cells, decreased photosynthetic capacity (Ren et al., 2016), and reduced DM accumulation, eventually leading to the loss of grain yield (Wang et al., 2020). Previous studies found that weak-light stress after silking significantly reduced the number and size of maize endosperm cells and reduced the enrichment of endosperm cells, which also led to smaller endosperm metastatic cells and the number of mitochondria, which eventually led to lower yield (Jia et al., 2011). Other studies have demonstrated that the IAA, ZR and GA contents in maize grain reduced and the ABA content increased under weak-light stress at post-silking stage, which inhibited grain growth and development (Gao et al., 2018). Studies on other crops also showed that weak-light stress significantly reduced grain yield of wheat (Li et al., 2010) and rice (Wei et al., 2018). N metabolism is an important process for the energy metabolism that determines crop yield and quality. Crop photosynthetic capacity is closely related to leaf N content (Sharwood et al., 2014). RuBPCase accounted for 50 ± 5% of the leaf soluble proteins in C_3 crop, and it accounted for 10%-25% in C_4 crop (Schmitt and Edwards, 1981). NR, GS, and GOGAT are the important enzymes involved in the assimilation of intracellular ammonium into organic compounds. Weak-light stress reduced NR, GS, and GOGAT activities in maize leaves, interfered with N metabolism, caused reduction of DM and N accumulation, and ultimately led loss of grain yield (Wang et al., 2020; Sun et al., 2023).

Weak-light stress posed a serious threat to maize production safety. However, there is few effective and reasonable protective measures to abate the influence. In recent years, a wide range of plant growth regulators, such as 6-benzylaminopurine (6-BA), gibberellic acid (GA_3), auxin (IAA) and cytokinin (CTK) have been widely used to reduce the damage of various abiotic stresses in crop production. The application of IAA and CTK increased grain yield, 1000-grain weight and filled-grain percentage of rice under salt stress (Javid et al., 2011). The application of GA_3 improved maize growth under salt stress (Rauf et al., 2022). It was well established and known that 6-BA could promote plant cell division, inhibit and scavenge free radicals, delay leaf senescence, increase DM and N accumulation (Roitsch and Ehneß, 2000). Exogenous application of 6-BA effectively alleviated the adverse effects of waterlogging on maize by increasing the leaf area index and chlorophyll content, reducing the MDA content, maintaining the stability of chloroplast ultrastructure (Ren et al., 2017), and reducing the ABA content (Hu et al., 2022). Exogenous 6-BA application during the fertile florets abortion stage of wheat increased the number of florets and number of grains by primarily suppressing the number of degenerated and aborted florets, which result in a further increase in grain yield (Li et al., 2019). Yuan et al. (2014) reported that soaking maize seeds by 6-BA could alleviate the physiological damage under drought stress. At present, most studies on 6-BA regulation of maize growth characteristics focused on waterlogging, drought and other stresses, and few studies reported on regulating growth of fresh waxy maize under weak-light stress. The main component of phytase Q9 is fulvic acid (fulvic acid content≥200 g/L) (Huang et al., 2020). Fulvic acid was reported to have significant effects in stress resistance. Exogenous fulvic acid application substantially reduced the damage of drought stress on maize by sustaining the chlorophyll contents and gas exchange possibly by enhanced SOD, POD and CAT activities and proline levels (Anjum et al., 2011). Huang et al. (2020) found that exogenous spraying phytase Q9 improved the leaf area index, SPAD value and net photosynthetic rate under weak-light conditions at the whole growth period (Huang et al., 2020). However, whether phytase Q9 could alleviate the effect of weak-light stress on fresh waxy maize and its regulation mechanism need further study. This study aimed to investigate the effects of exogenous spraying 6-BA and phytase Q9 on the yield and photosynthetic characteristics of fresh waxy maize under weak-light stress, and provide theoretical basis and technical

support for stress-resistant cultivation of fresh waxy maize under climate change.

Materials and methods

Experimental design

The field experiment was conducted at Yangzhou University farm (32°30′N, 119°25′E) in Jiangsu Province, China in the spring maize growing seasons of 2021-2022. Two fresh waxy maize hybrids, Suyunuo5 (SYN5, used in the national fresh waxy maize regional test as the control variety) and Jingkenuo2000 (JKN2000, having the largest planted area of waxy maize in China) were used as experimental materials. The sowing date was March 24 in 2021 and April 4 in 2022, and pollination date was June 14 in 2021 and June 9 in 2022. Maize was planted in double-row (0.8 and 0.4 m) according to local traditional method. Each plot was 10 m × 7.2 m with a plant density of 60000 plants/ha. Slow released compound fertilizer ($N/P_2O_5/K_2O$=27%/9%/9%) were applied at sowing time with the $N/P_2O_5/K_2O$ rates of 225/75/75 kg/ha. Two hybrids were harvested at milk stage on July 6 and July 1 in 2021 and 2022. After pollination, the shed was built with a black shading net of 50% shading degree (Figure 1). The distance between the shading net and the maize canopy was always 2-2.5 m to ensure that the field microclimate under the shading shed is basically consistent with the natural light conditions in the field. Five treatments including natural lighting in the field (CK), shading at 1-23 days after pollination (Z), spraying exogenous water (ZP1), 6-BA (ZP2) and Phytase Q9 (ZP3) under shading at 1-23 days after pollination were set. The concentration of 0.1 g/L 6-BA was used according to previous investigations (Chen et al., 2013). And the concentration of Phytase Q9 was 0.5 g/L. Both exogenous hormones were applied as foliar sprays at the rate of 150 ± 5 mL per plant on all leaves, from 16:00 to 18:00 the next day after shading.

Yield determination

Thirty ears were harvested from the middle three rows of each plot at milk stage (the 23rd day after pollination) using a continuous sampling method. Based on the average ear weight, three uniform ears were selected from each treatment to determine the fresh grain yield and moisture content.

Dry matter and N accumulation

Three representative plants of each treatment were collected and separated into leaves and stems (including sheaths and tassels) at silking stage, and into leaves, stems, cobs (including bracts) and grains at milk stage. All samples were oven dried to a constant weight at 80°C after de-enzyming at 105°C for 30 min and weighed separately. After weighing, the samples were ground using a cyclone sample mill with a fine mesh (0.5 mm). N concentrations of different organs were determined using the micro-Kjeldahl method. N accumulations of each fraction were calculated as the product of the concentration and DM.

Leaf gas exchange parameters

A portable photosynthetic apparatus system (LI-6400 Li-Cor, USA) was used to measure the net photosynthetic rate (Pn), stomatal conductance (Gs), transpiration rate (Tr) and intercellular CO_2 concentration (Ci) in ear leaves at 10 and 20 days after pollination (DAP). The measurements were performed as described previously (Guo et al., 2023).

Activities of enzymes involved in carbon, nitrogen metabolism and antioxidant system

At 5, 10, 15 and 21 DAP, Ear leaves of different treatments were collected in liquid N container immediately after sampling for enzyme activities. The activities of RuBPCase, PEPCase, NR, GS, GOGAT, SOD, POD, CAT and the contents of MDA, were measured using MLBIO Plant Sucrose Synthase ELISA Kit, following the manufacturer's instructions (Shanghai Enzyme-linked Biotechnology Co., Ltd., Shanghai, China) and a previously described method (Saiya-Cork et al., 2002; Zhang et al., 2020).

Statistical analysis

Statistical calculations were performed in Excel 2016 (Microsoft, Redmond, WA, United States), and figures generated in Sigma Plot 12.0 program. The data were subjected to ANOVA in

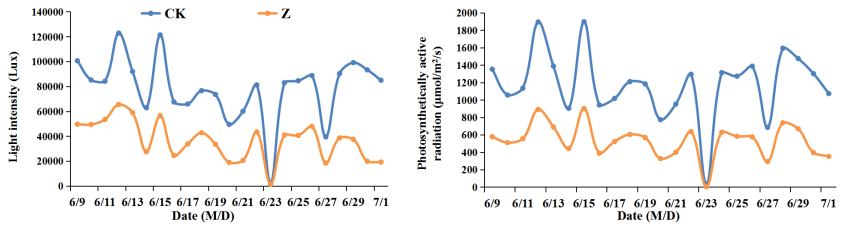

FIGURE 1
Light intensity and photosynthetically active radiation at daily 10:00 from June 9 to July 1 in 2022. CK, natural light; Z, weak-light after pollination.

the General Linear Model module of SPSS. Comparisons among treatments were based on Duncan's test at the 0.05 probability level (P<0.05).

Results

Yield

Weak-light stress after pollination decreased the fresh ear yield by 40.5% (SYN5) and 59.1% (JKN2000), and decreased by 41.2% and 54.5% in fresh grain yield compared with CK in two years, while increased the moisture content (Figure 2). The decrease in JKN2000 was more severe under weak-light stress. Spraying two exogenous hormones increased the fresh ear and grain yield compared with Z, and ZP1 had no significant difference with Z. The fresh ear yields of ZP2 and ZP3 were increased by 13.7% and 20.5%, and the fresh grain yields increased by 8.7% and 27.9% in SYN5. The fresh ear yields of ZP2 and ZP3 were increased by 22.0% and 30.0%, and the fresh grain yields increased by 25.7% and 31.1% in JKN2000. The increase was higher in JKN2000 under ZP3. And spraying exogenous hormones decreased the moisture content in grain to different extents under weak-light. The moisture content of ZP2 and ZP3 were both decreased by 5.8% in SYN5, and by 3.7% and 7.8% in JKN2000. The average yield in 2022 was higher than 2021, perhaps due to the high average temperature in 2022 compared to 2021 (Figure 3).

Dry matter and nitrogen accumulation

Weak-light stress after pollination significantly reduced DM and N accumulation at post-silking in two years (Figure 4). Compared with CK, the DM of Z at post-silking decreased by 53.8% (SYN5) and 52.7% (JKN2000), and the N accumulation of Z were reduced by 60.2% and 59.7%. Compared with Z, the DM of ZP2 and ZP3 at post-silking were increased by 42.5% and 48.9% in SYN5, and by 29.2%, 40.3% in JKN2000. N accumulation of ZP2 and ZP3 at post-silking were increased by 42.9%, 47.4% in SYN5, and by 42.2%, 57.3% in JKN2000. ZP1 had no significant difference

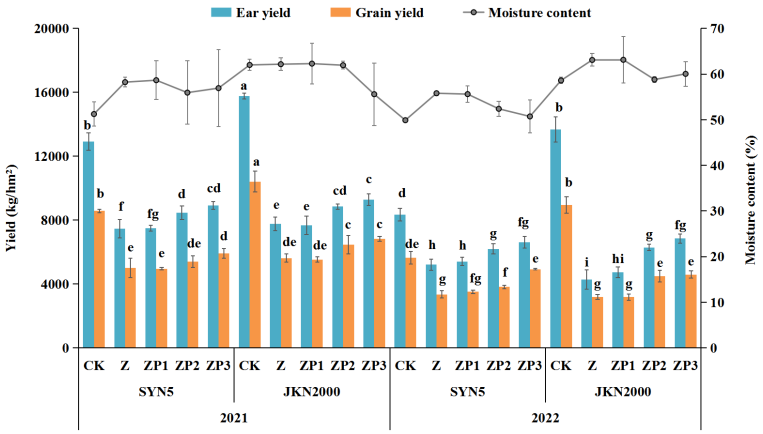

FIGURE 2
Effects of spraying exogenous hormones on fresh waxy maize yield under weak-light stress. Different letters above the bars represent significant differences at P < 0.05. SYN5, Suyunuo5; JKN2000, Jingkenuo2000; CK, natural light; Z, weak-light after pollination; ZP1, ZP2, and ZP3 represent spraying water, Phytase Q9 and 6-BA under weak-light stress after pollination.

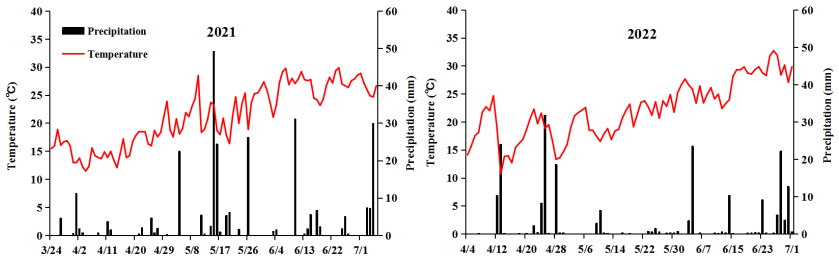

FIGURE 3
Daily precipitation and average temperature for maize growing season in 2021 and 2022.

10.3389/fpls.2023.1220827

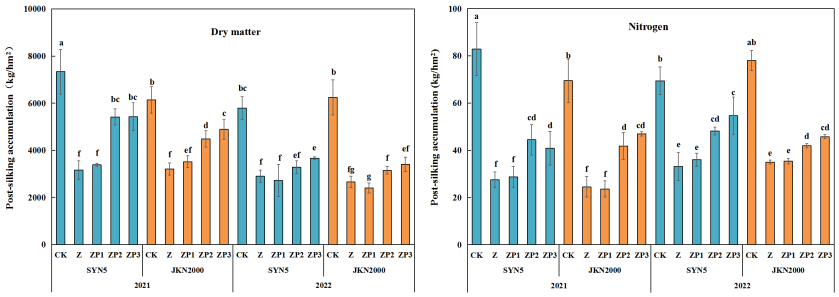

FIGURE 4
Effects of spraying exogenous hormones on the post-silking accumulation of dry matter and nitrogen in fresh waxy maize under weak-light stress. Different letters above the bars represent significant differences at $P < 0.05$. SYN5, Suyunuo5; JKN2000, Jingkenuo2000; CK, natural light; Z, weak-light after pollination; ZP1, ZP2, and ZP3 represent spraying water, Phytase Q9 and 6-BA under weak-light stress after pollination.

with Z. The effect on DM and N under ZP3 was greater than ZP2. The DM and N accumulation in 2022 was higher than 2021.

Leaf photosynthetic gas exchange parameters

Pn, Tr, Gs and Ci were higher at 10DAP than those at 20DAP. Compared with CK, Z treatment decreased Pn, Tr, and Gs, but increased Ci at 10DAP and 20DAP (Figure 5). ZP2 and ZP3 treatments increased the Pn of SYN5 and JKN2000 compared with Z, and the increase was higher at ZP3. The GS of ZP3 were increased significantly, but it had no significance with that of ZP2. The Tr of ZP2 and ZP3 were increased compared with Z. The Ci of two cultivars were decreased under ZP3 treatment, and ZP2 decreased the Ci in SYN5, but it had no significant effect on JKN2000. Overall, 6-BA had a more impact on the leaf photosynthetic gas exchange parameters.

Activities of enzymes involved in carbon and nitrogen metabolism

The activities of RuBPCase and PEPCase gradually decreased after pollination in two hybrids in 2022 (Figure 6). RuBPCase and PEPCase activities were decreased under Z treatment at all stages. Compared with

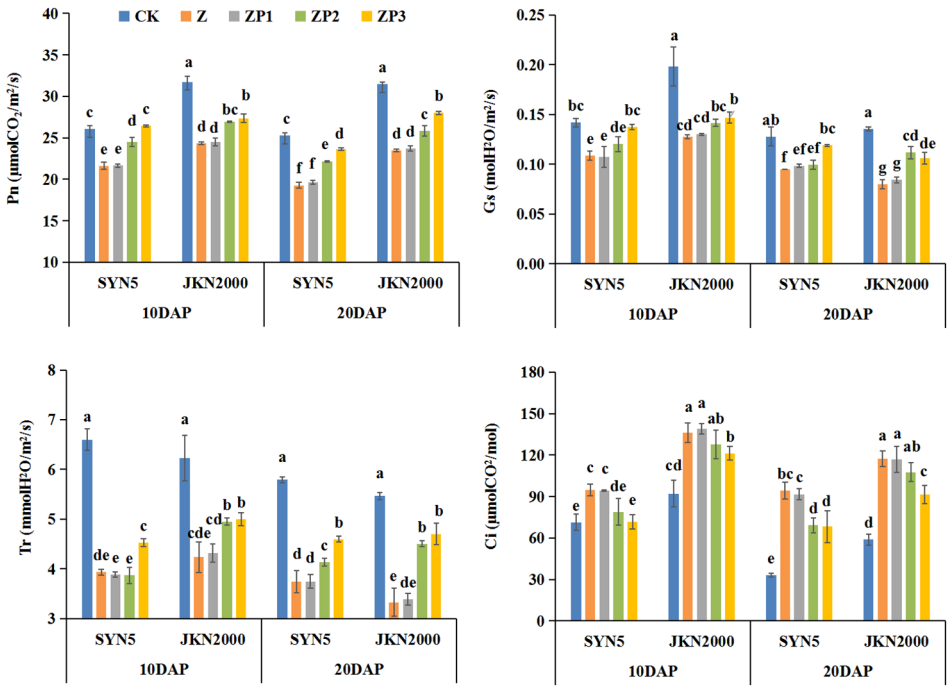

FIGURE 5
Effects of spraying exogenous hormones on photosynthetic gas exchange parameters in ear leaf of fresh waxy maize under weak-light stress. Different letters above the bars represent significant differences at $P < 0.05$ at same stage. SYN5, Suyunuo5; JKN2000, Jingkenuo2000; CK, natural light; Z, weak-light after pollination; ZP1, ZP2, and ZP3 represent spraying water, Phytase Q9 and 6-BA under weak-light stress after pollination. Pn, photosynthetic rate; Gs, stomatal conductance; Tr, transpiration rate; Ci, intercellular CO_2.

10.3389/fpls.2023.1220827

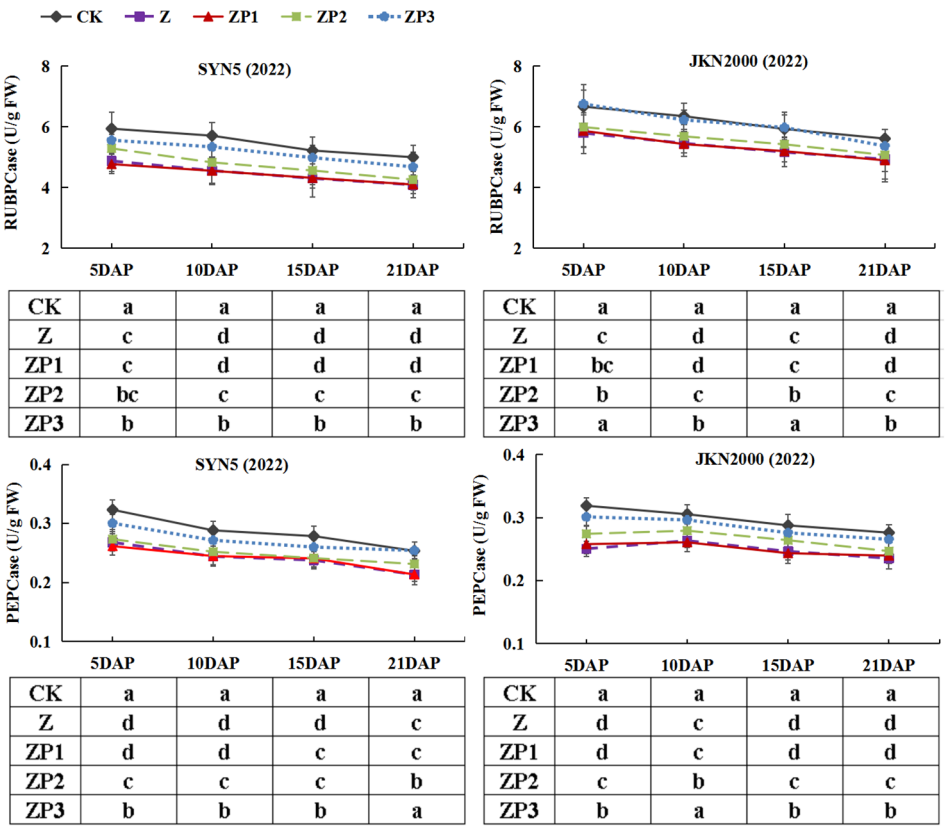

	5DAP	10DAP	15DAP	21DAP
CK	a	a	a	a
Z	c	d	d	d
ZP1	c	d	d	d
ZP2	bc	c	c	c
ZP3	b	b	b	b

	5DAP	10DAP	15DAP	21DAP
CK	a	a	a	a
Z	c	d	c	d
ZP1	bc	d	c	d
ZP2	b	c	b	c
ZP3	a	b	a	b

	5DAP	10DAP	15DAP	21DAP
CK	a	a	a	a
Z	d	d	d	c
ZP1	d	d	c	c
ZP2	c	c	c	b
ZP3	b	b	b	a

	5DAP	10DAP	15DAP	21DAP
CK	a	a	a	a
Z	d	c	d	d
ZP1	d	c	d	d
ZP2	c	b	c	c
ZP3	b	a	b	b

FIGURE 6
Effects of spraying exogenous hormones on the activities of RuBPCase and PEPCase in ear leaf of fresh waxy maize under weak-light stress. SYN5, Suyunuo5; JKN2000, Jingkenuo2000; CK, natural light; Z, weak-light after pollination; ZP1, ZP2, and ZP3 represent spraying water, Phytase Q9 and 6-BA under weak-light stress after pollination. RuBPCase, ribulose-1,5-bisphosphate carboxylase; PEPase, phosphoenolpyruvate carboxylase.

Z, ZP3 treatment increased the RuBPCase and PEPCase activities significantly. The RuBPCase activities in two hybrids and PEPCase activity in JKN2000 were increased under ZP2. ZP1 have no significant effect on activities of RuBPCase and PEPCase. In general, compared with Z, the average RuBPCase activities of the two hybrids under ZP2 and ZP3 were increased 6.6% and 15.9% in SYN5, 3.7% and 13.6% in JKN2000. And the average PEPCase activities of the two hybrids under ZP2 and ZP3 were increased 4.0% and 13.2% in SYN5, 6.2% and 13.6% in JKN2000.

NR, GS and GOGAT activities of the two hybrids increased initially, peaked at 10 DAP and decreased afterwards in two years (Figures 7–9). Weak-light stress decreased the activities of NR, GS and GOGAT after pollination in both hybrids. ZP2 and ZP3 treatments increased the activities of NR, GS and GOGAT compared with Z. And the increase was greater under ZP3. Compared with Z, the NR activities of SYN5 and JKN2000 were increased by 8.3% and 1.3% under ZP2 and increased by 11.4% and 6.9% under ZP3. The GS activities of SYN5 and JKN2000 were increased by 10.1% and 4.6% under ZP2 and increased by 15.4% and 7.4% under ZP3. And the activities of GOGAT in SYN5 and JKN2000 were increased by 1.9% and 4.5% under ZP2 and increased by 6.2% and 8.4% under ZP3. The trend of NR and GS activities were consistent between two hybrids and between two years.

Activities of antioxidant enzymes and MDA content

The SOD activities of the two hybrids increased initially, peaked at 15DAP and decreased afterwards in two years. Whereas the activities of CAT and POD gradually decreased with grain growth (Figures 10–12). The activities of SOD, CAT and POD were decreased under Z. ZP2 and ZP3 increased the activities of SOD, CAT and POD, but the increase was dependent on hybrid, stage and year. Compared with Z, the SOD activities of SYN5 and JKN2000 were increased by 3.4% and 2.7% under ZP2, and increased by 5.0% and 4.6% under ZP3. The CAT activities of SYN5 and JKN2000 were increased by 4.2% and 0.7% under ZP2, and increased by 5.3% and 2.9% under ZP3. POD activities of SYN5 and JKN2000 were increased by 4.9% and 4.0% under ZP2, and increased by 9.0% and 7.0% under ZP3. Meanwhile, the content of MDA gradually increased with grain growth, and it was increased under Z (Figure 13). But under ZP2 and ZP3, the contents of MDA decreased compared with Z. The content of MDA in SYN5 and JKN2000 were decreased by 12.0% and 12.1% under ZP2, and decreased by 9.6% and 13.7% under ZP3. The trend of SOD and POD activities were consistent between two hybrids and between two years.

10.3389/fpls.2023.1220827

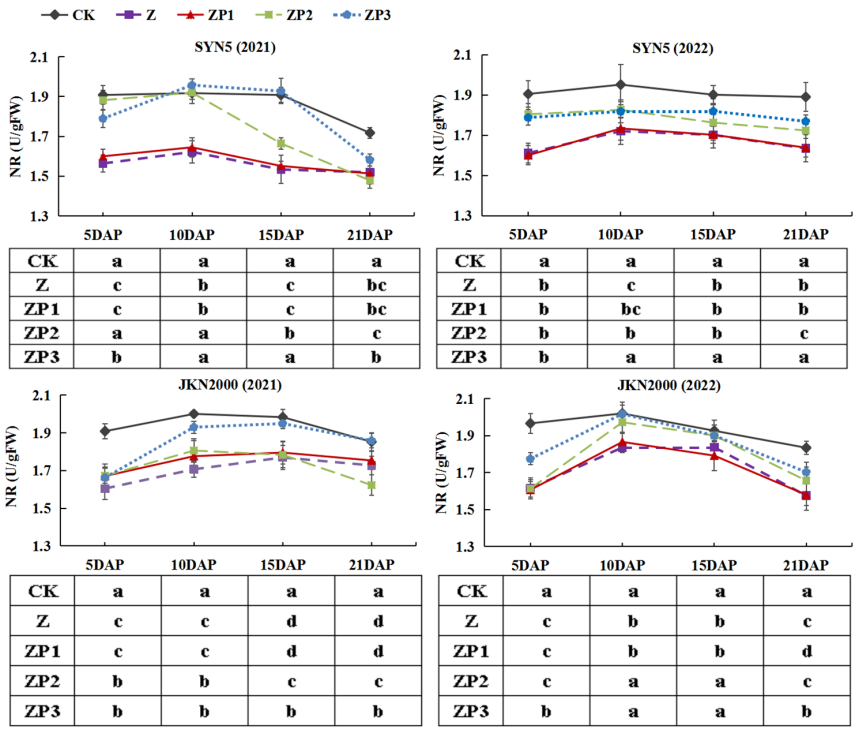

SYN5 (2021)	5DAP	10DAP	15DAP	21DAP
CK	a	a	a	a
Z	c	b	c	bc
ZP1	c	b	c	bc
ZP2	a	a	b	c
ZP3	b	a	a	b

SYN5 (2022)	5DAP	10DAP	15DAP	21DAP
CK	a	a	a	a
Z	b	c	b	b
ZP1	b	bc	b	b
ZP2	b	b	b	c
ZP3	b	a	a	a

JKN2000 (2021)	5DAP	10DAP	15DAP	21DAP
CK	a	a	a	a
Z	c	c	d	d
ZP1	c	c	d	d
ZP2	b	b	c	c
ZP3	b	b	b	b

JKN2000 (2022)	5DAP	10DAP	15DAP	21DAP
CK	a	a	a	a
Z	c	b	b	c
ZP1	c	b	b	d
ZP2	c	a	a	c
ZP3	b	a	a	b

FIGURE 7
Effects of spraying exogenous hormones on the activities of NR in ear leaf of fresh waxy maize under weak-light stress. SYN5, Suyunuo5; JKN2000, Jingkenuo2000; CK, natural light; Z, weak-light after pollination; ZP1, ZP2, and ZP3 represent spraying water, Phytase Q9 and 6-BA under weak-light stress after pollination. NR, nitrate reductase.

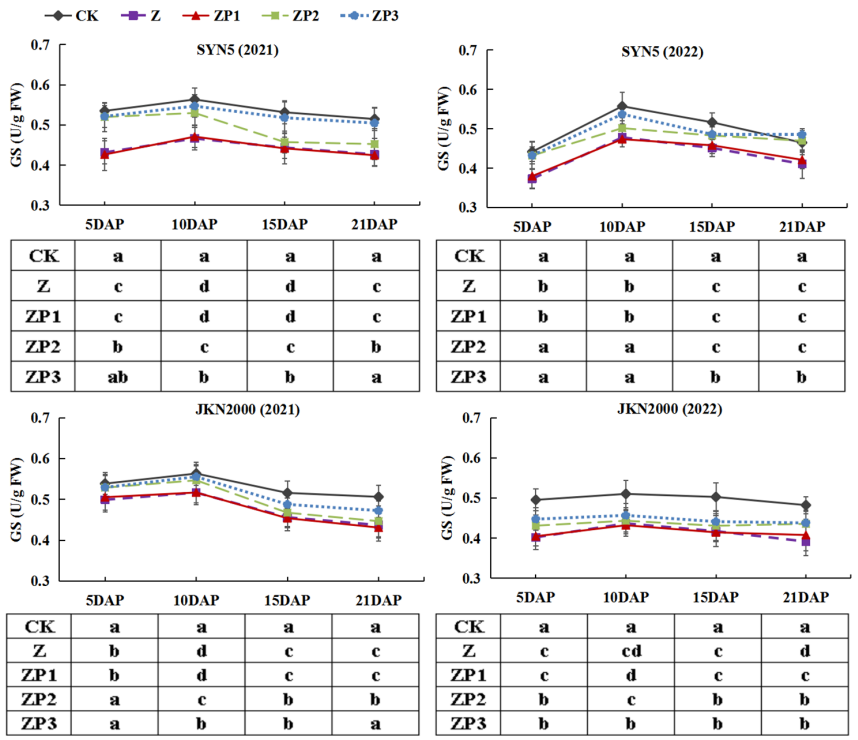

SYN5 (2021)	5DAP	10DAP	15DAP	21DAP
CK	a	a	a	a
Z	c	d	d	c
ZP1	c	d	d	c
ZP2	b	c	c	b
ZP3	ab	b	b	a

SYN5 (2022)	5DAP	10DAP	15DAP	21DAP
CK	a	a	a	a
Z	b	b	c	c
ZP1	b	b	c	c
ZP2	a	a	c	c
ZP3	a	a	b	b

JKN2000 (2021)	5DAP	10DAP	15DAP	21DAP
CK	a	a	a	a
Z	b	d	c	c
ZP1	b	d	c	c
ZP2	a	c	b	b
ZP3	a	b	b	a

JKN2000 (2022)	5DAP	10DAP	15DAP	21DAP
CK	a	a	a	a
Z	c	cd	c	d
ZP1	c	d	c	c
ZP2	b	c	b	b
ZP3	b	b	b	b

FIGURE 8
Effects of spraying exogenous hormones on the activities of GS in ear leaf of fresh waxy maize under weak-light stress. SYN5, Suyunuo5; JKN2000, Jingkenuo2000; CK, natural light; Z, weak-light after pollination; ZP1, ZP2, and ZP3 represent spraying water, Phytase Q9 and 6-BA under weak-light stress after pollination. GS, glutamine synthetase.

10.3389/fpls.2023.1220827

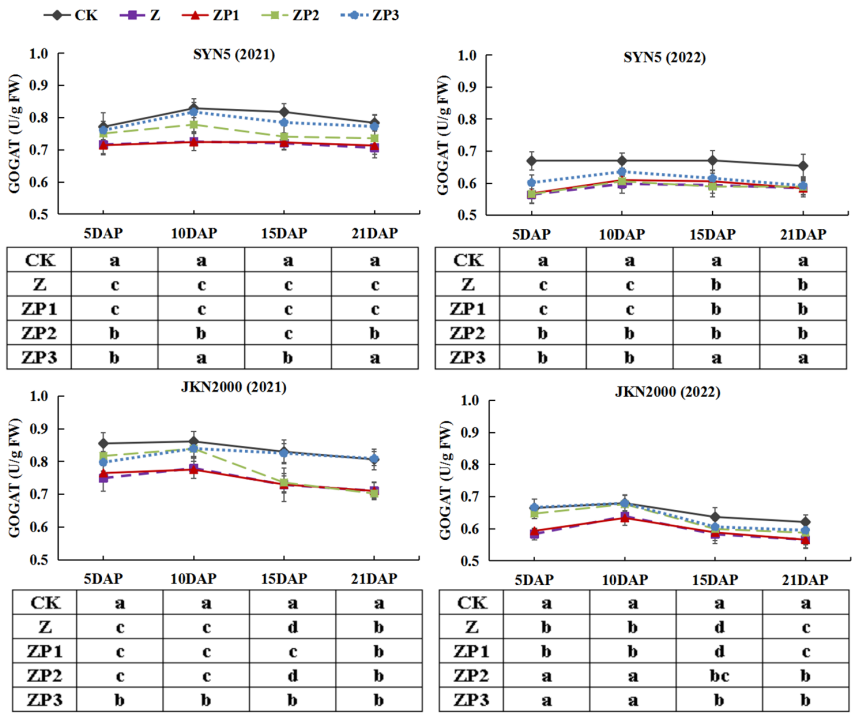

	5DAP	10DAP	15DAP	21DAP
CK	a	a	a	a
Z	c	c	c	c
ZP1	c	c	c	c
ZP2	b	b	c	b
ZP3	b	a	b	a

	5DAP	10DAP	15DAP	21DAP
CK	a	a	a	a
Z	c	c	b	b
ZP1	c	c	b	b
ZP2	b	b	b	b
ZP3	b	b	a	a

	5DAP	10DAP	15DAP	21DAP
CK	a	a	a	a
Z	c	c	d	b
ZP1	c	c	c	b
ZP2	c	c	d	b
ZP3	b	b	b	b

	5DAP	10DAP	15DAP	21DAP
CK	a	a	a	a
Z	b	b	d	c
ZP1	b	b	d	c
ZP2	a	a	bc	b
ZP3	a	a	b	b

FIGURE 9
Effects of spraying exogenous hormones on the activities of GOGAT in ear leaf of fresh waxy maize under weak-light stress. SYN5, Suyunuo5; JKN2000, Jingkenuo2000; CK, natural light; Z, weak-light after pollination; ZP1, ZP2, and ZP3 represent spraying water, Phytase Q9 and 6-BA under weak-light stress after pollination. GOGAT, glutamate synthase.

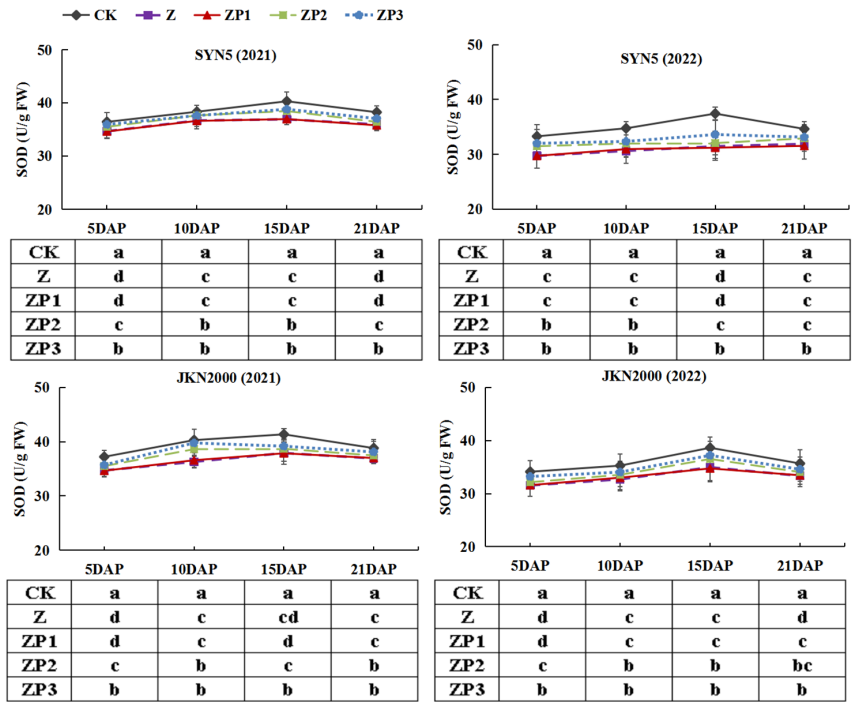

	5DAP	10DAP	15DAP	21DAP
CK	a	a	a	a
Z	d	c	c	d
ZP1	d	c	c	d
ZP2	c	b	b	c
ZP3	b	b	b	b

	5DAP	10DAP	15DAP	21DAP
CK	a	a	a	a
Z	c	c	d	c
ZP1	c	c	d	c
ZP2	b	b	c	c
ZP3	b	b	b	b

	5DAP	10DAP	15DAP	21DAP
CK	a	a	a	a
Z	d	c	cd	c
ZP1	d	c	d	c
ZP2	c	b	c	b
ZP3	b	b	b	b

	5DAP	10DAP	15DAP	21DAP
CK	a	a	a	a
Z	d	c	c	d
ZP1	d	c	c	c
ZP2	c	b	b	bc
ZP3	b	b	b	b

FIGURE 10
Effects of spraying exogenous hormones on the activities of SOD in ear leaf of fresh waxy maize under weak-light stress. SYN5, Suyunuo5; JKN2000, Jingkenuo2000; CK, natural light; Z, weak-light after pollination; ZP1, ZP2, and ZP3 represent spraying water, Phytase Q9 and 6-BA under weak-light stress after pollination. SOD, superoxide dismutase.

10.3389/fpls.2023.1220827

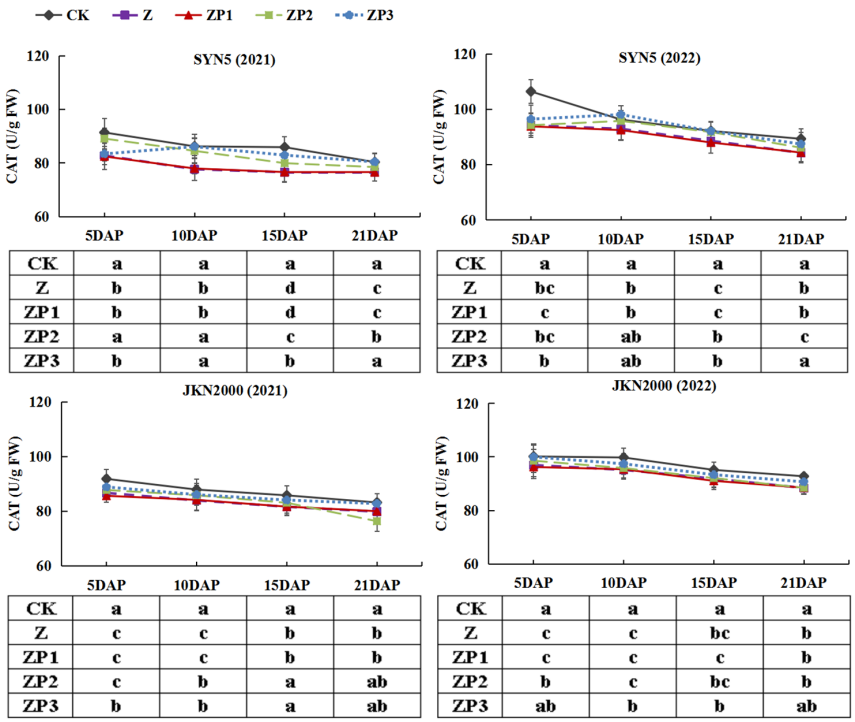

	5DAP	10DAP	15DAP	21DAP
CK	a	a	a	a
Z	b	b	d	c
ZP1	b	b	d	c
ZP2	a	a	c	b
ZP3	b	a	b	a

	5DAP	10DAP	15DAP	21DAP
CK	a	a	a	a
Z	bc	b	c	b
ZP1	c	b	c	b
ZP2	bc	ab	b	c
ZP3	b	ab	b	a

	5DAP	10DAP	15DAP	21DAP
CK	a	a	a	a
Z	c	c	b	b
ZP1	c	c	b	b
ZP2	c	b	a	ab
ZP3	b	b	a	ab

	5DAP	10DAP	15DAP	21DAP
CK	a	a	a	a
Z	c	c	bc	b
ZP1	c	c	c	b
ZP2	b	c	bc	b
ZP3	ab	b	b	ab

FIGURE 11
Effects of spraying exogenous hormones on the activities of CAT in ear leaf of fresh waxy maize under weak-light stress. SYN5, Suyunuo5; JKN2000, Jingkenuo2000; CK, natural light; Z, weak-light after pollination; ZP1, ZP2, and ZP3 represent spraying water, Phytase Q9 and 6-BA under weak-light stress after pollination. CAT, catalase.

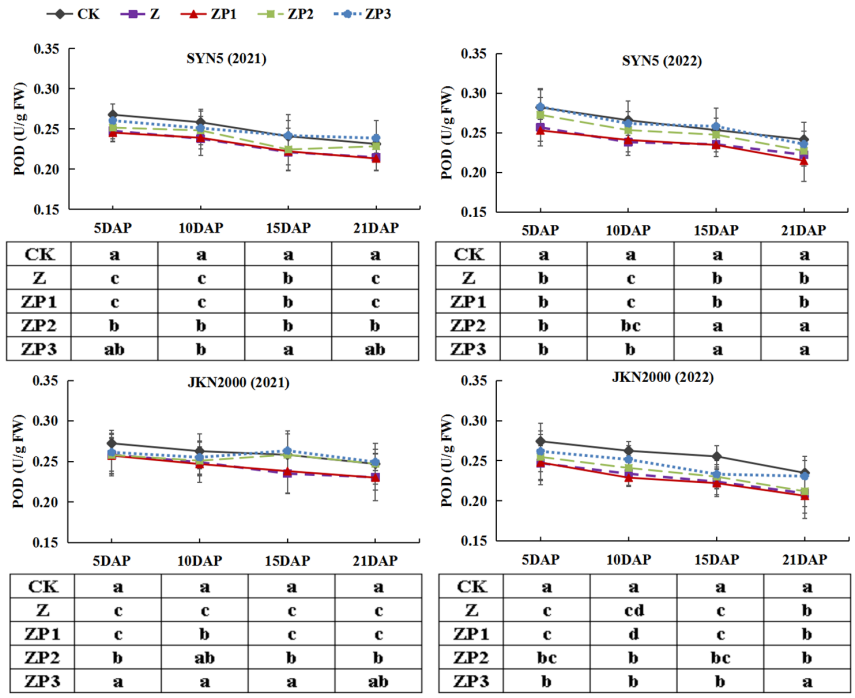

	5DAP	10DAP	15DAP	21DAP
CK	a	a	a	a
Z	c	c	b	c
ZP1	c	c	b	c
ZP2	b	b	b	b
ZP3	ab	b	a	ab

	5DAP	10DAP	15DAP	21DAP
CK	a	a	a	a
Z	b	c	b	b
ZP1	b	c	b	b
ZP2	b	bc	a	a
ZP3	b	b	a	a

	5DAP	10DAP	15DAP	21DAP
CK	a	a	a	a
Z	c	c	c	c
ZP1	c	b	c	c
ZP2	b	ab	b	b
ZP3	a	a	a	ab

	5DAP	10DAP	15DAP	21DAP
CK	a	a	a	a
Z	c	cd	c	b
ZP1	c	d	c	b
ZP2	bc	b	bc	b
ZP3	b	b	b	a

FIGURE 12
Effects of spraying exogenous hormones on the activities of POD in ear leaf of fresh waxy maize under weak-light stress. SYN5, Suyunuo5; JKN2000, Jingkenuo2000; CK, natural light; Z, weak-light after pollination; ZP1, ZP2, and ZP3 represent spraying water, Phytase Q9 and 6-BA under weak-light stress after pollination. POD, peroxidase.

10.3389/fpls.2023.1220827

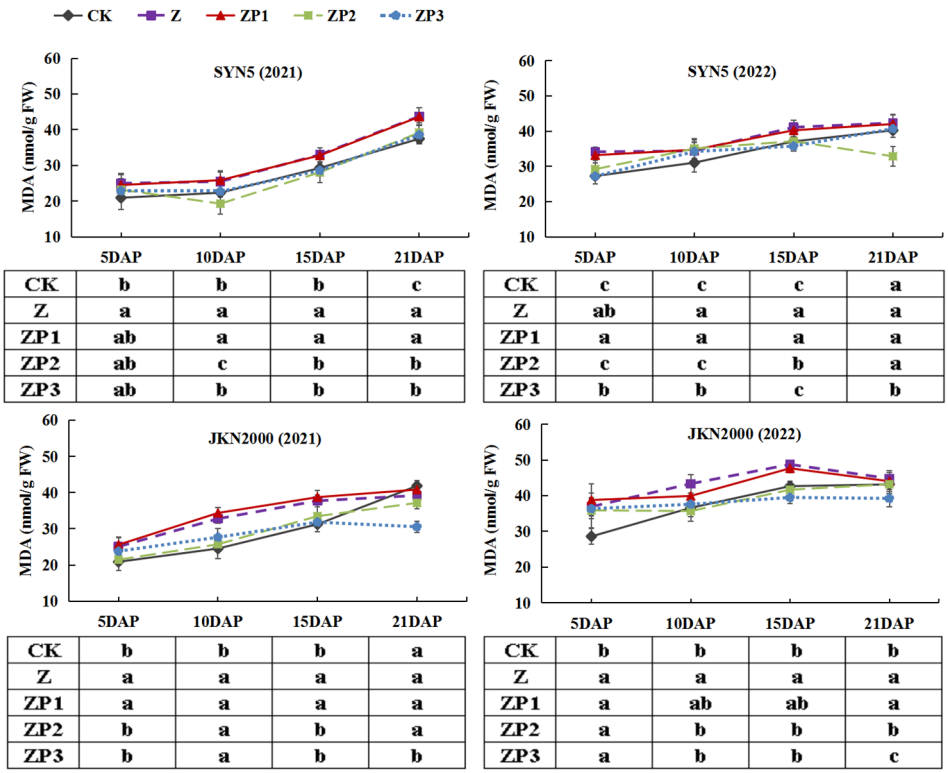

SYN5 (2021)	5DAP	10DAP	15DAP	21DAP
CK	b	b	b	c
Z	a	a	a	a
ZP1	ab	a	a	a
ZP2	ab	c	b	b
ZP3	ab	b	b	b

SYN5 (2022)	5DAP	10DAP	15DAP	21DAP
CK	c	c	c	a
Z	ab	a	a	a
ZP1	a	a	a	a
ZP2	c	c	b	a
ZP3	b	b	c	b

JKN2000 (2021)	5DAP	10DAP	15DAP	21DAP
CK	b	b	b	a
Z	a	a	a	a
ZP1	a	a	a	a
ZP2	b	a	b	a
ZP3	b	a	b	b

JKN2000 (2022)	5DAP	10DAP	15DAP	21DAP
CK	b	b	b	b
Z	a	a	a	a
ZP1	a	ab	ab	a
ZP2	a	b	b	b
ZP3	a	b	b	c

FIGURE 13
Effects of spraying exogenous hormones on MDA content in ear leaf of fresh waxy maize under weak-light stress. SYN5, Suyunuo5; JKN2000, Jingkenuo2000; CK, natural light; Z, weak-light after pollination; ZP1, ZP2, and ZP3 represent spraying water, Phytase Q9 and 6-BA under weak-light stress after pollination. MDA, malondialdehyde.

Correlation analysis

In this study, Pearson's correlation analysis revealed fresh ear and grain yield had positive correlations with DM and N accumulation, N metabolism enzymes (NR, GS, GOGAT), antioxidant enzymes (SOD, CAT, POD), photosynthetic gas exchange parameters (Pn, Tr, Gs), and carbon metabolism enzymes (RuBPCase, PEPCase) (Figure 14). The DM and N accumulation were positively correlated with carbon and N metabolism enzymes, antioxidant enzymes and photosynthetic gas exchange parameters. The carbon and N metabolism enzymes had positive correlations with antioxidant enzymes and photosynthetic gas exchange parameters. And the antioxidant enzymes had positive correlations with photosynthetic gas exchange parameters. The correlation analysis also indicated that photosynthetic gas exchange parameters were positively correlated with RuBPCase and PEPCase. Ci and MDA were negatively correlated with other indexes or parameters.

Discussion

Solar radiation is the energy source for the accumulation of photosynthates (Yang et al., 2021a). Photosynthate accumulation especially at post-silking is a key determinant of maize yield (Barnabás et al., 2008; Liu et al., 2020). The leaf N content is closely associated with plant photosynthetic capacity. A high N content in leaves enhanced photosynthesis and delayed leaf senescence (Sinclair et al., 2000). In this study, the results showed that weak-light stress decreased fresh ear and grain yield, DM and N accumulation in fresh waxy maize, which was consistent with the previous results (Yang et al., 2021a; Yang et al., 2021b). Exogenous hormone played an important role in the response to various abiotic stresses. Previous studies have showed that spraying phytase Q9 improved yield and DM accumulation on summer maize (Huang et al., 2020), and this is consistent with the results in this study on fresh waxy maize. Furthermore, we also found that spraying 6-BA and phytase Q9 both increased the yield, DM and N accumulation, and the increase was greater in 6-BA.

Photosynthetic capacity is the major determinant of crop productivity. Our study showed that weak-light stress decreased the Pn of ear leaves, which was consistent with the previous results on normal maize (Sinclair et al., 2000; Sharwood et al., 2014). Weak-light stress reduced leaf area index (LAI) and chlorophyll content and damaged the mesophyll cell ultrastructure, which led to the decrease of photosynthetic capacity, and thus resulted in significant yield loss (Ren et al., 2016). Previous study found that LAI, SPAD value and Pn of summer maize significantly increased under spraying phytase Q9 (Huang et al., 2020). In this study, we found that spraying 6-BA and phytase Q9 increased Pn significantly under weak-light stress, and the increase was higher in 6-BA. RuBPCase and PEPCase are key enzymes involved in carbon

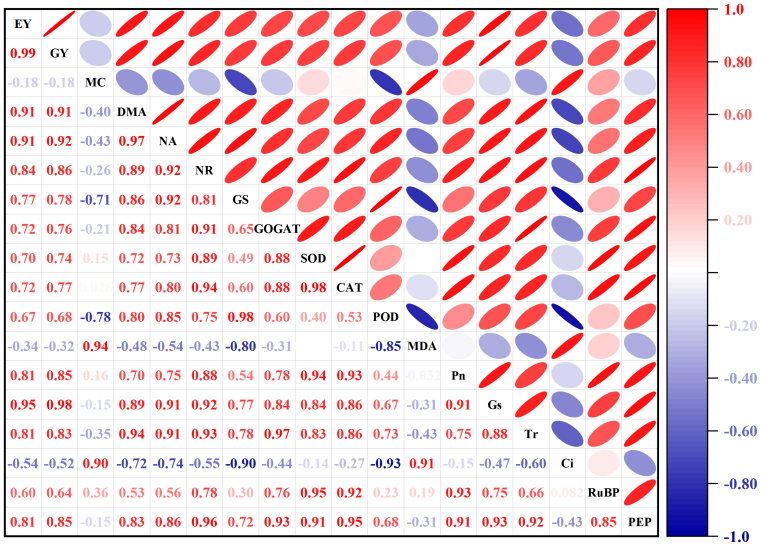

FIGURE 14
Pearson correlation matrix between yield, dry matter and N accumulation after pollination, and leaf related parameters. EY, fresh ear yield; GY, fresh grain yield; MC, moisture content; DMA, dry matter accumulation; NA, nitrogen accumulation; NR, nitrate reductase; GS, glutamine synthetase; GOGAT, glutamate synthase; SOD, superoxide dismutase; CAT, catalase; POD, peroxidase; MDA, malondialdehyde; Pn, photosynthetic rate; Gs, stomatal conductance; Tr, transpiration rate; Ci, intercellular CO_2; RuBP, ribulose-1,5-bisphosphate carboxylase; PEP, phosphoenolpyruvate carboxylase.

metabolism, and NR, GS, GOGAT are key enzymes involved in N metabolism. The activities of RuBPCase, PEPCase, NR, GS and GOGAT were decreased under weak-light on summer maize (Sharwood et al., 2014; Wang et al., 2020). This is generally consistent with the results of this experiment in fresh waxy maize. Studies reported that weak-light stress reduced the activities of photosynthesis-related enzymes in maize leaves (Sharwood et al., 2014), which reduced the net photosynthetic rate and led to the decrease of photosynthetic production capacity (Zhong et al., 2014). The decrease in grain weight and volume under weak-light may be due to reduced photosynthetic rate and decreased assimilate production capacity resulting from the inhibition of leaf N metabolism (Sharwood et al., 2014). In this study, spraying 6-BA and phytase Q9 increased the activities of PEPCase, RuBPCase, NR, GS and GOGAT under weak-light stress. This promoted the improvement of photosynthetic capacity, which in turn increased DM and N accumulation. Our experimental results also indicated that the spraying effect on carbon and N metabolism of 6-BA was better.

SOD, CAT and POD are key enzymes involved in antioxidant systems, and MDA is one of the products of membrane lipid peroxidation, its content can be used as one of the indicators to investigate the severity of cell stress. Previous study found that weak-light stress reduced the activities of SOD, CAT and POD, and increased the MDA content in ear leaves of summer maize (Huang et al., 2020). In this study, we also found that weak-light stress decreased the activities of SOD, CAT and POD, and increased the content of MDA, which accelerated the oxidative damage of leaf in fresh waxy maize. Under weak-light stress, plasmolysis occurred in mesophyll cells and the endomembrane system was destroyed, which resulted in the dissolution of cell membrane, karyotheca, mitochondria, and the mesophyll cell ultrastructure was damaged, which led to the decrease of photosynthetic capacity, and thus resulted in yield loss (Ren et al., 2016). Spraying phytase Q9 could increased the activities of SOD, CAT and POD (Huang et al., 2020). Our results also indicated that spraying 6-BA and phytase Q9 increased the activities of SOD, CAT and POD, and reduced the MDA content, which delayed the leaf senescence. We also found that the spraying effect on antioxidant systems of 6-BA was better than phytase Q9. Spraying exogenous hormones significantly alleviated the decline in anti-aging ability and photosynthetic productivity of fresh waxy maize under weak-light stress, thereby promoting dry matter accumulation and increasing the fresh ear and grain yield. Further research is needed on the hormone metabolism and molecular physiological mechanisms of exogenous regulators applied to improve the yield of fresh waxy maize under light stress.

Conclusions

The results showed that weak-light stress during the grain-filling stage severely limited photosynthetic production capacity by reducing the activity of enzymes involved in carbon and N metabolism, accelerating leaf senescence, and thereby reducing the accumulation of photosynthetic products, resulting in reduced yield in fresh waxy maize. The effect of weak-light stress was greater on JKN2000 than SYN5. Spraying exogenous phytase Q9 and 6-BA alleviated the decrease in carbon and nitrogen metabolism enzymes and antioxidant enzyme activities under weak-light stress, improved photosynthetic capacity, delayed leaf senescence, and thus increased dry matter and nitrogen accumulation, increasing yield. The improvement effect of 6-BA was more significant on JKN2000. These results indicated that in the actual production of

fresh waxy maize, 6-BA can be widely used as an effective regulator to alleviate weak-light stress.

Data availability statement

The raw data supporting the conclusions of this article will be made available by the authors, without undue reservation.

Author contributions

GL, WL, and DL designed the experiments. GL,WL, and YL did the field management. GL, WL, and WPL performed data analysis. GL, WL, and DL contributed to the preparation of the manuscript. All authors contributed to the article and approved the submitted version

Funding

This research was funded by the Natural Science Foundation of Jiangsu Province (BK20200952), National Natural Science Foundation of China (No.32101828), the Postgraduate Research and Practice Innovation Program of Jiangsu Province (SJCX22-1780), the Jiangsu Agricultural Industry Technology System of China (Grant No. JATS [2022]497) and the Priority Academic Program Development of Jiangsu Higher Education Institutions.

Conflict of interest

The authors declare that the research was conducted in the absence of any commercial or financial relationships that could be construed as a potential conflict of interest.

Publisher's note

References

Anjum, S. A., Wang, L., Farooq, M., Xue, L., and Ali, S. (2011). Fulvic acid application improves the maize performance under well-watered and drought conditions. *J. Agron. Crop Sci.* 197, 409–417. doi: 10.1111/j.1439-037X.2011.00483.x

Barnabás, B., Jäger, K., and Fehér, A. (2008). The effect of drought and heat stress on reproductive processes in cereals. *Plant Cell Environ.* 31, 11–38. doi: 10.1111/j.1365-3040.2007.01727.x

Che, H., Shi, G., Zhang, X., Arimoto, R., Zhao, J., Xu, L., et al. (2005). Analysis of 40 years of solar radiation data from china 1961–2000. *Geophys. Res. Lett.* 32. doi: 10.1029/2004GL022322

Chen, X., Li, G., Liu, P., Gao, H., Dong, S., Wang, Z., et al. (2013). Effects of exogenous hormone 6 benzyl adenine (6-BA) on photosystem II performance of maize during process of leaf senescence under different nitrogen fertilization levels. *Acta Agron. Sin.* 39, 1111–1118. doi: 10.3724/SP.J.1006.2013.01111

Chen, X., Wang, L., Niu, Z., Zhang, M., and Li, J. (2020). The effects of projected climate change and extreme climate on maize and rice in the Yangtze river basin, China. *Agric. For. Meteorol.* 282, 107867. doi: 10.1016/j.agrformet.2019.107867

Cui, H., Camberato, J. J., Jin, L., and Zhang, J. (2015). Effects of shading on spike differentiation and grain yield formation of summer maize in the field. *Int. J. Biometeorol.* 59, 1189–1200. doi: 10.1007/s00484-014-0930-5

Deng, F., Wang, L., Yao, X., Wang, J., Ren, W., and Yang, W. (2009). Effects of different-growing-stage shading on rice grain-filling and yield. *J. Sichuan Agric. Univ.* 27, 265–269.

Farooq, M., Bramley, H., Palta, J. A., and Siddique, K. H. (2011). Heat stress in wheat during reproductive and grain-filling phases. *Crit. Rev. Plant Sci.* 30, 491–507. doi: 10.1080/07352689.2011.615687

Gao, J., Shi, J., Dong, S., Liu, P., Zhao, B., and Zhang, J. (2018). Grain development and endogenous hormones in summer maize (Zea mays l.) submitted to different light conditions. *Int. J. Biometeorol.* 62, 2131–2138. doi: 10.1007/s00484-018-1613-4

Guo, J., Wang, Z., Wei, Q., Li, G., Yang, H., and Lu, D. (2023). Response of waxy maize (*Zea mays* l. var. ceratina kulesh) leaf photosynthesis to low temperature during the grain-filling stage. *Funct. Plant Biol.* 50, 335–346. doi: 10.1071/FP22252

Hu, J., Ren, B., Dong, S., Liu, P., Zhao, B., and Zhang, J. (2022). 6-benzyladenine increasing subsequent waterlogging-induced waterlogging tolerance of summer maize by increasing hormone signal transduction. *Ann. N. Y. Acad. Sci.* 1509, 89–112. doi: 10.1111/nyas.14708

Huang, X., Ren, B., Zhang, B., Liu, P., and Zhang, J. (2020). Effects of phytase Q9 on the yield and senescence characteristics of summer maize shaded in the field. *J. Appl. Ecol.* 31, 3433–3444. doi: 10.13287/j.1001-9332.202010.024

Javid, M. J., Sorooshzadeh, A., Sanavy, S. A. M. M., Allahdadi, I., and Moradi, F. (2011). Effects of the exogenous application of auxin and cytokinin on carbohydrate accumulation in grains of rice under salt stress. *Plant Growth Regul.* 65, 305–313. doi: 10.1007/s10725-011-9602-1

Jia, S., Li, C., Dong, S., and Zhang, J. (2011). Effects of shading at different stages after anthesis on maize grain weight and quality at cytology level. *Agric. Sci. China* 10, 58–69. doi: 10.1016/S1671-2927(11)60307-6

Kobata, T., Sugawara, M., and Takatu, S. (2000). Shading during the early grain filling period does not affect potential grain dry matter increase in rice. *Agron. J.* 92, 411–417. doi: 10.2134/agronj2000.923411x

Kumar, I., Swaminathan, K., Hudson, K., and Hudson, M. (2016). Evolutionary divergence of phytochrome protein function in zea mays PIF3 signaling. *J. Exp. Bot.* 67, 4231–4240. doi: 10.1093/jxb/erw217

Li, S., Song, M., Duan, J., Yang, J., Zhu, Y., and Zhou, S. (2019). Regulation of spraying 6-BA in the late jointing stage on the fertile floret development and grain setting in winter wheat. *Agron* 9, 546. doi: 10.3390/agronomy9090546

Li, W., Yan, S., Yin, Y., and Wang, Z. (2010). Starch granule size distribution in wheat grain in relation to shading after anthesis. *J. Agric. Sci.* 148, 183–189. doi: 10.1017/S0021859609990554

Liu, G., Yang, Y., Liu, W., Guo, X., Xue, J., Xie, R., et al. (2020). Leaf removal affects maize morphology and grain yield. *Agron* 10, 1–12. doi: 10.3390/agronomy10020269

Lu, D., Shen, X., Cai, X., Yan, F., Lu, W., and Shi, Y. (2014). Effects of heat stress during grain filling on the structure and thermal properties of waxy maize starch. *Food Chem.* 143, 313–318. doi: 10.1016/j.foodchem.2013.07.089

Ramanathan, V., and Feng, Y. (2009). Air pollution, greenhouse gases and climate change: global and regional perspectives. *Atmos. Environ.* 43, 37–50. doi: 10.1016/j.atmosenv.2008.09.063

Rauf, F., Ullah, M., Kabir, M. H., Mia, M., and Rhaman, M. S. (2022). Gibberellic acid enhances the germination and growth of maize under salinity stress. *Asian Plant Res. J.* 10, 5–15. doi: 10.9734/APRJ/2022/V10I3191

Ren, B., Cui, H., Camberato, J. J., Dong, S., Liu, P., Zhao, B., et al. (2016). Effects of shading on the photosynthetic characteristics and mesophyll cell ultrastructure of summer maize. *Sci. Nat.* 103, 1–12. doi: 10.1007/s00114-016-1392-x

Ren, B., Zhang, J., Dong, S., Liu, P., and Zhao, B. (2017). Regulations of 6-benzyladenine (6-BA) on leaf ultrastructure and photosynthetic characteristics of waterlogged summer maize. *J. Plant Growth Regul.* 36, 743–754. doi: 10.1007/s00344-017-9677-7

Roitsch, T., and Ehneß, R. (2000). Regulation of source/sink relations by cytokinins. *Plant Growth Regul.* 32, 359–367. doi: 10.1023/A:1010781500705

Saiya-Cork, K. R., Sinsabaugh, R. L., and Zak, D. R. (2002). The effects of long term nitrogen deposition on extracellular enzyme activity in an acer saccharum forest soil. *Soil Biol. Biochem.* 34, 1309–1315. doi: 10.1016/S0038-0717(02)00074-3

Schmitt, M. R., and Edwards, G. E. (1981). Photosynthetic capacity and nitrogen use efficiency of maize, wheat, and rice: a comparison between C3 and C4 photosynthesis. *J. Exp. Bot.* 32, 459–466. doi: 10.1093/jxb/32.3.459

Sharwood, R. E., Sonawane, B. V., and Ghannoum, O. (2014). Photosynthetic flexibility in maize exposed to salinity and shade. *J. Exp. Bot.* 65, 3715–3724. doi: 10.1093/jxb/eru130

Shi, K., Gu, X., Lu, W., and Lu, D. (2018). Effects of weak-light stress during grain filling on the physicochemical properties of normal maize starch. *Carbohydr. Polym.* 202, 47–55. doi: 10.1016/j.carbpol.2018.08.114

Sinclair, T. R., Pinter, P. J., Kimball, B. A., Adamsen, F. J., LaMorte, R. L., Wall, G. W., et al. (2000). Leaf nitrogen concentration of wheat subjected to elevated CO2 and either water or n deficits. *Agric. Ecosyst. Environ.* 79, 53–60. doi: 10.1016/S0167-8809(99)00146-2

Stanhill, G., and Cohen, S. (2001). Global dimming: a review of the evidence for a widespread and significant reduction in global radiation with discussion of its probable causes and possible agricultural consequences. *Agric. Meteorol.* 107, 255–278. doi: 10.1016/S0168-1923(00)00241-0

Sun, H., Li, W., Liang, Y., and Li, G. (2023). Shading stress at different grain filling stages affects dry matter and nitrogen accumulation and remobilization in fresh waxy maize. *Plants* 12, 1742. doi: 10.3390/plants12091742

Tollenaar, M., and Daynard, T. B. (1982). Effect of source-sink ratio on dry matter accumulation and leaf senesence of maize. *Can. J. Plant Sci.* 62, 855–860. doi: 10.4141/cjps82-128

Wang, J., Shi, K., Lu, W., and Lu, D. (2020). Post-silking shading stress affects leaf nitrogen metabolism of spring maize in southern China. *Plants* 9, 210. doi: 10.3390/plants9020210

Wei, H., Zhu, Y., Qiu, S., Han, C., Hu, L., Xu, D., et al. (2018). Combined effect of shading time and nitrogen level on grain filling and grain quality in japonica super rice. *J. Integr. Agric.* 17, 2405–2417. doi: 10.1016/S2095-3119(18)62025-8

Wen, Z., Shi, K., Lu, W., and Lu, D. (2019). Effects of postsilking weak-light stress on the flour quality of spring maize. *Cereal Chem.* 96, 742–753. doi: 10.1002/cche.10170

Yang, Y., Guo, X., Liu, H., Liu, G., Liu, W., Bo, M., et al. (2021b). The effect of solar radiation change on the maize yield gap from the perspectives of dry matter accumulation and distribution. *J. Integr. Agric.* 20, 482–493. doi: 10.1016/S2095-3119(20)63581-X

Yang, Y., Guo, X., Liu, G., Liu, W., Xue, J., Ming, B., et al. (2021a). Solar radiation effects on dry matter accumulations and transfer in maize. *Front. Plant Sci.* 12, 727134. doi: 10.3389/fpls.2021.727134

Yang, H., Shi, Y., Xu, R., Lu, D., and Lu, W. (2016). Effects of shading after pollination on kernel filling and physicochemical quality traits of waxy maize. *Crop J.* 4, 235–245. doi: 10.1016/j.cj.2015.12.004

Yang, Y., Xu, W., Hou, P., Liu, G., Liu, W., Wang, Y., et al. (2019). Improving maize grain yield by matching maize growth and solar radiation. *Sci. Rep.* 9, 3635. doi: 10.1038/s41598-019-40081-z

Yuan, Z., Wang, C., Li, S., Li, X., and Tai, F. (2014). Effects of different plant hormones or PEG seed soaking on maize resistance to drought stress. *Can. J. Plant Sci.* 94, 1491–1499. doi: 10.4141/cjps-2014-110

Zhang, C., Zhang, X., Kuzyakov, Y., Wang, H., Fu, X., Yang, Y., et al. (2020). Responses of c-, n- and p-acquiring hydrolases to p and n fertilizers in a subtropical Chinese fir plantation depend on soil depth. *Appl. Soil Ecol.* 150, 103465. doi: 10.1016/j.apsoil.2019.103465

Zhong, X., Shi, Z., Li, F., and Huang, H.. (2014). Photosynthesis and chlorophyll fluorescence of infertile and fertile stalks of paired near-isogenic lines in maize (*Zea mays* L.) under shade conditions. *Photosynthetica* 52, 597–603.

frontiers | Frontiers in Plant Science

TYPE Original Research
PUBLISHED 22 June 2023
DOI 10.3389/fpls.2023.1180734

OPEN ACCESS

EDITED BY
Jiwang Zhang,
Shandong Agricultural University, China

REVIEWED BY
Dalei Lu,
Yangzhou University, China
Congfeng Li,
Institute of Crop Sciences (CAAS), China

*CORRESPONDENCE
Laikun Xia
xialaikun@126.com
Wenchao Zhen
wenchao@hebau.edu.cn

†These authors have contributed equally to this work

RECEIVED 06 March 2023
ACCEPTED 06 April 2023
PUBLISHED 22 June 2023

CITATION
Gu L, Mu X, Qi J, Tang B, Zhen W and Xia L (2023) Nitrogen reduction combined with ET_c irrigation maintained summer maize yield and increased water and nitrogen use efficiency.
Front. Plant Sci. 14:1180734.
doi: 10.3389/fpls.2023.1180734

Nitrogen reduction combined with ET_c irrigation maintained summer maize yield and increased water and nitrogen use efficiency

Limin Gu[1,2], Xinyuan Mu[1], Jianshuang Qi[1], Baojun Tang[1], Wenchao Zhen[2,3*†] and Laikun Xia[1*†]

[1]Cereal Institute, Henan Academy of Agricultural Sciences, Zhengzhou, China, [2]State Key Laboratory of North China Crop Improvement and Regulation/Key Laboratory of Crop Growth Regulation of Hebei Province, College of Agronomy, Hebei Agricultural University, Baoding, China, [3]Key Laboratory of North China Water-saving Agriculture, Ministry of Agriculture and Rural Affairs, Baoding, Hebei, China

Introduction: High rainfall and excessive urea application are counterproductive to summer maize growth requirements and lower grain yield and water/nitrogen (N) use efficiency. The objective of this study was to determine whether ETc irrigation based on summer maize demand and reduced nitrogen rate in the Huang Huai Hai Plain increased water and nitrogen use efficiency without sacrificing yield.

Methods: To achieve this, we conducted an experiment with four irrigation levels [ambient rainfall (I0) and 50% (I1), 75% (I2), and 100% (I3) of actual crop evapotranspiration (ET_c)] and four nitrogen rates [no nitrogen fertilizer (N0), recommended nitrogen rate of urea (NU), recommended nitrogen rate of blending controlled-release urea with conventional urea fertilizer (BCRF) (NC), and reduced nitrogen rate of BCRF (NR)] in 2016–2018.

Results: The results show that reduced irrigation and nitrogen rate reduced Fv/Fm, ^{13}C-photosynthate, and nitrogen accumulation both in the kernel and plant. I3NC and I3NU accumulated higher ^{13}C-photosynthate, nitrogen, and dry matter. However, ^{13}C-photosynthate and nitrogen distribution to the kernel was decreased from I2 to I3 and was higher in BCRF than in urea. I2NC and I2NR promoted their distribution to the kernel, resulting in a higher harvest index. Compared with I3NU, I2NR increased root length density by 32.8% on average, maintaining considerable leaf Fv/Fm and obtaining similar kernel number and kernel weight. The higher root length density of I2NR of 40–60 cm promoted ^{13}C-photosynthate and nitrogen distribution to the kernel and increased the harvest index. As a result, the water use efficiency (WUE) and nitrogen agronomic use efficiency (NAUE) in I2NR increased by 20.5%–31.9% and 11.0%–38.0% than that in I3NU, respectively.

Discussion: Therefore, 75%ET_c deficit irrigation and BCRF fertilizer with 80% nitrogen rate improved root length density, maintained leaf Fv/Fm in the milking stage, promoted 13C-photosynthate, and distributed nitrogen to the kernel, ultimately providing a higher WUE and NAUE without significantly reducing grain yield.

KEYWORDS

blending controlled-release urea with conventional urea, deficit irrigation, summer maize, 13C-photosynthate distribution, nitrogen agronomic use efficiency, water use efficiency

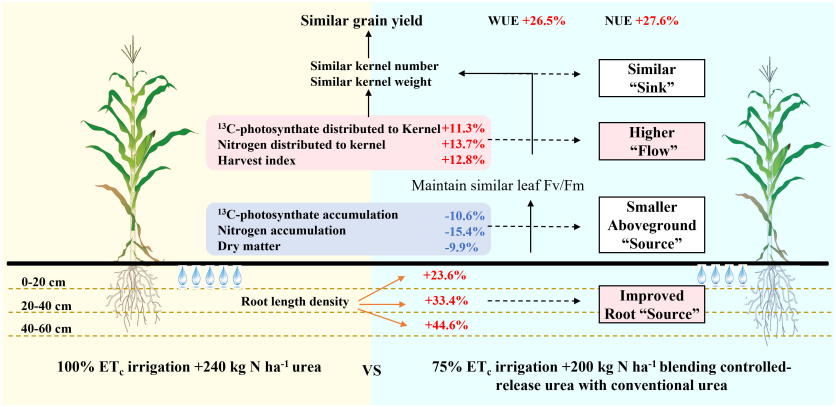

GRAPHICAL ABSTRACT
75%ETc deficit irrigation and BCRF fertilizer with 80% nitrogen rate improved root length density, maintained leaf Fv/Fm in the milking stage, promoted 13Cphotosynthate, and distributed nitrogen to the kernel, ultimately providing a higher WUE and NAUE without significantly reducing grain yield.

1 Introduction

Population expansion and climate change are generating water scarcity worldwide. As 70% of the fresh water supply is used by agriculture, water scarcity is a threat to the sustainability of agriculture (Mishra et al., 2021; Salehi, 2022). Increasing agricultural water use efficiency is a priority for food security and an effective way to mitigate water scarcity (Wang et al., 2019a). This problem is particularly serious in China, which hosts 6% of the world freshwater resources and feeds a significant amount of the world population.

With the greatest total output and acreage in China, maize is the most widely planted crop in the Huang-Huai-Hai Plain (Figure 1A), accounting for 35% of the national maize planting acreage and more than 40% of the corn grain output in China (Shu et al., 2021). Grown in the rainy season, summer maize received 310.0–536.4 mm of rainfall from 1961 to 2015 but only 115.5–166.0 mm of effective rainfall, which is significantly less than it requires (312.7–389.1 mm). Due to this misalignment between the rainfall and the maize's water demand (Tuan et al., 2011), local farmers must irrigate their crops two or three times each year to increase the maize yield. Flood irrigation averaging 90–100 mm of water increases evaporation loss and nitrogen leaching, reducing water and nitrogen use efficiencies while polluting the environment (Guo et al., 2010; Eekhout et al., 2018; Yu et al., 2019; Hou et al., 2021).

Deficit irrigation maximizes water productivity and achieves water delivery equal to or better than full irrigation cultivation (Zhang, 2003b; Geerts and Raes, 2009; Comas et al., 2019; Sandhu et al., 2019). Deficit irrigation reduces soil evaporation and regulates leaf stomatal opening to reduce transpiration water loss, maintaining high photosynthetic efficiency (Ullah et al., 2019; Jovanovic et al., 2020). Understanding maize water requirements is the basis of deficit irrigation strategy. Preliminary research demonstrated that maize water requirements varied by variety, weather, and soil conditions and that all these variables should be addressed when making irrigation decisions (Peng et al., 2019; Masupha and Moeletsi, 2020; Mirhashemi and Panahi, 2021). Nevertheless, the current irrigation strategy is mainly based on the field capacity (Guo et al., 2015; Liu et al., 2022a), ignoring crop requirements and meteorological conditions. Local stress irrigation based on surface irrigation (i.e., border irrigation) has a high single irrigation volume (approximately 60–120 mm) but low irrigation frequency, which is performed by two irrigations at the sowing and flowering stages (Wang et al., 2020). The high irrigation level induces higher soil evaporation between plants and the water

Abbreviations: WUE, water use efficiency; NAUE, nitrogen agronomic use efficiency; ^{13}C-AC, ^{13}C-photosynthate accumulation; ^{13}C-DR, ^{13}C-photosynthate distribution ratio; N-AC, nitrogen distribution accumulation; N-DR, nitrogen distribution ratio.

leachate (Srivastava et al., 2020; Yi et al., 2022). Currently, the most widely used conventional irrigation system is not compatible with advanced and efficient irrigation equipment, such as drip irrigation, sprinkler irrigation, or low-pressure pipe irrigation methods necessary to cover an area of $23{,}191\times10^3$ ha, 30.1% of the total irrigated area in 2020 in China (Ministry of Water Resources, 2020). It is critical, therefore, to investigate modern agricultural irrigation systems that are geared to water conservation, high land efficiency, and labor efficiency.

The crop evapotranspiration (ET_c) metric based on the FAO56 whitepaper is commonly used to make irrigation decisions, since it takes both crop requirements (growth phases) and climatic circumstances into account (Pereira et al., 2020). It also provides a precise and flexible irrigation schedule for an automatic or digital irrigation system, which is an excellent approach to cut labor expenses and water loss, and is accepted and employed by a growing number of farmers (Cancela et al., 2015). The majority of irrigation decision-making research has been conducted using models (Mancosu et al., 2016; López-Urrea et al., 2020), and the field performance of irrigation based on ET_c needs additional investigation. ET_c irrigation applied at 100% increases maize growth, net photosynthetic rate, and accumulation of dry matter (Guo et al., 2022). However, the effect of ET_c irrigation on photosynthetic transport, root length density, and water-saving potential of deficit ET_c irrigation on maize are currently unknown.

Numerous studies have demonstrated that soil moisture content and nitrogen availability have a complicated effect on crop yield (Sandhu et al., 2019). Irrigation that is appropriate for the soil could improve nitrogen use efficiency (NUE) by increasing nitrogen accumulation, translocation, and distribution (Yan et al., 2019). Blending controlled-release urea with conventional urea (BCRF) is both environment and economic friendly and has a wide range of applications (Vejan et al., 2021; Guo et al., 2022). Compared with urea, BCRF reduces N_2O emissions (Lyu et al., 2021) and nitrogen leachate (Adu-Gyamfi et al., 2019), meets crop nitrogen demands (Zheng et al., 2020), and increases photosynthetic efficiency (Guo et al., 2022), crop yield, and NUE (Zheng et al., 2016; Zhu and Zhang, 2016; Vejan et al., 2021). As a result, the optimal nitrogen rate for BCRF and ET_c irrigation levels may differ from the optimal nitrogen rate under standard irrigation and nitrogen management methods. While earlier research was focused on crop grain yield, water use efficiency (WUE), and NUE, the interplay between ET_c irrigation and BCRF on maize performance is less studied.

The purpose of this study was to (1) examine how reduced water and nitrogen input increase water and nitrogen use efficiency without compromising yield, (2) investigate the effect of deficit irrigation based on ET_c and BCRF on photosynthate accumulation and distribution, and (3) investigate the interaction between deficit ET_c irrigation and BCRF-dependent reduced nitrogen rates on WUE and NUE, to lay the groundwork for more precise irrigation and fertilization maize crop management strategies.

2 Materials and methods

2.1 Site and weather description

From 2016 to 2018, studies were conducted in the Henan Academy of Agricultural Sciences experimental base in Yuanyang, Henan Province, China (113°42′28.7′′N, 35°0′13.3′′E), 78 m above sea level). The regional climate is subhumid, warm temperate, continental, monsoon, and features four distinct seasons. This is a typical location on the Huang-Huai-Hai Plain (Figure 1A). The ET_c was calculated using weather data from 1983 to 2013 received from China's National Meteorological Information Center (climate data, Figure 2). Precipitation totaled 349.4, 193.6, and 239.4 mm during the maize growth period in 2016, 2017, and 2018, respectively.

The regional soil is fluvo-aquic, with 13.44 g kg^{-1} organic matter, 73.8 g kg^{-1} available N, 50.2 mg kg^{-1} available phosphate, and 134.5 mg kg^{-1} available potassium under a rainproof shelter and 13.86 g kg^{-1} organic matter, 86.13 g kg^{-1} available N, 53.5 mg kg^{-1} available phosphate, and 146.0 mg kg^{-1} available potassium in the field.

2.2 Experimental design

The experiment used a randomized complete block design with 16 treatments (4 irrigation levels and 4 nitrogen fertilizer

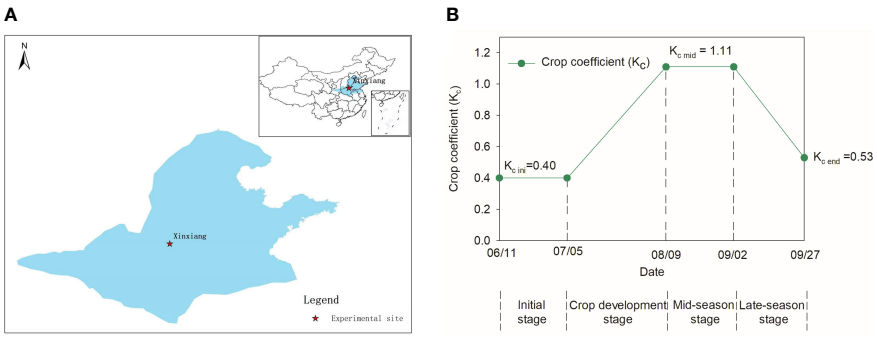

FIGURE 1
The experimental site in Huang-Huai-Hai maize region (blue area) of China **(A)** and the single crop coefficients K_c for the various development stages for summer maize in this experiment **(B)**.

treatments) in triplicate. The four irrigation levels were ambient rainfall (I0), 50% ET_c (I1), 75% ET_c (I2), and 100% ET_c (I3). The four nitrogen fertilizer treatments were as follows: no fertilizer (N0), urea with the recommended nitrogen rate (240 kg N ha^{-1}, NU), BCRF with the recommended nitrogen rate (240 kg N ha^{-1}, NC), and BCRF with a reduced nitrogen rate (200 kg N ha^{-1}, NR).

To avoid the potential impact of unforeseen rainfall on the experiment, maize, the experiment of I1, I2, and I3 was performed in microplots beneath an autonomously triple-folding rainproof shelter in 2016 and 2017. When it rained, the rainproof shelter was opened to cover the plots and keep the rain off. At other times, the rainproof shelter was stored adjacent to the experimental plots in an unoccupied location. The plants in I0 treatment received only rainfall with no supplemental irrigation from 2016 to 2018. In 2018, the experiment was conducted in a field 300 m away. That is, the water input in I0 was only rainfall in three maize seasons; the water input in I1, I2, and I3 in 2016 and 2017 under rainproof shelter was only irrigation; while water input in I1, I2, and I3 in field in 2018 was the sum of irrigation and rainfall.

The microplot was 2.9 m × 1.9 m in size, and the field plot was 4.2 m × 6.7 m in size. In 2016, 2017, and 2018, summer maize (Zhengdan 309, a national maize variety suitable for harvesting grain mechanically) was planted on June 16, June 16, and June 17 and harvested on September 30, October 3, and October 5, respectively. A precision irrigation equipment irrigated the maize. The previous crop, winter wheat, was irrigated fully and fertilized with no nitrogen to achieve identical soil moisture and nitrogen concentrations between microplots before planting maize. The maize was planting in 75,000 plans ha^{-1} with 60 cm plant row spacing. Pest, disease, and weed control strategies were similar to those used regionally.

2.2.1 Irrigation regime

Actual crop evapotranspiration (ET_c) was determined by the following formula:

$$ET_c = ET_0 \times K_c$$

ET_0 is averaged daily reference evapotranspiration (mm), calculated using daily meteorological data from 1983 to 2013 (from the National Meteorological Information Center of China) with the ET_0 calculator (Food and Agriculture Organization (FAO56). K_c is the crop coefficient, determined by the FAO56 guidelines. The lengths of the crop development phases for the initial stage, development stage, mid-season stage, and late-season stage were 26, 34, 24, and 20 days, respectively, according to FAO56. The K_c values for the initial stage, mid-season stage, and end of the late-season stage were 0.4, 1.11, and 0.53, respectively (Figure 1B).

The irrigation amounts for I1, I2, and I3 were calculated as follows:

$$I1 = 50\,\%\ ET_c - P_e$$

$$I2 = 75\,\%\ ET_c - P_e$$

$$I3 = 100\,\%\ ET_c - P_e$$

P_e is the effective precipitation amount (mm), and ET_c is the actual crop evapotranspiration. P = 0 for I1, I2, and I3 in 2016 and 2017 under rain shelter when it rains. P_e was calculated as P_e=a×P, in which a was 0, 1.0, and 0.75 when the precipitation<5 mm, 5 mm≤precipitation ≤ 50 mm, and precipitation >50 mm, respectively.

For both the microplot and field tests, 44.1 mm of water was irrigated after sowing to enable maize seedling emergence. Aside from the sowing irrigation, the plants were irrigated at the V6, V12, VT, R2, and R4 stages. The irrigation amounts and the precipitation levels at different irrigation levels in 2016–2017 and 2018 are shown in Tables 1, 2.

2.2.2 Fertilizer management

Four fertilizer treatments were tested: (i) a quick-release urea (46% N) with a 240 kg N kg^{-1} application rate, (ii) a BCRF (26% N, 10% P_2O_5, and 9% K_2O; Kingenta; controlled-release fertilizer: quick-acting fertilizer = 1:1) with a 240 kg N kg^{-1} application rate (NC), (iii) a BCRF with a 200 kg N kg^{-1} application rate (NR), and (Srivastava et al.) no nitrogen fertilizer (N0). All plots had the same phosphate and potassium rates of 150 kg P_2O_5 kg^{-1} and 120 kg K_2O kg^{-1}, respectively. Calcium superphosphate (12.0% P_2O_5) and potassium chloride (52.0% K_2O) fertilizers were used to compensate for the deficiency of phosphate and potassium. As a basal fertilizer, 100% BCRF, 50% urea, 100% calcium superphosphate, and potassium chloride fertilizer were applied. At the tasseling stage (VT), urea (50%) was applied as a

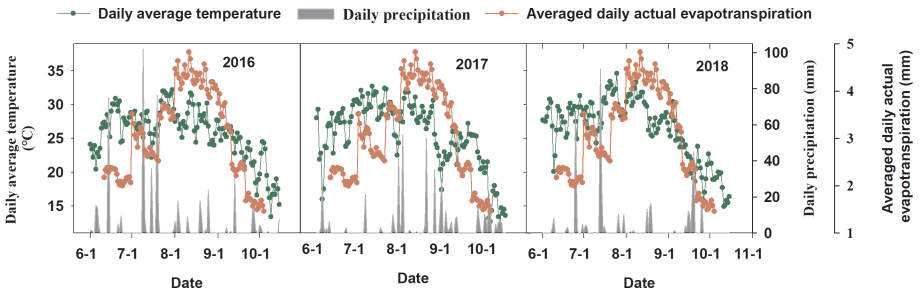

FIGURE 2
Daily mean temperature (°C) and precipitation (mm) during the summer maize season in 2016–2018 and the average daily actual evapotranspiration from 1983 to 2013.

10.3389/fpls.2023.1180734

TABLE 1 Irrigation volume of different irrigation levels at various summer maize growth stages in 2016 and 2017.

Item	Growth stage	Irrigation amount (mm)			
		I0	I1	I2	I3
Irrigation amount (mm)	Sowing	44.1	44.1	44.1	44.1
	V6	0	20.9	31.4	41.8
	V12	0	27.4	41.1	54.8
	VT	0	30.8	46.2	61.6
	R2	0	35.6	53.4	71.2
	R4	0	31.1	46.6	62.1
Irrigation total		44.1	189.9	262.8	335.6
Precipitation *	2016	349.4	0	0	0
	2017	193.6	0	0	0
Irrigation +precipitation	2016	393.5	189.9	262.8	335.6
	2017	237.7	189.9	262.8	335.6

*Precipitation in the whole growing season.

TABLE 2 Precipitation and irrigation volume of different irrigation levels at various summer maize growth stages in 2018.

Growth stage	Irrigation amount (mm)				Precipitation * (mm)
	I0	I1	I2	I3	
Sowing	44.1	44.1	44.1	44.1	87.6
V6	0	0	0	0	143.4
V12	0	0	0	0	15.6
VT	0	15.2	30.6	46	31.8
R2	0	3.8	21.6	39.4	111.4
R4	0	0	0	0	0
Total irrigation	44.1	63.1	96.3	129.5	–
Irrigation +precipitation	433.9	452.9	486.1	519.3	389.8

*Precipitation during the previous growth stage.

topdressing fertilizer. Winter wheat was planted prior to maize, and it was fertilized with nitrogen-free fertilizer to maintain a same soil nitrogen content prior to planting maize.

2.3 Sampling, measurements, and calculations

2.3.1 Meteorological data

Meteorological data, including rainfall, temperature, air humidity, and wind speed, were obtained automatically at a station 200 m from the trial site.

2.3.2 Labeling of selected plants with $^{13}CO_2$

Six representative plants from each plot were selected and labeled with $^{13}CO_2$ on silking stage. Ear leaves of each plant were covered in 0.1-mm thick mylar plastic bags, which permitted up to 95% of natural sunlight intensity. After sealing the bags at the base with Plasticine, 50 ml of $^{13}CO_2$ was injected. After 60 min, the $^{13}CO_2$ in each bag was extracted using a KOH washer to remove any residual radioactive $^{13}CO_2$, and the plastic bag was removed (Liu et al., 2015).

2.3.3 Dry matter, ^{13}C-photosynthate distribution ratio, and nitrogen distribution ratio among plant organs

The labeled plants were collected at physiological maturity and dissected into leaves, stem, sheath, ear bract, cob, and grain. The harvest index was calculated as the ratio of grain dry matter to total plant dry matter. All separated components were oven-dried to a constant weight at 80°C, weighed to determine dry matter (g plant^{-1}), and then milled into a powder. Subsamples of 4 mg were used to determine the isotopic abundance using an Isoprime 100 instrument (Isoprime 100, Cheadle, UK). Subsamples were

digested using an H_2SO_4–H_2O_2 method (Thomas et al., 1967), and total nitrogen was measured using a continuous flow autoanalyzer (AA3, SEAL Analytical, Germany). The ^{13}C-photosynthate accumulation (^{13}C-AC) and distribution ratio (^{13}C-DR) among different plant organs at physiological maturity (%/plant) and the nitrogen distribution accumulation (N-AC) and distribution ratio (N-DR) were calculated.

2.3.4 Ear leaf Fv/Fm and root length density

Using a continuous excitation fluorometer Pocket Plant Efficiency Analyzer (PEA, Hansatech, UK), the Fv/Fm of six representative ear leaves at the silking stage (R1) and milk stage (R3) were determined under dark conditions for 15 min. Three maize plants in each treatment were selected to evaluate root length density at the anthesis stage. In the 0–60-cm soil layer, a block of soil surrounding the plant (60 cm long, 22 cm wide, 20 cm deep; 26,400 cm^3) was removed for each plant sample. The root samples were carefully cleaned of non-root material. Root lengths were measured using WinRHIZO (Regent Instruments Inc., Canada) after the fresh roots were scanned using an Epson Perfection V800 scanner. Root length density was calculated by dividing root length by soil volume (26,400 cm^3).

2.3.5 Yield and harvest index

All ears in each plot were collected at the physiological maturity to investigate the yield and yield components. For each harvested ear, the kernel number per plant (KNP) was counted. Three 1,000-kernel samples were oven-dried at 80°C to a consistent weight and weighed to determine the kernel weight (KW). To determine grain yield, all kernels were air-dried, and grain yield was expressed at 14% moisture content.

2.3.6 Nitrogen agronomic use efficiency and water use efficiency

The nitrogen agronomic use efficiency (NAUE, kg kg N^{-1}) was calculated as follows:

$$\text{NAUE} = (Y_{\text{fertilizer N}} - Y_{N0})/\text{nitrogen rate}$$

$Y_{\text{Fertilizer N}}$ is the grain yield (kg ha^{-1}) for the nitrogen fertilizer treatment (NC, NR, and NU), and Y_{N0} is the grain yield for the N0 treatment. The nitrogen rate was the nitrogen fertilizer applied for the nitrogen fertilizer treatment.

The water use efficiency (WUE, kg m^{-3}) was calculated as follows:

$$\text{WUE} = Y/ET$$

$$ET = \rho W + I + P - R - D$$

Y is the grain yield (kg ha^{-1}), ET is evapotranspiration (mm), ρW is variation in soil water storage in the 0–100-cm soil layer between planting and maturity, I is the water input (the sum of irrigation, mm), and P is precipitation (i.e., rain in our study). R is the water lost to runoff from the ground surface, which was zero in this experiment due to the borders for each plot in both canopied (2016–2017) and in open-field (2018) microplots. D is deep percolation from the soil, which was ignored due to the low amount of irrigation in 2016 and 2017.

2.4 Statistical analyses

Data were analyzed using Microsoft Excel 2016 and mapped using Sigma Plot 10.0 and Origin 2021. The SAS software system for Windows 9.0 (SAS Institute, Cary, NC, USA) was used to perform analyses of variance (ANOVAs). An ANOVA was performed among all the irrigation and nitrogen treatments for grain yield, yield components, dry matter, harvest index, WUE, and NAUE (p<0.05). The multiple comparison procedure (SSR) test with Bonferroni correction for all treatments was used for multiple comparisons.

3 Results

3.1 Yield, dry matter, and harvest index

Irrigation, nitrogen fertilizer, and their interaction all had a substantial impact on the kernel number per ear, kernel weight, grain yield, dry matter, and harvest index (Table 3). The yield and dry matter increased with irrigation level, but there was no significant difference between the yields of I2 and I3. Compared with I3, I0 and I1 significantly decreased the kernels number per ear and kernel weight. I2 had a lower KNP but higher kernel weight than I3. For the same irrigation levels in I2 or I3, the kernels number per ear and kernel weight of three nitrogen fertilizers show the trend that NC>NR>NU, but there was no significant difference either between NC and NR or between NR and NU.

The harvest index rose with irrigation level, then subsequently fell with I2 representing the peak. The HI was highest in NR and lowest in NU. Over three seasons, the plants in I2NR produced a similar yield to those in I3NC treatments despite having a lower dry matter but a higher harvest index.

3.2 The ^{13}C-photosynthate/nitrogen accumulation and distribution ratio

The irrigation, nitrogen fertilizer, and their interaction had a significant effect on ^{13}C-photosynthate/nitrogen accumulation and distribution ratio (Supplementary Table S1). The ^{13}C-AC and N-AC of the plant and kernel increased with the irrigation level from I1 to I3, and nitrogen rate from 0 to 240 kg N ha^{-1} in the three growth seasons (Figure 3). Although there was no discernible difference between NU and NC in 2016, I3NC had the greatest ^{13}C-AC and N-AC of the plant and kernel, followed by I3NU, I2NC, and I2NU.

^{13}C-DR and N-DR both increased when irrigation level increased from I1 to I2, while they decreased from I2 to I3. The ^{13}C-DR of N0 was higher than that of NC, NU, and NR. Whereas the N-DR of N0 was lower than NC, NU, and NR. For the nitrogen fertilized treatments, the ^{13}C-DR and N-DR in the kernels was

TABLE 3 Effect of irrigation and nitrogen fertilizer on the grain yield, yield components, dry matter, and harvest index for summer maize in 2016–2018.

Treatment	2016					2017					2018				
	KNP	KW (g)	Yield(kg ha^{-1})	Dry matter(kg ha^{-1})	HI(%)	KNP	KW (g)	Yield (kg ha^{-1})	Dry matter (kg ha^{-1})	HI(%)	KNP	KW (g)	Yield (kg ha^{-1})	Dry matter (kg ha^{-1})	HI (%)
I0N0	264fg	263.3f	4430.6i	9657.4g	45.9e	267.3e	246.3d	4196.4h	9207.5h	43.3e	297.3g	258.8e	4899.9f	11765.9j	41.6g
I0NC	344bcd	303bc	6645.4d	13295.5bc	50.1bcd	314c	287.5b	5753.9d	10612.3def	51.5ab	384.7e	289.8c	7106d	16015.8f	44.4ef
I0NR	332cde	298.5c	6317.7e	12734.7cd	49.7bcde	309cd	287.4b	5660.5de	10440efg	51.5ab	391.7e	280.8cd	7012.2d	15328.4gh	45.8de
I0NU	324de	301.9bc	6231.9e	13099.9c	47.6de	310cd	288.6b	5703.7de	10902.7de	49.7bc	390.7e	282.9cd	7045.3d	16072.7f	43.8f
I1N0	240g	239.8g	3668.8j	7464h	49.3bcde	267.7e	246.4d	4202.4h	9074.5h	44.0e	363.3f	275.3d	6378.1e	13935.2i	45.7de
I1NC	332cde	279.1d	5905.2f	11326.4e	52.1bc	314.7c	283.2b	5680de	10619.3def	50.8ab	446.0c	313.6b	8914.4c	19478.7e	45.8de
I1NR	316e	273.9de	5517.3g	10699.1f	51.6bc	310.3cd	280.5b	5548.6ef	10267.9fg	51.3ab	444.7c	315.3b	8934.4c	19027e	47cd
I1NU	308e	272.2de	5344.2g	10966.8ef	48.8cde	306.3cd	281.1b	5486f	10957d	47.6cd	448.7c	305.6b	8738.3c	19419.3e	45ef
I2N0	276f	272de	4781.7h	9359.1g	51.1bcd	296.7d	265.1c	5012.6g	9965g	47.8cd	395.8e	282.1cd	7116.7d	14920.6h	47.7bc
I2NC	372ab	314.4a	7454.7a	13198.4c	56.5a	348.3ab	308.1a	6841.1ab	12604.7b	51.5ab	482.9b	338.7a	10427.5ab	21456.8bc	48.6bc
I2NR	367.3ab	308.9ab	7233b	12369d	58.5a	344.3b	307.3a	6743.7b	12090.9c	53.0a	480b	334.8a	10244.8ab	20261d	50.6a
I2NU	346bcd	311.2a	6929.7c	13003.8c	52.7b	336.3b	307a	6581.5c	12445.2bc	50.2b	482.3b	330.1a	10149.4b	21144.8c	48bc
I3N0	280f	268.8ef	4796.7h	9819.7g	48.9bcde	302cd	259c	4984.4g	10000.2g	47.4cd	411.6d	274.8d	7213.3d	15728.2fg	45.9de
I3NC	376.7a	311.6a	7479.6a	14378.2a	52bc	360a	303.6a	6966.2a	13472.3a	49.1bcd	500.2a	332.6a	10605.1a	22208.9a	47.7bc
I3NR	368ab	307.3ab	7193.1b	13841.7ab	52bc	350ab	301a	6715.8bc	12471.3bc	51.2ab	490.1ab	330.4a	10324ab	21099.1c	48.9ab
I3NU	354.7abc	310.8a	7001.1c	14338.9a	49.1bcde	340b	303.6a	6580.1c	13362.5a	46.8d	490.7ab	330.1a	10326.5ab	21667.6b	47.7bc
Two-factor ANOVA															
F value (Irrigation)	24.9**	171.2**	513.6**	165.3**	21.7**	70.7**	77.5**	505.2**	193.3**	7.5**	349.9**	111.1**	465.4**	1018**	50.8**
F value (Nitrogen)	91.0**	241.4**	1243.3**	367.8**	13.6**	91.4**	245.5**	920.2**	206.8**	54.4**	280.3**	134.5**	426.3**	1302.4**	16.0**
F value (Irrigation ×Nitrogen)	0.3ns	0.5ns	5.4**	3.6**	4.9**	0.4ns	3.4**	4.4**	7.8**	3.7**	1.1ns	4.1**	4.0**	10.6**	3.5**

KNP, KW and HI were kernel number per ear, 1000-kernel weight, and harvest index, respectively. Irrigation × Nitrogen was the interaction of irrigation and nitrogen fertilization. The value underlined was significantly higher than other treatments. Different letters in the same column indicate significant differences at the 0.05 level. *: significant at P ≤ 0.05; **: significant at P ≤ 0.01, NS: not significant at P ≤ 0.05.

10.3389/fpls.2023.1180734

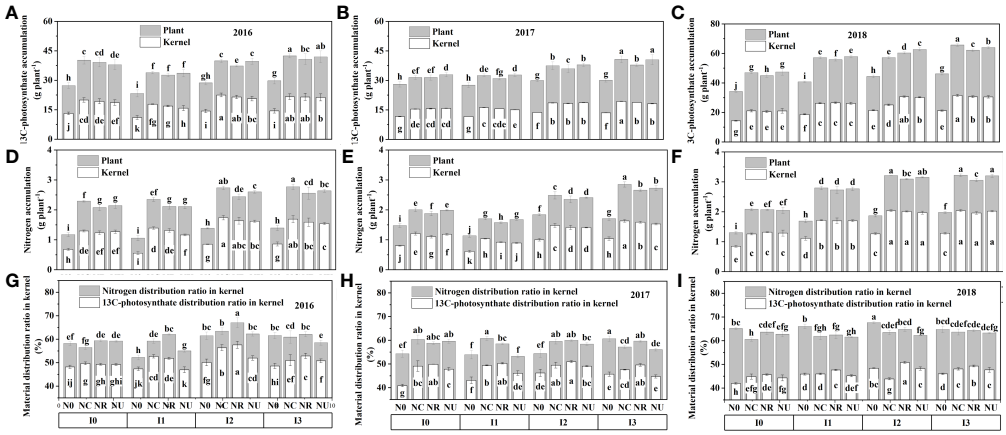

FIGURE 3
The effect of irrigation and nitrogen fertilizer on the 13C-photosynthate accumulation **(A–C)**, nitrogen accumulation **(D–F)**, and 13C-photosynthate distribution ratio and nitrogen distribution ratio **(G–I)** in the kernel at physiological maturity. The relative data in 2016 is shown in panels **(A, D, G)**; in 2017, panels **(B, E, H)**; and in 2018, **(C, F, I)**. Different letters in the same figure indicate significant differences at the 0.05 level.

higher in I2NR in 2016 and 2017 with no significant difference between I2NC, I2NR, and I3NC; that is, the BCRF fertilizer promoted the distribution of ^{13}C-photosynthate and nitrogen to the kernel. Thus, a higher ^{13}C-AC and N-AC were obtained in the I3NC and I3NU treatments, and the highest ^{13}C-DR and N-DR in the kernel were obtained in I2NR.

3.3 Root length density

There was a significant effect of irrigation treatment and nitrogen fertilizer on root length density (Supplementary Table S1). The root length density of 0–20 cm, 20–40 cm, and 40–60 cm accounted for 68.4%–76.4%, 18.8%–24.3%, and 4.3%–7.5% of total root length density (Figure 4). Root length density of either soil layer was increased with irrigation level from I0 to I2 and decreased from I2 to I3. In 0–60 cm, root length density was higher in NC and NR than in NU under the same irrigation level, while the difference was not statistically significant. There was no significant difference between root length density of NR and NC, except that NR was higher than NC under I2 and I1 irrigation levels at 40–60-cm soil layer. The I2NR treatment achieved the maximum root length density in the 0–20-cm and 40–60-cm soil layers, whereas I2NR, I2NC, and I2NU treatments achieved the highest root length density in the 20–40-cm soil layer. These results imply that (1) compared with urea, BCRF could improve maize root length density, and (2) Root length density of I2NR in the 0-60-cm soil layer, particularly in the 40-60-cm layer, was much higher than that of I3NC or I3NR.

3.4 Maximum photochemical efficiency of photosystem II (Fv/Fm)

Irrigation and nitrogen fertilizer management both had a significant impact on the Fv/Fm ratio (Supplementary Table S1). There was no significant difference between the Fv/Fm of NC, NR, and NU treatments, but the Fv/Fm for NC, NR, and NU were

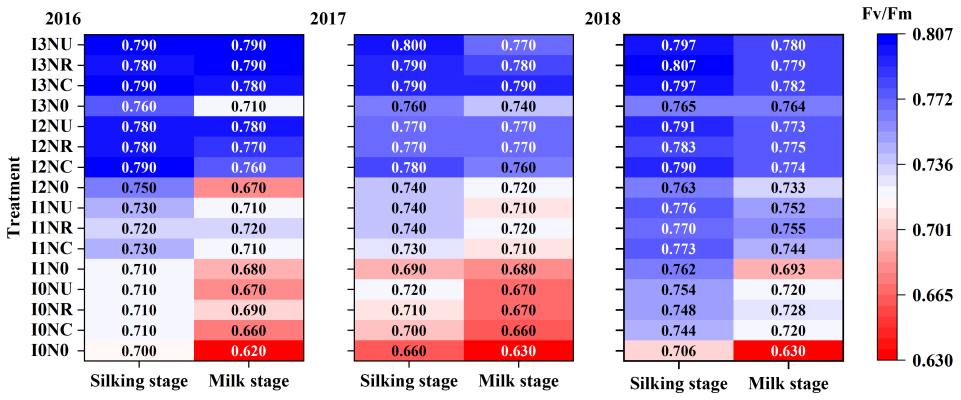

FIGURE 4
Effect of irrigation and nitrogen fertilizer on Fv/Fm at the silking stage and milk stage in 2016, 2017 and 2018.

significantly higher than that for N0 (Figure 5). With the application of nitrogen fertilizer, the I3 treatment had the highest Fv/Fm at the silking stage growth stage, followed by I2, I1, and I0. The Fv/Fm decreased significantly from silking stage to the milk stage, with average decreases of 6.2%, 3.1%, 2.6%, and 1.7% for I3, I2, I1, and I0, respectively. At the milk stage, Fv/Fm values were increased with irrigation level, but there was no significant difference between Fv/Fm values of I3 and I2. It may be concluded that irrigation at I3 and I2 benefited for maintaining a higher Fv/Fm of the ear leaves.

3.5 Evapotranspiration and water use efficiency

Along with the amount of rainfall, ET was highest in 2018 (442.8–532.8 mm) and lowest in 2017 (180.4–336.0 mm) (Figure 6). Both irrigation and nitrogen fertilizer and their interaction had an impact on ET, but the effect of irrigation was higher than that of nitrogen fertilizer. The ET was increased with irrigation or rainfall showing increased from I1 to I3 (Figure 6). The ET of nitrogen fertilizer treatments was highest in NC, followed by NR and NU, and was lowest in N0 (Figure 6). Maize grain yield showed a parabolic trend of opening downward as ET increased. The WUE was highest obtain in I1 in 2016 and 2017 but highest in I2 in 2018 (Table 4). Similar to yield, the WUE was highest in NC, but the difference between NC with NR or NU was significant in 2016.

3.6 Nitrogen use efficiency

Irrigation and nitrogen fertilizer management have a considerable impact on NAUE (5.3–15.6 kg N^{-1}) (Table 4). The NAUE increased with irrigation level from I1 to I2, but there was no significant difference between I2NC, I2NR, I3NC, and I3NR in 2017. The NAUE of the NC and NR was significantly higher than the NU by 15.25% and 27.20% averagely, where there was no significant difference between the NAUE of NC and NR.

3.7 Correlation analysis

Correlation analysis (Figure 7) revealed that the ^{13}C-AC, N-AC, Fv/Fm, and root length density were all significantly and positively linked with grain yield, KNP, 1,000 KW, and WUE (p<0.05). The ^{13}C-AC and N-AC of kernel were linearly related to kernel number per kernel, kernel weight, ET, and NAUE (Figure 8). The harvest index was increased linearly with the increase in ^{13}C-DR and N-DR of kernel, except harvest index versus N-DR in 2018.

4 Discussion

4.1 Effect of irrigation and nitrogen fertilizer on ^{13}C-photosynthate and nitrogen accumulation and distribution and harvest index

Maize grain yield is determined by dry matter and harvest index. The accumulation of dry matter is mostly determined by photosynthesis production, while the harvest index is primarily determined by the partitioning of photosynthate and biomass to kernels (Sinclair, 1998; Allison, 2010). ^{13}C-labeled CO_2 is an effective method for studying the accumulation and distribution characteristics of photosynthetic assimilate (Nouchi et al., 1995; Tremblay et al., 2012; Ren et al., 2021). ^{13}C-photosynthate allocation to grain is positive for kernel weight and grain yield (Liu et al., 2015; Ren et al., 2021). In this study, both ^{13}C-photosynthate and nitrogen accumulation in the kernel was positively related to kernel number per spike, kernel weight, and grain yield. Their distribution ratio to the kernel were found to be linearly related to harvest index. Increasing the harvest index was the primary strategy to increase maize grain yield at lower yield levels (<15 Mg ha^{-1}) (Liu et al., 2020). Thus, management that increases the accumulation and distribution of ^{13}C-photosynthate and nitrogen to the kernel could ultimately improve grain yield.

Researchers have demonstrated that ^{13}C-photosynthate allocation to grain increased with nitrogen fertilizer (Wei et al., 2019; Ren et al., 2021) but decreased when the nitrogen rate exceeded the acceptable

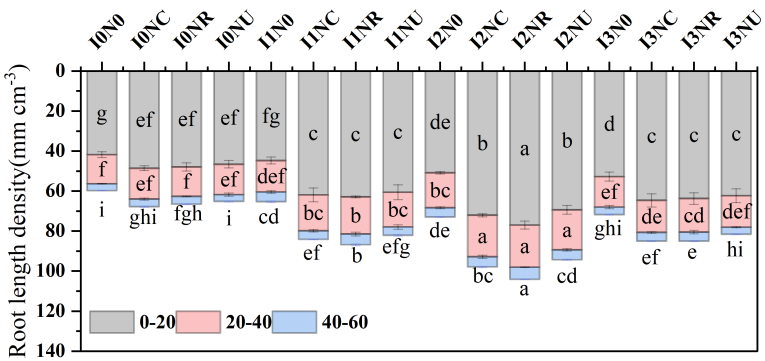

FIGURE 5
Effect of irrigation and nitrogen fertilizer on root length density. Different letters on the gray, pink, and blue histograms indicate significant differences at the 0.05 level.

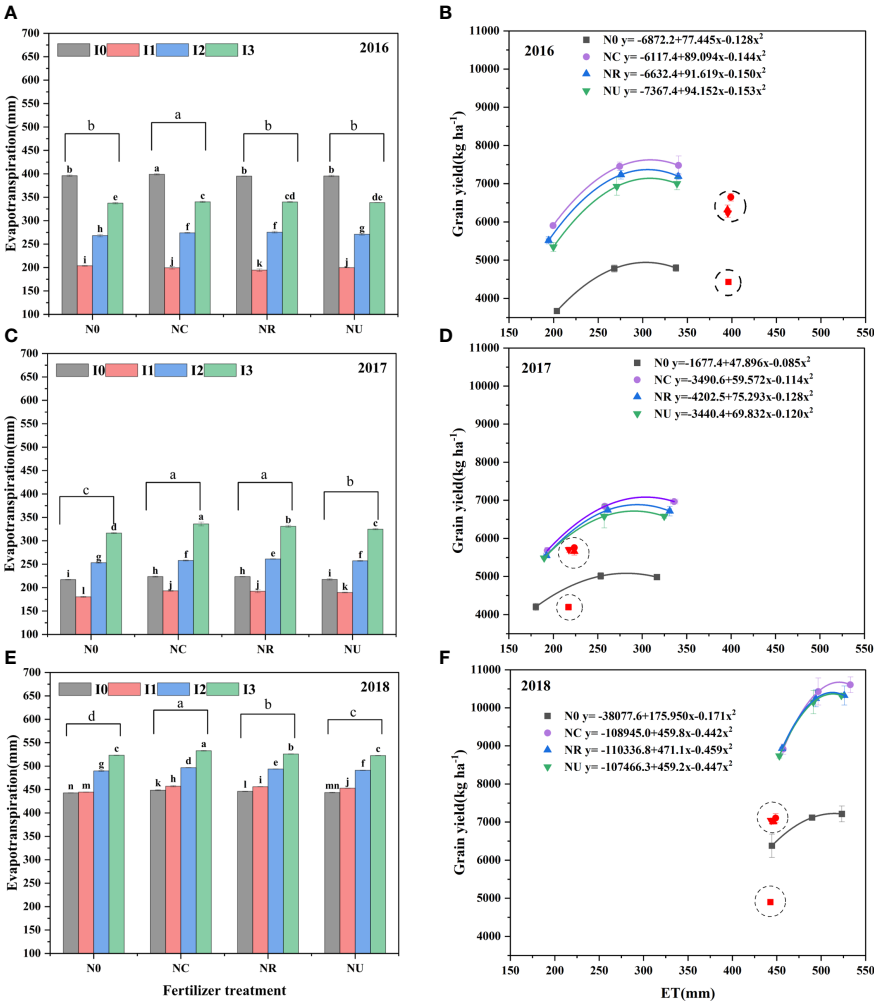

FIGURE 6
Effect of irrigation and nitrogen fertilizer on evapotranspiration and the relationship between grain yield and evapotranspiration. The data of I1, I2, and I3 were used to fit curves. Different letters on the gray, pink, and blue histograms indicate significant differences at the 0.05 level **(A, C, E)**. The curve with lines in blank, purple, blue, and green color was fitted with data of N0, NC, NR, and NU, **(B, D, F)** respectively.

rate (Zhang et al., 2021c). In this study, the nitrogen fertilization improved the ^{13}C-photosynthate and nitrogen accumulation and nitrogen distribution ratio to the kernel but reduced the ^{13}C-photosynthat distribution ratio to the kernel Figure 3).

In addition, ^{13}C-photosynthate and nitrogen accumulation and distribution characteristics were influenced by fertilizer type. Compared with common urea, controlled-release fertilizers and BCRF increased dry matter and nitrogen accumulation per plant and promoted its distribution to kernel (Zhao et al., 2010; Vejan et al., 2021). In this study, The NC treatment had a higher LAI and SPAD (not shown in this paper) (higher source) and a similar Fv/Fm value to the NU, resulting in a higher ^{13}C-AC and N-AC. The increased DM, ^{13}C-AC, N-AC, ^{13}C-DR, and N-DR in the BCRF treatments showed that the BCRF facilitated carbohydrate and nitrogen accumulation in plant tissue and subsequent remobilization to the kernels, resulting in an increased kernel per spike, kernel weight, and harvest index (Figure 8). These results are consistent with previous research (Qu et al., 2020; Guo et al., 2022). Compared with urea, plants grown with BCRF fertilizers had a similar "sink" (similar KNP and 1000 KW) but a greater "source" (Fv/Fm, ^{13}C-AC, and N-AC) and higher "flow" (^{13}C-DR, N-DR, and HI), resulting in more carbohydrate and nitrogen accumulation in the kernels and a higher yield (Graphical abstract).

4.2 Effect of irrigation and nitrogen fertilizer on root length density

Irrigation and nitrogen supply are the two important factors affecting the formation and development of the maize root system (Ning et al., 2015; Chilundo et al., 2017), and an active and deep rooting system was found to be favorably associated with water and nitrogen extraction and grain yield (Aina and Fapohunda, 1986). Root development rates were critical in enhancing plant biomass and cob yield under conditions of deficit irrigation (Flynn et al., 2020). In maize, a mild soil water deficit (50%–60%) resulted in the development of longer lateral roots and an increased root to shoot ratio (Kang et al., 2000), but severe water stress had an adverse effect

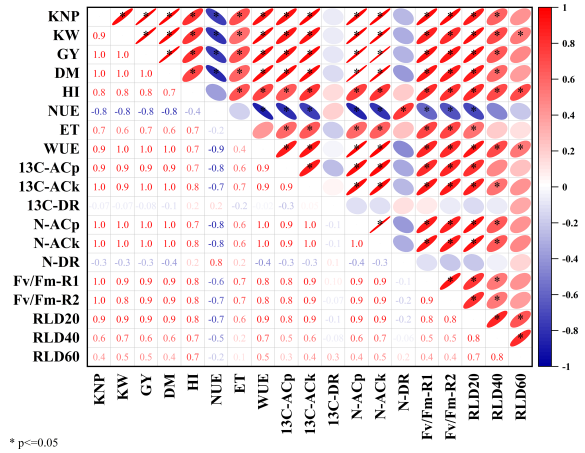

FIGURE 7
Correlation coefficients between maize grain yield, dry matter, ^{13}C-photosynthate and nitrogen accumulation and distribution characteristics, leaf maximum photochemical efficiency of photosystem II, root length density, and nitrogen and water use efficiency. KNP, kernel number per ear; KW, kernel weight; GY, grain yield; NI, harvest index; NUE, nitrogen agronomic use efficiency; ET, evapotranspiration; WUE, water use efficiency; 13C-ACp, 13C-photosynthate accumulation in plant; 13C-ACk, 13C-photosynthate accumulation in kernel; 13C-DR, 13C-photosynthate distribution ratio in kernel; N-ACp, nitrogen accumulation in plant; N-ACk, nitrogen accumulation in kernel; N-DR, nitrogen distribution ratio in kernel; Fv/Fm-R1 and Fv/Fm-R2, maximum photochemical efficiency of photosystem II (Fv/Fm) in silking stage and milk stage, respectively; RLD20, RLD40 and RLD60, root length density for 0-20cm, 20-40cm and 40-60cm, respectively.

on lateral root spread (Sampathkumar et al., 2012). In this study, root length density increased from I1 to I2 and decreased from I2 to I3. Compared with I2, the I1 and I3 treatments reduced root length density by 9.0%–14.6% and 10.6%–24.4%, respectively. In other words, both excessive and deficient irrigation amount may inhibit root elongation. In this study, maize plants in deficit irrigation increased root depth (increased root length density) and water extraction from deeper soil profiles (Li et al., 2022) while simultaneously decreasing leaf area to minimize transpiration, resulting in lower water consumption (Pandey et al., 2000).

In the cold–dry season, the effect of irrigation on root density was weaker than fertilizer type, and slow-release fertilization resulted in overall higher root density, above-ground biomass, and grain yield than quick-release fertilization (Chilundo et al., 2017). In this study, nitrogen fertilizer had a significant impact on root length density, increasing from 0 kg N ha^{-1} to 200–240 kg N ha^{-1}, but the effect was less than that observed with changes in irrigation. Compared with I3NU treatment, I2NR treatment increased root length density by 26.4% in 0–60-cm soil layer and by 41.0% in 40–60 cm. The result was consistent with other studies (Flynn et al., 2020; Halli et al., 2021). Appropriate water and nitrogen deficiency induced root elongation in search of more water and nutrients. The moderate water-stress and low nitrogen rate treatments resulted in an optimal root distribution defined by increased root length density and a bigger and deeper penetration scale throughout the soil layers, resulting in fewer drought responses and the best WUE and NUE (Wang et al., 2019b). Additionally, the root length density of BCRF fertilizers was greater than that of urea in this investigation, both at the same and reduced nitrogen rates. The blend product consistently supplies sufficient nitrogen to maize crops (Zheng et al., 2020), demonstrating that BCRF can alter the abundance of microbial colonies and improve soil nitrate content, root growth, and nitrogen uptake throughout the maize growing season (Li et al., 2021; Zhang et al., 2021b). Root length density was positive to photosynthesis (Fv/Fm) on the milk stage, harvest index, 13C-photosynthate, and nitrogen distribution ratio. Suitable root length is beneficial to optimize root–shoot ratio and increase dry matter accumulation in aboveground and underground parts simultaneously (Elazab et al., 2016; Ordonez et al., 2020). In this study, the first increased and then decreased with the increase in irrigation level, which was consistent to previous studies (Elazab et al., 2016; Gao et al., 2022). Furthermore, the higher root length density treatment, with higher water and nitrogen assimilating capacity, delayed the leaf senescence process with higher photosynthetic rate (Figure 4) and ultimately increased photosynthate and nitrogen accumulation and distribution in kernel (Chilundo et al., 2017). In this study, a higher root length density in I2NR maintains higher maize photosynthesis (Fv/Fm) in the milk stage, delayed leaf senescence in the later stage, and results in similar kernel weights as with I3NU.

4.3 Effect of irrigation and nitrogen fertilizer on grain yield, NAUE, and WUE

Water shortage is worsening, and droughts are becoming more common in the Huang-Huai-Hai Plain, China's key summer maize-producing region (Kang and Zhang, 2016; Chen et al., 2021). Effective irrigation practice is critical for maintaining high summer maize yields while improving WUE. Deficit irrigation is preferable to full irrigation for eco-agriculture (Zhang, 2003a; Tavakkoli and Oweis, 2004; Geerts and Raes, 2009). Researchers have reported that 75% ET_c in winter wheat (Lu et al., 2021) and 80% ET_c in maize (Guo et al., 2022) produced higher yield and WUE due to higher net photosynthetic efficiency and leaf area index. In this study, the plants in I1 were severely drought stressed and had the lowest Fv/Fm, dry matter, kernel number, kernel weight, and yield but the highest WUE. Fv/Fm, optimal/maximal quantum yield of PSII, was the indicator for adjusting leaf growth status under water deficit (Song et al., 2018; Li et al., 2019). The I1 significantly decreased the maximum light energy absorption and capture efficiency and accumulated low energy for photosynthesis, limiting the maize dry matter accumulation. When compared with I3, the maize growth in I1 was severely limited, with yield losses of 10.9%–32.0%; hence, this treatment is not recommended for maize production. I2 maize had lower dry matter, ^{13}C-AC, and N-AC than I3, but it produced the same yield due to higher root length density, HI, ^{13}C-DR, and N-DR. This finding was consistent with previous reports (Tolk et al., 1999; Oktem et al., 2003; Payero et al., 2006; Imma and Maria, 2007; Lu et al., 2021; Guo et al., 2022) that appropriate deficit irrigation optimizes yield and WUE. As a result, a mild water deficit of 75% ET_c promoted deeper root growth (40–60 cm), maintaining long-term Fv/Fm benefits for leaf photosynthesis, and promoted more photosynthate and nitrogen from other organs to kernel tissues, resulting in increased grain yield and WUE.

10.3389/fpls.2023.1180734

TABLE 4 Effect of irrigation and fertilizer treatment on water use efficiency and nitrogen agronomic use efficiency for summer maize in 2016–2018.

Treatment	WUE(kg m^{-3})			NAUE (kg kg N^{-1})		
	2016	2017	2018	2016	2017	2018
I0N0	1.12j	1.94h	1.11f			
I0NC	1.67h	2.57bcd	1.58d	9.2b	6.5d	9.0f
I0NR	1.60h	2.54d	1.57d	9.5b	7.3bc	11.8cde
I0NU	1.58h	2.62bc	1.59d	7.5cd	6.3d	9.8ef
I1N0	1.80g	2.33e	1.44e			
I1NC	2.96a	2.94a	1.95c	9.3b	6.2d	11def
I1NR	2.84b	2.89a	1.96c	9.2b	6.7cd	13.3bc
I1NU	2.68c	2.89a	1.93c	7.0d	5.3e	10.2ef
I2N0	1.79g	1.98gh	1.45e			
I2NC	2.72c	2.65b	2.10a	11.2a	7.6b	13.8abc
I2NR	2.63cd	2.58bcd	2.07ab	12.2a	8.7a	15.6a
I2NU	2.56d	2.56cd	2.07ab	8.7bc	6.5d	12.6bcd
I3N0	1.43i	1.58i	1.38e			
I3NC	2.21e	2.08f	1.99bc	11.2a	8.3a	14.1ab
I3NR	2.12ef	2.03fg	1.96c	12.0a	8.6a	15.6a
I3NU	2.07f	2.03fg	1.98c	9.3b	6.6d	13bcd
Irrigation(I)						
I0	1.49d	2.42b	1.46c	8.7b	6.7b	10.2c
I1	2.57a	2.76a	1.82b	8.5b	6.1c	11.5b
I2	2.42b	2.44b	1.92a	10.7a	7.6a	14.0a
I3	1.96c	1.93c	1.83b	10.8a	7.8a	14.2a
Nitrogen treatment(N)						
N0	1.53d	1.96c	1.35b	10.2a	7.1b	12.0b
NC	2.39a	2.56a	1.90a	10.7a	7.8a	14.1a
NR	2.30b	2.51b	1.89a	8.1b	6.2c	11.4b
NU	2.22c	2.53ab	1.89a			
F values						
I	771.18**	713.97**	202.7**	20.8**	41.9**	25.8**
N	493.37**	495.9**	375.87**	35.4**	57.1**	17.3**
I×N	11.03**	3.23**	1.81ns	3.0*	3.8*	0.5ns

WUE and NAUE were water use efficiency (kg m^{-3}) and nitrogen agronomic use efficiency (kg kg N^{-1}), respectively. Different letters in the same column indicate significant differences at the 0.05 level. *: significant at $P \leq 0.05$; **: significant at $P \leq 0.01$, NS: not significant at $P \leq 0.05$.

The tolerance of maize to drought stress varied depending on the stage of growth. Drought from the tasseling stage to the milk stage had the largest impact on maize output, followed by drought from the seventh leaf stage to the tasseling stage and drought from the sowing to the seventh leaf stage (Zhang et al., 2021a; Zhu et al., 2021). A hypothetical lower degree of drought stress in the sensitive period and a higher degree of drought stress in the non-sensitive period could further improve the yield and WUE than drought stress during the entire growth period. The degree of drought stress based on ET_c criteria during the maize growing season needs to be further studied (Mansouri-Far et al., 2010).

Clarifying the relationship between ET and maize grain yield, WUE and NAUE could improve our understanding of regulatory mechanisms when facing persistent water scarcity and climate change (Chen et al., 2021). The trend of grain yield, WUE, and ET in 2018 was consistent to previous studies (Grassini et al., 2009; Hernández et al.,

2015). The lower ET for highest grain and WUE in 2016 and 2017 may be attributed to the higher productivity for limited irrigation when rainfall was prevented. Increased with ET, the grain yield were quadratic (Figure 6). Without taking soil evaporation into account, larger daily ET rates could be the result of increased root capacity for water and nitrogen extraction (Canales et al., 2021) and/or a greater canopy capacity, resulting in higher photosynthate accumulation (Hernández et al., 2015). While photosynthesis increased initially and then stayed consistent as leaf stomatal opening increased, excessive stomatal opening resulted in excessive water loss and decreased the leaf immediate water use efficiency. Furthermore, the grain yield in 2016 and 2017 under rainproof shelter was significantly lower than that in 2018 and the farmer field in this region. With rainproof shelter, the irrigation effect on maize performance could be studied clearly, reducing the risk of unforeseen rainfall affecting (Kundel et al., 2018). However, the temperature was higher than the field, resulting in higher evapotranspiration, shorter growth period, and lower yield. The maize performance under rainproof shelter could provide referential value for dryland or dry years.

The actual average ET (526.2 mm) for I3 in 2018 was much higher than the average ET_c (335.9 mm, calculated by FAO56) from 1981 to 2015, which was higher than the precipitation in 2016 and 2017 but lower than the precipitation in 2018 (349.4, 193.6, and 389.8 mm in the three growing seasons, respectively). The discrepancy between real ET and estimated ET_c was partly related to an imbalance in the timing and quantity of rainfall and maize need (Liu et al., 2022b). The ineffective evaporation was compounded by more precipitation prior to the V12 stage (231 mm) but a lower maize demand (94.6 mm). Rainfall exceeds maize demand by a substantial margin, resulting in significant water losses through soil evaporation (Jia et al., 2021) and leachate (Nouchi et al., 1995; Li et al., 2020), whereas the rainfall (15.6 mm) was much lower than the maize demand (61.6 mm) during V12 stage to anthesis stage, the water critical period. The low yield and WUE of I0 treatment throughout the three seasons indicated that additional irrigation was

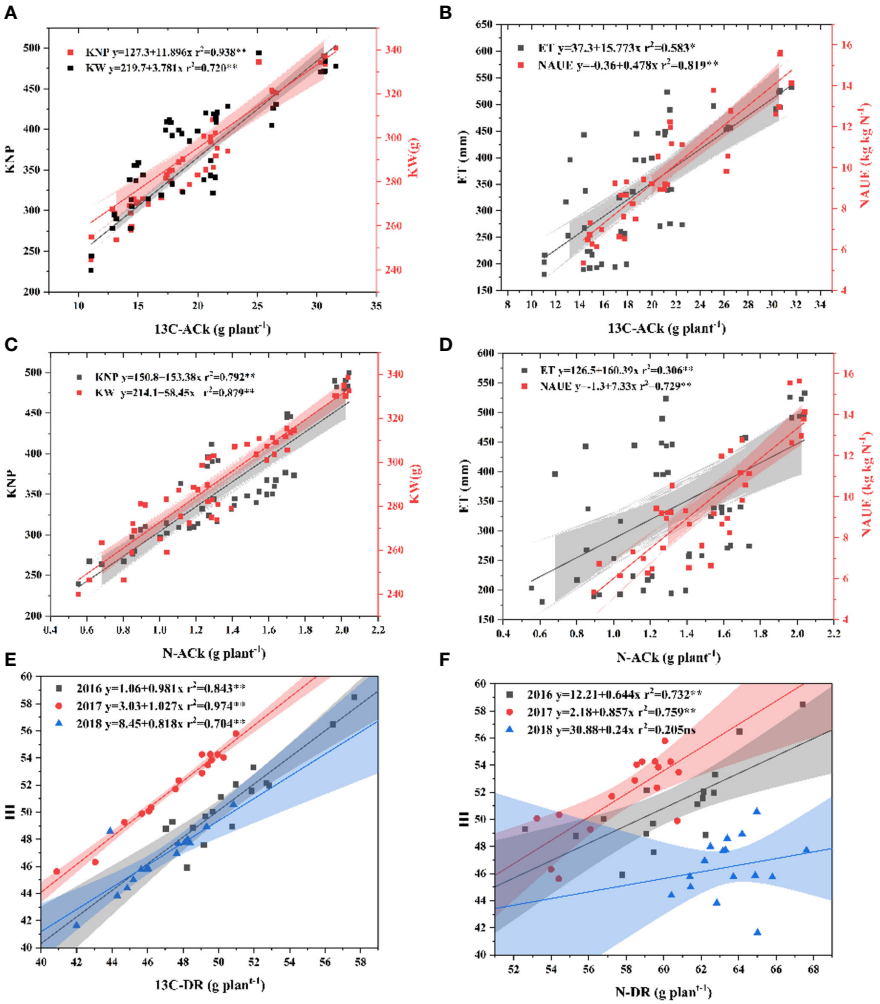

FIGURE 8
Scatterplots of kernel number per spike (KNP), kernel weight (KW), evapotranspiration (ET), and nitrogen agronomic use efficiency (NAUE) versus ^{13}C-photosynthate accumulation in kernel (^{13}C-ACk) **(A, B)** and nitrogen accumulation in kernel (N-ACk) **(C, D)**, ^{13}C-photosynthate distribution ratio in kernel (^{13}C-DR), and nitrogen distribution ratio in kernel (N-DR) versus harvest index (HI) **E, F)**, respectively. The colored areas indicate the 95% confidence intervals of the fitted curves.

required for the summer maize season, despite the fact that rainfall was greater than ET_c in 2018 (Ren et al., 2022).

Improved grain yield and NAUE requires better coordination of crop nitrogen requirements and multiple-source availability (Cui et al., 2010; Ciampitti and Vyn, 2012; Zhang et al., 2012; Meng et al., 2016). A larger LAI and SPAD (not shown) and a similar Fv/Fm value (for the same nitrogen rate treatment) in the NC treatment resulted in increased ^{13}C-AC and N-AC. The higher dry matter, ^{13}C-AC, N-AC, ^{13}C-DR, and N-DR in the BCRF treatments indicate that the BCRF enhanced the carbohydrate and nitrogen accumulation in plant tissue and subsequent remobilization to the kernels, ultimately resulting in greater yield. These results are consistent with previous research (Qu et al., 2020; Guo et al., 2022). Compared with plants grown using urea, plants grown with BCRF fertilizer had the same "sink" (similar kernel number per spike) and higher "source" (^{13}C-AC and N-AC) and "flow" (^{13}C-DR, N-DR and HI), resulting in more carbohydrate and nitrogen accumulation in the kernels and a higher yield Graphical abstract.

The coupling effect of irrigation amount and nitrogen management was significant. Blending control-release fertilizer and urea could dramatically alleviate grain yield loss due to water stress (Guo et al., 2022). In this study, the grain yield of NC was 6.6%–10.6%, 0.9%–3.5%, and 0.9%–2.0% higher than that of NU in the 2016, 2017, and 2018 growing seasons, respectively. However, the difference between NU and NC was greater under I2 and I3 treatments. In addition, drought stress was lessened because of the nitrogen fertilizer (Tilling et al., 2007; Sandhu et al., 2019). In this study, the nitrogen-fertilized treatments, especially the I1 and I0 treatments, significantly increased the Fv/Fm, ^{13}C-AC, N-AC, and grain yield compared with the N0 treatments. Drought-stressed maize had a lower root density (Chilundo et al., 2017; Gheysari et al., 2017), excessive nutrients remaining in the soil (Ge et al., 2012), and a reduced nitrogen uptake (Xiao et al., 2021). Proper irrigation (I2 in this study) helped to enhance N-AC and ^{13}C-AC in the kernels and NAUE. Excessive irrigation resulted in ineffective plant development and decreased N-DR content in kernels and raised the danger of nutrient leaching (Ren et al., 2016; Srivastava et al., 2020).

5 Conclusion

Compared with the I3NU treatment, the I2NC and I2NR treatments increased the kernel number per ear (sink size), maintained a higher Fv/Fm in the milk stage (Ministry of Water Resources), increased ^{13}C-photosynthate and nitrogen accumulation, and promoted ^{13}C-photosynthate and nitrogen transport from nutritive organs to the kernels (flow), resulting in a higher harvest and a comparable yield. Meanwhile, I2NC and I2NR had a reduced irrigation input and topdressing cost while synchronously increasing the WUE and NAUE. Due to its balanced "source-flow-sink" characteristics, the 75% ET_c-based irrigation combined with 200 kg N ha^{-1} of BCRF is an effective treatment in terms of yield, WUE, and NAUE. Additional field experiments on a 75% ET_c irrigation treatment with different water deficits in the water-sensitive and water-insensitive stages of the plants should be undertaken to optimize the potential for greater yields and resource use efficiency.

Data availability statement

The original contributions presented in the study are included in the article/Supplementary Material. Further inquiries can be directed to the corresponding authors.

Author contributions

LG: data curation, writing—original draft, visualization, investigation, and funding acquisition. XM: writing—review and editing. JQ: supervision. BT: funding acquisition and supervision. WZ: conceptualization and writing—review and editing. LX: conceptualization and writing—review and editing. All authors contributed to the article and approved the submitted version.

Funding

This work was supported by the National Natural Science Foundation of China (31601259), Project of Corn Industry Technology System Construction in Henan (HARS-22-02-G2), scientific and technological innovation team project of Henan Academy of Agricultural Sciences (2023TD37), and Special Fund for Agro-scientific Research in the Public Interest (201503130). We thank LetPub (www.letpub.com) for linguistic assistance and pre-submission expert review.

Conflict of interest

The authors declare that the research was conducted in the absence of any commercial or financial relationships that could be construed as a potential conflict of interest.

Publisher's note

Supplementary material

The Supplementary Material for this article can be found online at: https://www.frontiersin.org/articles/10.3389/fpls.2023.1180734/full#supplementary-material

References

Adu-Gyamfi, R., Agyin-Birikorang, S., Tindjina, I., Manu, Y., and Singh, U. (2019). Minimizing nutrient leaching from maize production systems in northern Ghana with one-time application of multi-nutrient fertilizer briquettes. *Sci. Total Environ.* 694, 133667. doi: 10.1016/j.scitotenv.2019.133667

Aina, P. O., and Fapohunda, H. O. (1986). Root distribution and water uptake patterns of maize cultivars field-grown under differential irrigation. *Plant Soil* 94 (2), 257–265. doi: 10.1007/BF02374349

Allison, J. (2010). Effect of plant population on the production and distribution of dry matter in maize. *Ann. Appl. Biol.* 63 (1), 135–144. doi: 10.1111/j.1744-7348.1969.tb05474.x

Canales, F. J., Rispail, N., García-Tejera, O., Arbona, V., Pérez-de-Luque, A., and Prats, E. (2021). Drought resistance in oat involves ABA-mediated modulation of transpiration and root hydraulic conductivity. *Environ. Exp. Bot.* 182, 104333. doi: 10.1016/j.envexpbot.2020.104333

Cancela, J. J., Fandiño, M., Rey, B. J., and Martínez, E. M. (2015). Automatic irrigation system based on dual crop coefficient, soil and plant water status for vitis vinifera (cv godello and cv mencía). *Agric. Water Manage.* 151, 52–63. doi: 10.1016/j.agwat.2014.10.020

Chen, L., Chang, J., Wang, Y., Guo, A., Liu, Y., Wang, Q., et al. (2021). Disclosing the future food security risk of China based on crop production and water scarcity under diverse socioeconomic and climate scenarios. *Sci. Total Environ.* 790, 148110. doi: 10.1016/j.scitotenv.2021.148110

Chilundo, M., Joel, A., Wesström, I., Brito, R., and Messing, I. (2017). Response of maize root growth to irrigation and nitrogen management strategies in semi-arid loamy sandy soil. *Field Crops Res.* 200, 143–162. doi: 10.1016/j.fcr.2016.10.005

Ciampitti, I. A., and Vyn, T. J. (2012). Physiological perspectives of changes over time in maize yield dependency on nitrogen uptake and associated nitrogen efficiencies: a review. *Field Crops Res.* 133, 48–67. doi: 10.1016/j.fcr.2012.03.008

Comas, L. H., Trout, T. J., DeJonge, K. C., Zhang, H., and Gleason, S. M. (2019). Water productivity under strategic growth stage-based deficit irrigation in maize. *Agric. Water Manage.* 212, 433–440. doi: 10.1016/j.agwat.2018.07.015

Cui, Z., Chen, X., and Zhang, F. (2010). Current nitrogen management status and measures to improve the intensive wheat–maize system in China. *Ambio* 39 (5/6), 376–384. doi: 10.1007/s13280-010-0076-6

Eekhout, J. P. C., Hunink, J. E., Terink, W., and de Vente, J. (2018). Why increased extreme precipitation under climate change negatively affects water security. *Hydrol. Earth System Sci.* 22 (11), 5935–5946. doi: 10.5194/hess-22-5935-2018

Elazab, A., Serret, M. D., and Araus, J. L. (2016). Interactive effect of water and nitrogen regimes on plant growth, root traits and water status of old and modern durum wheat genotypes. *Planta* 244 (1), 125–144. doi: 10.1007/s00425-016-2500-z

Flynn, N. E., Stewart, C. E., Comas, L. H., and Fonte, S. J. (2021). Deficit irrigation drives maize root distribution and soil microbial communities with implications for soil carbon dynamics. *Soil Sci. Soc. America J.* 85, 412–422. doi: 10.1002/saj2.20201

Gao, Y., Chen, J., Wang, G., Liu, Z., Sun, W., Zhang, Y., et al. (2022). Different responses in root water uptake of summer maize to planting density and nitrogen fertilization. *Front Plant Sci.* 13, 918043. doi: 10.3389/fpls.2022.918043

Ge, T., Sun, N., Bai, L., Tong, C., and Sui, F. (2012). Effects of drought stress on phosphorus and potassium uptake dynamics in summer maize (Zea mays) throughout the growth cycle. *Acta Physiol. Plant.* 34 (6), 2179–2186. doi: 10.1007/s11738-012-1018-7

Geerts, S., and Raes, D. (2009). Deficit irrigation as an on-farm strategy to maximize crop water productivity in dry areas. *Agric. Water Manage.* 96 (9), 1275–1284. doi: 10.1016/j.agwat.2009.04.009

Gheysari, M., Sadeghi, S.-H., Loescher, H. W., Amiri, S., Zareian, M. J., Majidi, M. M., et al. (2017). Comparison of deficit irrigation management strategies on root, plant growth and biomass productivity of silage maize. *Agric. Water Manage.* 182, 126–138. doi: 10.1016/j.agwat.2016.12.014

Grassini, P., Yang, H., and Cassman, K. G. (2009). Limits to maize productivity in Western corn-belt: a simulation analysis for fully irrigated and rainfed conditions. *Agric. For. Meteorol.* 149 (8), 1254–1265. doi: 10.1016/j.agrformet.2009.02.012

Guo, J., Fan, J., Xiang, Y., Zhang, F., Yan, S., Zhang, X., et al. (2022). Maize leaf functional responses to blending urea and slow-release nitrogen fertilizer under various drip irrigation regimes. *Agric. Water Manage.* 262, 107396. doi: 10.1016/j.agwat.2021.107396

Guo, J. H., Liu, X. J., Zhang, Y., Shen, J. L., Han, W. X., Zhang, W. F., et al. (2010). Significant acidification in major Chinese croplands. *Science* 327 (5968), 1008–1010. doi: 10.1126/science.1182570

Guo, Z., Shi, Y., Yu, Z., and Zhang, Y. (2015). Supplemental irrigation affected flag leaves senescence post-anthesis and grain yield of winter wheat in the Huang-Huai-Hai plain of China. *Field Crops Res.* 180, 100–109. doi: 10.1016/j.fcr.2015.05.015

Halli, H. M., Angadi, S., Kumar, A., Govindasamy, P., Madar, R., El-Ansary, D. O., et al. (2021). Influence of planting and irrigation levels as physical methods on maize root morphological traits, grain yield and water productivity in semi-arid region. *Agronomy* 11 (2), 294. doi: 10.3390/agronomy11020294

Hernández, M., Echarte, L., Della Maggiora, A., Cambareri, M., Barbieri, P., and Cerrudo, D. (2015). Maize water use efficiency and evapotranspiration response to n supply under contrasting soil water availability. *Field Crops Res.* 178, 8–15. doi: 10.1016/j.fcr.2015.03.017

Hou, P., Jiang, Y., Yan, L., Petropoulos, E., Wang, J., Xue, L., et al. (2021). Effect of fertilization on nitrogen losses through surface runoffs in Chinese farmlands: a meta-analysis. *Sci. Total Environ.* 793, 148554. doi: 10.1016/j.scitotenv.2021.148554

Imma, F., and Maria, F. J. (2007). Comparative response of maize (Zea mays l.) and sorghum (Sorghum bicolor l. moench) to deficit irrigation in a Mediterranean environment. *Agric. Water Manage.* 83 (1), 135–143. doi: 10.1016/j.agwat.2005.11.001

Jia, Q., Shi, H., Li, R., Miao, Q., Feng, Y., Wang, N., et al. (2021). Evaporation of maize crop under mulch film and soil covered drip irrigation: field assessment and modelling on West liaohe plain, China. *Agric. Water Manage.* 253, 106894. doi: 10.1016/j.agwat.2021.106894

Jovanovic, N., Pereira, L. S., Paredes, P., Pôças, I., Cantore, V., and Todorovic, M. (2020). A review of strategies, methods and technologies to reduce non-beneficial consumptive water use on farms considering the FAO56 methods. *Agric. Water Manage.* 239, 106267. doi: 10.1016/j.agwat.2020.106267

Kang, S., Shi, W., and Zhang, J. (2000). An improved water-use efficiency for maize grown under regulated deficit irrigation. *Field Crops Res.* 67 (3), 207–214. doi: 10.1016/S0378-4290(00)00095-2

Kang, L., and Zhang, H. (2016). A comprehensive study of agricultural drought resistance and background drought levels in five main grain-producing regions of China. *Sustainability* 8 (4), 346. doi: 10.3390/su8040346

Kundel, D., Meyer, S., Birkhofer, H., Fliessbach, A., Mäder, P., Scheu, S., et al. (2018). Design and manual to construct rainout-shelters for climate change experiments in agroecosystems. *Front. Environ. Sci.* 6, 14. doi: 10.3389/fenvs.2018.00014

Li, R., Gao, Y., Chen, Q., Li, Z., Gao, F., Meng, Q., et al. (2021). Blended controlled-release nitrogen fertilizer with straw returning improved soil nitrogen availability, soil microbial community, and root morphology of wheat. *Soil Tillage Res.* 212, 105045. doi: 10.1016/j.still.2021.105045

Li, Y., Huang, G., Chen, Z., Xiong, Y., Huang, Q., Xu, X., et al. (2022). Effects of irrigation and fertilization on grain yield, water and nitrogen dynamics and their use efficiency of spring wheat farmland in an arid agricultural watershed of Northwest China. *Agric. Water Manage.* 260, 107277. doi: 10.1016/j.agwat.2021.107277

Li, Y., Song, H., Zhou, L., Xu, Z., and Zhou, G. (2019). Vertical distributions of chlorophyll and nitrogen and their associations with photosynthesis under drought and rewatering regimes in a maize field. *Agric. For. Meteorol.* 272-273, 40–54. doi: 10.1016/j.agrformet.2019.03.026

Li, Z., Wen, X., Hu, C., Li, X., Li, S., Zhang, X., et al. (2020). Regional simulation of nitrate leaching potential from winter wheat-summer maize rotation croplands on the north China plain using the NLEAP-GIS model. *Agricult. Ecosyst. Environ.* 294, 106861. doi: 10.1016/j.agee.2020.106861

Liu, T., Gu, L., Dong, S., Zhang, J., Liu, P., and Zhao, B. (2015). Optimum leaf removal increases canopy apparent photosynthesis, 13C-photosynthate distribution and grain yield of maize crops grown at high density. *Field Crops Res.* 170, 32–39. doi: 10.1016/j.fcr.2014.09.015

Liu, W., Hou, P., Liu, G., Yang, Y., Guo, X., Ming, B., et al. (2020). Contribution of total dry matter and harvest index to maize grain yield–a multisource data analysis. *Food Energy Secur.* 9 (4), e256. doi: 10.1002/fes3.256

Liu, Y., Lin, Y., Huo, Z., Zhang, C., Wang, C. , Xue, J., et al. (2022b). Spatio-temporal variation of irrigation water requirements for wheat and maize in the yellow river basin, china 1974–2017. *Agric. Water Manage.* 262, 107451. doi: 10.1016/j.agwat.2021.107451

Liu, S., Lin, X., Wang, W., Zhang, B., and Wang, D. (2022a). Supplemental irrigation increases grain yield, water productivity, and nitrogen utilization efficiency by improving nitrogen nutrition status in winter wheat. *Agric. Water Manage.* 264, 107505. doi: 10.1016/j.agwat.2022.107505

López-Urrea, R., Domínguez, A., Pardo, J. J., Montoya, F., García-Vila, M., and Martínez-Romero, A. (2020). Parameterization and comparison of the AquaCrop and MOPECO models for a high-yielding barley cultivar under different irrigation levels. *Agric. Water Manage.* 230, 105931. doi: 10.1016/j.agwat.2019.105931

Lu, J., Hu, T., Geng, C., Cui, X., Fan, J., and Zhang, F. (2021). Response of yield, yield components and water-nitrogen use efficiency of winter wheat to different drip fertigation regimes in Northwest China. *Agric. Water Manage.* 255, 107034. doi: 10.1016/j.agwat.2021.107034

Lyu, X., Wang, T., Song, X., Zhao, C., Rees, R. M., Liu, Z., et al. (2021). Reducing N2O emissions with enhanced efficiency nitrogen fertilizers (EENFs) in a high-yielding spring maize system. *Environ. pollut.* 273, 116422. doi: 10.1016/j.envpol.2020.116422

Mancosu, N., Spano, D., Orang, M., Sarreshteh, S., and Snyder, R. L. (2016). SIMETAW# - a model for agricultural water demand planning. *Water Resour. Manage.* 30 (2), 541–557. doi: 10.1007/s11269-015-1176-7

Mansouri-Far, C., Modarres Sanavy, S. A. M., and Saberali, S. F. (2010). Maize yield response to deficit irrigation during low-sensitive growth stages and nitrogen rate under semi-arid climatic conditions. *Agric. Water Manage.* 97 (1), 12–22. doi: 10.1016/j.agwat.2009.08.003

Masupha, T. E., and Moeletsi, M. E. (2020). The use of water requirement satisfaction index for assessing agricultural drought on rain-fed maize, in the luvuvhu river catchment, south Africa. *Agric. Water Manage.* 237, 106142. doi: 10.1016/j.agwat.2020.106142

Meng, Q. F., Yue, S. C., Hou, P., Cui, Z. L., and Chen, X. P. (2016). Improving yield and nitrogen use efficiency simultaneously for maize and wheat in China: a review. *Pedosphere* 26 (2), 137–147. doi: 10.1016/S1002-0160(15)60030-3

Ministry of Water Resources (2020) *2020 statistic bulletin on China water activities* (China: Water and Power Press). Available at: http://www.mwr.gov.cn/sj/tjgb/slfztjgb/202202/t20220209_1561588.html (Accessed 9 2021).

Mirhashemi, S. H., and Panahi, M. (2021). Investigation and prediction of maize water requirements in four growth stages under the influence of natural factors (Case study: qazvin plain, Iran). *Environ. Technol. Innovation* 24, 102062. doi: 10.1016/j.eti.2021.102062

Mishra, B. K., Kumar, P., Saraswat, C., Chakraborty, S., and Gautam, A. (2021). Water security in a changing environment: concept, challenges and solutions. *Water* 13 (4), 490. doi: 10.3390/w13040490

Ning, S., Shi, J., Zuo, Q., Wang, S., and Ben-Gal, A. (2015). Generalization of the root length density distribution of cotton under film mulched drip irrigation. *Field Crops Res.* 177, 125–136. doi: 10.1016/j.fcr.2015.03.012

Nouchi, I., Ito, O., Harazono, Y., and Kouchi, H. (1995). Acceleration of 13C-labelled photosynthate partitioning from leaves to panicles in rice plants exposed to chronic ozone at the reproductive stage. *Environ. pollut.* 88 (3), 253. doi: 10.1016/0269-7491(95)93437-5

Oktem, A., Simsek, M., and Oktem, G. A. (2003). Deficit irrigation effects on sweet corn (Zea mays saccharata sturt) with drip irrigation system in a semi-arid region: i. water-yield relationship. *Agric. Water Manage.* 61 (1), 63–74. doi: 10.1016/S0378-3774(02)00161-0

Ordonez, R. A., Archontoulis, S. V., Martinez-Feria, R., Hatfield, J. L., Wright, E. E., and Castellano, M. J. (2020). Root to shoot and carbon to nitrogen ratios of maize and soybean crops in the US Midwest. *J. Eur. J. Agron.* 120 (1), 123130. doi: 10.1016/j.eja.2020.126130

Pandey, R. K., Maranville, J. W., and Chetima, M. M. (2000). Deficit irrigation and nitrogen effects on maize in a sahelian environment: II. shoot growth, nitrogen uptake and water extraction. *Agric. Water Manage.* 46 (1), 15–27. doi: 10.1016/S0378-3774(00)00074-3

Payero, J. O., Melvin, S. R., Irmak, S., and Tarkalson, D. D. (2006). Yield response of corn to deficit irrigation in a semiarid climate. *Agric. Water Manage.* 84 (1), 101–112. doi: 10.1016/j.agwat.2006.01.009

Peng, Y., Xiao, Y., Fu, Z., Dong, Y., Zheng, Y., Yan, H., et al. (2019). Precision irrigation perspectives on the sustainable water-saving of field crop production in China: water demand prediction and irrigation scheme optimization. *J. Cleaner Product.* 230, 365–377. doi: 10.1016/j.jclepro.2019.04.347

Pereira, L. S., Paredes, P., and Jovanovic, N. (2020). Soil water balance models for determining crop water and irrigation requirements and irrigation scheduling focusing on the FAO56 method and the dual kc approach. *Agric. Water Manage.* 241, 106357. doi: 10.1016/j.agwat.2020.106357

Qu, Z., Qi, X., Shi, R., Zhao, Y., Hu, Z., Chen, Q., et al. (2020). Reduced n fertilizer application with optimal blend of controlled-release urea and urea improves tomato yield and quality in greenhouse production system. *J. Soil Sci. Plant Nutr.* 20 (4), 1741–1750. doi: 10.1007/s42729-020-00244-8

Ren, P., Huang, F., and Li, B. (2022). Spatiotemporal patterns of water consumption and irrigation requirements of wheat-maize in the Huang-Huai-Hai plain, China and options of their reduction. *Agric. Water Manage.* 263 (H032649), 107468. doi: 10.1016/j.agwat.2022.107468

Ren, H., Jiang, Y., Zhao, M., Qi, H., and Li, C. (2021). Nitrogen supply regulates vascular bundle structure and matter transport characteristics of spring maize under high plant density. *Front. Plant Sci.* 11. doi: 10.3389/fpls.2020.602739

Ren, B., Zhu, Y., Zhang, J., Dong, S., Liu, P., and Zhao, B. (2016). Effects of spraying exogenous hormone 6-benzyladenine (6-BA) after waterlogging on grain yield and growth of summer maize. *Field Crops Res.* 188, 96–104. doi: 10.1016/j.fcr.2015.10.016

Salehi, M. (2022). Global water shortage and potable water safety; today's concern and tomorrow's crisis. *Environ. Int.* 158, 106936. doi: 10.1016/j.envint.2021.106936

Sampathkumar, T., Pandian, B. J., and Mahimairaja, S. (2012). Soil moisture distribution and root characters as influenced by deficit irrigation through drip system in cotton–maize cropping sequence. *Agric. Water Manage.* 103 (103), 43–53. doi: 10.1016/j.agwat.2011.10.016

Sandhu, O. S., Gupta, R. K., Thind, H. S., Jat, M. L., Sidhu, H. S., and Yadvinder, S. (2019). Drip irrigation and nitrogen management for improving crop yields, nitrogen use efficiency and water productivity of maize-wheat system on permanent beds in north-west India. *Agric. Water Manage.* 219, 19–26. doi: 10.1016/j.agwat.2019.03.040

Shu, G., Cao, G., Li, N., Wang, A., Wei, F., Li, T., et al. (2021). Genetic variation and population structure in China summer maize germplasm. *Sci. Rep.* 11 (1), 8012. doi: 10.1038/s41598-021-84732-6

Sinclair, T. R. (1998). Historical changes in harvest index and crop nitrogen accumulation. *Crop Sci.* 38 (3), 638–643. doi: 10.1016/j.agwat.2011.10.016

Song, H., Li, Y., Zhou, L., Xu, Z., and Zhou, G. (2018). Maize leaf functional responses to drought episode and rewatering. *Agric. For. Meteorol.* 249, 57–70. doi: 10.1016/j.agrformet.2017.11.023

Srivastava, R. K., Panda, R. K., and Chakraborty, A. (2020). Quantification of nitrogen transformation and leaching response to agronomic management for maize crop under rainfed and irrigated condition. *Environ. pollut.* 265, 114866. doi: 10.1016/j.envpol.2020.114866

Tavakkoli, A. R., and Oweis, T. Y. (2004). The role of supplemental irrigation and nitrogen in producing bread wheat in the highlands of Iran. *Agric. Water Manage.* 65 (3), 225–236. doi: 10.1016/j.agwat.2003.09.001

Thomas, R. L., Sheard, R. W., and Moyer, J. R. (1967). Comparison of conventional and automated procedures for nitrogen, phosphorus, and potassium analysis of plant material using a single digestion. *Agron. J.* 59 (3), 240–243. doi: 10.2134/agronj1967.00021962005900030010x

Tilling, A. K., O'Leary, G. J., Ferwerda, J. G., Jones, S. D., Fitzgerald, G. J., Rodriguez, D., et al. (2007). Remote sensing of nitrogen and water stress in wheat. *Field Crops Res.* 104 (1-3), 77–85. doi: 10.1016/j.fcr.2007.03.023

Tolk, J. A., Howell, T. A., and Evett, S. R. (1999). Effect of mulch, irrigation, and soil type on water use and yield of maize. *Soil Tillage Res.* 50 (2), 137–147. doi: 10.1016/S0167-1987(99)00011-2

Tremblay, P., Grover, R., Maguer, J. F., Legendre, L., and Ferrier-Pages, C. (2012). Autotrophic carbon budget in coral tissue: a new 13C-based model of photosynthate translocation. *J. Exp. Biol.* 215 (8), 1384–1393. doi: 10.1242/jeb.065201

Tuan, N. T., Qiu, J.-j., Verdoodt, A., Li, H., and Van Ranst, E. (2011). Temperature and precipitation suitability evaluation for the winter wheat and summer maize cropping system in the Huang-Huai-Hai plain of China. *Agric. Sci. China* 10 (2), 275–288. doi: 10.1242/jeb.06520110.1016/s1671-2927(11)60005-9

Ullah, H., Santiago-Arenas, R., Ferdous, Z., Attia, A., and Datta, A. (2019). "Chapter two - improving water use efficiency, nitrogen use efficiency, and radiation use efficiency in field crops under drought stress: a review," in *Advances in agronomy*. Ed. D. L. Sparks (Academic Press), 109–157.

Vejan, P., Khadiran, T., Abdullah, R., and Ahmad, N. (2021). Controlled release fertilizer: a review on developments, applications and potential in agriculture. *J. Controlled Release* 339, 321–334. doi: 10.1016/j.jconrel.2021.10.003

Wang, S., Hu, Y., Yuan, R., Feng, W., Pan, Y., and Yang, Y. (2019a). Ensuring water security, food security, and clean water in the north China plain – conflicting strategies. *Curr. Opin. Environ. Sustain.* 40, 63–71. doi: 10.1016/j.cosust.2019.09.008

Wang, Y., Li, S., Qin, S., Guo, H., Yang, D., and Lam, H.-M. (2020). How can drip irrigation save water and reduce evapotranspiration compared to border irrigation in arid regions in northwest China. *Agric. Water Manage.* 239, 106256. doi: 10.1016/j.agwat.2020.106256

Wang, Y., Zhang, X., Chen, J., Chen, A., Wang, L., Guo, X., et al. (2019b). Reducing basal nitrogen rate to improve maize seedling growth, water and nitrogen use efficiencies under drought stress by optimizing root morphology and distribution. *Agric. Water Manage.* 212, 328–337. doi: 10.1016/j.agwat.2018.09.010

Wei, S., Wang, X., Li, G., Jiang, D., and Dong, S. (2019). Maize canopy apparent photosynthesis and (13)C-photosynthate reallocation in response to different density and n rate combinations. *Front. Plant Sci.* 10. doi: 10.3389/fpls.2019.01113

Xiao, C., Zou, H., Fan, J., Zhang, F., Li, Y., Sun, S., et al. (2021). Optimizing irrigation amount and fertilization rate of drip-fertigated spring maize in northwest China based on multi-level fuzzy comprehensive evaluation model. *Agric. Water Manage.* 257, 107157. doi: 10.1016/j.agwat.2021.107157

Yan, S., Wu, Y., Fan, J., Zhang, F., Qiang, S., Zheng, J., et al. (2019). Effects of water and fertilizer management on grain filling characteristics, grain weight and productivity of drip-fertigated winter wheat. *Agric. Water Manage.* 213, 983–995. doi: 10.1016/j.agwat.2018.12.019

Yi, J., Li, H., Zhao, Y., Shao, M.a., Zhang, H., and Liu, M. (2022). Assessing soil water balance to optimize irrigation schedules of flood-irrigated maize fields with different cultivation histories in the arid region. *Agric. Water Manage.* 265, 107543. doi: 10.1016/j.agwat.2022.107543

Yu, C., Huang, X., Chen, H., Godfray, H. C. J., Wright, J. S., Hall, J. W., et al. (2019). Managing nitrogen to restore water quality in China. *Nature* 567 (7749), 516–520. doi: 10.1038/s41586-019-1001-1

Zhang, H. (2003a). *Improving water productivity through deficit irrigation: examples from Syria, the north China plain and Oregon, USA* (International Water Management Institute).

Zhang, H. (2003b). Production and quality of the sugar beet (Beta vulgaris l.) cultivated under controlled deficit irrigation conditions in a semi-arid climate. *Agric. Water Manage.* 62 (3), 215–227. doi: 10.1079/9780851996691.0301

Zhang, F., Cui, Z., Chen, X., Ju, X., Shen, J., Chen, Q., et al. (2012). Chapter one – integrated nutrient management for food security and environmental quality in China. *Adv. Agron.* 116, 1–40. doi: 10.1016/B978-0-12-394277-7.00001-4

Zhang, L., Liang, Z., Hu, Y., Schmidhalter, U., Zhang, W., Ruan, S., et al. (2021b). Integrated assessment of agronomic, environmental and ecosystem economic benefits of blending use of controlled-release and common urea in wheat production. *J. Cleaner Product.* 287, 125572. doi: 10.1016/j.jclepro.2020.125572

Zhang, H., Ma, L., Douglas-Mankin, K. R., Han, M., and Trout, T. J. (2021a). Modeling maize production under growth stage-based deficit irrigation management with RZWQM2. *Agric. Water Manage.* 248, 106767. doi: 10.1016/j.agwat.2021.106767

Zhang, Z., Yu, Z., Zhang, Y., and Shi, Y. (2021c). Split nitrogen fertilizer applicationimproved grain yield in winter wheat (Triticum aestivumL.) *via* modulating antioxidant capacity and13C photosynthate mobilization under water-saving irrigation conditions. *Ecol. Processes* 10 (1), 21. doi: 10.1186/S13717-021-00290-9

Zhao, B., Shuting, D., and Zhang, J.W.J.A.A.S. (2010). Effects of controlled-release fertilizer on yield and nitrogen accumulation and distribution in summer maize. *Acta Agronom. Sin.* 10 (2), 301–304. doi: 10.2966/scrip.100213.301

Zheng, W., Wan, Y., Li, Y., Liu, Z., Chen, J., Zhou, H., et al. (2020). Developing water and nitrogen budgets of a wheat-maize rotation system using auto-weighing lysimeters: effects of blended application of controlled-release and un-coated urea. *Environ. pollut.* 263, 114383. doi: 10.1016/j.envpol.2020.114383

Zheng, W., Zhang, M., Liu, Z., Zhou, H., Lu, H., Zhang, W., et al. (2016). Combining controlled-release urea and normal urea to improve the nitrogen use efficiency and yield under wheat-maize double cropping system. *Field Crops Res.* 197, 52–62. doi: 10.1016/j.fcr.2016.08.004

Zhu, X., Xu, K., Liu, Y., Guo, R., and Chen, L. (2021). Assessing the vulnerability and risk of maize to drought in China based on the AquaCrop model. *Agric. Syst.* 189, 103040. doi: 10.1016/j.agsy.2020.103040

Zhu, L. X., and Zhang, W. J. (2016). Effects of controlled-release urea combined with conventional urea on nitrogen uptake, root yield, and quality of platycodon grandiflorum. *J. Plant Nutr.* 40 (5), 662–672. doi: 10.1080/01904167.2016.1249799

frontiers | Frontiers in Plant Science

TYPE Review
PUBLISHED 05 September 2023
DOI 10.3389/fpls.2023.1206829

OPEN ACCESS

EDITED BY
Baizhao Ren,
Shandong Agricultural University, China

REVIEWED BY
Baozhong Yin,
Hebei Agricultural University, China
Umesh Yadav,
University of North Texas, United States
Jagesh Kumar Tiwari,
Indian Institute of Vegetable Research (ICAR), India

*CORRESPONDENCE
Si Shen
shensi@cau.edu.cn
Shun-Li Zhou
zhoushl@cau.edu.cn

†These authors have contributed equally to this work

RECEIVED 16 April 2023
ACCEPTED 14 August 2023
PUBLISHED 05 September 2023

CITATION
Liang X-G, Gao Z, Fu X-X, Chen X-M, Shen S and Zhou S-L (2023) Coordination of carbon assimilation, allocation, and utilization for systemic improvement of cereal yield. *Front. Plant Sci.* 14:1206829. doi: 10.3389/fpls.2023.1206829

Coordination of carbon assimilation, allocation, and utilization for systemic improvement of cereal yield

Xiao-Gui Liang[1,2,3†], Zhen Gao[3†], Xiao-Xiang Fu[1], Xian-Min Chen[2], Si Shen[2*] and Shun-Li Zhou[2*]

[1]Key Laboratory of Crop Physiology, Ecology and Genetic Breeding, Ministry of Education and Jiangxi Province/The Laboratory for Phytochemistry and Botanical Pesticides, College of Agriculture, Jiangxi Agricultural University, Nanchang, China, [2]College of Agronomy and Biotechnology, China Agricultural University, Beijing, China, [3]State Key Laboratory of North China Crop Improvement and Regulation, Hebei Agricultural University, Baoding, Hebei, China

The growth of yield outputs is dwindling after the first green revolution, which cannot meet the demand for the projected population increase by the mid-century, especially with the constant threat from extreme climates. Cereal yield requires carbon (C) assimilation in the source for subsequent allocation and utilization in the sink. However, whether the source or sink limits yield improvement, a crucial question for strategic orientation in future breeding and cultivation, is still under debate. To narrow the knowledge gap and capture the progress, we focus on maize, rice, and wheat by briefly reviewing recent advances in yield improvement by modulation of i) leaf photosynthesis; ii) primary C allocation, phloem loading, and unloading; iii) C utilization and grain storage; and iv) systemic sugar signals (e.g., trehalose 6-phosphate). We highlight strategies for optimizing C allocation and utilization to coordinate the source–sink relationships and promote yields. Finally, based on the understanding of these physiological mechanisms, we envisage a future scenery of "smart crop" consisting of flexible coordination of plant C economy, with the goal of yield improvement and resilience in the field population of cereals crops.

KEYWORDS

photosynthesis, carbon utilization, sugar transport, systemic signaling, trehalose 6-phosphate, carbon allocation, source-sink relationship, smart crop

Introduction

Global primary food production needs to double by 2050 to meet the growing demand for food and nutrition (Grassini et al., 2013; Ray et al., 2013). Simultaneously, there is increasing pressure from sustainable development and global climate change, including bioenergy demand, arable land constraints, and extreme weather (Clark et al., 2020; Ortiz-Bobea et al., 2021). Crops in the future will have to be "resilient" and "smart" to cope with

unpredictable stresses and thus increase yields in practice. Carbohydrates are pivotal for a crop to balance its maintenance, growth, and yield formation, providing a carbon (C) skeleton, energy substrates, and indispensable sugar signals. Assimilation of C in leaves by light energy conversion export to growing shoots and root systems in specific spatiotemporal patterns is mediated by transporters. Many relevant reviews, based mainly on new findings on carbohydrate transport, sugar sensing, and systemic improvement in model plants, such as *Arabidopsis* and tobacco, have been published (for example, Rolland et al., 2006; Ruan, 2014; Fichtner and Lunn, 2021; Burgess et al., 2023). Maize, wheat, and rice are major food crops worldwide, but their carbohydrate flow and correlated regulation measures have not been well summarized. Here, we briefly review the pathways of C fixation, transport, and storage, mainly in the three cereals, and the key sugar signals that have come to light in systemic regulation during the past few years. We discuss published strategies for the regulation of the plant C economy ("C economy" in this paper refers to the production, circulation, and use of carbohydrates) for crop yield and resilience. We proposed that "systemic enhancement" from source to sink together with "specific optimization" in C allocation management depending on spatial–temporal demand may be the way for both crop yield potential and stress resistance and/or resilience.

Photosynthesis improvement is showing promise in limited field application

Plants convert light energy into chemical energy *via* photosynthesis (Figure 1A). The theoretical maximum efficiencies of photosynthetic energy conversion are approximately 4.6% and 6% for C3 and C4 plants, respectively, as estimated using biomass (Zhu et al., 2010). However, efficiency in the real world, even under favorable conditions, is only half or less than the theoretical value (Yin and Struik, 2015). As a well-studied pathway, the limitations of photosynthesis have been modeled. The improvement of the photosynthetic system is mainly projected into three phases: near-term (including photorespiration bypass, canopy structure improvement, RuBP regeneration, and chlorophyll optimization), mid-term (including photoprotective recovery and RubisCO carboxylation improvement), and long-term (including RubisCO oxygenase decline, mesophyll conductance, and conversion of C3 to C4) (Zhu et al., 2010; von Caemmerer and Furbank, 2016; Leister, 2023).

In the past two decades, researchers have proposed yield-improvement strategies based on enhanced photosynthesis using synthetic biology or gene editing in *Arabidopsis* and tobacco (Long et al., 2018; Hart et al., 2019; Papanatsiou et al., 2019; Chen et al., 2020; Lopez-Calcagno et al., 2020). A few recent studies have shown promise for field crops. One synthetic photorespiratory pathway boosted tobacco biomass by up to 40%, whereas another led to an observable increase in photosynthesis and grain yield under high light in field-grown rice plants (Shen et al., 2019; South et al., 2019). Transgenic rice overexpressing a RuBisCO subunit improved yield performance and nitrogen (N) use efficiency for biomass production when receiving sufficient N fertilization in an experimental paddy field (Yoon et al., 2020). The total spikelet number of transgenic rice did not change, but the ratio of filled spikelets increased, resulting in a 20%–28% higher yield than the wild type (Yoon et al., 2020). In *Arabidopsis* and soybean, a large increase in grain yield under fluctuating light conditions was achieved by accelerating the recovery from photoprotection. However, when lodging (caused by storms) and/or reduced cloud cover resulted in a lack of sun-flecks in the canopy, the yield gain brought by genetically modified soybeans disappeared (Kromdijk et al., 2016; De Souza et al., 2022). These examples show that increases in photosynthetic efficiency can improve crop yield, under nutrient availability or specific light conditions. However, under adverse conditions such as drought or barren, which occur frequently around the world today, the yield gains shrink or disappear. As Sinclair et al. (2019) refuted, photosynthesis depends on N (and other nutrients). When nitrogen is reduced, plants with high photosynthetic efficiency may not increase crop yield but will cause resource competition and waste, further leading to insufficient transport of sugars into sink tissues. Cross-scale model studies validated that under water-limited conditions, high photosynthetic efficiency could lead to early consumption of soil water and later-growth-period drought and reduce crop yield; however, under water-abundant conditions, improvement of RubisCO and SeBP increased the yield of wheat and sorghum in Australia (Wu et al., 2019a; Wu et al., 2023). In contrast, elevated CO_2 and phosphate pools have been modeled to synergistically enhance C3 photosynthesis (Khurshid et al., 2020).

Scholars engaged in photosynthetic efficiency research have notice that proper field nutrition management and coordinated plant C economy are critical to yield as photosynthesis. Transgenic rice plants with modified photorespiration and enhanced photosynthesis undergo massive grain abortion, consistent with a marked reduction in sugar transport from source to sink, as tracked by ^{13}C isotope labeling (Wang et al., 2020). Therefore, sustainable C economic growth of plants is proposed here to depend on further timely and reasonable allocation and utilization after photosynthesis enhancement.

Primary C allocation in photosynthetic leaves indicates sink growth and resilience

While photosynthesis occurs only in light, growth and respiration occur throughout the day–night cycle (Smith and Stitt, 2007). The immediate photo-assimilate is partitioned into a fraction for glycolysis consumption, a fraction for sucrose transport, and a fraction for temporary storage in leaves and remobilized during the night (Figure 1B). In *Arabidopsis*, starch is the main transitional reserve in leaves (up to 50% or more) and is synthesized and degraded linearly in a diurnal cycle to maximize C utilization and prevent starvation in changing environments (Stitt and Zeeman, 2012; Ruan, 2014). Furthermore, precisely controlled starch

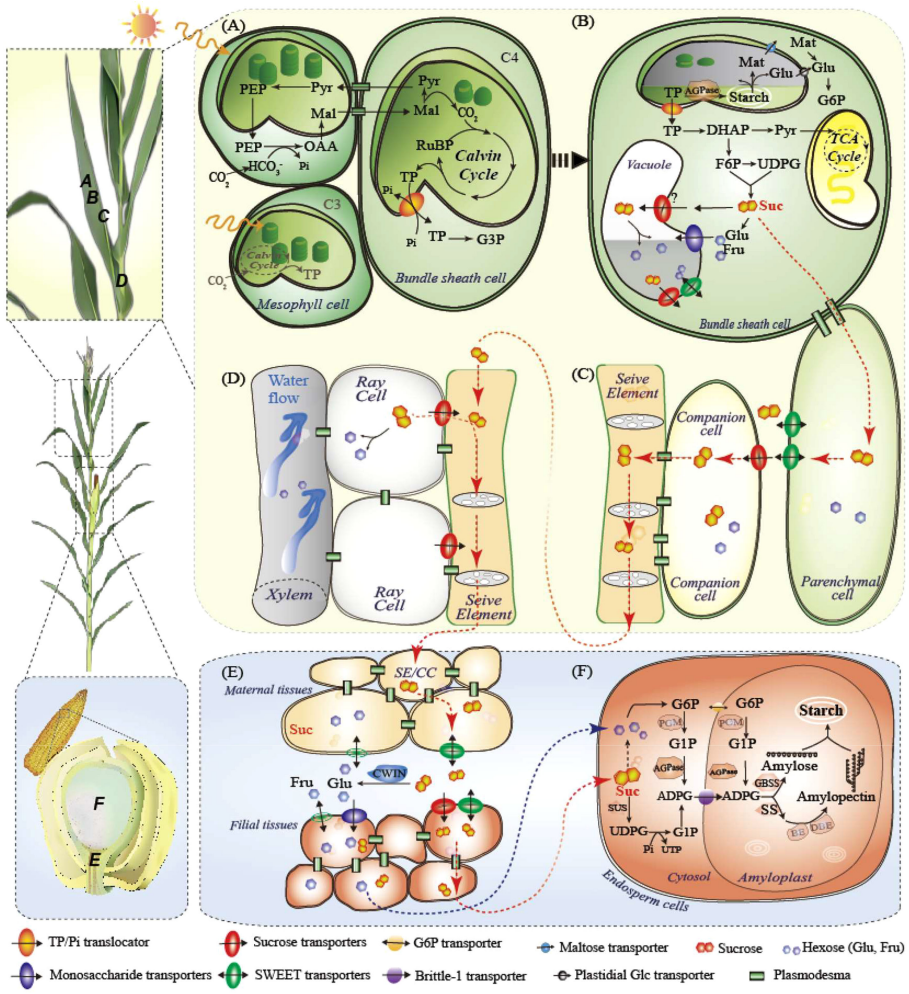

FIGURE 1
Carbon fixation and sugar flux from leaves to grains, taking maize plants as an example. **(A)** C4 photosynthesis in maize leaves in mesophyll and bundle sheath cells. C3 is also shown in gray in mesphyll cells only. **(B)** Primary carbon partitioning in the diurnal cycle, demonstrating three fates of leaf sugars: glycolysis, temporary storage in chloroplasts or vacuoles, and transport as sucrose; **(C)** Phloem loading of sucrose by SWEET and SUT; **(D)** Sucrose retrieval in vascular; **(E)** Phloem unloading from maternal to filial tissues; **(F)** Starch synthesis in endosperm cells. ADPG, adenosine 5′-diphosphoglucose; AGPase, ADPG pyrophosphorylase; BE, branching enzymes; CBC, Calvin Benson cycle; CC, companion cells; CWIN, cell wall invertase; DBE, debranching enzymes; DHAP, dihydroxyacetone phosphate; Fru, fructose; GBSS, Granule-bound starch synthase; Glu, glucose; G3P, glucose 3-phosphate; INV, invertase; ISA, Mal, maleic acid; Mat, maltose; MT, monosaccharide transporter; OAA, oxaloacetic acid; PEP, phosphoenolpyruvate; RUBP, ribulose 1,5-bisphosphate; SE, sieve elements; SS, soluble starch synthase; SWEET, sugars will eventually be exported transporters; SUT, sucrose transporter; SuS, sucrose synthase; PGM, phosphoglucomutase; Pyr, pyruvate; SSS, soluble starch synthase; TCA cycle, tricarboxylic acid cycle; TP, triose phosphate. UDPG, Uridine 5′-diphosphoglucose; UTP, uridine triphosphate.

turnover has been shown to be negatively correlated with growth rate or biomass accumulation (Cross et al., 2006; Sulpice et al., 2009; Sulpice et al., 2014), reflecting that the more C reserved in leaves, the less sink obtained for growth. Similarly, the ratio of daily starch accumulation to net C assimilation is negatively correlated with the ground biomass and final yield of three representative maize hybrids (Liang et al., 2019). Under low light or prolonged darkness, maize leaves allocate an even lower proportion of reduced photosynthetic products to sink ends, such as the developing ears, leading to biomass and/or yield losses (Liang et al., 2020; Liang et al., 2021). Thus, it may be possible to increase crop yield potential and resilience by allocating more primary C to sinks under certain circumstances (Oszvald et al., 2018). However, compared to the starchy leaves in *Arabidopsis*, crops such as wheat and rice prefer soluble sugar leaves, while maize leaves are intermediate (Smith and Stitt, 2007; Liang et al., 2021), the role of C storage in cereal leaves deserves further validation.

Some transporters are directly responsible for the primary C allocation. Sucrose transporter 2 (SUT2), located on the vacuolar membrane, transiently stores sucrose for subsequent growth in cereals (Leach et al., 2017; Prasad et al., 2023). Both loss-of-function mutants of *ossut2* and *zmsut2* exhibit severe growth restriction and accumulate more sucrose, fructose, glucose, and starch in the leaves (Eom et al., 2011; Leach et al., 2017). Rice cultivars with increased yield under elevated CO_2 conditions exhibited elevated expression of *OsSUT1* and *OsSUT2* and increased photosynthetic capacity of flag leaves, suggesting that enhanced export can prevent inhibition of photosynthesis by sugar

accumulation (Zhang et al., 2020a). Other transporters that control sugar transport across vacuole in mesophyll cells, such as the tonoplast monosaccharide transporters (TMTs, TMT1, 2), the class IV sugars will eventually be exported transporters (SWEETs, SWEET16, 17), has also been shown to regulate plant growth and stress resistance in several species (Wingenter et al., 2010; Liu et al., 2022b; Zhu et al., 2022). But as far as we know, related studies on major cereal crops are rare.

In summary, our preliminary findings indicate that daily C turnover in expanded leaves is directly related to crop growth and resistance. Boosting diurnal leaf sucrose export appears to be a strategy to improve cereal yield or stress tolerance in sink tissues, at least in some cases. However, it remains unclear whether this sacrifices the ability of the source leaves to survive extreme stress with fewer sugar reserves. The primary C allocation characteristics and underlying physiological mechanisms in different crops and varieties require further investigation.

Phloem loading and unloading: the linkage between leaves and sinks

Long-distance sugar transport requires phloem loading and unloading to coordinate leaf C supply and sink growth in different environments. Phloem tissue is composed of three cell types: companion cells (CC), sieve elements (SE), and phloem parenchyma cells (PP), which act as highway linking sources and sinks for sugar transport. Proteins responsible for sugar transport, including SUT, SWEETs, and monosaccharide transporters (MTs), have receive much attention (Julius et al., 2017; Braun, 2022; Xue et al., 2022; Singh et al., 2023). Here, we focus on maize, rice, and wheat and discuss the importance of the coordination of C transport for crop production in some recent cases.

Sucrose, the principal sugar for transport, is produced in mesophyll cells (C3) or bundle sheath cells (C4) and moves into adjacent phloem parenchyma cells through plasmodesmata (symplastic movement). In the subsequent apoplastic transport, sucrose is excreted into the intercellular space by clade III SWEETs and collected by SUT1, which is located on the plasma membrane of CC cells against the concentration gradient in the CC–SE complex (Figure 1C; Xue et al., 2022). Mutants of *Zmsut1* and *Ossut1* are severely debilitated in growth and grain filling (Scofield et al., 2002; Slewinski et al., 2009). However, both mutants could grow to maturity and produce fertile seeds, suggesting that sugars could be transferred by other SUTs (perhaps *OsSUT5* in rice, see Wang et al., 2021b) or paths. Through hydrostatic pressure established in the phloem, sucrose is transported to the sink organ by the SE, where sucrose leakage is retrieved by SUT1 during long-distance transport (Figure 1D; Ohshima et al., 1990; Knoblauch et al., 2016). Sucrose unloading occurs symplasmically in growing radicles and shoot apices, while in cereal grains, SWEETs, SUT1, cell wall invertases (CWINs), and MTs are required for maternal-to-filial transport (Figure 1E; Apoplastic path, see details below; Haupt et al., 2001; Dhungana and Braun, 2021; Ruan, 2022; Shen et al., 2022).

SWEETs may be among the most complex sugar transporter families (Chen et al., 2012; Eom et al., 2015; Xue et al., 2022; Singh et al., 2023). The number of SWEETs are 24, 21, and 59, while the SUTs are 5, 5, and 18 in maize, rice, and wheat, respectively (Zhu et al., 2022; Prasad et al., 2023). In maize, SWEET13, including *ZmSWEET13a*, *b*, and *c*, is responsible for sucrose efflux to the SE–CC complex. The triple-knockout mutants exhibited similar but milder growth to *Zmsut1*, implying greater genetic redundancy among clade III SWEETs (Bezrutczyk et al., 2018). Similarly, *OsSWEET11, 13*, *14*, and *15* are expressed in the rice leaf phloem and are thought to play a role in phloem loading (Yuan et al., 2014; Eom et al., 2019; Mathan et al., 2021a). Single-knockout mutants of *Ossweet 11*, *13*, and *14* showed milder or no yield penalty, whereas double-knockout mutants of *Ossweet11* and *14* had severe phenotypes (Eom et al., 2019; Fei et al., 2021). Blocking sugar transmembrane loading by overexpressing CWIN or by knocking down *OsDOF11* (DNA binding with one finger 11), which binds and activates gene expression of *OsSUT1*, *OsSWEET11*, and *OsSWEET14*, resulted in restricted vegetable growth and decreased grain yields (Wu et al., 2018; Wang et al., 2021b). In contrast, enhanced apoplastic phloem loading under low nitrogen conditions was attributed to increased gene expression of *OsSUT1*, *OsSWEET11*, and *OsSWEET14* in leaves and stems (Li et al., 2022a). Furthermore, the lack of symplastic connection between the SE–CC complex and surrounding parenchyma cells in leaves and stems was verified by the phloem-mobile symplastic tracer carboxyfluorescein (Li et al., 2022a).

Both SUTs and SWEETs are believed to have undergone post-domestication selection for higher-caloric harvests (Sosso et al., 2015; Mathan et al., 2021a; Singh et al., 2023). Researchers have attempted to modify the expression of SUT1 and/or clade III SWEETs to coordinate C transport. However, unexpectedly, constitutive overexpression of *OsSWEET11*, *OsSWEET14*, *OsDOF1*, *OsSUT1*, and *OsSWEET11* and *14* in rice resulted in attenuated growth and yield penalty, similar to the *AtSWEET11* and *12* OE lines in *Arabidopsis* (Gao et al., 2018; Kim et al., 2021; Singh et al., 2021; Fatima et al., 2023). Surprisingly, the *OsDOF11* and Os*SWEET 14* OE lines showed improved resistance to plant pathogens, such as *Xanthomonas oryzae pv oryzae* and *Rhizoctonia solani*, which are known to induce the expression of SWEETs for sugar secretion and nutrition hijacking (Eom et al., 2019; Oliva et al., 2019; Wu et al., 2022). Constitutive overexpression of SWEET may induce a series of plant defense reactions, leading to a trade-off between growth and resistance (Xue et al., 2022). Thus, specific regulations are more reasonable. Field rice plants overexpressing *AtSUT2* under the control of a phloem-specific promoter, showed a 16% increase in grain yield (Wang et al., 2015). Tissue-specific activation of *OsDOF11* increases both yield and resistance to *R. solani* (Kim et al., 2021). More ingeniously, by creating genomic mutations in the SWEET (*OsSWEET11*, *13*, *14*)-specific promoter, where pathogen-secreted transcription activator-like effectors bind to induce gene expression, endowing rice lines with robust, broad-spectrum resistance (Eom et al., 2019; Oliva et al., 2019).

Sugar loading and unloading clues and the significance of these transporters in improving crop performance remain to be explored. First, new sugar transporters are yet to be discovered, although it has been suggested that most sugar transporters have been

identified (Chen et al., 2015). Recently, a nitrate transporter 1/peptide transporter family member named *ZmSUGCAR1* was shown to carry both sucrose and glucose for grain filling and was proposed to be conserved in wheat and sorghum (Yang et al., 2022). Whether other nitrate/peptide transporters in this family are involved in sugar transport and whether substrate competition affects transporter selectivity is unclear. Second, the substrate selectivity of sugar transporters in crops and their correlation with growth and abiotic stress resistance need to be explored. Clade III SWEETs and clade I SWEET3a glucose transporters can transport gibberellin hormones in addition to sugars (Morii et al., 2020; Wu et al., 2022). *OsSWEET13* and *15* were strongly expressed under drought, salt, and ABA treatment, which revealed that the ABA-responsive transcription factor *OsbZIP72* directly binds to the promoters of *OsSWEET13* and *15* and activates their expression, likely to improve the root-shoot ratio for higher tolerance (Mathan et al., 2021b; Chen et al., 2022a). Third, functional redundancy within the family or clade and interactions among different types of sugar transporters are largely unknown. In general, exploration of the above issues would further deepen our understanding of the critical role of sugar transporters in coordinating the plant C economy and simultaneously improving crop yield and resilience.

Phloem unloading: how sugar transport from maternal to filial tissues determines crop yield

Besides the endosperm and embryo, cereal grains also comprise multiple distinctive or even transgenerational tissues, such as the maternal placentachalaza in maize, filial basal endosperm transfer cells (named endosperm transfer cells in wheat), and embryo-surrounding region (ESR) (see details in Liu et al., 2022a; Shen et al., 2022). Within developmentally specific but functionally coordinated tissues, sugar transporters and CWIN set a typical manifestation in which their locations mandate functions in phloem unloading and determine grain development. We recently built a holistic view of sugar transporters that control sucrose unloading in maize grains (Shen et al., 2022). *ZmSWEET11* and *13b* located in the placento-chalazal zone, expel sucrose into the apoplasmic space and, *ZmSUT1*, *ZmSWEET11/13a* (sucrose transporters), and *ZmSTP3*, *ZmSWEET3a/4c* (monosaccharide transporters), located in the basal endosperm transfer cells, retrieved sucrose or hexoses after hydrolysis by CWIN (Figure 1E). Sucrose could be further transported by the embryo-surrounding region (ESR) located in *ZmSWEET14a/15a*, broken down by the ESR-embryo junction located in CWIN, and retrieved by embryo-located *ZmSUT4* for embryo development (Shen et al., 2022). Sucrose synthase (SUS) and invertase are responsible for sucrose cleavage in the endosperm and embryo. Similarly, sucrose or monosaccharides derived from *GIF1* (also named *OsCWIN2*) in the vascular bundle are transported by *OsSWEET11*, *14*, and *15* in rice. *OsSUT1*, *3*, and *4*, *OsSWEET4*, *11*, and *14*, as well as possibly *OsMT4* and *6*, are responsible for transporting sugar to the aleurone layer for grain growth and C storage (Ma et al., 2017; Yang et al., 2018; Solomon and Drea, 2019; Fei et al., 2021; Li et al., 2022b; Liu et al., 2022a). Although the assimilate acquisition route in wheat differs that from rice and maize (Solomon and Drea, 2019; Liu et al., 2022a), the transporters responsible for apoplast transport may be similar. A recent study showed that TraesCS4B02G287800 and TraesCS4D02G286500 (homologous to *OsSUT1*), and TraesCS2D02G293200 and TraesCS2B02G311900 (homologous to *OsGIF1*) are involved in low-light induced sugar transport in wheat grains (Yang et al., 2023).

CWIN is proposed to play a major role in early grain development, probably promoting glucose-activated nuclear division for large endosperm capacity and embryo fertility (Ruan, 2014; Ruan, 2022). Both mutants of *Mn1* (also named *ZmCWIN2*) in maize and the ortholog gene *OsGIF1* in rice exhibited reduced grain size, indicating the irreplaceable roles of hexose supply and sugar signaling generated by CWIN (Wang et al., 2008; Li et al., 2013). Ubiquitously expressed *Mn1* has the highest expression in developing maize seeds, specifically at the grain set stage (Li et al., 2013). Constitutive overexpression of *AtGIF1*, *OsGIF1*, or *Mn1* in the maize inbred line Ye478 results in increased grain number, grain weight, starch content, and final yield (Li et al., 2013). In rice, 35S or *Waxy*-promoted ectopic expression of the *OsGIF1* gene showed small grains similar to the *gif1* mutant, but the native promotor-driven Os*GIF1* increased yield production (Wang et al., 2008). The interactions between CWIN and sugar transporters remain largely unknown. CWIN is co-expressed with hexose transporters located at the plasma membrane of sinks. Sosso et al. (2015) proposed that SWEET4-mediated hexose transport acts downstream of a CWIN in maize and rice. Both *ZmSWEET4c* and *OsSWEET4* mutants are defective in seed-filling (Sosso et al., 2015).

Sugar transporters and invertases in phloem loading and unloading are essential for yield. However, the specific function of each transporter and its responses to C availability (and external stimuli) need to be elucidated. During drought-induced kernel abortion, C shortage suppressed ZmSWEET effluxers (located on the PC and ESR), CWIN, and SUS, but stimulated ZmSTPs and ZmSUTs, which are responsible for sugar uptake in filial tissues (Shen et al., 2020; Shen et al., 2022). When the C supply was boosted, the doomed kernels were reformed, and drought-induced changes in the transporters were mostly prevented (Shen et al., 2022). Sugar signals may regulate transporters and their coordination; however, the specific mechanisms remain unclear. In addition, how these proteins respond to other signaling pathways, such as phytohormones, remains largely unknown.

Regulation of starch synthesis increases sink demand and crop yield

After maize kernel capacity was established, CWIN expression was repressed and sucrose was directly transported into the endosperm in maize, where SUSs such as shrunken1 (*ZmSh1*) and sucrose synthase 1, 2, and 4 (*ZmSUS1/2/4*) were highly expressed during the grain-filling stage (Figure 1F; Larkins, 2017; Shen et al., 2022). Starch is the main storage site in the cereal

endosperm, accounting for more than 70% of the endosperm dry weight. Starch synthesis is highly regulated by enzymes including adenosine diphosphate (ADP)-glucose pyrophosphorylases (AGPases), soluble starch synthases (SSs), granule-bound starch synthases (GBSSs), starch branching enzymes (BEs), and starch debranching enzymes (DBEs) (Jeon et al., 2010). Interestingly, the order of starch accumulation in different parts of one grain is highly conserved in maize, rice, and probably wheat, starting from the distal end of the sugar unloading position and gradually moving to the proximal end (Chen, 2022; Liu et al., 2022a). Sucrose, but not hexose, is thought to be resynthesized at the base of the maize endosperm (the site of sugar unloading) and transported to the site of starch synthesis, which is inconsistent with the substantial upregulation of SUSs during grain filling (Shannon et al., 1986; Olsen, 2020; Shen et al., 2022). AGPase is a key enzyme in starch synthesis. Overexpression of AGPase or SS has been reported to increase cereal grain weight, starch content, and yield (Smidansky et al., 2002; Tian et al., 2018; Paul et al., 2020). A recent study engineered heat-stable 6-phosphogluconate dehydrogenase in maize to improve grain yield under heat stress (Ribeiro et al., 2020). By altering these critical metabolic enzymes, yield performance can be improved by increasing sink demand; however, further efforts are needed in field applications.

Systemic sugar signaling regulates C partitioning

Many of the details related to sugar sensing, signaling, and crosstalk with phytohormones and environmental nutrients are largely performed in model plants (Wu et al., 2019b; Baena-Gonzalez and Lunn, 2020; Fichtner et al., 2021; Li et al., 2021; Meng et al., 2022), while for cereals, the understanding of sugar signal transduction and regulation is still insufficient. Here, we briefly introduce the core networks of sugar sensing and signaling. Specifically, recent examples of the regulation of trehalose-6-phosphate in cereal crops are discussed, with the aim of revealing the potential of systemic regulation to coordinate source-sink C balance and synchronously enhance crop yield and resilience.

There are two main mechanisms for sensing and transducing sugar signals in plants, called: direct and indirect (Figure 2; Li et al., 2021). The former is triggered by sugar-binding sensors, such as the glucose signaling sensor hexokinase (HXK), and possibly the regulators of G-protein signaling1 (RGS1), trehalose 6-phosphate (T6P) synthase1 (TPS1), and T6P phosphatase (TPP). The latter includes sugar-derived bioenergetic molecules and metabolite-regulated signaling proteins, such as the glucose-activated target of rapamycin (TOR) and sugar-inhibited SNF1-related protein kinase 1 (SnRK1). HXK1 controls multiple biological processes, including photosynthesis, phytohormone production, growth, and senescence, which are uncoupled from sugar metabolism (Moore et al., 2003). T6P, known as plant "insulin" is a key signal indicating sucrose availability and regulating sucrose homeostasis systemically (Fichtner and Lunn, 2021). TOR kinase acts as a GPS of nutrient, energy, and environmental cues to orchestrate growth and development, whereas SnRK1 antagonizes TOR by phosphorylating RAPTOR, a subunit of the TOR complex (Figure 2A). The SnRK1 complex plays a central role in nutrient sensing and stress responses and is activated under nutrient deprivation, such as darkness and starvation, but is inhibited by sugar phosphates, such as glucose 1-phosphate and T6P (Zhang et al., 2009; Li et al., 2021). By downregulating anabolism and upregulating catabolism, SnRK1 restores cellular energy homeostasis and coordinates tissue response to the environment.

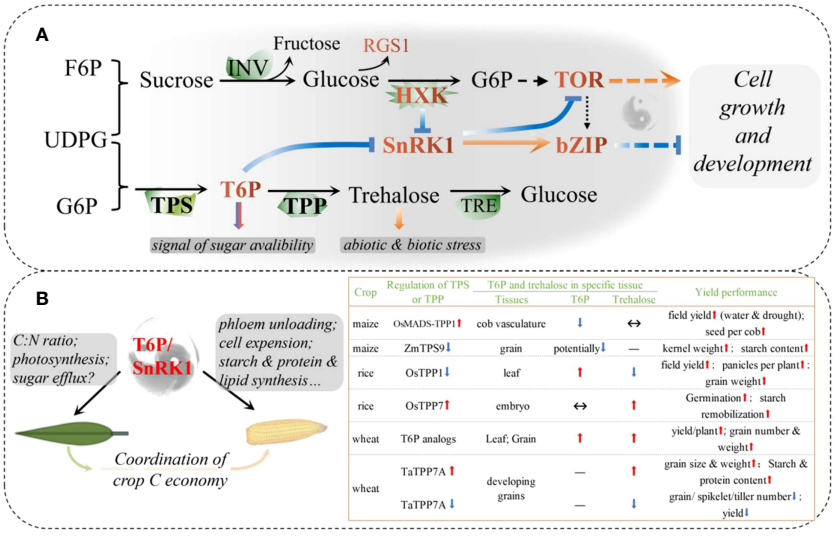

Crop	Regulation of TPS or TPP	T6P and trehalose in specific tissue: Tissues	T6P	Trehalose	Yield performance
maize	OsMADS-TPP1↑	cob vasculature	↓	↔	field yield↑ (water & drought); seed per cob↑
maize	ZmTPS9↓	grain	potentially↓	—	kernel weight↑; starch content↑
rice	OsTPP1↓	leaf	↑	↓	field yield↑; panicles per plant↑; grain weight↑
rice	OsTPP7↑	embryo	↔	↑	Germination↑; starch remobilization↑
wheat	T6P analogs	Leaf; Grain	↑	↑	yield/plant↑; grain number & weight↑
wheat	TaTPP7A↑	developing grains	—	↑	grain size & weight↑; Starch & protein content↑
	TaTPP7A↓		—	↓	grain/ spikelet/tiller number↓; yield↓

FIGURE 2
Systemic sugar signals. **(A)** Interactions in core sugar sensing and signaling; **(B)** Schematic diagram of source-sink carbon balance regulated by a possible T6P/SnRK1 complex in cereals. Recent reports on the regulation of T6P signaling in maize, rice, and wheat have been summarized. bZIP, The basic leucine zipper domain; F6P, fructose 6-phosphate; G6P, glucose 6-phosphate; HXK, hexokinase; INV, invertase; RGS1, regulator of G-protein signaling1; SnRK1, sucrose non-fermenting related kinase 1; T6P, trehalose 6-phosphate; TOR, target of Rapamycin; TPP, T6P phosphatase; TPS, T6P synthase; TRE, trehalase; UDPG, Uridine 5′-diphosphoglucose.

T6P is an intermediate in the trehalose biosynthesis pathway mediated by TPS1 and TPP. As a signal and regulator of sucrose status, T6P functions, at least partly, if not all, through the inhibition of SnRK1, and trehalose has long been implicated in plant biotic and abiotic stress responses (Baena-Gonzalez and Lunn, 2020). Recent studies on the regulation of T6P have shown promising results in major crops, with a significant increase in both yield and stress resistance or resilience (Figure 2B; Paul et al., 2018). In maize, floral promoter *OsMads6* driven overexpression of the rice TPP1 gene in developing maize ears improved yield under both drought and non-drought conditions over multiple field sites and seasons (Nuccio et al., 2015). *OsMads6* is most active in phloem CC cells in florets and piths, leading to the largest decrease in T6P levels, but significantly increased expression of SWEETs in these tissues. Hence, an increase in both sucrose in ear spikelets and photosynthesis in leaves during the flowering period can be explained by boosted phloem unloading (Nuccio et al., 2015; Oszvald et al., 2018). A common drought-induced phenomenon in maize production is the abortion of apical kernels, where the expression of TPS is elevated, but TPP is lower when compared to set kernels. Abortion can be largely rescued by synchronous pollination and/or incomplete basal pollination, accompanied by downregulation of TPS and upregulation of TPP expression (Shen et al., 2018; Shen et al., 2020). *ZmTPS9* was recently identified as a non-starch pathway gene that contributes to starch synthesis. Gene editing to knockout *ZmTPS9* results in increased starch accumulation and kernel weight (Hu et al., 2021).

The contributions of T6P, TPS, and TPP genes to source- and sink-related traits were further confirmed by gene-based mapping and T6P-precursors in wheat (Griffiths et al., 2016; Lyra et al., 2021). Using plant-permeable analogs and sunlight-triggered release of T6P, a chemical intervention was proposed to increase wheat grain yield spraying during grain filling and to prevent drought during the vegetative stage (Griffiths et al., 2016). However, unlike maize, the increased yield was associated with increased T6P in wheat grains, suggesting that the role of T6P may differ among species. Another possibility is that T6P has different effects on the source and the sink. The sprayed T6P-precursors to the ears only or to the whole plant cannot enter the grain without affecting other tissues, although the T6P in the grain was elevated (Griffiths et al., 2016). T6P in other parts (including leaves, glumes, and vasculature) is not known, and there may be huge differences in the pericarp and endosperm in one grain owing to unclear transport characteristics. T6P-precursors spraying not only increased gene expression related to the cell wall, starch, and protein synthesis in grains, and increased sugar availability in new-born leaves after post-drought spraying, but also increased photo-assimilation and preserved less C in source tissues, including flag leaves, aging leaves, and potentially pericarps (Liang, 2019). As a systemic signaling pathway, the role of T6P in cereal crops may be similar, but there are existing spatiotemporal differences.

In general, we propose that the increase in T6P could accelerate sucrose transport and/or conversion in source tissues (here, where net C outcomes above zero are defined as "source") and hence boosts photosynthesis in leaves, while increased sugar accumulation in the sink tissues (where net C incomes above zero are defined as "sink") could be associated with decreased T6P (Figure 2B). Consistent with this speculation, *TaTPP-7A* was detected as a QTL that was significantly associated with grain weight, and overexpression of *TaTPP-7A* greatly enhanced grain weight and wheat yield (Liu et al., 2023). Overexpression of *OsTPP7* located in coleoptile tips enhanced rice germination under both anaerobic stress and an aerobic environment by stimulation of endosperm starch remobilization, whereas *Ostpp1* mutants germinated slower than the wild type (Kretzschmar et al., 2015; Wang et al., 2021a). Recently, a sugar-inducible rice transcription factor, *OsNAC23*, was found to directly repress *OsTPP1* expression to simultaneously elevate T6P, thereby facilitating C partitioning from the source to sink. Plants overexpressing *OsNAC23* showed elevated T6P levels, sugar transport, and photosynthesis in flag leaves and increased sink organ size and rice yields in three elite-variety backgrounds and two locations (Li et al., 2022c). These results further confirmed our speculation and showed promise for future T6P modulation of both yield potential and resistance/resilience (Figure 2B). Future research may need to explore different strategies to regulate T6P in sources and/or sinks and to further clarify the roles of different TPSs and TPPs in the processes of yield production and resilience.

The source-sink system: the Yin–Yang balance

High photoassimilation is the basis for yield and resistance only if the carbohydrates can be effectively stored or transported in downstream processes. First, triose phosphate (TP) from the Calvin cycle must be exported from the chloroplast into the cytoplasm in exchange for inorganic phosphate (Pi). High TP in chloroplasts results in high levels of 3-phosphoglyceraldehyde, low Pi, and photosynthetic inhibition, thereby activating AGPase and starch synthesis. However, a low TP leads to the opposite (Mugford et al., 2014). Starch accumulation in leaves can relieve photosynthetic inhibition but is negatively correlated with maize growth (Liang et al., 2019; Liang et al., 2020). Hence, increasing P availability could be a feasible way to improve the yield of photosynthetically improved crops (Khurshid et al., 2020). Second, excessive soluble sugars in the cytoplasm also feedback-inhibit photosynthesis, which could be alleviated by TMT-mediated temporary storage in the vacuole or by an efficient transport system that is co-controlled by SWEETs and SUT1 in leaves. Third, stems have multiple roles in carbohydrate coordination, acting as a transfer tissue, temporary sink, and donator as needed (Slewinski, 2012). Regulation of stem sugars has been shown to boost yield and resilience as early as the first green revolution. Finally but most importantly, sugars loaded into the phloem must be utilized promptly and appropriately. Sugar unloading strength and sink growth activity ultimately determine the persistence of the source strength.

There is still no verdict about the debate on whether cereal yield is source or sink-limited. Researchers focusing on the source (e.g., photosynthesis system) and sink (e.g., sugar unloading and

utilization) both believe that their work could solely improve yield output, while usually reaching an opposite or unexpected result. The so-called "source limitation" or "sink limitation" is more a matter of, at least partly, synergies between organ growth, phase transition, and environmental changes. As mentioned above, the flow of C (and other nutrients) in plants determines that the development of the source-sink relationship always maintains a dynamic balance, rather than mutual independence or even antagonism. The status between the source and sink can be described as Yin and Yang in Tai Ji, the two opposing and unifying principles in nature (Figure 3). Uncoordinated relationships in the crop are generally divided into two cases, i.e., sufficient source supply with insufficient sink demand and the opposite, in which the plant as a whole system tries to turn to but probably never attains a balance. There is no doubt that the strengthening or weakening of one can pull or feedback inhibits the development of the other. For example, evaluated leaf photosynthesis by CO_2 concentration increased yield performance, whereas a larger sink capacity facilitated higher power of C fixation and higher ratios of transfer (Arp, 1991; Paul and Foyer, 2001; O'Leary et al., 2015).

The question is, will the improvement of one be sufficient to stimulate the other to achieve a high level of source-sink balance? A combined approach using both 'pull' and 'push' has been reported for yield improvement (Rossi et al., 2015). The long time-scale adaptation of the crop to the environment makes it difficult to bring out ideal results by one or two gene modifications, although silencing or knockout of particular genes has resulted in phenotype defects. Metabolic engineering also suggests that an optimal balance of enzyme activities is more important than simply overexpressing a suite of enzymes (Sweetlove et al., 2017). Therefore, rather than improving only the source or sink, systemic improvement and whole-plant C balance may be more important for crop production. This can be achieved by introducing multiple targeted engineered genes from both the source and sink tissues, such as transporters, critical enzymes, and systemic signals, into crops.

Optimizing plant C economy for both yield and resilience

Empirically, crop yield and stress resistance often contradicts each other. However, by optimizing the plant C economy, several genetic strategies have emerged that can increase crop tolerance to stress while increasing, or at least not reducing, yield. Editing of the SWEETs promoter mentioned above is a precise strategy to improve disease resistance while maintaining functional SWEETs for crops (Eom et al., 2019; Oliva et al., 2019). ABA is a key response signal for abiotic stresses such as drought. Sustained ABA signaling is considered to significantly increase plant resistance but at the expense of a growth penalty. Overexpression of ABA signaling receptors (TaPYLs), which can respond rapidly to drought-induced ABA signals, improves wheat yield under drought conditions without affecting non-drought growth and yield (Mega et al., 2019). Overexpression of the brassinosteroid receptor BRL3 confers drought resistance without affecting plant growth (Fàbregas et al., 2018). Trehalose accumulates under various conditions and protects plants from damage. Researchers have used fusion gene coding for TPS and TPP driven by an ABA-inducible promoter to generate transgenic rice. Trehalose overproduction contributes to lower yield penalties under drought, saline, and sodic conditions, while the yield potential remains unchanged (Joshi et al., 2020). These examples, together with the above-mentioned T6P modulation are not representative of all, but raise the point of view that carbohydrates can be allocated to the right place at the right time by spatiotemporal expression of certain gene(s) through manipulation of specific promoters (conditionally induced or tissue-specific). This flexible C economy strategy could simultaneously endow crops with both high-yield traits and good resistance/resilience.

In field production, several strategies for simultaneously improving crop resistance and yield by targeting C allocation have gradually emerged. Ovary or grain abortion is an adaptive response in cereal domestication, but is agronomically undesirable as it prevents crop yields from reaching their potential. The window period for ovary pollination and grain establishment is considered highly sensitive to stress (Shen et al., 2018; Gao et al., 2023). Shortening maize ASI in the

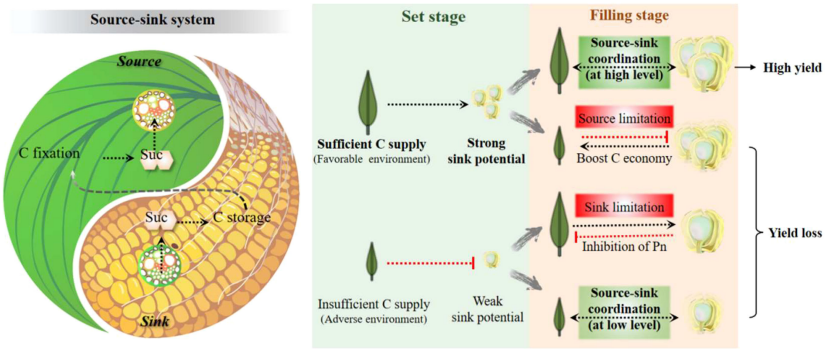

FIGURE 3
The dialectical relationship between source and sink from a systemic perspective with the example of carbohydrates. This relationship is described as the balance of Yin and Yang, the wisdom crystallization of ancient Chinese. The different scenarios of the source-sink relationship during the grain set and filling stages are briefly summarized. It is proposed that the C supply from the source determines the sink capacity during the grain-set stage, whereas in the grain-filling stage, the realization of a potentially high yield requires a high-level balance between the source and sink. C, carbon; Suc, sucrose.

past has improved grain yield due to, at least partly, increased C allocation into the ear tissue. Furthermore, the pollination time gap (PTG) of ovaries on different parts of a panicle/cob will lead to uneven distribution of C allocation among grain siblings, resulting in abortion of inferior spikelets, which usually occur at the top of maize ears, the upper and lower parts of rice, and wheat spikes, especially under adverse conditions such as drought (Shen et al., 2018; Shen et al., 2023). Shortening PTG by measures, such as synchronizing pollination or adoption of stubby ear hybrids, has been shown to coordinate C allocation within siblings and improve both yield and drought resistance in maize (Shen et al., 2018; Shen et al., 2020; Chen et al., 2022b). Strategies aimed at shortening PTG for rice and wheat might work equally well. Moreover, increased distribution of C in the ovary or grain can be achieved by stem manipulation. In wheat, drought-induced abortion of inferior ovaries or grains is associated with suppressed ABA signal transduction in the stems (Zhang et al., 2020b). In contrast, moderate post-anthesis drought in rice-induced ABA signaling and ABA–IAA interactions promotes the remobilization of stem-stored C reserves and enhances inferior grain filling (Wang and Zhang, 2020; Teng et al., 2022). Similarly, recent research has highlighted ways to increase maize grain number and final yield under both optimal and unsuitable environments by tuning stem elongation and ear development. Two maize genotypes with similar plant heights and yield potentials but different drought tolerances were subjected to water scarcity. The ear grain number and final yield of the tolerant genotype were 38.1% and 35.1% higher, respectively, but the plant height was 17.6% short than that under drought (Gao et al., 2023). ^{13}C labeling, together with transcript analysis revealed that the inhibited stem elongation and promoted assimilate allocation to the ear in the tolerant hybrid were induced by signals including ABA and T6P in the stem (Gao et al., 2023). Exogenous application of plant growth regulators, such as ethephon and cycocel at the V15 stage of maize hybrids was proved to reduce internode length and facilitate assimilate partitioning to the ear, which in turn increases the final yield (Zhao et al., 2022). In general, as evidenced by the first green revolution, it is still an important way to increase yield and resistance by reducing or reactivating stem carbohydrates and increasing ovary or grain allocation during the critical growth period.

In summary, some promising strategies, such as rapid environmental response, optimized ear traits, and specific gene regulation in certain tissues or circumstances, aimed at optimizing the C economy within plant systems and increasing C flow to sink organs, have achieved synergistic improvements in yield and resistance/resilience. Based on these strategies, future research may lead to yield breakthroughs in multiple crops using different means (breeding and/or cultivation).

Concluding thoughts

In conclusion, systemic improvement of crops should include the synergistic promotion of C fixation, transport, and utilization. Although the photosynthetic capacity of the field population of modern varieties is believed to be relatively high, as indicated by the traits of canopy leaf area, stay green, and stress tolerance, further improvements in photosynthetic efficiency and coupling with nutrients (N, P, and others) are still needed. One of the keys to high yields in the field is the efficient and economical use of photosynthetically produced assimilates. Unlike currently common adaptation strategies (for example, less C allocation under drought, seed abortion due to insufficient C supply, etc.), the C economy of future "smart crops" needs to be well designed, and the key lies in the flexible adjustment of C flow according to tissue needs at specific growth periods, aiming to improve yield and/or resilience. Both breeding and cultivation methods as well as crop physiology should be considered. In particular, understanding how a field crop manipulates its C economy is the basis for precise control. A recent study found that rapid phosphorylation of SWEET11 and 12 in *Arabidopsis* promotes carbohydrate transport to the roots during drought (Chen et al., 2022a). However, root C allocation and adjustment in crops have received limited attention. Hence, further research is needed to determine which tissue(s) should be stimulated during the growth process in the face of changing environments. Currently, some appropriate strategies, such as specifically overexpressing the TPP gene in maize and spraying T6P precursors after flowering or seedling drought in wheat, have been developed and applied (Griffiths et al., 2016; Oszvald et al., 2018). It is believed that in the future, "smart crops" created through means such as targeted gene editing, or "smart cultivation systems" based on precise C regulation will significantly contribute to the actual yield improvement.

Author contributions

X-GL and ZG drafted and edited the manuscript and figure. XXF surveyed and analyzed the literature. X-GL and X-MC revised the manuscript. SS and S-LZ conceived the study, contributed to drafting, and edited both the text and figure. X-MC did a lot of work in the revision of the paper, including language & logic revision, re-creation and addition of figures. All authors contributed to the article and approved the submitted version.

Funding

This work was supported by the National Natural Science Foundation of China (32160445), the fellowship of China Postdoctoral Science Foundation (2022M723432), the Natural Science Funds of Jiangxi Province (20202BABL215004, 20202BABL215008), the earmarked fund for Innovation team of Jiangxi Agricultural University (JXAUCXTD002), and the earmarked fund for CARS (CARS-02-16). Support is acknowledged from the State Key Laboratory of North China Crop Improvement and Regulation to X-GL.

Conflict of interest

The authors declare that the research was conducted in the absence of any commercial or financial relationships that could be construed as a potential conflict of interest.

The reviewer BY declared a shared affiliation with the author ZG to the handling editor at the time of review.

Publisher's note

References

Arp, W. J. (1991). Effects of source-sink relations on photosynthetic acclimation to elevated CO_2. *Plant Cell Environ.* 14, 869–875. doi: 10.1111/j.1365-3040.1991.tb01450.x

Baena-Gonzalez, E., and Lunn, J. E. (2020). SnRK1 and trehalose 6-phosphate - two ancient pathways converge to regulate plant metabolism and growth. *Curr. Opin. Plant Biol.* 55, 52–59. doi: 10.1016/j.pbi.2020.01.010

Bezrutczyk, M., Hartwig, T., Horschman, M., Char, S. N., Yang, J., Yang, B., et al. (2018). Impaired phloem loading in *zmsweet13a,b,c* sucrose transporter triple knock-out mutants in *Zea mays*. *New Phytol.* 218, 594–603. doi: 10.1111/nph.15021

Braun, D. M. (2022). Phloem loading and unloading of sucrose: what a Long, strange trip from source to sink. *Annu. Rev. Plant Biol.* 73, 553–584. doi: 10.1146/annurev-arplant-070721-083240

Burgess, A. J., Masclaux-Daubresse, C., Strittmatter, G., Weber, A. P. M., Taylor, S. H., Harbinson, J., et al. (2023). Improving crop yield potential: underlying biological processes and future prospects. *Food Energy Secur.* 12, e435. doi: 10.1002/fes3.345

Chen, X. M. (2022). Spatio-temporal heterogeneity of carbon metabolism and its regulational mechanism in maize endosperm. *PhD thesis China Agric. University Beijing*.

Chen, J. H., Chen, S. T., He, N. Y., Wang, Q. L., Zhao, Y., Gao, W., et al. (2020). Nuclear-encoded synthesis of the D1 subunit of photosystem II increases photosynthetic efficiency and crop yield. *Nat. Plants* 6, 570–580. doi: 10.1038/s41477-020-0629-z

Chen, L. Q., Cheung, L. S., Feng, L., Tanner, W., and Frommer, W. B. (2015). Transport of sugars. *Ann. Rev. Biochem.* 84, 865–894. doi: 10.1146/annurev-biochem-060614-033904

Chen, Q., Hu, T., Li, X., Song, C. P., Zhu, J. K., Chen, L., et al. (2022a). Phosphorylation of SWEET sucrose transporters regulates plant root:shoot ratio under drought. *Nat. Plants* 8, 68–77. doi: 10.1038/s41477-021-01040-7

Chen, X. M., Li, F. Y., Dong, S., Liu, X. F., Li, B. B., Xiao, Z. D., et al. (2022b). Stubby or slender? ear architecture is related to drought resistance in maize. *Front. Plant Sci.* 13, 901186. doi: 10.3389/fpls.2022.901186

Chen, L. Q., Qu, X. Q., Hou, B. H., Sosso, D., Osorio, S., Fernie, A. R., et al. (2012). Sucrose efflux mediated by SWEET proteins as a key step for phloem transport. *Science* 335, 207–211. doi: 10.1126/science.1213351

Clark, M. A., Domingo, N. G. G., Colgan, K., Thakrar, S. K., Tilman, D., Lynch, J., et al. (2020). Global food system emissions could preclude achieving the 1.5° and 2°C climate change targets. *Science* 370, 705–708. doi: 10.1126/science.aba7357

Cross, J. M., von Korff, M., Altmann, T., Bartzetko, L., Sulpice, R., Gibon, Y., et al. (2006). Variation of enzyme activities and metabolite levels in 24 *Arabidopsis* accessions growing in carbon-limited conditions. *Plant Physiol.* 142, 1574–1588. doi: 10.1104/pp.106.086629

De Souza, A. P., Burgess, S. J., Doran, L., Hansen, J., Manukyan, L., Maryn, N., et al. (2022). Soybean photosynthesis and crop yield are improved by accelerating recovery from photoprotection. *Science* 377, 851–854. doi: 10.1126/science.adc9831

Dhungana, S. R., and Braun, D. M. (2021). Sugar transporters in grasses: Function and modulation in source and storage tissues. *J. Plant Physiol.* 266, 153541. doi: 10.1016/j.jplph.2021.153541

Eom, J. S., Chen, L. Q., Sosso, D., Julius, B. T., Lin, I. W., Qu, X. Q., et al. (2015). SWEETs, transporters for intracellular and intercellular sugar translocation. *Curr. Opin. Plant Biol.* 25, 53–62. doi: 10.1016/j.pbi.2015.04.005

Eom, J. S., Cho, J. I., Reinders, A., Lee, S. W., Yoo, Y., Tuan, P. Q., et al. (2011). Impaired function of the tonoplast-localized sucrose transporter in rice, *OsSUT2*, limits the transport of vacuolar reserve sucrose and affects plant growth. *Plant Physiol.* 157, 109–119. doi: 10.1104/pp.111.176982

Eom, J. S., Luo, D., Atienza-Grande, G., Yang, J., Ji, C., Thi Luu, V., et al. (2019). Diagnostic kit for rice blight resistance. *Nat. Biotechnol.* 37, 1372–1379. doi: 10.1038/s41587-019-0268-y

Fàbregas, N., Lozano-Elena, F., Blasco-Escamez, D., Tohge, T., Martinez-Andujar, C., Albacete, A., et al. (2018). Overexpression of the vascular brassinosteroid receptor *BRL3* confers drought resistance without penalizing plant growth. *Nat. Commun.* 9, 4680. doi: 10.1038/s41467-018-06861-3

Fatima, U., Balasubramaniam, D., Khan, W. A., Kandpal, M., Vadassery, J., Arockiasamy, A., et al. (2023). *AtSWEET11* and *AtSWEET12* transporters function in tandem to modulate sugar flux in plants. *Plant Direct* 7, e481. doi: 10.1002/pld3.481

Fei, H., Yang, Z., Lu, Q., Wen, X., Zhang, Y., Zhang, A., et al. (2021). *OsSWEET14* cooperates with *OsSWEET11* to contribute to grain filling in rice. *Plant Sci.* 306, 110851. doi: 10.1016/j.plantsci.2021.110851

Fichtner, F., Dissanayake, I. M., Lacombe, B., and Barbier, F. (2021). Sugar and nitrate sensing: A multi-billion-year story. *Trends Plant Sci.* 26, 352–374. doi: 10.1016/j.tplants.2020.11.006

Fichtner, F., and Lunn, J. E. (2021). The Role of Trehalose 6-Phosphate (Tre6P) in plant metabolism and development. *Annu. Rev. Plant Biol.* 72, 3.1–3.24. doi: 10.1146/annurev-arplant-050718-095929

Gao, Y., Zhang, C., Han, X., Wang, Z. Y., Ma, L., Yuan, P., et al. (2018). Inhibition of *OsSWEET11* function in mesophyll cells improves resistance of rice to sheath blight disease. *Mol. Plant Pathol.* 19, 2149–2161. doi: 10.1111/mpp.12689

Gao, J., Zhang, Y., Xu, C., Wang, X., Wang, P., and Huang, S. (2023). Abscisic acid collaborates with lignin and flavonoid to improve pre-silking drought tolerance by tuning stem elongation and ear development in maize (*Zea mays* L.). *Plant J.* 114, 437–454. doi: 10.1111/tpj.16147

Grassini, P., Eskridge, K. M., and Cassman, K. G. (2013). Distinguishing between yield advances and yield plateaus in historical crop production trends. *Nat. Commun.* 4, 2918. doi: 10.1038/ncomms3918

Griffiths, C. A., Sagar, R., Geng, Y., Primavesi, L. F., Patel, M. K., Passarelli, M. K., et al. (2016). Chemical intervention in plant sugar signalling increases yield and resilience. *Nature* 540, 574–578. doi: 10.1038/nature20591

Hart, J. E., Sullivan, S., Hermanowicz, P., Petersen, J., Diaz-Ramos, L. A., Hoey, D. J., et al. (2019). Engineering the phototropin photocycle improves photoreceptor performance and plant biomass production. *P. Natl. Acad. Sci.* 116, 12550–12557. doi: 10.1073/pnas.1902915116

Haupt, S., Duncan, G. H., Holzberg, S., and Oparka, K. J. (2001). Evidence for symplastic phloem unloading in sink leaves of barley. *Plant Physiol.* 125, 209–218. doi: 10.1104/pp.125.1.209

Hu, S., Wang, M., Zhang, X., Chen, W., Song, X., Fu, X., et al. (2021). Genetic basis of kernel starch content decoded in a maize multi-parent population. *Plant Biotechnol. J.* 19, 2192–2205. doi: 10.1111/pbi.13645

Jeon, J. S., Ryoo, N., Hahn, T. R., Walia, H., and Nakamura, Y. (2010). Starch biosynthesis in cereal endosperm. *Plant Physiol. Biochem.* 48, 383–392. doi: 10.1016/j.plaphy.2010.03.006

Joshi, R., Sahoo, K. K., Singh, A. K., Anwar, K., Pundir, P., Gautam, R. K., et al. (2020). Enhancing trehalose biosynthesis improves yield potential in marker-free transgenic rice under drought, saline, and sodic conditions. *J. Exp. Bot.* 71, 653–668. doi: 10.1093/jxb/erz462

Julius, B. T., Leach, K. A., Tran, T. M., Mertz, R. A., and Braun, D. M. (2017). Sugar transporters in plants: New insights and discoveries. *Plant Cell Physiol.* 58, 1442–1460. doi: 10.1093/pcp/pcx090

Khurshid, G., Abbassi, A. Z., Khalid, M. F., Gondal, M. N., Naqvi, T. A., Shah, M. M., et al. (2020). A cyanobacterial photorespiratory bypass model to enhance photosynthesis by rerouting photorespiratory pathway in C_3 plants. *Sci. Rep.* 10, 20879. doi: 10.1038/s41598-020-77894-2

Kim, P., Xue, C. Y., Song, H. D., Gao, Y., Feng, L., Li, Y., et al. (2021). Tissue-specific activation of *DOF11* promotes rice resistance to sheath blight disease and increases grain weight *via* activation of SWEET14. *Plant Biotechnol. J.* 19, 409–411. doi: 10.1111/pbi.13489

Knoblauch, M., Knoblauch, J., Mullendore, D. L., Savage, J. A., Babst, B. A., Beecher, S. D., et al. (2016). Testing the Munch hypothesis of long distance phloem transport in plants. *eLife* 5, e15341. doi: 10.7554/eLife.15341.025

Kretzschmar, T., Pelayo, M. A., Trijatmiko, K. R., Gabunada, L. F., Alam, R., Jimenez, R., et al. (2015). A trehalose-6-phosphate phosphatase enhances anaerobic germination tolerance in rice. *Nat. Plants* 1, 15124. doi: 10.1038/nplants.2015.124

Kromdijk, J., Glowacka, K., Leonelli, L., Gabilly, S. T., Iwai, M., Niyogi, K. K., et al. (2016). Improving photosynthesis and crop productivity by accelerating recovery from photoprotection. *Science* 354, 857–861. doi: 10.1126/science.aai8878

B. A. Larkins (Ed.) (2017). *Maize kernel development* (Boston, MA: CABI), ISBN: .

Leach, K. A., Tran, T. M., Slewinski, T. L., Meeley, R. B., and Braun, D. M. (2017). Sucrose transporter2 contributes to maize growth, development, and crop yield. *J. Integr. Plant Biol.* 59, 390–408. doi: 10.1111/jipb.12527

Leister, D. (2023). Enhancing the light reactions of photosynthesis: Strategies, controversies, and perspectives. *Mol. Plant* 16, 4–22. doi: 10.1016/j.molp.2022.08.005

Li, L., Liu, K. H., and Sheen, J. (2021). Dynamic nutrient signaling networks in plants. *Annu. Rev. Cell Dev. Bi.* 37, 341–367. doi: 10.1146/annurev-cellbio-010521-015047

Li, B., Liu, H., Zhang, Y., Kang, T., Zhang, L., Tong, J., et al. (2013). Constitutive expression of cell wall invertase genes increases grain yield and starch content in maize. *Plant Biotechnol. J.* 11, 1080–1091. doi: 10.1111/pbi.12102

Li, P., Wang, L., Liu, H., and Yuan, M. (2022b). Impaired SWEET-mediated sugar transportation impacts starch metabolism in developing rice seeds. *Crop J.* 10, 98–108. doi: 10.1016/j.cj.2021.04.012

Li, Z., Wei, X., Tong, X., Zhao, J., Liu, X., Wang, H., et al. (2022c). The OsNAC23-Tre6P-SnRK1a feed-forward loop regulates sugar homeostasis and grain yield in rice. *Mol. Plant* 15, 706–722. doi: 10.1016/j.molp.2022.01.016

Li, G., Zhou, C., Yang, Z., Zhang, C., Dai, Q., Huo, Z., et al. (2022a). Low nitrogen enhances apoplastic phloem loading and improves the translocation of photoassimilates in rice leaves and stems. *Plant Cell Physiol.* 63, 991–1007. doi: 10.1093/pcp/pcac066

Liang, X. G. (2019). *The quantification of photoassimilate in crop Leaves and the adjustment of C-balance by trehalose pathway* (Beijing: China Agricultural University).

Liang, X. G., Gao, Z., Shen, S., Paul, M. J., Zhang, L., Zhao, X., et al. (2020). Differential ear growth of two maize varieties to shading in the field environment: effects on whole plant carbon allocation and sugar starvation response. *J. Plant Physiol.* 251, 153194. doi: 10.1016/j.jplph.2020.153194

Liang, X. G., Gao, Z., Zhang, L., Shen, S., Zhao, X., Liu, Y. P., et al. (2019). Seasonal and diurnal patterns of non-structural carbohydrates in source and sink tissues in field maize. *BMC Plant Biol.* 19, 1–11. doi: 10.1186/s12870-019-2068-4

Liang, X. G., Shen, S., Gao, Z., Zhang, L., Zhao, X., and Zhou, S. L. (2021). Variation of carbon partitioning in newly expanded maize leaves and plant adaptive growth under extended darkness. *J. Integr. Agr.* 20, 2360–2371. doi: 10.1016/S2095-3119(20)63351-2

Liu, T., Kawochar, M. A., Liu, S., Cheng, Y., Begum, S., Wang, E., et al. (2022b). Suppression of the tonoplast sugar transporter, *StTST3.1*, affects transitory starch turnover and plant growth in potato. *Plant J.* 113, 342–356. doi: 10.1111/tpj.16050

Liu, H., Si, X., Wang, Z., Cao, L., Gao, L., Zhou, X., et al. (2023). *TaTPP-7A* positively feedback regulates grain filling and wheat grain yield through T6P-SnRK1 signalling pathway and sugar-ABA interaction. *Plant Biotechnol. J* 21, 1159–1175. doi: 10.1111/pbi.14025

Liu, J., Wu, M. W., and Liu, C. M. (2022a). Cereal endosperms: Development and storage product accumulation. *Annu. Rev. Plant Biol.* 73, 255–291. doi: 10.1146/annurev-arplant-070221-024405

Long, B. M., Hee, W. Y., Sharwood, R. E., Rae, B. D., Kaines, S., Lim, Y.-L., et al. (2018). Carboxysome encapsulation of the CO_2-fixing enzyme Rubisco in tobacco chloroplasts. *Nat. Commun.* 9, 3570. doi: 10.1038/s41467-018-06044-0

Lopez-Calcagno, P. E., Brown, K. L., Simkin, A. J., Fisk, S. J., Vialet-Chabrand, S., Lawson, T., et al. (2020). Stimulating photosynthetic processes increases productivity and water-use efficiency in the field. *Nat. Plants* 6, 1054–1063. doi: 10.1038/s41477-020-0740-1

Lyra, D. H., Griffiths, C. A., Watson, A., Joynson, R., Molero, G., Igna, A. A., et al. (2021). Gene-based mapping of trehalose biosynthetic pathway genes reveals association with source- and sink-related yield traits in a spring wheat panel. *Food Energy Secur.* 10, e292. doi: 10.1002/fes3.292

Ma, L., Zhang, D., Miao, Q., Yang, J., Xuan, Y., and Hu, Y. (2017). Essential role of sugar transporter *OsSWEET11* during the early stage of rice grain filling. *Plant Cell Physiol.* 58, 863–873. doi: 10.1093/pcp/pcx040

Mathan, J., Singh, A., and Ranjan, A. (2021a). Sucrose transport and metabolism control carbon partitioning between stem and grain in rice. *J. Exp. Bot.* 72, 4355–4372. doi: 10.1093/jxb/erab066

Mathan, J., Singh, A., and Ranjan, A. (2021b). Sucrose transport in response to drought and salt stress involves ABA-mediated induction of *OsSWEET13* and *OsSWEET15* in rice. *Physiol. Plant* 171, 620–637. doi: 10.1111/ppl.13210

Mega, R., Abe, F., Kim, J. S., Tsuboi, Y., Tanaka, K., Kobayashi, H., et al. (2019). Tuning water-use efficiency and drought tolerance in wheat using abscisic acid receptors. *Nat. Plants* 5, 153–159. doi: 10.1038/s41477-019-0361-8

Meng, Y., Zhang, N., Li, J., Shen, X., Sheen, J., and Xiong, Y. (2022). TOR kinase, a GPS in the complex nutrient and hormonal signaling networks to guide plant growth and development. *J. Exp. Bot.* 73, 7041–7054. doi: 10.1093/jxb/erac282

Moore, B., Zhou, L., Rolland, F., Hall, Q., Cheng, W.-H., Liu, Y.-X., et al. (2003). Role of the *Arabidopsis* glucose sensor HXK1 in nutrient, light, and hormonal signaling. *Science* 300, 332–336. doi: 10.1126/science.1080585

Morii, M., Sugihara, A., Takehara, S., Kanno, Y., Kawai, K., Hobo, T., et al. (2020). The dual function of *OsSWEET3a* as a gibberellin and glucose transporter is important for young shoot development in rice. *Plant Cell Physiol.* 61, 1935–1945. doi: 10.1093/pcp/pcaa130

Mugford, S. T., Fernandez, O., Brinton, J., Flis, A., Krohn, N., Encke, B., et al. (2014). Regulatory properties of ADP glucose pyrophosphorylase are required for adjustment of leaf starch synthesis in different photoperiods. *Plant Physiol.* 166, 1733–1747. doi: 10.1104/pp.114.247759

Nuccio, M. L., Wu, J., Mowers, R., Zhou, H. P., Meghji, M., Primavesi, L. F., et al. (2015). Expression of trehalose-6-phosphate phosphatase in maize ears improves yield in well-watered and drought conditions. *Nat. Biotechnol.* 33, 862–869. doi: 10.1038/nbt.3277

O'Leary, G. J., Christy, B., Nuttall, J., Huth, N., Cammarano, D., Stockle, C., et al. (2015). Response of wheat growth, grain yield and water use to elevated CO_2 under a Free-Air CO_2 Enrichment (FACE) experiment and modelling in a semi-arid environment. *Global Change Biol.* 21, 2670–2686. doi: 10.1111/gcb.12830

Ohshima, T., Hayashi, H., and Chino, M. (1990). Collection and chemical composition of pure phloem sap from *Zea mays* L. *Plant Cell Physiol.* 31, 735–737. doi: 10.1093/oxfordjournals.pcp.a077972

Oliva, R., Ji, C., Atienza-Grande, G., Huguet-Tapia, J. C., Perez-Quintero, A., Li, T., et al. (2019). Broad-spectrum resistance to bacterial blight in rice using genome editing. *Nat. Biotechnol.* 37, 1344–1350. doi: 10.1038/s41587-019-0267-z

Olsen, O. A. (2020). The modular control of cereal endosperm development. *Trends Plant Sci.* 25, 279–290. doi: 10.1016/j.tplants.2019.12.003

Ortiz-Bobea, A., Ault, T. R., Carrillo, C. M., Chambers, R. G., and Lobell, D. B. (2021). Anthropogenic climate change has slowed global agricultural productivity growth. *Nat. Clim. Change* 11, 306–312. doi: 10.1038/s41558-021-01000-1

Oszvald, M., Primavesi, L. F., Griffiths, C. A., Cohn, J., Basu, S. S., Nuccio, M. L., et al. (2018). Trehalose 6-Phosphate regulates photosynthesis and assimilate partitioning in reproductive tissue. *Plant Physiol.* 176, 2623–2638. doi: 10.1104/pp.17.01673

Papanatsiou, M., Petersen, J., Henderson, L., Wang, Y., Christie, J. M., and Blatt, M. R. (2019). Optogenetic manipulation of stomatal kinetics improves carbon assimilation, water use, and growth. *Science* 363, 1456–1459. doi: 10.1126/science.aaw0046

Paul, M. J., and Foyer, C. H. (2001). Sink regulation of photosynthesis. *J. Exp. Bot.* 52, 1383–1400. doi: 10.1093/jexbot/52.360.1383

Paul, M. J., Gonzalez-Uriarte, A., Griffiths, C. A., and Hassani-Pak, K. (2018). The role of trehalose 6-phosphate in crop yield and resilience. *Plant Physiol.* 177 (1), 12–23. doi: 10.1104/pp.17.01634

Paul, M. J., Watson, A., and Griffiths, C. A. (2020). Linking fundamental science to crop improvement through understanding source and sink traits and their integration for yield enhancement. *J. Exp. Bot.* 71, 2270–2280. doi: 10.1093/jxb/erz480

Prasad, D., Jung, W. J., and Seo, Y. W. (2023). Identification and molecular characterization of novel sucrose transporters in the hexaploid wheat (*Triticum aestivum* L.). *Gene* 860, 147245. doi: 10.1016/j.gene.2023.147245

Ray, D. K., Mueller, N. D., West, P. C., and Foley, J. A. (2013). Yield trends are insufficient to double global crop production by 2050. *PloS One* 8, e66428. doi: 10.1371/journal.pone.0066428

Ribeiro, C., Hennen-Bierwagen, T. A., Myers, A. M., Cline, K., and Settles, A. M. (2020). Engineering 6-phosphogluconate dehydrogenase improves grain yield in heat-stressed maize. *P. Natl. Acad. Sci.* 117, 33177–33185. doi: 10.1073/pnas.2010179117

Rolland, F., Baena-Gonzalez, E., and Sheen, J. (2006). Sugar sensing and signaling in plants: conserved and novel mechanisms. *Annu. Rev. Plant Biol.* 57, 675–709. doi: 10.1146/annurev.arplant.57.032905.105441

Rossi, M., Bermudez, L., and Carrari, F. (2015). Crop yield: challenges from a metabolic perspective. *Curr. Opin. Plant Biol.* 25, 79–89. doi: 10.1016/j.pbi.2015.05.004

Ruan, Y. L. (2014). Sucrose metabolism: gateway to diverse carbon use and sugar signaling. *Annu. Rev. Plant Biol.* 65, 33–67. doi: 10.1146/annurev-arplant-050213-040251

Ruan, Y. L. (2022). CWIN-sugar transporter nexus is a key component for reproductive success. *J. Plant Physiol.* 268, 153572. doi: 10.1016/j.jplph.2021.153572

Scofield, G. N., Hirose, T., Gaudron, J. A., Furbank, R. T., Upadhyaya, N. M., and Ohsugi, R. (2002). Antisense suppression of the rice transporter gene, *OsSUT1*, leads to impaired grain filling and germination but does not affect photosynthesis. *Funct. Plant Biol.* 29, 815–826. doi: 10.1071/PP01204

Shannon, J. C., Porter, G. A., and Knlevel, D. P. (1986). "Phloem unloading and transfer of sugars into developing corn endosperm,". In: Phloem Transport Eds. J. Cronshaw, W. J. Lucas and R. T. Giaquinta (New York: Phloem Transport, Alan Liss, Inc.), 265–277.

Shen, S., Liang, X. G., Zhang, L., Zhao, X., Liu, Y. P., Lin, S., et al. (2020). Intervening in sibling competition for assimilates by controlled pollination prevents seed abortion under postpollination drought in maize. *Plant Cell Eviron.* 43, 903–919. doi: 10.1111/pce.13704

Shen, S., Ma, S., Chen, X. M., Yi, F., Li, B. B., Liang, X. G., et al. (2022). A transcriptional landscape underlying sugar import for grain set in maize. *Plant J.* 110, 228–242. doi: 10.1111/tpj.15668

Shen, S., Ma, S., Wu, L., Zhou, S. L., and Ruan, Y. L. (2023). Winners-take-all: Competition of carbon resource for grain set. *Trends Plant Sci* 28, 893–901. doi: 10.1016/j.tplants.2023.03.015

Shen, B. R., Wang, L. M., Lin, X. L., Yao, Z., Xu, H. W., Zhu, C. H., et al. (2019). Engineering a new chloroplastic photorespiratory bypass to increase photosynthetic efficiency and productivity in rice. *Mol. Plant* 12, 199–214. doi: 10.1016/j.molp.2018.11.013

Shen, S., Zhang, L., Liang, X. G., Zhao, X., Lin, S., Qu, L. H., et al. (2018). Delayed pollination and low availability of assimilates are major factors causing maize kernel abortion. *J. Exp. Bot.* 69, 1599–1613. doi: 10.1093/jxb/ery013

Sinclair, T. R., Rufty, T. W., and Lewis, R. S. (2019). Increasing photosynthesis: Unlikely solution for world food problem. *Trends Plant Sci.* 24, 1032–1039. doi: 10.1016/j.tplants.2019.07.008

Singh, J., Das, S., Jagadis Gupta, K., Ranjan, A., Foyer, C. H., and Thakur, J. K. (2023). Physiological implications of SWEETs in plants and their potential applications in improving source-sink relationships for enhanced yield. *Plant Biotechnol. J* 21, 1528–1541. doi: 10.1111/pbi.13982

Singh, J., James, D., Achary, V. M. M., Patel, M. K., Thakur, J. K., Reddy, M. K., et al. (2021). Coordinated overexpression of *OsSUT1*, *OsSWEET11* and *OsSWEET14* in rice impairs carbohydrate metabolism that has implications in plant growth, yield and susceptibility to *Xanthomonas oryzae pv oryzae* (*Xoo*). *bioRxiv*, 425507. doi: 10.1101/2021.01.07.425507

Slewinski, T. L. (2012). Non-structural carbohydrate partitioning in grass stems: a target to increase yield stability, stress tolerance, and biofuel production. *J. Exp. Bot.* 63, 4647–4670. doi: 10.1093/jxb/ers124

Slewinski, T. L., Meeley, R., and Braun, D. M. (2009). Sucrose transporter1 functions in phloem loading in maize leaves. *J. Exp. Bot.* 60, 881–892. doi: 10.1093/jxb/ern335

Smidansky, E. D., Clancy, M., Meyer, F. D., Lanning, S. P., Blake, N. K., Talbert, L. E., et al. (2002). Enhanced ADP-glucose pyrophosphorylase activity in wheat endosperm increases seed yield. *P. Natl. Acad. Sci.* 99, 1724–1729. doi: 10.1073/pnas.022635299

Smith, A. M., and Stitt, M. (2007). Coordination of carbon supply and plant growth. *Plant Cell Environ.* 30, 1126–1149. doi: 10.1111/j.1365-3040.2007.01708.x

Solomon, C. U., and Drea, S. (2019). Delineation of post-phloem assimilate transport pathway into developing caryopsis of Brachypodium distachyon. *bioRxiv*. doi: 10.1101/718569

Sosso, D., Luo, D., Li, Q. B., Sasse, J., Yang, J., Gendrot, G., et al. (2015). Seed filling in domesticated maize and rice depends on SWEET-mediated hexose transport. *Nat. Genet.* 47, 1489–1493. doi: 10.1038/ng.3422

South, P. F., Cavanagh, A. P., Liu, H. W., and Ort, D. R. (2019). Synthetic glycolate metabolism pathways stimulate crop growth and productivity in the field. *Science.* 363, eaat9077. doi: 10.1126/science.aat9077

Stitt, M., and Zeeman, S. C. (2012). Starch turnover: pathways, regulation and role in growth. *Curr. Opin. Plant Biol.* 15, 282–292. doi: 10.1016/j.pbi.2012.03.016

Sulpice, R., Flis, A., Ivakov, A. A., Apelt, F., Krohn, N., Encke, B., et al. (2014). *Arabidopsis* coordinates the diurnal regulation of carbon allocation and growth across a wide range of photoperiods. *Mol. Plant* 7, 137–155. doi: 10.1093/mp/sst127

Sulpice, R., Pyl, E. T., Ishihara, H., Trenkamp, S., Steinfath, M., Witucka-Wall, H., et al. (2009). Starch as a major integrator in the regulation of plant growth. *P. Natl. Acad. Sci.* 106, 10348–10353. doi: 10.1073/pnas.0903478106

Sweetlove, L. J., Nielsen, J., and Fernie, A. R. (2017). Engineering central metabolism - a grand challenge for plant biologists. *Plant J.* 90, 749–763. doi: 10.1111/tpj.13464

Teng, Z., Yu, H., Wang, G., Meng, S., Liu, B., Yi, Y., et al. (2022). Synergistic interaction between ABA and IAA due to moderate soil drying promotes grain filling of inferior spikelets in rice. *Plant J.* 109, 1457–1472. doi: 10.1111/tpj.15642

Tian, B., Talukder, S. K., Fu, J., Fritz, A. K., and Trick, H. N. (2018). Expression of a rice soluble starch synthase gene in transgenic wheat improves the grain yield under heat stress conditions. *In Vitro Cell.Dev.Biol.-Plant* 54, 216–227. doi: 10.1007/s11627-018-9893-2

von Caemmerer, S., and Furbank, R. T. (2016). Strategies for improving C4 photosynthesis. *Curr. Opin. Plant Biol.* 31, 125–134. doi: 10.1016/j.pbi.2016.04.003

Wang, G., Li, X., Ye, N., Huang, M., Feng, L., Li, H., et al. (2021a). *OsTPP1* regulates seed germination through the crosstalk with abscisic acid in rice. *New Phytol.* 230, 1925–1939. doi: 10.1111/nph.17300

Wang, L., Lu, Q., Wen, X., and Lu, C. (2015). Enhanced sucrose loading improves rice yield by increasing grain size. *Plant Physiol.* 169, 2848–2862. doi: 10.1104/pp.15.01170

Wang, L. M., Shen, B. R., Li, B. D., Zhang, C. L., Lin, M., Tong, P. P., et al. (2020). A synthetic photorespiratory shortcut enhances photosynthesis to boost biomass and grain yield in rice. *Mol. Plant* 13, 1802–1815. doi: 10.1016/j.molp.2020.10.007

Wang, E., Wang, J., Zhu, X., Hao, W., Wang, L., Li, Q., et al. (2008). Control of rice grain-filling and yield by a gene with a potential signature of domestication. *Nat. Genet.* 40, 1370–1374. doi: 10.1038/ng.220

Wang, G., Wu, Y., Ma, L., Lin, Y., Hu, Y., Li, M., et al. (2021b). Phloem loading in rice leaves depends strongly on the apoplastic pathway. *J. Exp. Bot.* 72, 3723–3738. doi: 10.1093/jxb/erab085

Wang, G., and Zhang, J. (2020). Carbohydrate, hormone and enzyme regulations of rice grain filling under post-anthesis soil drying. *Environ. Exp. Bot.* 178, 104165. doi: 10.1016/j.envexpbot.2020.104165

Wingenter, K., Schulz, A., Wormit, A., Wic, S., Trentmann, O., Hoermiller, I. I., et al. (2010). Increased activity of the vacuolar monosaccharide transporter TMT1 alters cellular sugar partitioning, sugar signaling, and seed yield in *Arabidopsis*. *Plant Physiol.* 154, 665–677. doi: 10.1104/pp.110.162040

Wu, A., Brider, J., Busch, F. A., Chen, M., Chenu, K., Clarke, V. C., et al. (2023). A cross-scale analysis to understand and quantify the effects of photosynthetic enhancement on crop growth and yield across environments. *Plant Cell Environ.* 46, 23–44. doi: 10.1111/pce.14453

Wu, L. B., Eom, J. S., Isoda, R., Li, C., Char, S. N., Luo, D., et al. (2022). *OsSWEET11b*, a potential sixth leaf blight susceptibility gene involved in sugar transport-dependent male fertility. *New Phytol.* 234, 975–989. doi: 10.1111/nph.18054

Wu, A., Hammer, G. L., Doherty, A., von Caemmerer, S., and Farquhar, G. D. (2019a). Quantifying impacts of enhancing photosynthesis on crop yield. *Nat. Plants* 5, 380–388. doi: 10.1038/s41477-019-0398-8

Wu, Y., Lee, S. K., Yoo, Y., Wei, J., Kwon, S. Y., Lee, S. W., et al. (2018). Rice transcription factor *OsDOF11* modulates sugar transport by promoting expression of sucrose transporter and SWEET genes. *Mol. Plant* 11, 833–845. doi: 10.1016/j.molp.2018.04.002

Wu, Y., Shi, L., Li, L., Fu, L., Liu, Y., Xiong, Y., et al. (2019b). Integration of nutrient, energy, light, and hormone signalling *via* TOR in plants. *J. Exp. Bot.* 70, 2227–2238. doi: 10.1093/jxb/erz028

Xue, X., Wang, J., Shukla, D., Cheung, L. S., and Chen, L. Q. (2022). When SWEETs turn tweens: Updates and perspectives. *Annu. Rev. Plant Biol.* 73, 379–403. doi: 10.1146/annurev-arplant-070621-093907

Yang, H., Li, Y., Qiao, Y., Sun, H., Liu, W., Qiao, W., et al. (2023). Low light stress promotes new tiller regeneration by changing source-sink relationship and activating expression of expansin genes in wheat. *Plant Cell Environ.* 46, 1562–1581. doi: 10.1111/pce.14548

Yang, J., Luo, D., Yang, B., Frommer, W. B., and Eom, J. S. (2018). SWEET11 and 15 as key players in seed filling in rice. *New Phytol.* 218, 604–615. doi: 10.1111/nph.15004

Yang, B., Wang, J., Yu, M., Zhang, M., Zhong, Y., Wang, T., et al. (2022). The sugar transporter *ZmSUGCAR1* of the nitrate transporter 1/peptide transporter family is critical for maize grain filling. *Plant Cell* 34, 4232–4254. doi: 10.1093/plcell/koac256

Yin, X., and Struik, P. C. (2015). Constraints to the potential efficiency of converting solar radiation into phytoenergy in annual crops: from leaf biochemistry to canopy physiology and crop ecology. *J. Exp. Bot.* 66, 6535–6549. doi: 10.1093/jxb/erv371

Yoon, D.-K., Ishiyama, K., Suganami, M., Tazoe, Y., Watanabe, M., Imaruoka, S., et al. (2020). Transgenic rice overproducing Rubisco exhibits increased yields with improved nitrogen-use efficiency in an experimental paddy field. *Nat. Food* 1, 134–139. doi: 10.1038/s43016-020-0033-x

Yuan, M., Zhao, J., Huang, R., Li, X., Xiao, J., and Wang, S. (2014). Rice MtN3/saliva/SWEET gene family: Evolution, expression profiling, and sugar transport. *J. Integr. Plant Biolo.* 56, 559–570. doi: 10.1111/jipb.12173

Zhang, Z., Huang, J., Gao, Y., Liu, Y., Li, J., Zhou, X., et al. (2020b). Suppressed ABA signal transduction in the spike promotes sucrose use in the stem and reduces grain number in wheat under water stress. *J. Exp. Bot.* 71, 7241–7256. doi: 10.1093/jxb/eraa380

Zhang, J., Li, D., Xu, X., Ziska, L. H., Zhu, J., Liu, G., et al. (2020a). The potential role of sucrose transport gene expression in the photosynthetic and yield response of rice cultivars to future CO_2 concentration. *Physiol. Plantarum* 168, 218–226. doi: 10.1111/ppl.12973

Zhang, Y., Primavesi, L. F., Jhurreea, D., Andralojc, P. J., Mitchell, R. A., Powers, S. J., et al. (2009). Inhibition of SNF1-related protein kinase1 activity and regulation of metabolic pathways by trehalose-6-phosphate. *Plant Physiol.* 149, 1860–1871. doi: 10.1104/pp.108.133934

Zhao, Y., Zhang, S., Lv, Y., Ning, F., Cao, Y., Liao, S., et al. (2022). Optimizing ear-plant height ratio to improve kernel number and lodging resistance in maize (*Zea mays* L.). *Field Crops Res.* 276, 108376. doi: 10.1016/j.fcr.2021.108376

Zhu, X. G., Long, S. P., and Ort, D. R. (2010). Improving photosynthetic efficiency for greater yield. *Annu. Rev. Plant Biol.* 61, 235–261. doi: 10.1146/annurev-arplant-042809-112206

Zhu, J., Zhou, L., Li, T., Ruan, Y., Zhang, A., Dong, X., et al. (2022). Genome-wide investigation and characterization of SWEET gene family with focus on their evolution and expression during hormone and abiotic stress response in maize. *Genes* 13, 1682. doi: 10.3390/genes13101682

Frontiers in Plant Science

Cultivates the science of plant biology and its applications

The most cited plant science journal, which advances our understanding of plant biology for sustainable food security, functional ecosystems and human health.

Discover the latest Research Topics

See more →

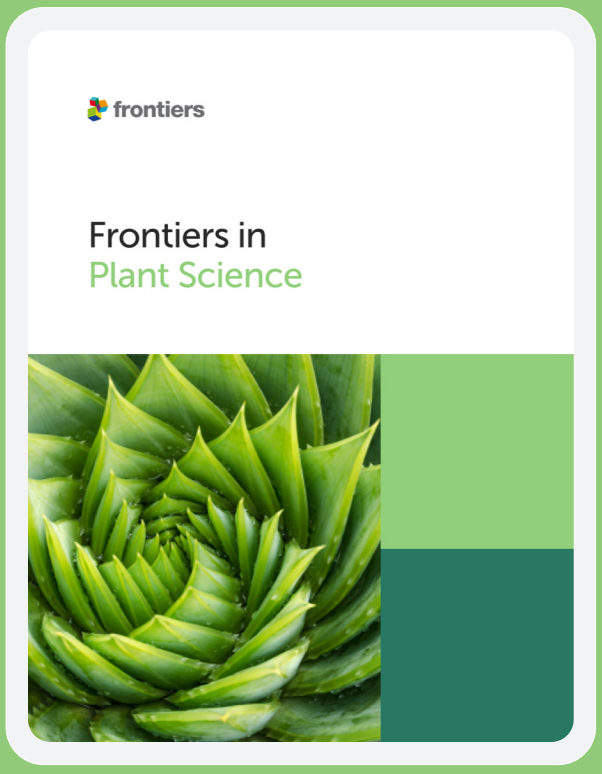

Frontiers

Avenue du Tribunal-Fédéral 34
1005 Lausanne, Switzerland
frontiersin.org

Contact us

+41 (0)21 510 17 00
frontiersin.org/about/contact